



HAL
open science

Photooxidation of hypercoordinate silicate for the generation of carbon centered radicals : radical processes and dual catalysis

Christophe Lévêque

► **To cite this version:**

Christophe Lévêque. Photooxidation of hypercoordinate silicate for the generation of carbon centered radicals : radical processes and dual catalysis. Catalysis. Université Pierre et Marie Curie - Paris VI, 2017. English. NNT : 2017PA066209 . tel-01754038

HAL Id: tel-01754038

<https://theses.hal.science/tel-01754038>

Submitted on 30 Mar 2018

HAL is a multi-disciplinary open access archive for the deposit and dissemination of scientific research documents, whether they are published or not. The documents may come from teaching and research institutions in France or abroad, or from public or private research centers.

L'archive ouverte pluridisciplinaire **HAL**, est destinée au dépôt et à la diffusion de documents scientifiques de niveau recherche, publiés ou non, émanant des établissements d'enseignement et de recherche français ou étrangers, des laboratoires publics ou privés.

Thèse de Doctorat de Chimie Moléculaire de
l'Université Pierre et Marie Curie

Ecole doctorale de Chimie Moléculaire de Paris Centre – ED 406

Institut Parisien de Chimie Moléculaire / Equipe MACO

**Photooxydation de silicates hypercoordinés pour la
génération de radicaux carbonés: processus
radicalaires et catalyse duale**

Présentée par

M. Christophe LÉVÊQUE

Pour obtenir le grade de
Docteur de l'Université Pierre et Marie Curie

Soutenance prévue le 29 Septembre 2017

Devant un jury composé de :

M. Yannick LANDAIS, Professeur à l'Université de Bordeaux	Rapporteur
M. Sami LAKHDAR, Chargé de recherche CNRS à l'Université de Caen	Rapporteur
Mme Kirsten ZEITLER, Professeur à l'Université de Leipzig	Examineur
M. Nicolas RABASSO, Maître de conférences à l'Université Paris-Sud 11	Examineur
M. Alejandro PEREZ-LUNA, Directeur de recherche CNRS à l'Université Pierre et Marie Curie	Examineur
M. Cyril OLLIVIER, Directeur de recherche CNRS à l'Université Pierre et Marie Curie	Examineur
M. Louis FENSTERBANK, Professeur à l'Université Pierre et Marie Curie	Examineur

Thèse de Doctorat de Chimie Moléculaire de
l'Université Pierre et Marie Curie

Ecole doctorale de Chimie Moléculaire de Paris Centre – ED 406

Institut Parisien de Chimie Moléculaire / Equipe MACO

**Photooxydation de silicates hypercoordinés pour la
génération de radicaux carbonés: processus
radicalaires et catalyse duale**

Présentée par

M. Christophe LÉVÊQUE

Pour obtenir le grade de
Docteur de l'Université Pierre et Marie Curie

Soutenance prévue le 29 Septembre 2017

Devant un jury composé de :

M. Yannick LANDAIS, Professeur à l'Université de Bordeaux	Rapporteur
M. Sami LAKHDAR, Chargé de recherche CNRS à l'Université de Caen	Rapporteur
Mme Kirsten ZEITLER, Professeur à l'Université de Leipzig	Examineur
M. Nicolas RABASSO, Maître de conférences à l'Université Paris-Sud 11	Examineur
M. Alejandro PEREZ-LUNA, Directeur de recherche CNRS à l'Université Pierre et Marie Curie	Examineur
M. Cyril OLLIVIER, Directeur de recherche CNRS à l'Université Pierre et Marie Curie	Examineur
M. Louis FENSTERBANK, Professeur à l'Université Pierre et Marie Curie	Examineur

Remerciements

Les travaux de ce projet de thèse ont été réalisés à l'Institut Parisien de Chimie Moléculaire dirigé par le Docteur Corinne Aubert.

Je tiens tout d'abord à remercier les membres du jury pour avoir accepté de participer à mon jury de thèse en tant que rapporteurs: M. Yannick Landais, professeur à l'Université de Bordeaux et M. Sami Lakhdar, Chargé de recherche CNRS à l'université de Caen, et en tant qu'examineurs: Mme Kirsten Zeitler, professeur à l'université de Leipzig, M. Nicolas Rabasso, maître de conférence à l'université Paris-Sud 11 et M. Alejandro Perez-Luna, directeur de recherche CNRS à l'université Pierre et Marie Curie.

Je souhaite particulièrement remercier mes encadrants, Cyril Ollivier et Louis Fensterbank pour m'avoir permis de réaliser mon doctorat au sein de l'équipe MACO. Merci pour votre disponibilité, vos conseils et remarques, ainsi que pour votre compréhension. Bien que le début de doctorat ait pu être compliqué, le chemin parcouru pendant ces trois années sur le plan professionnel et personnel a été très enrichissant et je souhaite une nouvelle fois vous remercier pour cela.

Je remercie aussi les membres de l'équipe MACO, membres permanents ainsi qu'étudiants présents ou passés, pour la bonne ambiance et les bons moments passés à vos côtés.

Enfin, un grand merci aux personnes de mon entourage, famille et amis, qui ont su me soutenir pendant ces trois années.

Sommaire

Remerciements	5
Sommaire	7
Abbreviations	11
Résumé en français	15
Chapter I. Photoredox catalysis, an opportunity for sustainable chemistry	39
1.1 Evolution of radical chemistry	41
1.1.1 Introduction to radical synthesis	41
1.1.2 Challenges in radical chemistry	43
1.2 The photoredox catalysis as an alternative	43
1.2.1 Nature as a source of inspiration	44
1.2.2 Artificial redox photocatalysts	45
1.2.2.1 Photophysical properties	48
1.2.2.2 Molecular orbital approach and redox potentials	50
1.2.3 Principle of photoredox catalysis	52
1.2.4 Formation of carbon centered radicals	57
1.2.4.1 Formation of aryl radicals by photoreduction	57
1.2.4.2 Photoreductive processes for the generation of alkyl radicals	58
1.2.4.3 Photooxidative processes for the formation of alkyl radicals	63
1.3 Conclusion	69
Chapter II Merging photoredox and organometallic catalysis for cross-coupling reactions	71
2.1 Context	73
2.2 Radical trapping by transition-metals	73
2.3 Ruthenium and Palladium: Genesis of the photoredox/transition metal dual catalysis	79
2.4 Towards photoredox/transition-metal dual catalysis processes	82
2.4.1 Processes without radical formation: Catalysis of Redox Steps	82
2.4.2 Processes with radical formation: Catalysis of Downstream Steps	88

2.4.2.1	Gold mediated catalysis	88
2.4.2.2	Copper-mediated catalysis	92
2.5	Conclusion	94
Chapter III Oxidation of alkyl bis-catecholato silicates: a mild way for the formation of carbon centered radicals		97
3.1	Definition of silicates	99
3.2	Oxidation of hypercoordinate silicon compounds	99
3.2.1	Metal mediated oxidation of organopentafluorosilicates	100
3.2.2	Photon-induced electron transfers with alkyl bis-catecholato silicates	102
3.3	Alkyl bis-catecholato silicates in synthesis	105
3.3.1	Formation of alkyl bis-catecholato silicates	105
3.3.2	Structural analysis and properties	108
3.3.2.1	Hypercoordination of the silicon atom in alkyl bis-catecholato silicates	108
3.3.2.2	Redox properties	111
3.4	Studies on photooxidation of alkyl bis-catecholato silicates	113
3.4.1	Photooxidation by polypyridine transition metal photocatalysts	113
3.4.2	To a metal free oxidation	116
3.4.2.1	Stoichiometric oxidation	116
3.4.2.2	Organic dyes as photooxidant	120
3.5	Conclusion	124
Chapter IV Combining photooxidation of alkyl bis-catecholato silicates and Nickel catalysis: functionalization of electrophiles		127
4.1	Progress in Nickel catalysis	129
4.2	Development of visible-light photoredox/nickel dual catalysis	136
4.2.1	Pioneer works	136
4.2.2	Advances on photoredox/nickel dual catalysis	140
4.3	Alkyl bis-catecholato silicates in photoredox/nickel dual catalysis: formation of C(sp²)-C(sp³) bonds	148
4.3.1	Process involving a metal based photocatalyst	148
4.3.2	Toward a green dual catalytic system	155

4.4	Alkyl bis-catecholato silicates in photoredox/nickel dual catalysis: formation of C(sp³)-C(sp³) bonds	162
4.4.1	C(sp ³)-C(sp ³) cross-coupling reactions involving alkyl carboxylates	162
4.4.2	Silicates as nucleophilic partners	163
4.4.2.1	Optimization of the cross-coupling reaction	163
4.4.2.2	Scope of the reaction and limitations	166
4.5	Extension to other catalytic systems	169
4.5.1	Concept of non-innocent ligands	169
4.5.2	Preliminary results	172
4.6	Conclusion	176
Experimental Section		179
5.1	General informations	181
5.2	Synthesis of photocatalysts	182
5.3	Synthesis of silicates	186
5.4	Synthesis of electrophiles	205
5.5	Radical additions reactions	214
5.6	Cross-coupling reactions: photoredox/nickel dual catalysis	227
5.6.1	C(sp ²)-C(sp ³) bond formation	227
5.6.2	C(sp ³)-C(sp ³) bond formation	267
5.7	Synthesis of non-inocent ligand complexes	278
General Conclusion		281

Abbreviations

[18-C-6]: 1,4,7,10,13,16-hexaoxacyclooctadecane

AcO: acetate

Ar: aryl

BDE: Bond Dissociation Energy

Bn: benzyl

Boc: *tert*-butoxycarbonyl

bpy: 2,2'-bipyridyl

bpz: 2,2'-bipyrazine

COD: 1,5-cyclooctadiene

Cp: cyclopentadienyl

d: doublet

DBU: 1,8-diazabicyclo[5.4.0]undec-7-ene

DCM: dichloromethane

dme: dimethoxyethane

DIPEA: diisopropylethylamine

DMF: *N,N'*-dimethylformamide

DMP: Dess-Martin Periodinane

DMSO: dimethylsulfoxide

Et: ethyl

equiv.: equivalent

ESI: Electro-Spray Ionisation

EWG: Electron Withdrawing Group

dppe: ethylenebis(diphenylphosphine)

dtbbpy: 4,4'-di-*tert*-butyl-2,2'-bipyridyl

HOMO: Highest Occupied Molecular Orbital

HRMS: High Resolution Mass Spectrometry

IR: infrared

ISC: Inter-System Crossing

LEDs: Light-Emitting Diodes

LUMO: Lowest Unoccupied Molecular Orbital

nm: nanometer

NMP: *N*-methyl-2-pyrrolidone

NMR: Nuclear Magnetic Resonance

PC: photocatalyst

ppy: 2-phenylpyridine

Pybox: 2,6-bis(4,5-dihydrooxazol-2-yl)pyridine

q: quadruplet

rt: room temperature

RISC: Reverse Inter-System Crossing

s: singlet

SCE: Saturated Calomel Electrode

SET: Single Electron Transfer

t: triplet

TEMPO: (2,2,6,6-Tetramethylpiperidin-1-yl)oxyl

TfO: triflate

THF: tetrahydrofuran

TMS: trimethylsilyl

Ts: tosyl

V: Volt

W: Watt

Résumé en français

Bien que les réactions ioniques occupent une place importante en chimie de synthèse, les processus impliquant des espèces radicalaires ont réussi à s'imposer comme des alternatives de choix. Le premier radical de synthèse a été mis en évidence en 1900 par Moses Gomberg. Il s'agit du radical triphénylméthyle.¹ Malgré cette découverte, l'intérêt pour la chimie radicalaire de synthèse a mis du temps à émerger. Grâce aux travaux de plusieurs chimistes, dont notamment ceux de Paneth, Hey et Kharasch, et la découverte de la RPE dans les années 40, l'étude des réactions faisant intervenir des radicaux a été simplifiée et a permis d'élargir les applications de la chimie radicalaire à la synthèse organique. Parmi les processus mettant en jeu des espèces radicalaires, la mise au point de processus en chaînes médiés par l'hydrure d'étain, les réactions de transfert d'atome ou de groupe d'atomes, mais aussi les réactions de cyclisation ainsi que les processus en cascade ont en partie fortement contribué au développement de la chimie radicalaire de synthèse.

Malgré tous ces efforts, leurs utilisations dans des procédés industriels restent limités. La polymérisation radicalaire ou l'oxydation du cumène pour la production de phénol méritent toutefois d'être citées. En effet, les radicaux ont longtemps été considérés comme des espèces très réactives hors de contrôle par une partie des chimistes. Pourtant, les contributions de Kochi, Davis, Giese, Minisci, Curran, Hart et d'autres ont pu démystifier la réactivité des radicaux et en faire des candidats valables pour la chimie de synthèse. A l'opposé des réactifs organométalliques de type Grignards, organolithiens, cuprates,... qui doivent être manipulés avec précautions, les précurseurs radicalaires permettent d'engendrer les radicaux en solvant partiellement hydraté. De plus, les réactions radicalaires ont l'avantage de ne pas être sensibles à la nature du solvant, d'être chimiosélectives et peuvent être réalisées sans avoir à utiliser de groupes protecteurs. De fait, plusieurs options pour la formation de radicaux sont utilisables. Pour des réactions en chaîne, plusieurs initiateurs (trialkylboranes, peroxydes, composés azo,...) et médiateurs radicalaires (stannanes, silanes, thiols,...) sont à disposition. La formation des espèces radicalaires peut aussi se faire par transfert monoélectronique à l'aide de sels métalliques en quantité stœchiométriques, en oxydation (manganèse, cérium, argent,...) ou en réduction (samarium, titane, zinc, nickel,...). Toutes ces alternatives sont

¹ (a) M. Gomberg, *J. Am. Chem. Soc.*, 1900, **22**, 757–771. (b) M. Gomberg, *J. Am. Chem. Soc.*, 1901, **23**, 496–502. (c) M. Gomberg, *J. Am. Chem. Soc.*, 1902, **24**, 597–628.

autant d'outils à disposition du chimiste pour la formation de liaisons carbone-carbone ou carbone-hétéroatome.²

Bien qu'elle possède des avantages, la chimie radicalaire a aussi ces limitations. En effet, les réactions radicalaires doivent être réalisées en milieu dilué, ce qui limite la possibilité de les réaliser sur large échelle. De plus, afin de piéger de façon efficace les radicaux, un excès d'accepteur radicalaire est souvent nécessaire. A noter que, les initiateurs radicalaires présentent des risques d'explosion. Mais l'aspect le plus négatif de cette chimie est l'utilisation trop récurrente de médiateurs à base d'étain, toxiques pour l'Homme et difficiles à éliminer. Avec l'avènement du concept de chimie verte à la fin des années 1990,³ de nombreux efforts ont été réalisés pour éviter l'utilisation des dérivés de l'étain dans les méthodes de synthèse.

Progressivement, des alternatives ont été proposées pour remplacer les médiateurs stannylés. Des méthodes utilisant des quantités catalytiques de ces dérivés ou bien des supports solides à base d'étain ont d'abord été considérées. L'utilisation d'autres médiateurs radicalaires tels que des silanes, phosphines ou thiols moins toxiques se sont révélés de bon réactifs mais moins efficaces. Les métaux mettant en jeu des transferts monoélectroniques ont aussi été considérés comme alternatives mais doivent être utilisés en quantités stœchiométriques ou sur-stœchiométriques, de plus ils sont spécifiques d'une fonction chimique. D'un point de vue développement durable et écologique, ces alternatives aux dérivés de l'étain sont limitées. Pour autant, un domaine de recherche amorcé à la fin des années 1970, permettant de former des radicaux par transfert monoélectronique grâce à un complexe métallique photoactivé à travers le développement d'une catalyse photorédox en lumière visible, a attiré depuis une dizaine d'années de nombreux groupes de recherche.

² Pour des ouvrages sur les aspects de la chimie radicalaire de synthèse, voir: a) C. Chatgililoglu and A Studer in *Encyclopedia of Radicals in Chemistry, Biology and Materials*, Eds. John Wiley & Sons Ltd, Chichester, 2012. (b) P. Renaud, M. P. Sibi in *Radicals in Organic Synthesis, Vol. 1 & 2*, Wiley-VCH, Weinheim, 2001. (c) D. P. Curran, N. A. Porter, B. Giese in *Stereochemistry of Radical Reactions*, VCH, Weinheim, 1996. (d) A. Gansäuer in *Radicals in Synthesis I & II, Topics in Current Chemistry*, Springer, Heidelberg, Vols 263 & 264, 2006.

³ Pour des ouvrages sur les aspects de la chimie verte: (a) J. A. Linthorst in *An overview: origins and development of green chemistry, Foundations of Chemistry*. 2009, **12**, 55–68. (b) E. J. Woodhouse, S. Breyman in *Green chemistry as social movement?, Science, Technology, & Human Values.*, 2005, **30**, 199–222. (c) P. T. Anastas and J. C. Warner in *Green Chemistry: Theory and Practice*, Oxford University Press, Oxford, 1988. (d) M. Malacria, J.-P. Goddard et C. Ollivier, 2009, K1200.

Après activation par un photon suivie de la promotion d'un électron dans une orbitale de plus haute énergie, certains complexes métalliques ou photocatalyseurs, ont la faculté de réduire ou oxyder par transfert monoélectronique un substrat, engendrant ainsi une espèce radicalaire. Les radicaux ainsi formés peuvent être employés de la même façon qu'avec les méthodes précédentes dans des processus radicalaires unitaires, incluant la recombinaison, le transfert d'électrons, la β -fragmentation, l'addition homolytique et la substitution homolytique. Les processus d'oxydation et de réduction sont en partie régis par des facteurs thermodynamiques et plus particulièrement par les potentiels redox des espèces mises en jeu. Afin de moduler le potentiel d'oxydation ou de réduction des photocatalyseurs, le métal (Cu, Ru, Ir,...) ou les ligands peuvent être modifiés, ceci permettant ainsi d'obtenir une large gamme de potentiels redox utilisable selon les substrats à réduire ou oxyder (**Schéma 1**).⁴ Même si la plupart des photocatalyseurs sont des complexes métalliques, un nombre croissant de colorants organiques, tels que la fluorescéine, l'Eosin Y, le rose Bengal et bien d'autres, se sont révélés être des photocatalyseurs aussi efficaces.⁵

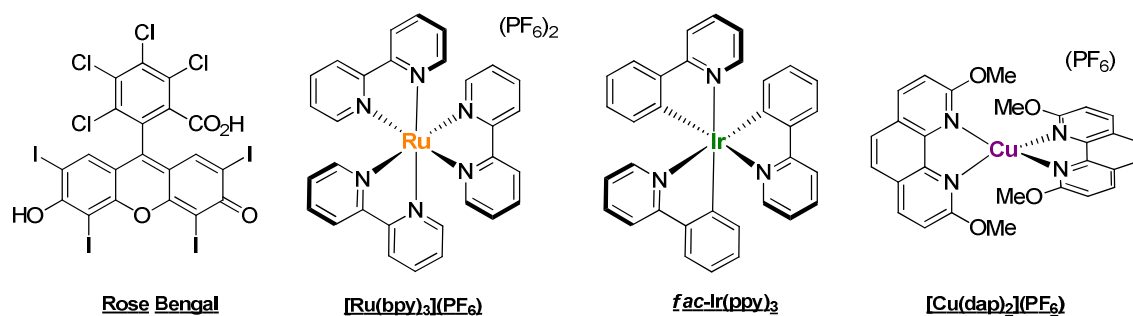


Schéma 1. Exemples de photocatalyseurs organiques et de complexes organométalliques photoactifs

Grâce à l'ensemble des photocatalyseurs à disposition, des radicaux carbonés ou centrés sur un hétéroatome (par exemple l'oxygène, l'azote ou le soufre) peuvent être formés et utilisés en synthèse. Malgré tout, la formation des radicaux carbonés alkyles non stabilisés reste difficile à engendrer de façon efficace. De nombreux exemples de processus de

⁴ C. K. Prier, D. A. Rankic and D. W. V. MacMillan, *Chem. Rev.*, 2013, **113**, 5322–5363.

⁵ (a) N. A. Romero and D. A. Nicewicz, *Chem. Rev.*, 2016, **116**, 10075–10166. (b) M. Neumann, S. Fldner, B. König and K. Zeitler, *Angew. Chem. Int. Ed.*, 2011, 50, 951 – 954.

photoréduction ont rapportés la formation de radicaux alkyles stabilisés, notamment par réduction de α -halo-esters,⁶ de dérivés d'acides⁷ ou d'époxydes⁸ par exemple (**Schéma 2**).

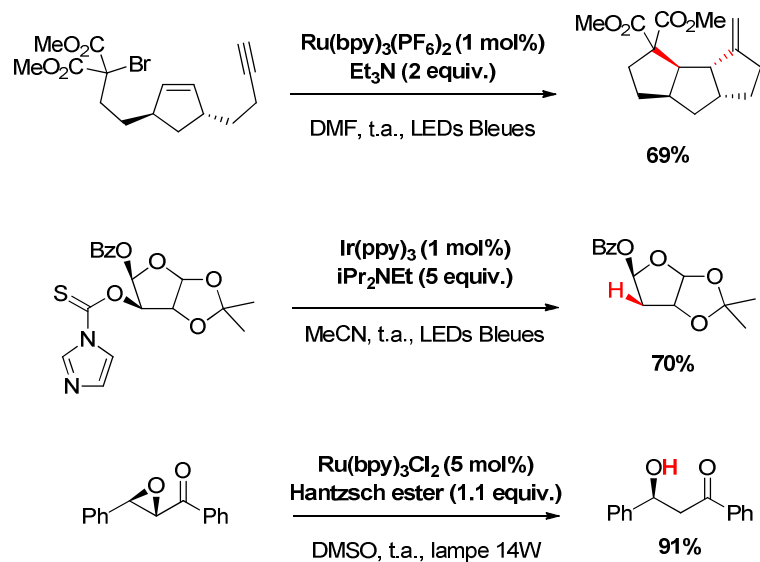


Schéma 2. Formation de radicaux carbonés par photoréduction

Peu de travaux ont permis la formation de radicaux alkyles non stabilisés par photoréduction. En 2012, Stephenson a réussi à montrer la formation de telles espèces par réduction d'iodures d'alkyles primaires. Les radicaux ont pu ensuite être engagés dans une étape de cyclisation ou bien directement abstraire un atome d'hydrogène.⁹ Néanmoins, peu d'exemples ont été rapportés dans ces travaux.

⁶ W. Tucker, J. D. Nguyen, J. M. R. Narayanam, S. W. Krabbe and C. R. J. Stephenson, *Chem. Commun.*, 2010, **46**, 4985–4987.

⁷ L. Chenneberg, A. Baralle, M. Daniel, L. Fensterbank, J.-P. Goddard and C. Ollivier, *Adv. Synth. Catal.*, 2014, **356**, 2756–2762.

⁸ E. Hasegawa, S. Takizawa, T. Seida, A. Tamaguchi, N. Yamaguchi, N. Chiba, T. Takahashi, H. Ideka and K. Akiyama, *Tetrahedron*, 2006, **62**, 6581–6588.

⁹ J. D. Nguyen, E. M. D'Amato, J. M. R. Narayanam and Corey R. J. Stephenson, *Nature Chem.*, 2012, **4**, 854–859.

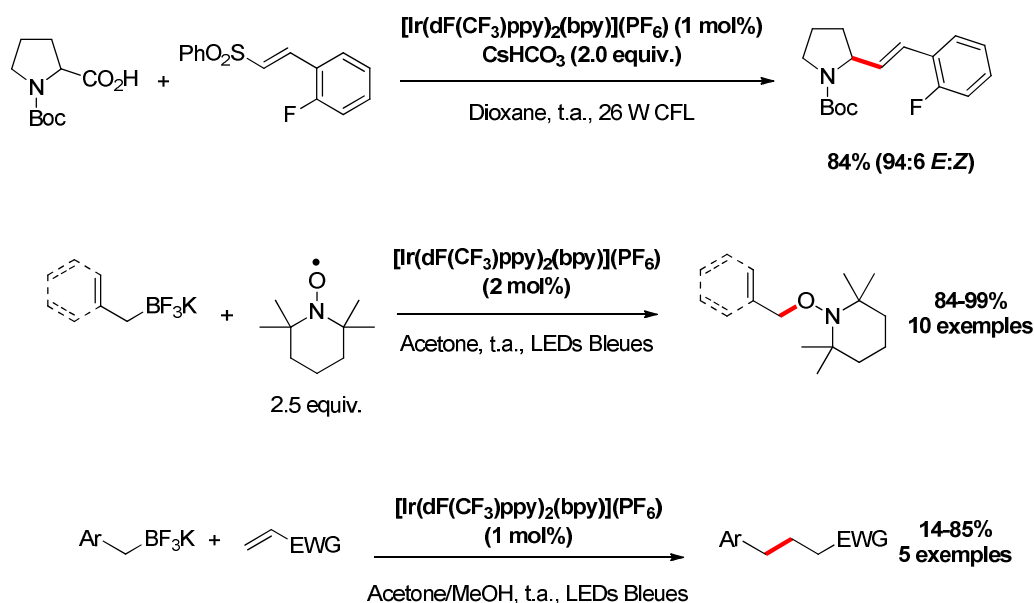


Schéma 4. Photooxydation d' α -amino acides et d'organotrifluoroborates

Dans notre groupe, nous avons montré que des espèces hypervalentes du silicium en conditions de photooxydation peuvent former des radicaux carbonés non stabilisés. Les alkyles bis-catécholato silicates dont les premières synthèses ont été effectuées par Frye¹² puis Corriu,¹³ peuvent être formés à partir de trialkoxysilanes ou trichlorosilanes et de catéchol. Ces espèces anioniques possèdent des potentiels d'oxydation relativement faible ($\sim +0.3$ – $+0.9\text{V}$ vs ESC).¹⁴ Une version ammonium ainsi qu'une version potassium de ces espèces ont pu être obtenus. Dans notre cas, les potassiums alkyles bis-catécholato silicates ont été le cœur de notre étude. Cependant, il a été remarqué que la version potassium des silicates se décompose progressivement. L'ajout d'un éther couronne, le [18-C-6], permet de complexer le potassium et d'éviter la dégradation observée.

¹²C. L. Frye, *J. Am. Chem. Soc.*, 1964, **86**, 3170–3171.

¹³ (a) G. Cerveau, C. Chuit, R. J. P. Corriu, L. Gerbier, C. Reye, J.-L. Aubagnac and B. El Amrani, *Int. J. Mass Spectrom. Ion Phys.*, 1988, **82**, 259. (b) A. Boudin, G. Cerveau, C. Chuit, R. J. P. Corriu and C. Reye, *Bull. Chem. Soc. Jpn.*, 1988, **61**, 101–106.

¹⁴ V. Corcé, L.-M. Chamoreau, E. Derat, J.-P. Goddard, C. Ollivier and L. Fensterbank *Angew. Chem. Int. Ed.* 2015, **54**, 11414–11418.

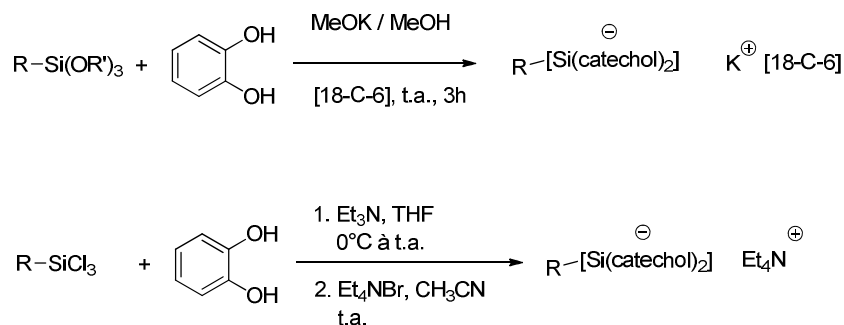


Schéma 5. Synthèse des alkyles bis-catécholato silicates

Après photooxydation par un photocatalyseur d'iridium activé par des LEDs bleues, les intermédiaires radicalaires, stabilisés ou non, ont pu être directement piégés par le TEMPO ou engagés dans des réactions d'allylation, de vinylation ou d'alcynylation.¹⁴

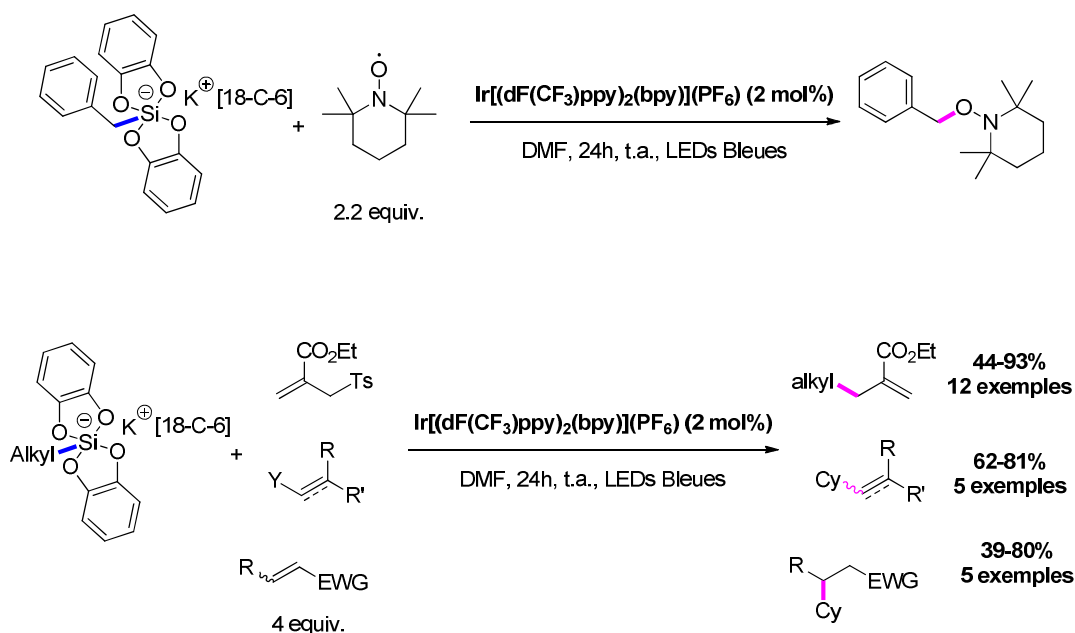


Schéma 6. Photooxydation des alkyles bis-catécholato silicates de potassium

Après activation lumineuse, le complexe d'iridium oxyde l'alkyle bis-catécholato silicate pour former le radical alkyle. Le radical obtenu est ensuite piégé par un accepteur pour conduire à un intermédiaire radicalaire nécessaire à la régénération du photocatalyseur ainsi qu'au produit désiré. Dans le cas d'un piégeage par le TEMPO, un second équivalent est nécessaire pour reformer l'espèce catalytique.

Grâce à ces substrats, la formation de radicaux alkyles primaires, secondaires, et tertiaires, stabilisés ou non, est désormais possible par photooxydation.

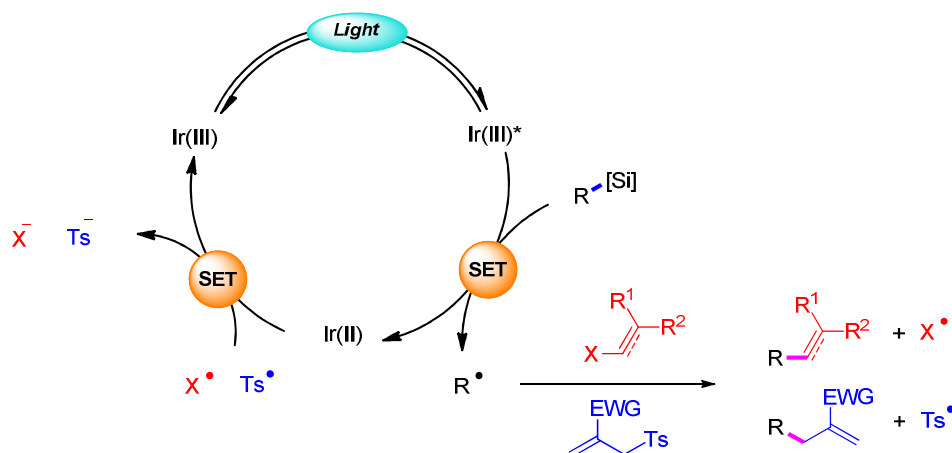


Schéma 7. Mécanisme d'allylation, de vinylation et d'alcylation

Depuis la fin des années 2000, les recherches sur la catalyse photoredox se sont intensifiées de façon exponentielle. Un domaine d'étude particulièrement attirant concerne la catalyse duale photorédox/organométallique. Initialement portée sur des processus de photoréduction, des travaux ont ensuite montré la possibilité de coupler des électrophiles aromatiques avec des radicaux engendrés par photooxydation, grâce à des complexes de nickel. Les premiers travaux sur ce type de couplage ont été réalisés de façon simultanée par Molander en utilisant des benzyltrifluoroborates¹⁵ comme source de radicaux d'une part, et d'autre part à partir de α -amino carboxylates et anilines grâce aux études de MacMillan et Doyle.¹⁶

¹⁵ J. C. Tellis, D. N. Primer and G. A. Molander, *Science*, 2014, **345**, 433436.

¹⁶ Z. Zuo, D. T. Ahneman, L. Chu, J. A. Terrett, A. G. Doyle, D. W. C. MacMillan, *Science*, 2014, **345**, 437440.

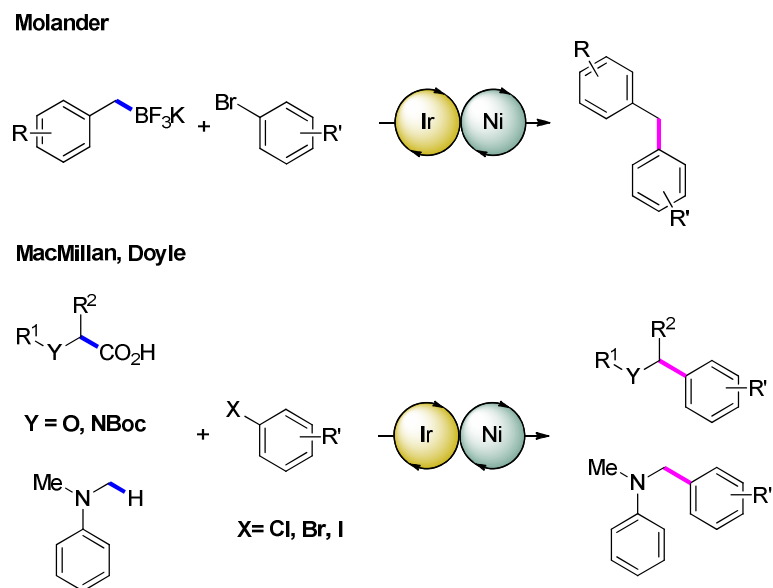
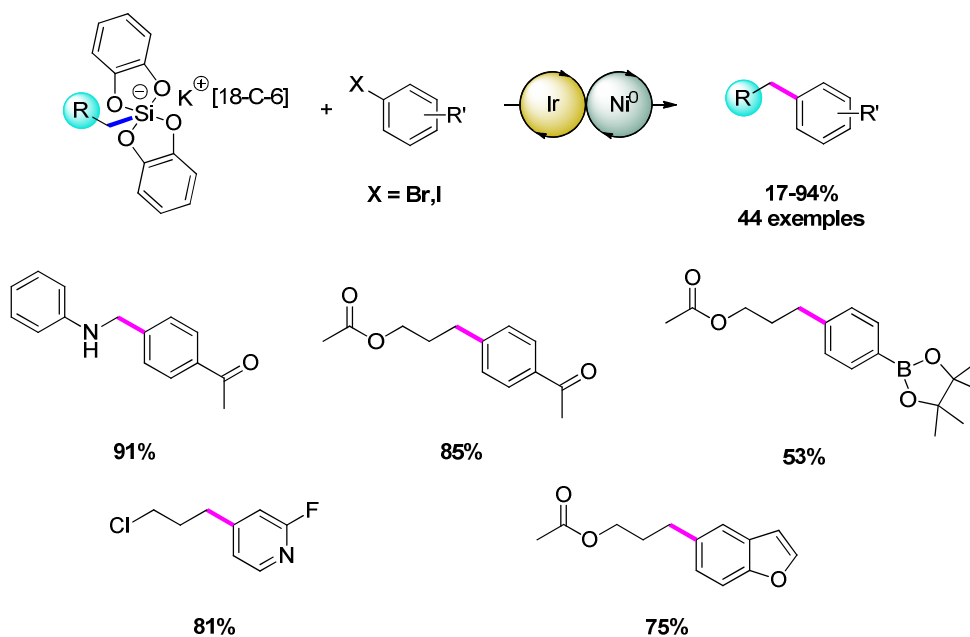


Schéma 8. Premiers exemples de catalyse duale photoredox/nickel

Tout comme les carboxylates et les trifluoroborates, les alkyles bis-catécholato silicates permettent d'engendrer des radicaux carbonés par photooxydation lesquels peuvent ensuite participer à des réactions de couplages croisés catalysés par des complexes de nickel. Mais le principal avantage de ces espèces est leur capacité à former des radicaux primaires non stabilisés. Ainsi, les travaux que nous avons réalisés se sont tout d'abord portés sur le couplage d'alkyles silicates primaires avec des bromures d'aryles ou d'hétéroaryles. Un large panel de silicates portant diverses fonctions chimiques (halogènes, esters, nitriles, époxydes...) ont pu être couplés avec divers halogénures d'(hétéro)aryles portant des groupes électroattracteurs (carbonyle, $-\text{CF}_3$) ou électrodonneurs ($-\text{TMS}$, $-\text{OMe}$), en présence de 2 mol% d'un photocatalyseur d'iridium $[\text{Ir}(\text{dF}(\text{CF}_3)\text{ppy})_2\text{bpy}](\text{PF}_6)$ et 3 mol% d'un complexe de nickel(0) $[\text{Ni}(\text{dtbbpy})]$.¹⁷

¹⁷ C. Lévêque, L. Chenneberg, V. Corcé, J.-P. Goddard, C. Ollivier and L. Fensterbank, *Org. Chem. Front.*, 2016, **3**, 462-465.



Dans un souci de rendre toujours plus “vertes” les conditions réactionnelles, nous avons par la suite envisagé de remplacer le photocatalyseur d’iridium (très coûteux et non recyclable après catalyse) par un photocatalyseur organique. Cependant, ces derniers ont des propriétés moins favorables pour la catalyse photoredox que les analogues métalliques. Les temps de vie à l’état excité étant trop courts, la probabilité de pouvoir effectuer des transferts monoélectroniques est donc diminuée. Parmi les chromophores ayant prouvé leur efficacité en catalyse photoredox, nous avons sélectionné la fluorescéine, l’Eosin Y et le catalyseur de Fukuzumi. Lors d’expériences de piégeage avec le TEMPO, seul le catalyseur de Fukuzumi a montré une activité modérée vis-à-vis du silicate de benzyle. En effet, les alkyles silicates non activités n’ont pas pu être converti de façon efficace dans ces conditions.¹⁸

¹⁸ L. Chenneberg, C. Lévêque, V. Corcé, A. Baralle, J.-P. Goddard, C. Ollivier and L. Fensterbank, *Synlett*, 2016, **27**, 731–735.

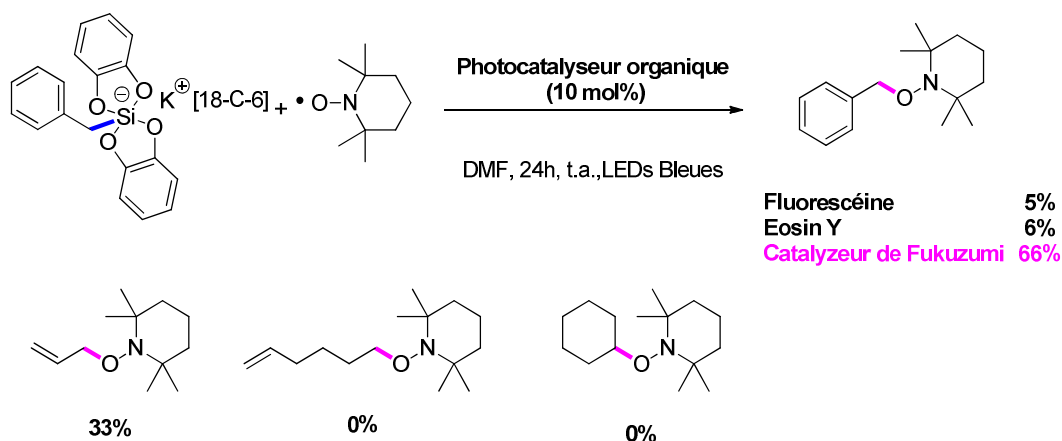


Schéma 10. Photooxydation des alkyles bis-catécholato silicates par des photocatalyseurs organiques

En 2012, le groupe d'Adachi, en quête de nouvelles molécules pour la préparation de diodes organiques électroluminescentes (OLEDs), a décrit une famille de *N*-carbazolyl dicyanobenzène qui avait des propriétés particulièrement performantes pour ce type d'applications.¹⁹ Quelques années plus tard, après avoir déterminé les potentiels rédox de ces composés, Zhang a montré que le 1,2,3,5-tetrakis-(carbazol-yl)-4,6-dicyanobenzène (4CzIPN) pouvait être utilisé en tant que photocatalyseur²⁰ dans des conditions de catalyse duale photorédox/nickel en reproduisant les réactions décrites par Molander et MacMillan.

¹⁹ H. Uoyama, K. Goushi, K. Shizu, H. Nomura and C. Adachi, *Nature*, 2012, **492**, 234–238.

²⁰ J. Luo and J. Zhang, *ACS Catal.*, 2016, **6**, 873–877.

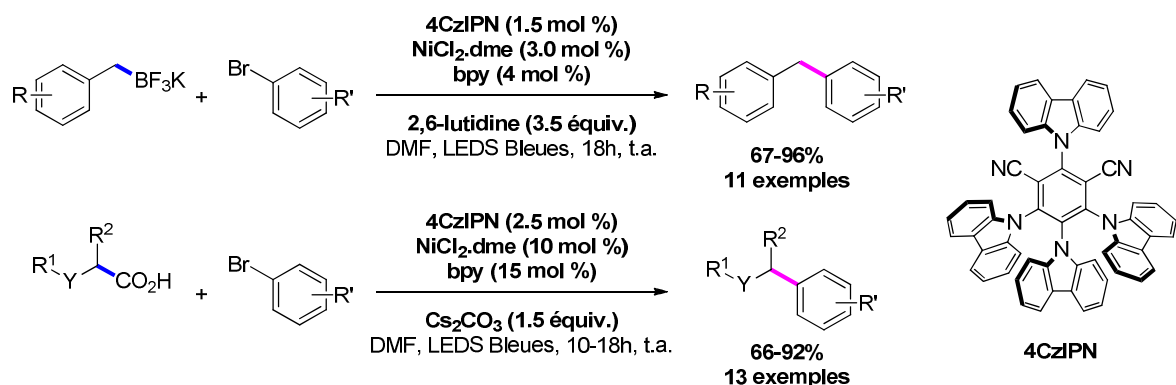


Schéma 11. Catalyse duale photorédox/nickel en présence de 4CzIPN

Ce photocatalyseur organique ayant démontré sa faculté à oxyder des benzyltrifluoroborates et α -amino carboxylates, son utilisation pour oxyder les alkyles bis-catécholato silicates a donc été envisagée. Des expériences de piégeage avec le TEMPO ont montré qu'une faible charge catalytique de 4CzIPN (1 mol%) permet de photooxyder efficacement les silicates. Des réactions radicalaires d'allylation, de vinylation ou d'addition conjuguée de type Giese ont donné de très bons résultats démontrant ainsi l'efficacité de ce photocatalyseur organique.²¹

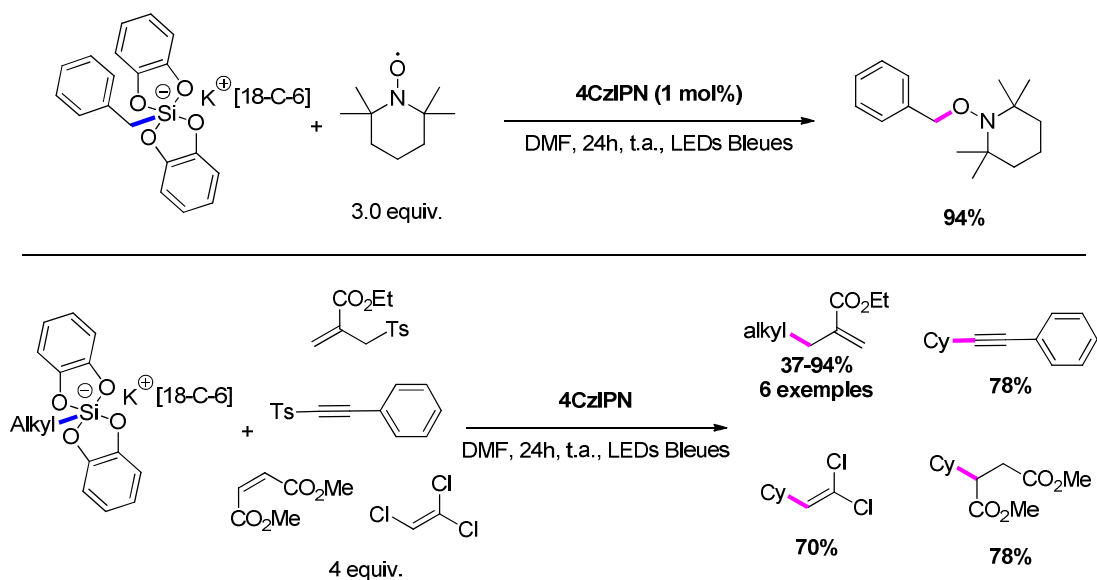


Schéma 12. Photooxydation des alkyles bis-catécholato silicates–piégeage des radicaux alkyles engendrés

²¹ C. Lévêque, L. Cheneberg, V. Corcé, C. Ollivier and L. Fensterbank, *Chem Commun*, 2016, **52**, 9877–9880.

Après avoir montré que les alkyles bis-catécholato silicates pouvaient être photooxydés par le 4CzIPN, nous avons tout naturellement envisagé de développer un système catalytique de couplage croisé mettant en jeu ce photocatalyseur. Dans ce cas, l'optimisation précédente nous a conduits à utiliser la même charge catalytique en photocatalyseur que pour les réactions de piégeage des radicaux (1 mol%). Cependant, le complexe de nickel(0) utilisé dans les conditions précédentes s'est révélé inefficace. L'utilisation d'un complexe de nickel(II) nous a permis de palier à ce problème et de pouvoir effectuer le couplage entre divers alkyles bis-catécholato silicates et des bromures d'aryles ou d'hétéroaryles.²¹

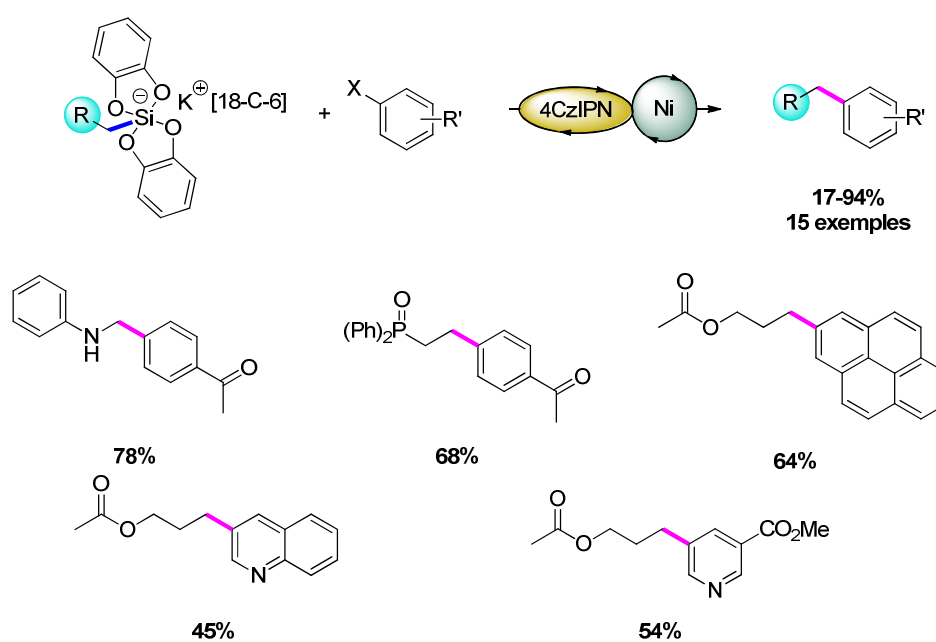


Schéma 13. Catalyse duale en présence 4CzIPN et d'alkyles bis-catécholato silicates

Les conditions de catalyse duale développées nous ont par la suite permis de coupler des bromures éthyléniques avec le [18-Crown-6] bis(catécholato)-acétoxypropylsilicate de potassium. Les bromures éthyléniques non activés ont pu être convertis en produits de couplage avec des rendements modérés, même si les bromures éthyléniques activés ont donné de meilleurs résultats. L'utilisation de β -bromo/chlorostyrènes diastéréomériquement purs en tant qu'électrophiles a permis d'obtenir des produits de couplage avec conservation de la géométrie de la double liaison lorsque le 4CzIPN a été utilisé.²¹

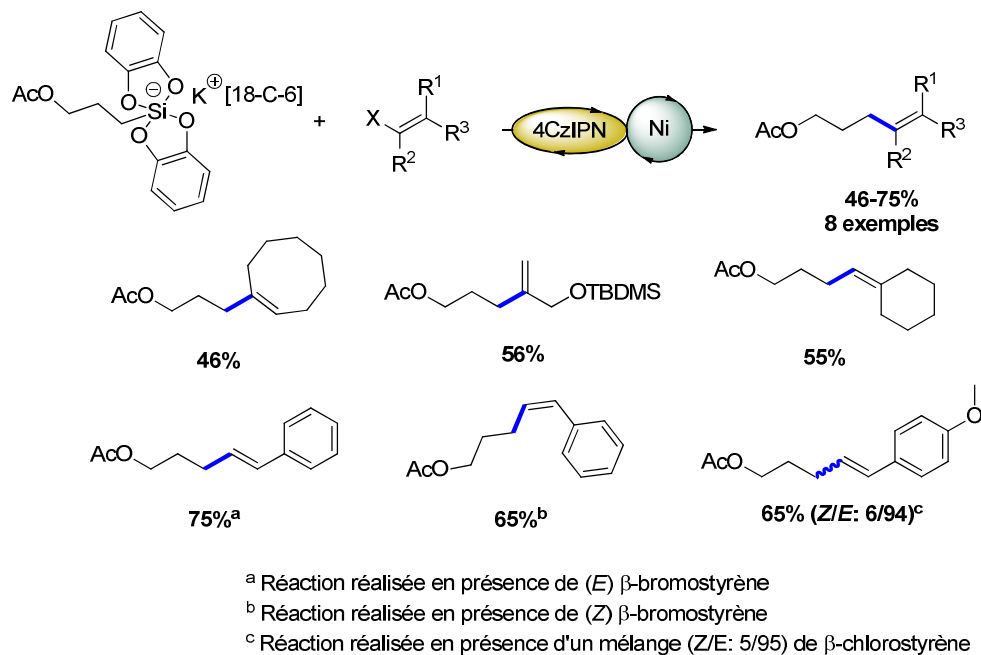


Schéma 14. Extension de la méthode de couplage aux halogénures éthyléniques

En outre, nous avons observé que les dérivés styryles engagés en catalyse pouvaient s'isomériser sous irradiation lumineuse en présence du photocatalyseur organique. Au vu de ces résultats, nous avons pu conclure que le 4CzIPN peut être un photooxydant mais aussi un simple photosensibilisateur. Toutefois, l'oxydation des silicates s'est révélée être plus rapide que le processus de photosensibilisation conduisant à l'isomérisation.²¹

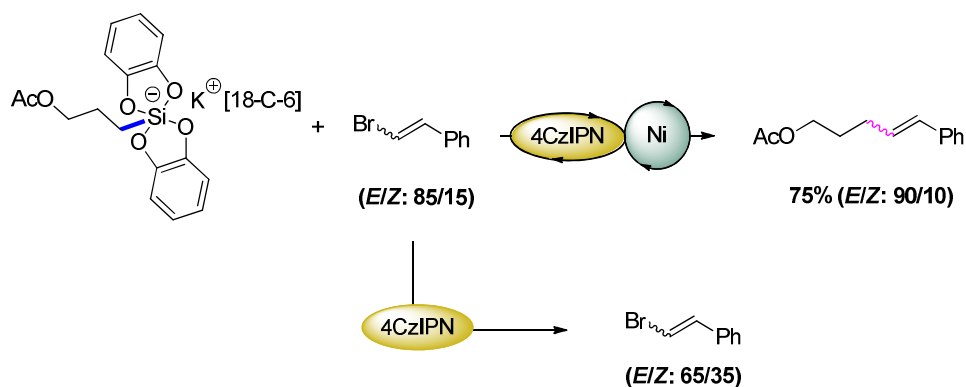


Schéma 15. Photosensibilisation vs. photooxydation par le 4CzIPN

Après avoir étudié le couplage croisé de type $C(sp^3)-C(sp^2)$ en conditions de catalyse duale photoredox/nickel entre des alkyles silicates et des halogénures éthyléniques ou aromatiques, nos travaux se sont tournés vers la formation de liaisons $C(sp^3)-C(sp^3)$ en utilisant cette fois des halogénures d'alkyles.²² Les premières expériences d'optimisation nous ont permis d'obtenir le produit de couplage entre le 4-bromobutyrate d'éthyle et le *n*-hexylsilicate avec un rendement modéré (34%). Ce résultat s'explique par la formation d'un produit secondaire qui s'est avéré être le produit d'homocouplage du bromure utilisé avec un rendement similaire (38%). Plusieurs axes d'optimisation ont été explorés pour favoriser la formation du produit de couplage croisé par rapport au produit d'homocouplage. Les modifications apportées sur la nature du ligand complexé au nickel, du photocatalyseur, des charges catalytiques ou encore du solvant de réaction, n'ont pas permis de former exclusivement le produit de couplage croisé. Dans les meilleures conditions, le produit attendu a pu être obtenu avec un rendement de 43% et le produit secondaire avec un rendement de 38%.

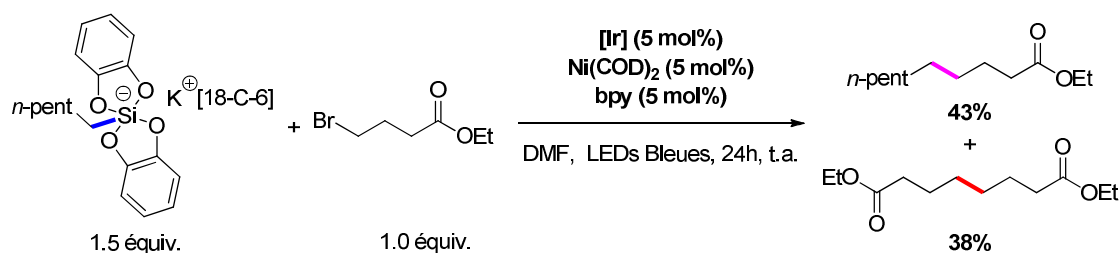


Schéma 16. Conditions optimisées de catalyse duale photoredox/nickel pour la formation de liaisons $C(sp^3)-C(sp^3)$

Après optimisation des conditions réactionnelles, plusieurs alkyles silicates ont été engagés en présence du 4-bromobutyrate d'éthyle comme partenaire électrophile. Malheureusement, pour l'ensemble des silicates engagés dans le processus catalytique, le produit d'homocouplage a toujours été isolé avec un rendement proche de ceux des produits de couplage croisé, lesquels restent encore faibles. Par la suite, le partenaire électrophile a été modifié. Plusieurs bromures primaires et secondaires ont été couplés avec

²² C. Lévêque, V. Corcé, L. CHenneberg, C. Ollivier and L. Fensterbank, *Eur. J. Org. Chem.* **2017**, 2118–2121.

l'acétoxypropylsilicate. Une fois encore les rendements en produits de couplage croisé sont demeurés faibles. En outre, le bromure de hex-5-ényle a conduit à la formation de trois produits de couplage croisé dont un produit de cyclisation. Ce dernier est probablement le résultat d'une cyclisation radicalaire 5-*exo*-trig. Ce résultat nous a laissé penser qu'un radical hex-5-ényle a pu être formé durant la réaction, ce qui signifie que nos conditions réactionnelles permettent alors la formation d'un radical à partir des bromures d'alkyles. Ainsi, deux radicaux sont en compétition lors de la réaction de couplage, ce qui expliquerait la formation du produit d'homocouplage. Des études mécanistiques plus approfondies permettraient de mieux rationaliser ces résultats.

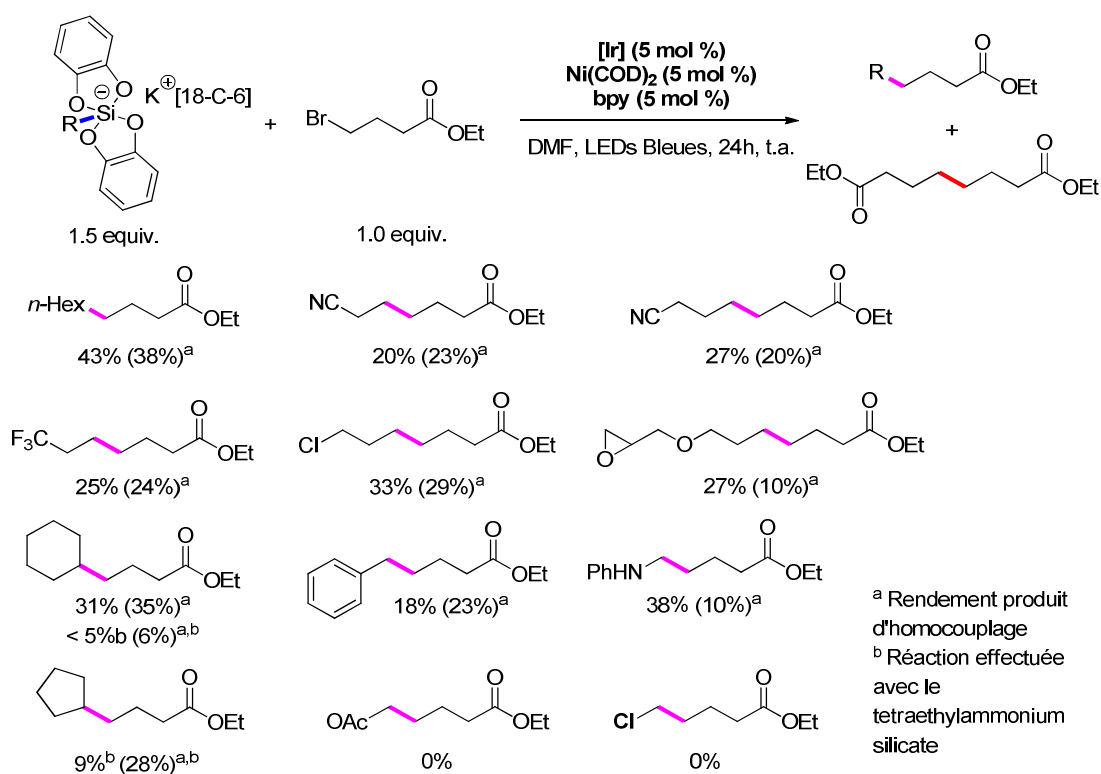


Schéma 17. Catalyse duale photoredox/nickel: couplage croisé entre des alkyles silicate et le 4-bromobutyrate d'éthyle

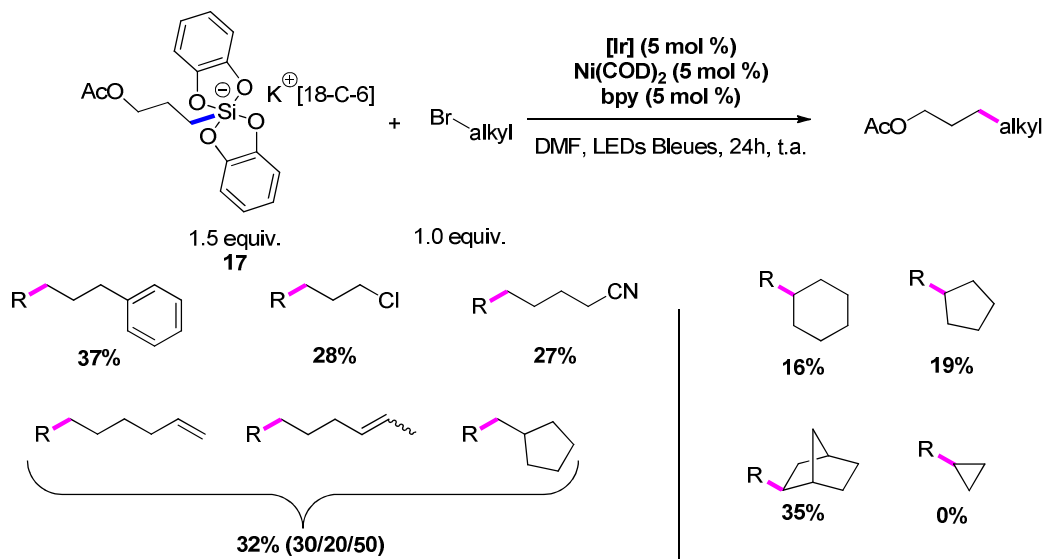


Schéma 18. Catalyse dual photoredox/nickel: couplage croisé entre l'acétoxypropyl silicate et divers bromures d'alkyles

Après avoir démontré tout le potentiel des alkyles bis-catécholato silicates pour la formation de liaisons carbone-carbone en catalyse photoredox ainsi qu'en catalyse duale photoredox/nickel, nous nous sommes tournés vers un autre système catalytique mettant aussi en jeu des transferts monoélectroniques. Une thématique développée au sein de notre laboratoire, concerne la catalyse par des métaux de transition portant des ligands non-innocents. Un ligand est considéré non-innocent lorsque le degré d'oxydation du métal, sur lequel il est complexé, ne peut être clairement défini. En particulier, le complexe bis(iminosemiquinonate) de cuivre ($\text{Cu(L}_{\text{SQ}})_2$) possède la particularité d'être un complexe sur lequel les deux ligands ont un caractère radicalaire. Chaque ligand pouvant être oxydé ou réduit, le complexe peut exister sous cinq formes différentes.²³

²³ P. Chaudhuri, C. Nazari Veani, E. Bill, E. Bothe, T. Weyhermüller, K. Wieghardt, *J. Am. Chem. Soc.*, 2001, **123**, 2213–2223.

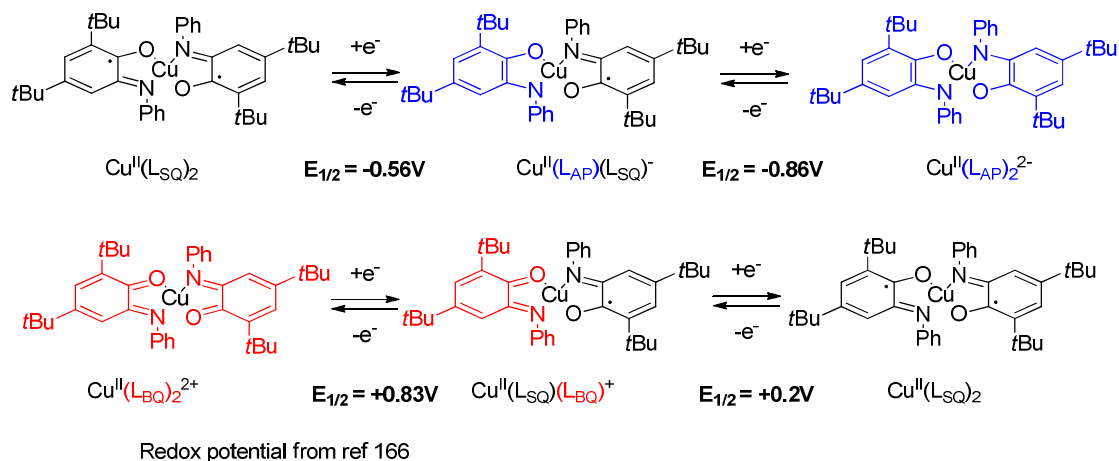


Schéma 19. Propriétés redox du complexe $\text{Cu}(\text{L}_{\text{SQ}})_2$

Des travaux réalisés au sein de notre équipe ont montré que le complexe $\text{Cu}(\text{L}_{\text{SQ}})_2$ utilisé en quantité catalytique pouvait former des radicaux $\text{CF}_3\cdot$ par réduction d'une source de CF_3 électrophile tel que le réactif d'Umemoto ou le réactif de Togni II. Ce dernier a notamment été utilisé pour former ces radicaux $\text{CF}_3\cdot$ et les engager dans des processus d'addition radicalaire sur des alcènes, des alcyne, des éthers d'énols silylés ainsi que sur des hétérocycles tels que le pyrrole ou le furane.²⁴

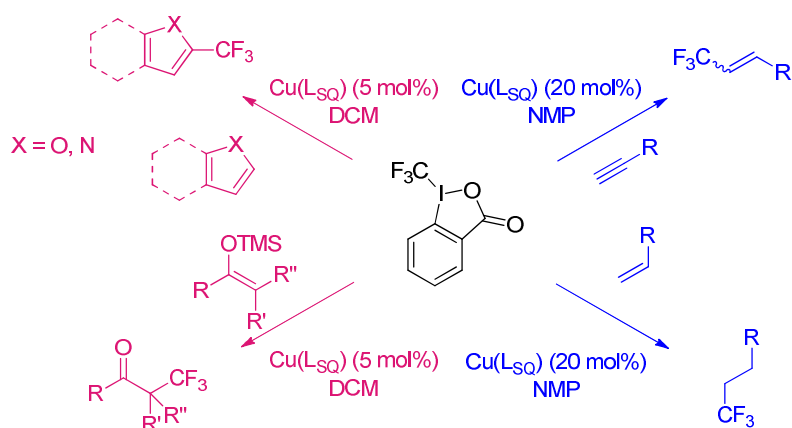


Schéma 20. Piégeage des radicaux $\text{CF}_3\cdot$ formés par réduction du réactif de Togni II avec le complexe $\text{Cu}(\text{L}_{\text{SQ}})_2$.

²⁴ J. Jacquet, S. Blanchard, E. Derat, M. Desage-El Murr and L. Fensterbank, *Chem. Sci.*, 2016, 7, 2030–2036.

Dans notre cas, nous avons tenté d'utiliser ce type de complexe pour engendrer des radicaux alkyles par oxydation des alkyles bis-catécholato silicates. Les silicates possèdent un potentiel d'oxydation relativement bas (~0.3 – 0.9V vs SCE). Par rapport à ces valeurs, le complexe $\text{Cu}(\text{L}_{\text{BQ}})_2(\text{OTf})_2$ (L_{BQ} = iminobenzoquinone) a donc été choisi (+0.83V vs SCE). Des premières expériences de piégeage par le TEMPO ont été réalisées. En conditions catalytiques ou stœchiométriques dans le DMF, de faibles rendements d'adduit benzyl-TEMPO ont été obtenus. De plus, la présence d'allylsulfone à la place du TEMPO n'entraîne aucune formation de produit d'allylation.

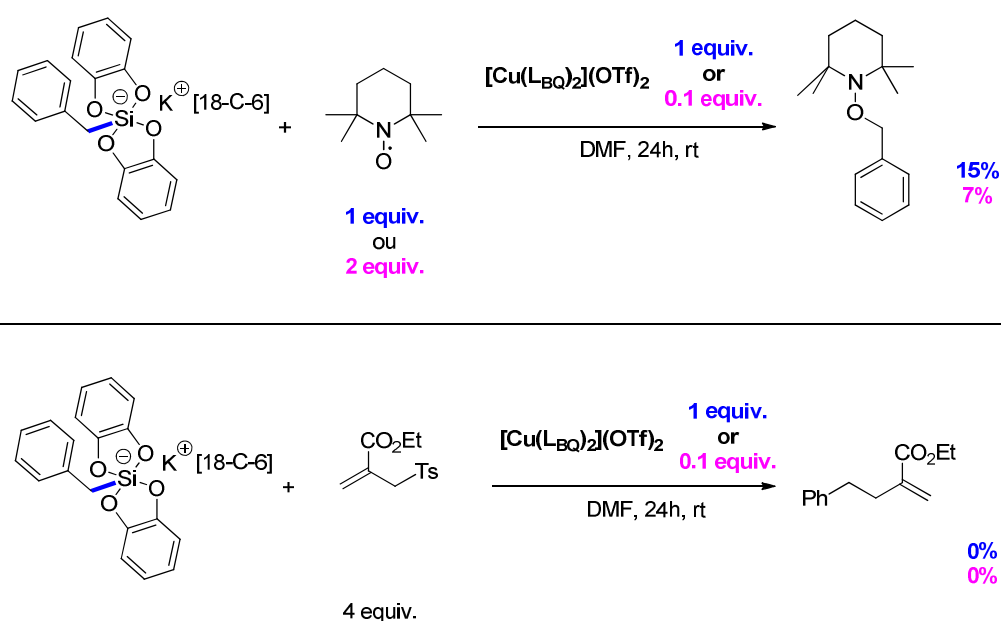


Schéma 21. Oxydation du benzylsilicate par le complexe $\text{Cu}(\text{L}_{\text{BQ}})_2(\text{OTf})_2$

Par la suite, nous avons remplacé de solvant DMF par le dichlorométhane ainsi que le précurseur radicalaire par l'anilinoéthyle silicate, étant plus facile à oxyder. En présence d'allylsulfone comme accepteur radicalaire, nous avons pu cette fois-ci observer la formation du produit d'allylation avec un rendement moyen de 48%. Après quelques étapes d'optimisation (augmentation de la charge catalytique en complexe de cuivre, de la quantité d'accepteur et de la concentration), un rendement de 66% en produit d'addition radicalaire a

pu être atteint. Même si l'optimisation et l'exploration de cette nouvelle voie d'oxydation des silicates restent encore à développer, ces résultats préliminaires sont prometteurs.

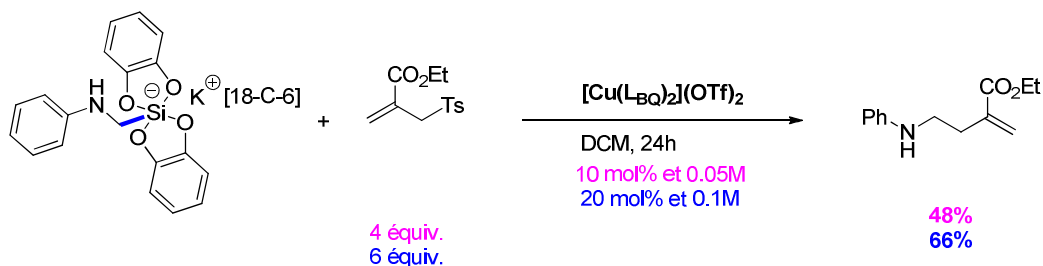


Schéma 22. Résultats préliminaires d'addition radicalaire sur l'allylsulfone

En conclusion, les travaux réalisés au cours de cette thèse se sont centrés sur la transformation de l'énergie lumineuse en énergie chimique avec la formation d'espèces radicalaires à partir de substrats organiques. Dans notre cas, nous nous sommes intéressés plus particulièrement à la formation de radicaux alkyles primaires par photooxydation d'alkyles bis-catécholato silicates. Ces espèces présentant un atome de silicium hypervalent possèdent plusieurs avantages en terme de synthèse, de stabilité mais aussi de faibles potentiel d'oxydation, ce qui en fait des précurseurs de choix pour la génération de radicaux par photooxydation. En effet, l'oxydation de ces espèces par des photocatalyseurs métalliques d'iridium ou de ruthénium photoactivés a permis de former des radicaux carbonés stabilisés ou non. Des radicaux primaires, secondaires et tertiaires ont pu être engagés dans des réactions d'addition radicalaire en conditions catalytiques. Par la suite, les études ont montré que ces radicaux pouvaient être piégés par des complexes de nickel et couplés avec des électrophiles aromatiques ou hétéroaromatiques en conditions de catalyse duale, avec de bon rendements. Afin de rendre ce type de catalyse plus éco-compatible, nous avons donc cherché à remplacer le photocatalyseur d'iridium par un organophotocatalyseur. Le 4CzIPN a démontré qu'il pouvait photooxyder les silicates avec la même efficacité que les complexes métalliques. En catalyse duale, cet organophotocatalyseur nous a permis d'obtenir des produits de couplage croisé avec des bromures aromatiques ou hétéroaromatiques mais aussi avec des bromures éthyléniques. Enfin, le couplage alkyl-alkyl en conditions de catalyse duale avec les silicates a pu être réalisé, mais malheureusement avec de faibles rendements.

Actuellement, des travaux sont à l'étude sur l'oxydation des silicates par des complexes métalliques avec des ligands non-innocents. Des résultats préliminaires ont montré que le complexe de cuivre $\text{Cu}(\text{L}_{\text{BQ}})_2(\text{OTf})_2$ en quantité catalytique peut former un radical α -aminé à partir du silicate correspondant et que ce radical peut être piégé en réaction d'allylation. L'optimisation du système permettra de développer de nouveaux systèmes catalytiques mettant en jeu les silicates comme précurseurs de radicaux carbonés.

Chapter I.
**Photoredox catalysis, an opportunity for sustainable
chemistry**

Chapter I.

Photoredox catalysis, an opportunity for sustainable chemistry

1.1 Evolution of radical chemistry

1.1.1 Introduction to radical synthesis

Radicals are chemical intermediates which display one or more atoms with an unpaired electron. The discovery of such species has been reported first by Moses Gomberg in 1900 with evidences of the formation of the triphenylmethyl radical. However, much of the chemist community did not approve the existence of radicals. During the next 50 years a growing numbers of proofs brought by Paneth,¹ Hey² and Kharasch³ allowed to support the idea of radical species. The discovery of EPR⁴ confirmed definitely their existence. Like the ionic species, radicals exist in nature and play key roles in biologic processes. Several enzymes showed radical behaviors pathways like the ribonucleotide reductase that allows the transformation of ribonucleosides to deoxyribonucleosides, essential building blocks of DNA. An equivalent of this biological reaction has been developed in radical synthesis with the Barton-McCombie reaction (Figure 1).⁵

¹ F. Paneth and W. Hofeditz, *Chem. Ber.*, 1929, **62**, 1335–1247.

² D. H. Hey and W. A. Walters, *Chem. Rev.*, 1937, **21**, 169–208.

³ For selected reports see: (a) Herbert C. Brown, M. S. Kharasch and T. H. Chao, *J. Am. Chem. Soc.*, 1940, **62**, 3435–3439. (b) M. S. Kharasch, S. S. Kane and H. C. Brown *J. Am. Chem. Soc.*, 1941, **63**, 526–528. (c) M. S. Kharasch, E. V. Jensen and W. H. Urry, *Science*, 1945, **102**, 128–128. (d) M. S. Kharasch, E. V. Jensen and W. H. Urry, *J. Am. Chem. Soc.*, 1946, **68**, 154–155

⁴ E. Zavoisky, *Fizicheskii Zhurnal*, 1945, **9**, 211–245.

⁵ L. Chenneberg and C. Ollivier, *Chimia*, 2016, **70**, 67–76.

Deoxyribonucleotides synthesis



Barton-McCombie reaction

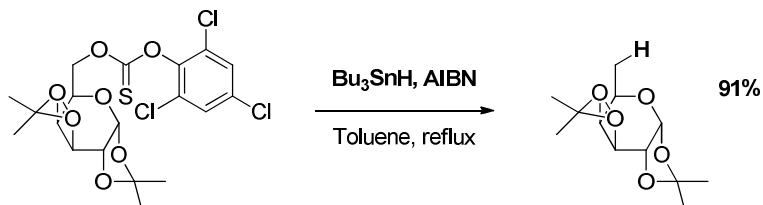


Figure 1. Bio-catalyzed dehydroxylation of alcohols

This analogous natural reaction is one of all the reactions and methodologies developed by the radical chemistry community. The Giese reaction, the Minisci reaction, atom-transfer, cascade and cyclization reactions are few examples of all the work done on this field. Despite these progresses, industrial processes involving radicals are not very common. But some examples can be mentioned like the radical polymerization or the production of phenol from oxidation of cumene. Although radicals have remained mysterious and considered as out of control by a part of the chemists, the contribution of Kochi, Curran, Giese, Hart and others⁶ demystified the radicals and turned this species as alternatives of usual anionic reactions. Indeed, contrary to organometallic reagents, radical precursors can provide highly reactive neutral radicals in smooth conditions, under air atmosphere and non-distilled solvents. In addition, radical reactions are highly chemoselective and can be performed without protected functions. Indeed, several conditions for the generation of radicals are available. Radical initiators (Et_3B , peroxides, azo compounds ...) and mediators (stannanes, silanes, thiols...) can provide radicals for chain reactions. Single electron transfers from stoichiometric metallic oxidants (manganese, cerium) or reductants (samarium, titanium, zinc, nickel) are as many alternatives for the formation of radicals.

⁶ For a comprehensive account on all aspect of radical chemistry in synthesis, see: a) C. Chatgililoglu and A Studer in *Encyclopedia of Radicals in Chemistry, Biology and Materials*, Eds. John Wiley & Sons Ltd, Chichester, 2012. (b) P. Renaud and M. P. Sibi in *Radicals in Organic Synthesis Vol.1 & 2*, Wiley-VCH, Weinheim, 2001. (c) D. P. Curran, N. A. Porter and B. Giese in *Stereochemistry of Radical Reactions*, VCH, Weinheim, 1996. (d) A. Gansäuer in *Radicals in Synthesis I & II, Topics in Current Chemistry*, Springer, Heidelberg, Vols 263 & 264, 2006.

1.1.2 Challenges in radical chemistry

Radical chemistry offers many advantages (vide supra) and promising features compared to anionic reactions. However, it suffers of several drawbacks which limit their use in synthesis. Because the reactions are performed in diluted conditions, the scale up is quite complicated. Some of the processes also require an excess of radical acceptor. But, the most problematic aspects are the use of explosive initiators (peroxides, azo compounds) or toxic mediators like the tin (IV) derivatives which are also difficult to remove from the product. In this context, solutions have been proposed to escape from “the tyranny of tin” and to offer the opportunity of using sustainable methods.

In order to progressively substitute the use of tin reagents, methodologies involving only catalytic amounts of these reagents or tin-supported surfaces have been reported.⁷ Processes employing stoichiometric mediators such as silanes, phosphines or thiols are also potential alternatives. Organoboranes, as substrates or radical initiators for chain-reactions, showed promising results as well.^{6b,8} Less toxic metals responsible of one-electron transfers were also considered as a possible solution. However, methodologies involving metal complexes based on iron, copper, manganese, titanium, samarium... require excess amounts. Unfortunately, in terms of sustainability and eco-compatibility, it is important to develop alternatives even more efficient. At the end of the 70's, some pioneering works⁹ mentioned the generation of radicals thanks to a single electron transfer (SET) mediated by a photoactivated metal complex.

1.2 The photoredox catalysis as an alternative

The radical chemistry allowed chemists to develop a wide range of processes for the carbon-carbon bond formation. Many efforts, to avoid the use of toxic tin reagents and to find others alternatives have been done so far, but many reactions are still performed under these conditions. Since the end of the 2000s, photoredox catalysis has emerged as a powerful and versatile eco-compatible approach for the generation of radicals.

⁷ A. Studer and S. Amrein, *Synthesis*, 2002, **7**, 835–849.

⁸ C. Ollivier and P. Renaud, *Chem. Rev.*, 2001, **101**, 3415–3434.

⁹ D. M. Hedstrand, W. H. Kruizinga and R. M. Kellogg, *Tetrahedron Lett.*, 1978, **19**, 1255–1258.

1.2.1 Nature as a source of inspiration

The evolution has allowed living organism to develop sustainable and highly sophisticated process. Among them, the photosynthesis of plants has early interested scientists. The chlorophyll present in plant cells absorbs the sunlight in the visible range and initiates the transformation of CO₂ and water to saccharides and oxygen. This natural synthetic process highlights the fundamental and efficient conversion of energy from sunlight into chemical energy.

Taking advantage of this process, increasing efforts from the radical chemistry community has been realized to develop new methodologies using the visible light as a promotor of redox reactions for the generation of radicals. Visible-light photoredox catalysis has emerged as a powerful methodology for radical formation in terms of selectivity and sustainability. Since the pioneering work on this field, more and more groups have incremented the photoredox catalysis as a part of their research and the number of publications on this topic demonstrates its growing popularity (Figure 2). Inspired by the photoredox process of natural photosynthesis, chemists were interested on the development of photocatalysts absorbing light in the visible region and with a large range of potential values to perform efficient redox transformations. The first man-made photocatalyst mainly reported and still frequently used is the photoactive complex Ru(bpy)₃Cl₂. First reported as a photoredox catalyst for organic synthetic purposes by Kellog,⁹ Pac¹⁰ and Deronzier,¹¹ this complex has been essentially used in inorganic chemistry for devices applications¹² or transformation of small molecules¹³ (CO₂, H₂O). This is only from 2008 and the advances of

¹⁰ C. Pac, M. Ihama, M. Yasuda, Y. Miyauchi and H. Sakurai, *J. Am. Chem. Soc.*, 1981, **103**, 6495–6497.

¹¹ H. Cano-Yelo and A. Deronzier, *Tetrahedron Lett.*, 1984, **25**, 5517–5520.

¹² For reviews on the use of Ru(bpy)₂²⁺ in photoredox processes: (a) S. Campagna, F. Puntoriero, F. Nastasi, G. Bergamini, V. Balzani, *Top. Curr.Chem.*, 2007, **280**, 117. (b) K. Kalyanasundaram, *Coord. Chem. Rev.*, 1982, **46**, 159–244. (c) A. Juris, V. Balzani, F. Barigelletti, S. Campagna, P. Belser and A. von Zelewsky, *Coord. Chem. Rev.*, 1988, **84**, 85–277. (d) F. Teplý, *Collect. Czechoslov. Chem. Commun.*, 2011, **76**, 859–917.

¹³ (a) K. Kalyanasundaram, J. Kiwi and M. Grätzel, *Helv. Chim. Acta*, 1978, **61**, 2720–2730. (b) J. Kiwi and M. Graetzel, *J. Am. Chem. Soc.*, 1979, **101**, 7214–7217. (c) J. Hawecker, J.-M. Lehn and R. Ziessel, *J. Chem. Soc. Chem. Commun.*, 1985, 56–58. (d) K. Kalyanasundaram and M. Grätzel, *Coord. Chem. Rev.*, 1998, **177**, 347–414.

MacMillan,¹⁴ Yoon,¹⁵ and Stephenson,¹⁶ that organic photoredox catalysis has definitely taken off.

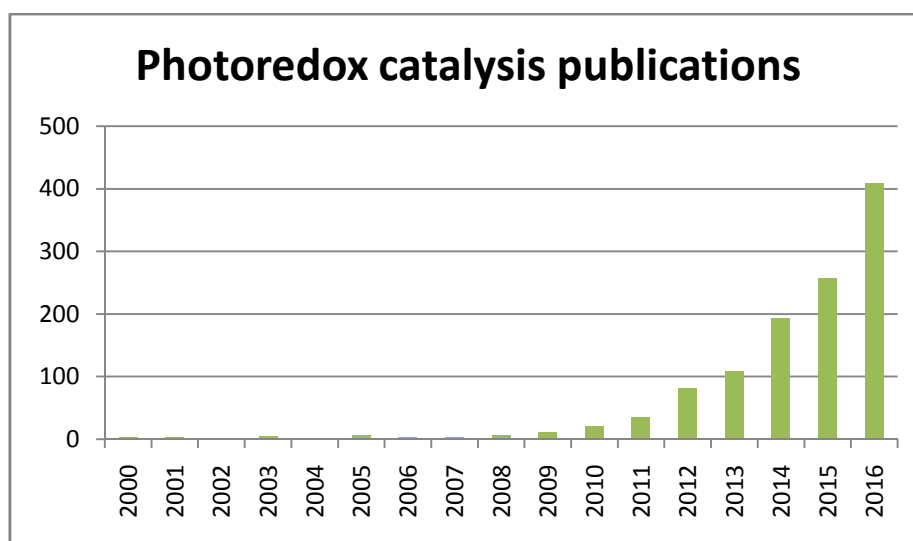


Figure 2. Number of publications on photoredox catalysis since 2000

1.2.2 Artificial redox photocatalysts

The photosynthesis led to the development of catalytic processes involving chromophores as light harvesters to promote electron transfers for photoelectrochemical cells, photocatalytic water splitting systems or photobioreactors. In this context, chemists tuned photocatalysts which could act as chlorophyll. The complex $\text{Ru}(\text{bpy})_3\text{Cl}_2$ first synthesized by Burstall¹⁷ in 1936 has shown photophysical and redox properties to perform single electron processes under visible light activation. Thus, many efforts have been done to widen the range of transition metal-based photocatalysts. In order to get closer to the principles of green chemistry, organic dyes have also attracted interest. In terms of efficiency, a valuable photocatalyst has to absorb the visible light, get fitting redox properties and a long lifetime at the excited state to enable electron transfers. Several polypyridyl complexes of metal from the fourth to sixth periods showed these properties. Most of them are ruthenium,¹² rhenium¹⁸ or

¹⁴ D. A. Nicewicz and D. W. C. MacMillan, *Science*, 2008, **322**, 77–80.

¹⁵ M. A. Ischay, M. E. Anzovino, J. Du and T. P. Yoon, *J. Am. Chem. Soc.*, 2008, **130**, 12886–12887.

¹⁶ J. M. R. Narayanam, J. W. Tucker and C. R. J. Stephenson, *J. Am. Chem. Soc.*, 2009, **131**, 8756–8757.

¹⁷ F. H. Burstall, *J. Chem. Soc.*, 1936, 173-175.

¹⁸ S. Campagna, F. Puntoriero, F. Nastasi, G. Bergamini, and V. Balzani, *Top. Curr.Chem.*, 2007, **281**, 45.

iridium¹⁹ based complexes (**Scheme 1**) but some gold,²⁰ copper,²¹ chromium²² or iron²³ complexes, are also reported. Besides the organometallic complexes, organic dyes are also good candidates for artificial photosynthesis processes (**Scheme 1**).

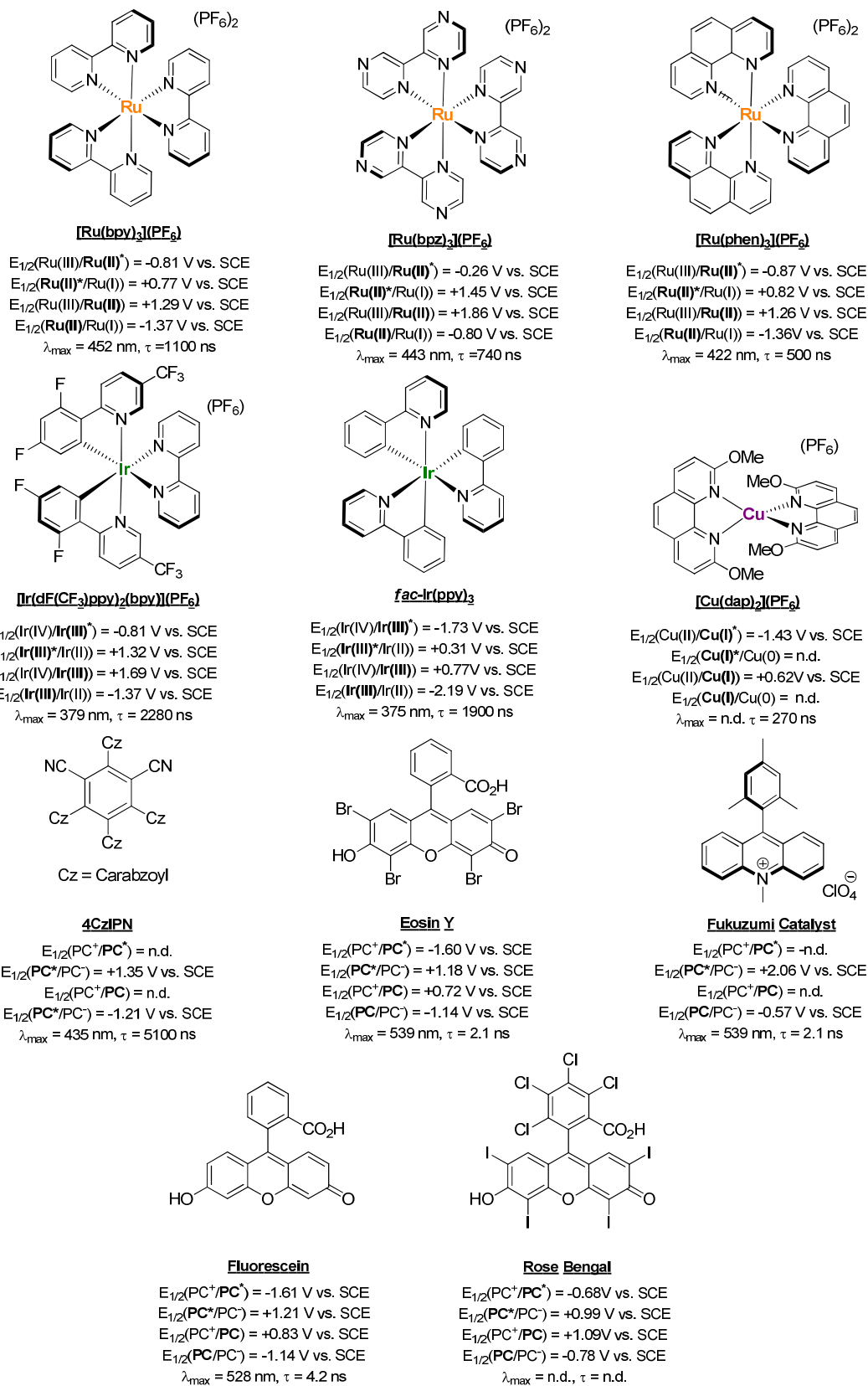
¹⁹ (a) R. D. Costa, E. Ortí, H. J. Bolink, F. Monti, G. Accorsi and N. Armaroli, *Angew. Chem. Int. Ed.*, 2012, **51**, 8178–8211. (b) Campagna, F Puntoriero, F Nastasi, G. Bergamini and V. Balzani, *Top. Curr.Chem.*, 2007, **281**, 143.

²⁰ T. McCallum, S. Rohe and L. Barriault, *Synlett*, 2017, **13**, 289–305.

²¹ S. Campagna, F Puntoriero, F Nastasi, G. Bergamini and V. Balzani, *Top. Curr.Chem.*, 2007, **280**, 69.

²² (a) N. A. P. Kane-Maguire, R. C. Kerr and J. R. Walters, *Inorganica Chim. Acta*, 1979, **33**, L163–L165. (b) D. Pagliero and G. A. Argüello, *J. Photochem. Photobiol. Chem.*, 2001, **138**, 207–211.

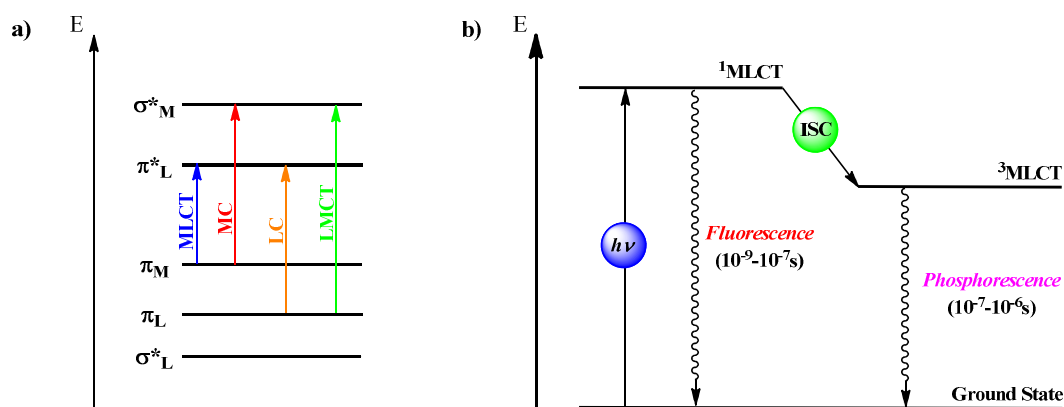
²³ J. Zhang, D. Campolo, F Dumur, X. Piao, J.-P. Fouassier, D. Gimes, J. Lalevée, *J. Polym. Science, Polym. Chem.*, 2016, **54**, 2247–2253.



Scheme 1. Examples of photocatalysts

1.2.2.1 Photophysical properties

The mainly used metal-based photocatalysts are the ruthenium and iridium complexes due to their photophysical properties and the range of redox potential accessible. Considering the photophysical properties of such complexes, the UV/visible absorption spectrum displays four kinds of absorption bands. The LC (Ligand-Centered) transition, the MC (Metal-Centered) transition or d-d transition, the MLCT (Metal-to-Ligand Charge Transfer) transition and the LMCT (Ligand-to-Metal Charge Transfer) transition (**Scheme 2 a**). For example, an electronic absorption spectrum of $[\text{Ru}(\text{bpy})_3](\text{PF}_6)_2$ in ethanol is mentioned in **Figure 3** and showed four bands (LC at 285nm, MC at 322 and 344 nm, and two MLCT at 240 and 450 nm)



Scheme 2. a) Simplified molecular orbital diagram for Ruthenium and Iridium photocatalysts. b) Simplified energy diagram of absorbing and emitting processes.

This MLCT transition is actually the most important one since the absorption is in the visible-light region spectra and it allows to reach a $^3\text{MLCT}$ after an Inter-System Crossing (ISC) thanks to a strong spin-orbit coupling, usually observed with the heavy metal atom (**Scheme 2 b**). The consequence is a longer luminescence lifetime (10^{-7} - 10^{-6} s)^{12a,19b} compared to 3d metal complexes and so the possibility of electrons transfers.

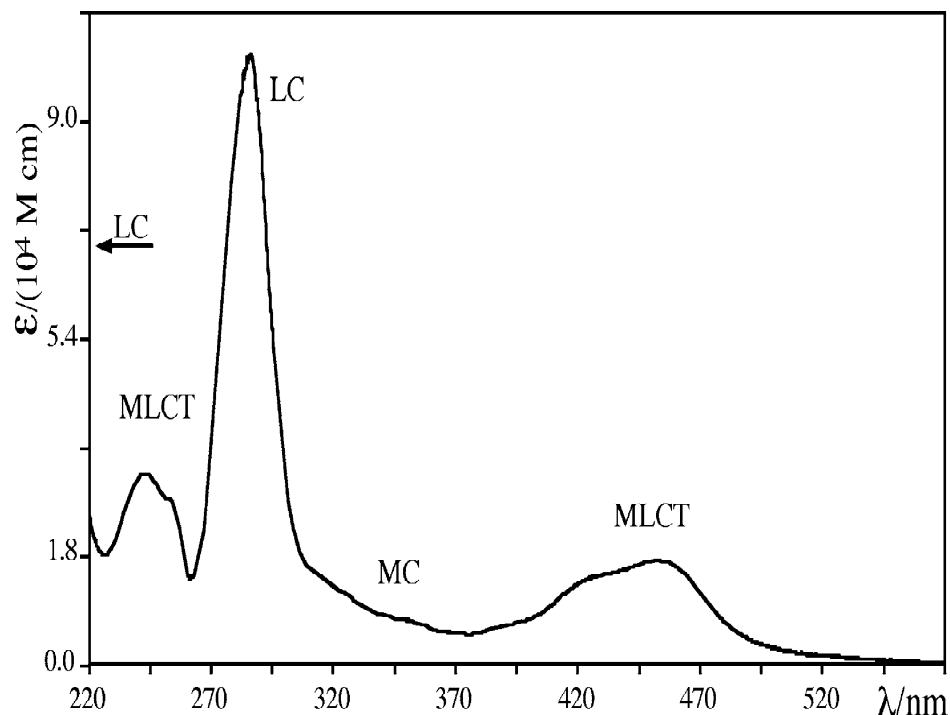


Figure 3. Electronic absorption spectrum of $[\text{Ru}(\text{bpy})_3](\text{PF}_6)_2$ in EtOH.

Constantly trying to evolve toward a greener chemistry, many photoredox processes involve organic dyes as photocatalyst such as fluorescein, Eosin Y or rose bengal.²⁴ As organic molecules, the strongest light absorption results in the promotion of an electron of a π orbital to a π^* orbital. Because of the lack of heavy atoms and so the inefficient intersystem crossover, the light emission is mainly fluorescence. The consequence for these photocatalysts is a very short lifetime of the S_1 excited state (2 to 20 ns for most of the organic photocatalysts). The envisaged electron transfers must be at least as fast as the deexcitation of the chromophore. Recent work on the development of OLEDs has shown new perspective in terms of organic photocatalysts design.²⁵ Thanks to a short gap between singlet and triplet state and efficient spin conversion processes, a series of tetracarbazolyl dicyanobenzene with

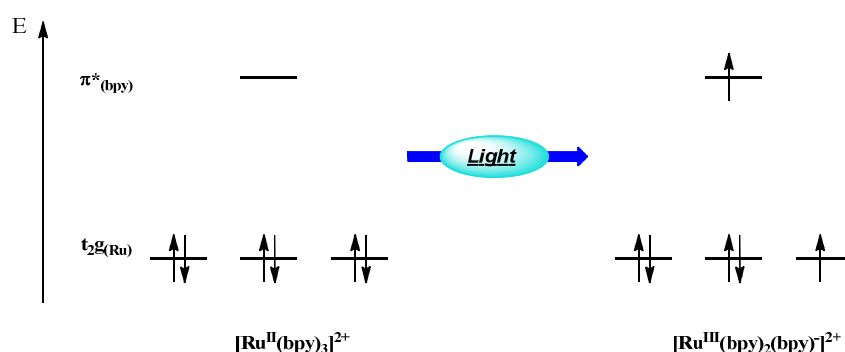
²⁴ For reviews on the use of organic photocatalysts: (a) S. Fukuzumi and K. Ohkubo, *Org. Biomol. Chem.*, 2014, **12**, 6059–6071. (b) N. A. Romero and D. A. Nicewicz, *Chem. Rev.*, 2016, **116**, 10075–10166. (c) M. Neumann, S. Fldner, B. König and K. Zeitler, *Angew. Chem. Int. Ed.*, 2011, **50**, 951–954.

²⁵ (a) M.A Baldo, S. Lamabsky, P. E. Burrows, M. E. Thompson and S. R. Forrest, *Appl. Phys. Lett.*, 1999, **75**, 4–6. (b) A. Endo, K. Sato, K. Yoshimura, T. Kai, A. Kawada, H. Miyazaki and C. Adachi, *Appl. Phys. Lett.*, 2011, **98**, 083302. (c) S. Y. Lee, T. Yasuda, H. Nomura and C. Adachi, *Appl. Phys. Lett.*, 2012, **101**, 093306. (e) H Uoyama, K. Goushi, K. Shizu, H. Nomura and C. Adachi, *Nature*, 2012, **492**, 234–238.

excited state lifetimes of few micro-seconds have shown optimal features for photoredox catalyzed processes.²⁶

1.2.2.2 Molecular orbital approach and redox potentials

In this part, we will focus on the description of metal-based photocatalysts and especially on the $\text{Ru}(\text{bpy})_3^{2+}$ which is the most studied. However, the mentioned statements are applicable to homo- and heteroleptic iridium photocatalysts. As previously detailed, ruthenium and iridium photocatalysts reach a triplet state ($^3\text{MLCT}$) after visible-light absorption. About the $\text{Ru}^{\text{II}}(\text{bpy})_3^{2+}$, it corresponds to the promotion of an electron from the $t_{2g}(\text{Ru})$ orbitals of the metal to a π^* orbital of the ligand. The excited complex can be formally written as “ $[\text{Ru}^{\text{III}}(\text{bpy})_2(\text{bpy})]^{2+}$ ”, equivalent to $[\text{Ru}^{\text{II}}(\text{bpy})_3^{2+}]^*$ where respectively the metal becomes oxidant and a ligand bpy reductant (**Scheme 3**).

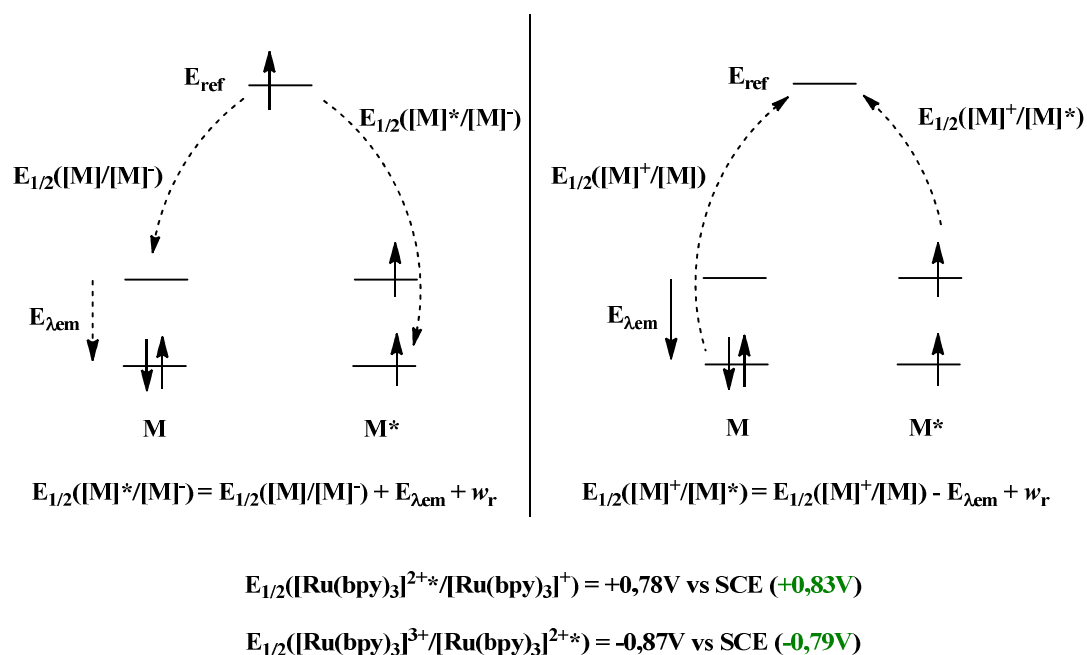


Scheme 3. Simplified orbital diagram of $\text{Ru}(\text{bpy})_3^{2+}$ during light absorption

The photoexcited complex $[\mathbf{M}]$ can then oxidize or reduce a substrate by a SET giving the opportunity to generate radicals. In order to have an idea on the tolerant substrates for the SET, the redox potentials of photocatalysts at the excited-state have to be determined. From electrochemical and fluorescence data, a qualitative estimation of the excited-state redox potentials can be given. The minimum difference of energy between the ground state of the catalyst and its excited state corresponds to the wavelength of the emission maximum $E_{\lambda\text{em}}$. Therefore, the required energy to reduce the photocatalyst in the excited state $E([\mathbf{M}]^*/[\mathbf{M}])$ equals the sum of the required energy to reduce the photocatalyst in the ground state

²⁶ J. Luo and J. Zhang, *ACS Catal.*, 2016, **6**, 873–877.

$E([M]/[M^-])$ and $E_{\lambda_{em}}$ (Scheme 4. left). Also, the energy necessary to oxidize the photocatalyst at the excited-state $E([M]^+/[M^*])$ equals the difference between the energy necessary to oxidize the photocatalyst in the ground state $E([M]^+/[M])$ and $E_{\lambda_{em}}$ (Scheme 4. right). However, an electrostatic work term w_r , describing the charge generation and separation within the electron-transfer complex, must be taken in account but is difficult to estimate. Thus the calculated potentials are slightly over- or underrated, but experimental values can be measured²⁷ by phase-modulated voltammetry, showing a good match with the calculated ones. Fine tuning of the redox potential can be realized changing the ligand (bipyridine, bipyrazine, phenanthroline...) or modifying the metal. In this context, heteroleptic iridium complexes are particularly interesting due to their two ligands type (cyclometalating ligand and bidentate ligand) which can be both modified.

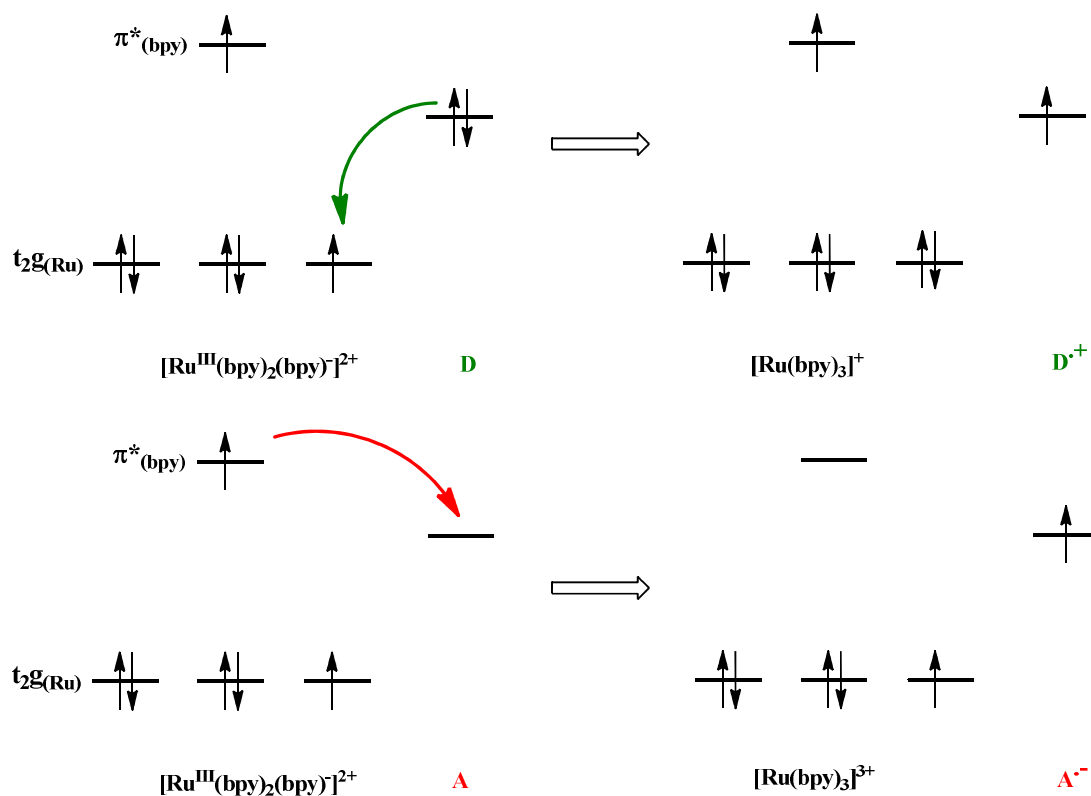


Scheme 4. Calculation of the redox potential of photocatalysts at the excited-state and comparison with the measured values.

Therefore, the photocatalyst excited state may pick up or give out an electron to a substrate if the redox potentials match. In terms of orbital, if the HOMO of a donor **D** is between the t_{2g} and π^* orbitals of the $Ru(bpy)_3^{+2}$, a SET can happen giving the oxidized

²⁷ W. E. Jones and M. A. Fox, *J. Phys. Chem.*, 1994, **98**, 5095–5099.

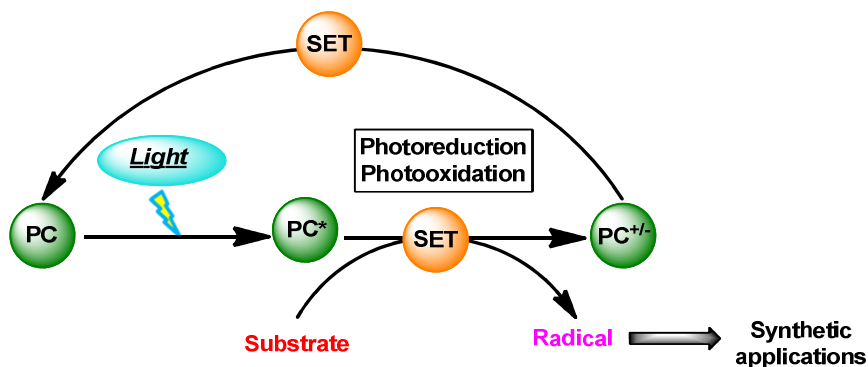
substrate $\mathbf{D}^{\bullet+}$ and $\text{Ru}(\text{bpy})_3^{3+}$ (**Scheme 5**). In the case of an acceptor \mathbf{A} , if the LUMO is in the same energy range, the electron transfer would form the radical anion $\mathbf{A}^{\bullet-}$ and $\text{Ru}(\text{bpy})_3^{3+}$



Scheme 5. SET between excited $\text{Ru}(\text{bpy})_3^{2+}$ and donor or acceptor.

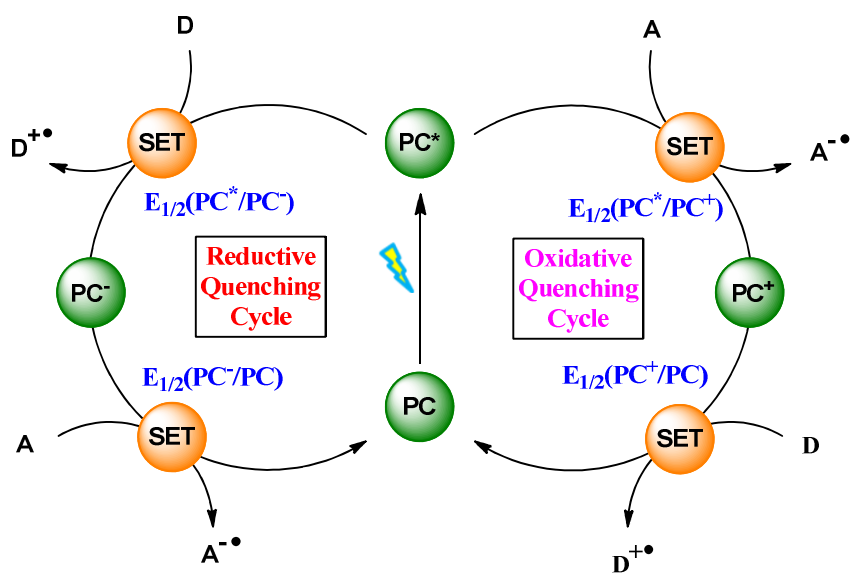
1.2.3 Principle of photoredox catalysis

As we have seen above, photoexcited chromophores (PC^*) can transfer one electron to substrates providing radicals which can be involved in radical processes. However, to render the overall process catalytic, the photocatalyst ($\text{PC}^{+/}$) should undergo another SET with an intermediate or an additive. When the substrate is reduced by the photocatalyst, the process would be named **Photoreduction** and **Photooxidation** if the substrate is oxidized (**Scheme 6**).



Scheme 6. General catalytic process of photoredox catalysis

More precisely, after light absorption the excited PC^* reacts with an electron donor **D** so called a “reductive quencher” leading to the reduced photocatalyst PC^- . The altered photocatalyst transfers its excess of electron to an acceptor **A**, regenerating the starting photocatalyst to end the “**reductive quenching cycle**”. The “**oxidative quenching cycle**” is the reaction of PC^* with an acceptor **A**, which acts as an oxidative quencher. The oxidized photocatalyst PC^+ then reacts with a donor **D** and regenerates PC (**Scheme 7**).



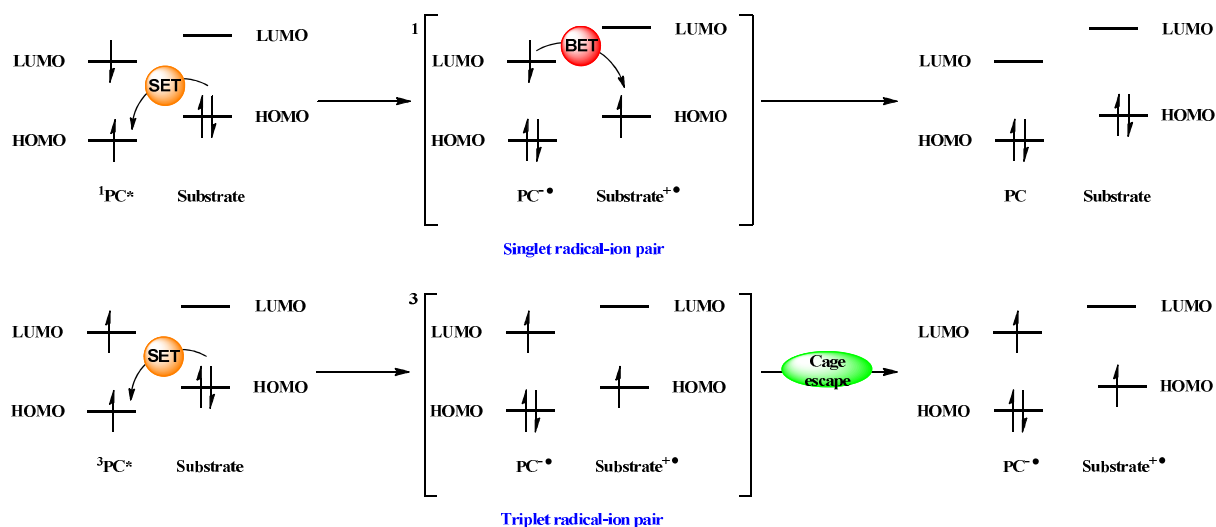
Scheme 7. Reductive and oxidative quenching cycles.

The radicals engaged in synthetic applications can be generated by photoreduction or photooxidation. Concerning the photoreduction, a substrate (or acceptor in this case) would be directly reduced by the photoexcited catalyst if the redox potentials fit well. But sometimes,

the potential of the light excited photocatalyst is not enough high to reduce the substrate. A sacrificial electron donor (amines, Hantzsch ester...) would react first with PC^* to generate PC^- and provide a stronger reductant capable to reduce the substrate. In photooxidation, the photoexcited catalyst may directly oxidize a radical precursor (or donor in this case). As mentioned previously, if the PC^* is not enough oxidizing, addition of a sacrificial electron acceptor (oxygen, methylviologen, persulfate agent...) would provide the much stronger oxidant PC^+ . The oxidation of the substrate then should give the radical.

After oxidation or reduction of the substrate by the photocatalyst, the formed radical-ion pairs may undergo back electron transfer (BET) giving back both reactants. After reductive quenching, the spin multiplicity of the system should remain unchanged. If the electron transfer happens when the photocatalyst is in a singlet excited state, the radical-ion pair is also in a singlet state. In this case, the BET results in an overall singlet state without restraint. However, regarding a triplet state, the spin multiplicity must change during the BET which is less favored. Therefore, free radicals are more likely to be formed in the reaction once the photocatalyst is in a triplet excited state (**Scheme 8**). Metal complexes reach easily the triplet excited state thanks to the heavy metal atom which increases the spin-orbit coupling and so the inter-system crossover (ISC). For organic molecules, the most populated excited state is most of the times the singlet state which limits their efficiency in photoredox catalysis. Despite this property, some organic dyes have already attested to be used as photocatalysts in redox processes.²⁸ At the moment, no explanation can rationalize these observations inconsistent with the theory.

²⁸ (a) D. Ravelli and M Fagnoni, *ChemCatChem*, 2012, **4**, 169–171 (b) N. A. Romero and D. A. Nicewicz, *Chem. Rev.*, 2016, **116**, 10075–10166.



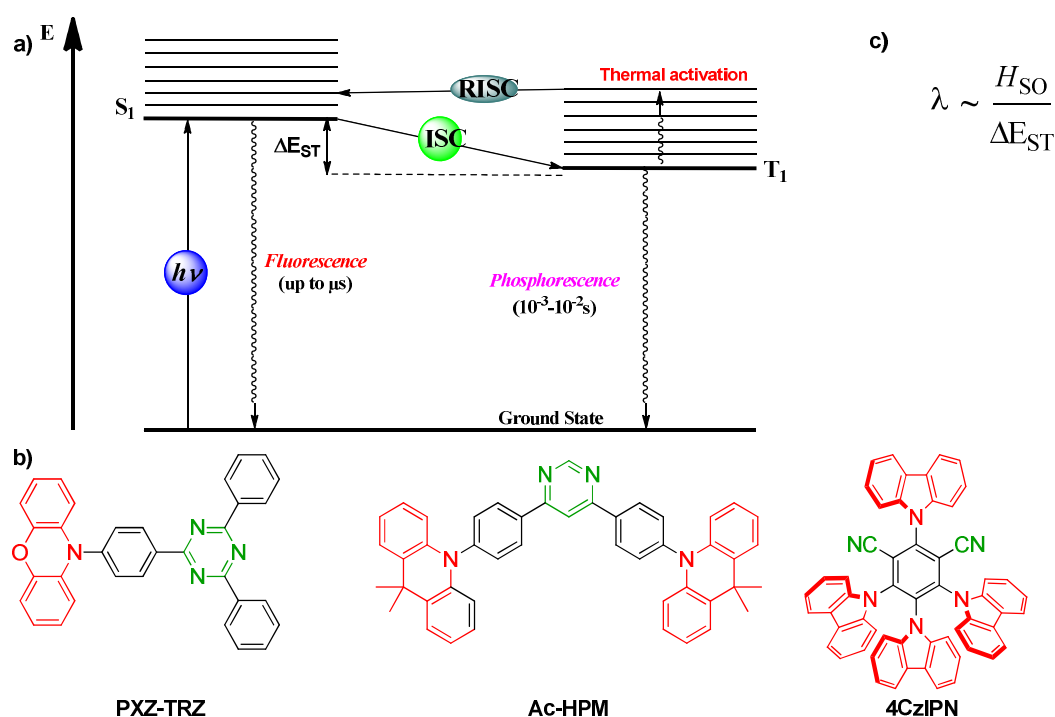
Scheme 8. Cage escape and BET in singlet and triplet ion pairs for photooxidation of a substrate

Since the triplet excited state is more likely to provide radical processes, organic dyes reaching efficiently this state would be more promising for photoredox catalysis. Organic Thermally Activated Delayed Fluorescence (TADF) materials have begun to be exploited in this field. As mentioned in the name category of these molecules, they are chromophores with a very long luminescence lifetime compared to other common organic molecules. Usually, organic dyes or complexes reaching a triplet state after ISC lose their excess of energy by phosphorescence or vibrational relaxation. In the case of TADF materials, a reverse intersystem crossover is possible (RISC) thanks to the thermal activation by the surrounding environment (**Scheme 9 a**). This pathway is possible only if the energy difference between S_1 and T_1 (ΔE_{ST}) is enough low and particularly in the range of the thermal energy. Thanks to a quantum mechanical analysis, Adachi^{25b} found that the reduction in the overlap between the HOMO and the LUMO results in a small ΔE_{ST} . In this context, molecules displaying a donor(red)-acceptor(green) scaffold are unavoidable candidates such as phenoxazine–triphenyltriazine (PXZ-TRZ),²⁹ 4,6-bis[4-(9,9-dimethyl-9,10-dihydroacridine)-phenyl] pyrimidine (Ac-HMP)³⁰ or 4CzIPN^{25e} (**Scheme 9 b**).

²⁹ H. Tanaka, K. Shizu, H. Miyazaki and C. Adachi, *Chem. Commun.*, 2012, **48**, 11392–11394.

³⁰ R. Komatsu, H. Sasabe, Y. Seino, K. Nakao and J. Kido, *J. Mater. Chem. C*, 2016, **4**, 2274–2278.

For TADF materials, the kinetics values of ISC, RISC and fluorescence processes are crucial to obtain the enhancement of luminescence lifetime. The fluorescence process is usually in the range of nanoseconds. In order to avoid this direct desexcitation pathway, the ISC kinetics must be in the range of the fluorescence. Also, the luminescence lifetime would be increased if the RISC is slower than the ISC. Actually, for this kind of molecules, the ISC process is rather efficient. The spin conversion efficiency is correlated to the first-order mixing coefficient between singlet and triplet states (λ). This parameter is inversely proportional to ΔE_{ST} and proportional to H_{SO} which is the spin-orbit interaction (**Scheme 9 c**).³¹ Because the ΔE_{ST} is low, the overall spin-orbit coupling is important. In consequence, TADF materials can exist in their triplet excited state and perform electron transfers. Particularly, the 4CzIPN proved to be an efficient photocatalyst in photoredox/nickel dual catalysis.^{26,32}



Scheme 9. a) Energy diagram for TADF materials. b) Examples of Organic Donor(red)-Acceptor(green) TADF materials. c) First-order spin-orbit coupling parameter

³¹ N. J. Turro, *Modern Molecular Photochemistry*, 98–100 (Benjamin Cummings, 1978)

³² (a) C. L  v  que, L. Chenneberg, V. Corc  , C. Ollivier and L. Fensterbank, *Chem Commun*, 2016, **52**, 9877–9880. (b) B. A. Vara, M. Jouffroy and G. A. Molander, *Chem Sci*, 2017, **8**, 530–535. (c) E. E. Stache, T. Rovis and A. G. Doyle, *Angew. Chem. Int. Ed.*, 2017, **56**, 3679–3683.

1.2.4 Formation of carbon centered radicals

In terms of synthetic interests, the photoredox catalysis found opportunities to generate various types of radicals by photoreduction or photooxidation of different chemical functions. Radicals centered on carbon, nitrogen,³³ sulphur³⁴ or phosphorus³⁵ can be obtained by photoredox catalysis and engaged in the formation of carbon carbon bonds or heteroatom carbon bonds. The wide diversity of carbon-centered radicals generated (aryl, alkenyl, alkyl) makes this method of great interest. Thus, many works on the generation by photocatalysis of such intermediates have been realized, starting with the formation of aryl radicals.

1.2.4.1 Formation of aryl radicals by photoreduction

The pioneering example developed by Deronzier was the reduction of arenediazonium salts with Ru(bpy)₃Cl₂ as photocatalyst. The excited ruthenium complex enables the formation of an aryl radical by photoreduction of the diazonium salt to perform a Pschorr type reaction (**Scheme 10 a**)).³⁶ More recently, König extended this catalytic process to intermolecular Meerwein type arylation reactions with Eosin Y as photocatalyst (**Scheme 10 b**)).³⁷ Aryl radicals were further obtained by photoreduction of sulfonium³⁸ or iodonium³⁹ salts and engaged in intermolecular radical allylation reactions. Although aryl radicals are obtained efficiently, alkyl radicals are more of interest for the formation of molecular scaffolds.

³³ L. J. Allen, P. J. Cabrera, M. Lee and M. S. Sanford, *J. Am. Chem. Soc.*, 2014, **136**, 5607–5610. (b) Q. Qin and S. Yu, *Org. Lett.*, 2014, **16**, 3504–3507. (c) W. Greulich, C. G. Daniliuc and A. Studer, *Org. Lett.*, 2015, **17**, 254–257. (d) X.-Q. Hu, J.-R. Chen, Q. Wei, F.-L. Liu, Q.-H. Deng, A. M. Beauchemin and W.-J. Xiao, *Angew. Chem., Int. Ed.*, 2014, **53**, 12163–12167.

³⁴ (a) E. L. Tyson, M. S. Ament and T. P. Yoon, *J. Org. Chem.*, 2013, **78**, 2046–2050 (b) P.D. Morse and D. A. Nicewicz, *Chem. Sci.*, 2015, **6**, 270–274. (c) J.-G. Sun, H. Yang, P. Li and B. Zhang, *Org. Lett.*, 2016, **18**, 5114–5117.

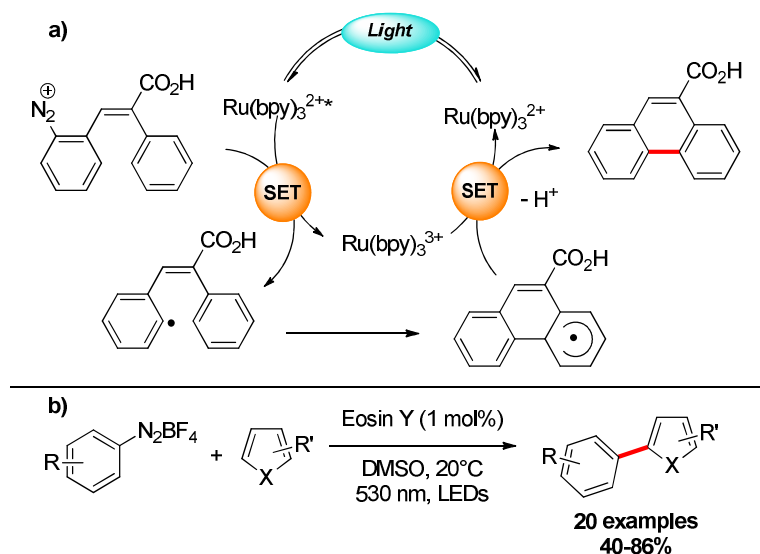
³⁵ (a) W.-J. Yoo and Shu Kobayashi, *Green Chem.*, 2013, **15**, 1844–1848. (b) V. Quint, F. Morlet-Savary, J.-F. Lohier, Jacques Lalevée, A.-C. Gaumont and S. Lakhdar, *J. Am. Chem. Soc.* 2016, **138**, 7436 – 7441. (c) M.-J. Bu, Guo-ping Lu and Chun Cai, *Catal. Sci. Technol.*, 2016, **6**, 413–416. (d) K. Luo, Y.-Z. Chen, W.-C. Yang, J. Zhu and L. Wu, *Org. Lett.*, 2016, **18**, 452–455.

³⁶ (a) H. Cano-Yelo and A. Deronzier, *J. Chem. Soc. Perkin Trans. 2*, 1984, 1093–1098. (b) H. Cano-Yelo and A. Deronzier, *J. Photochem.*, 1987, **37**, 315–321.

³⁷ (a) P. Schroll, D. P. Hari, B. König, *ChemistryOpen*, 2012, **1**, 130–133. (b) D. P. Hari, P. Schroll, B. König, *J. Am. Chem. Soc.*, 2012, **134**, 2958–2961.

³⁸ S. Donck, A. Baroudi, L. Fensterbank, J.-P. Goddard, C. Ollivier, *Adv. Synth. Catal.*, 2013, **355**, 1477–1482.

³⁹ A. Baralle, L. Fensterbank, J.-P. Goddard, C. Ollivier, *Chem. Eur. J.* 2013, **19**, 10809–10813.



Scheme 10. a) Photocatalyzed Pschorr reaction. b) Photocatalyzed Meerwein arylation

1.2.4.2 Photoreductive processes for the generation of alkyl radicals

- **Reduction of alkyl halides**

Halides are substrates of choice for reduction processes to generate alkyl radicals. Fukuzumi⁴⁰ was the first to report the photoreduction of alkyl halides. Recently, inspired by this work, MacMillan¹⁴ managed to merge photoredox catalysis and organocatalysis, and to perform enantioselective α -alkylation of aldehydes with bromoalkanes as radical precursors. In the presence of a chiral imidazolidinone, an enamine is formed. Reduction of the bromoalkane by $[\text{Ru}(\text{bpy})_3^+]$ leads to an alkyl radical which adds to the enamine double bond. The resulting α -amino radical is then oxidized by $[\text{Ru}(\text{bpy})_3^{2+}]^*$, generating an iminium intermediate which after hydrolysis liberates the α -alkylated aldehyde (**Scheme 11**). This methodology was also extended to the reduction of trifluoroiodomethane⁴¹ and benzyl bromide⁴² with iridium photocatalysts.

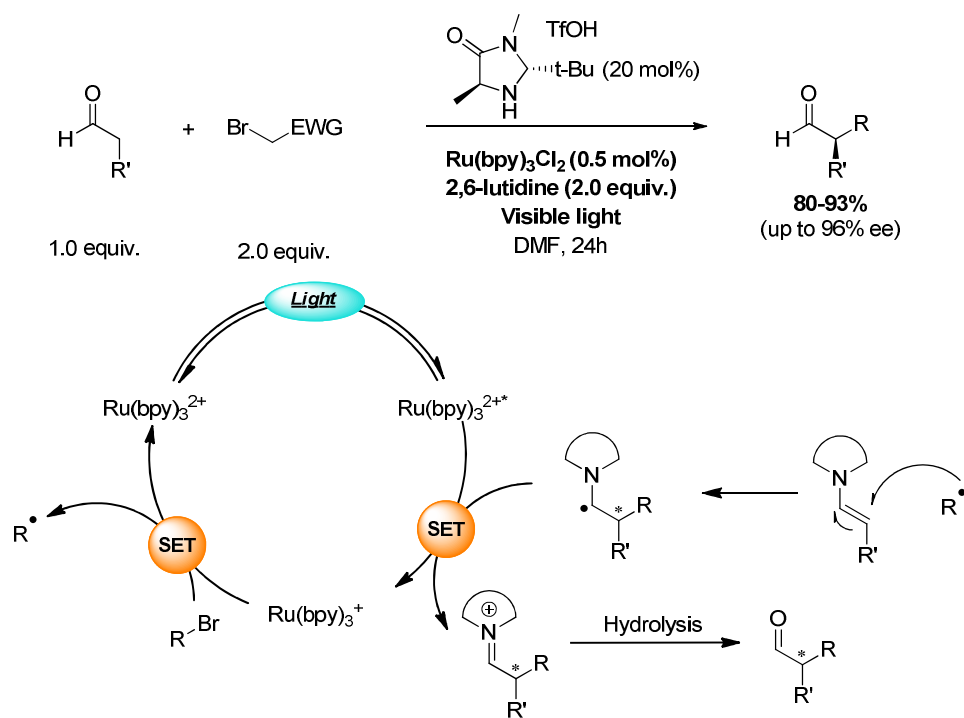
In this field, Stephenson reported the direct reduction of several chloro, bromo and iodo alkanes involving $[\text{Ru}(\text{bpy})_3^{2+}]$ as photocatalyst and DIPEA as sacrificial electron donor

⁴⁰ S. Fukuzumi, S. Mochizuki and T. Tanaka, *J. Phys. Chem.*, 1990, **94**, 722–726.

⁴¹ D. A. Nagib, M. E. Scott and D. W. C. MacMillan, *J. Am. Chem. Soc.*, 2009, **131**, 10875–10877.

⁴² H.-W. Shih, M. N. Vander Wal, R. L. Grange and D. W. C. MacMillan, *J. Am. Chem. Soc.*, 2010, **132**, 13600–13603.

and formic acid.⁴³ The presence of formic acid favored the formation of an excellent donor of hydrogen, the ammonium salt ($\text{H}^+\text{NEt}_2\text{Pr}_2\cdot\text{HCO}_2^-$). In similar conditions (Et_3N instead of DIPEA), radicals obtained from the reduction of bromomalonate could also be engaged in radical cyclizations with alkenes, alkynes⁴⁴, indoles and pyrroles⁴⁵ moieties (**Scheme 12 a**). More interestingly, polyene substrates gave polycyclic compounds after cascade cyclizations.



Scheme 11. Enantioselective α -alkylation of aldehydes

Although the processes look efficient, the main limitation is the nature of the halide. Indeed, reductive potentials of non-activated alkyl iodides or bromides are lower than $[\text{Ru}^{2+}]^*$ or $[\text{Ru}^+]$ and measured between -1.61V and -2.5V vs SCE⁴⁶. Stephenson showed that they are reduced with the highly reductant $\text{Ir}(\text{ppy})_3$ (-1.73V vs SCE at the excited state) and the generated radical can be engaged in 5-*exo*-trig and 5-*exo*-dig cyclization processes (**Scheme**

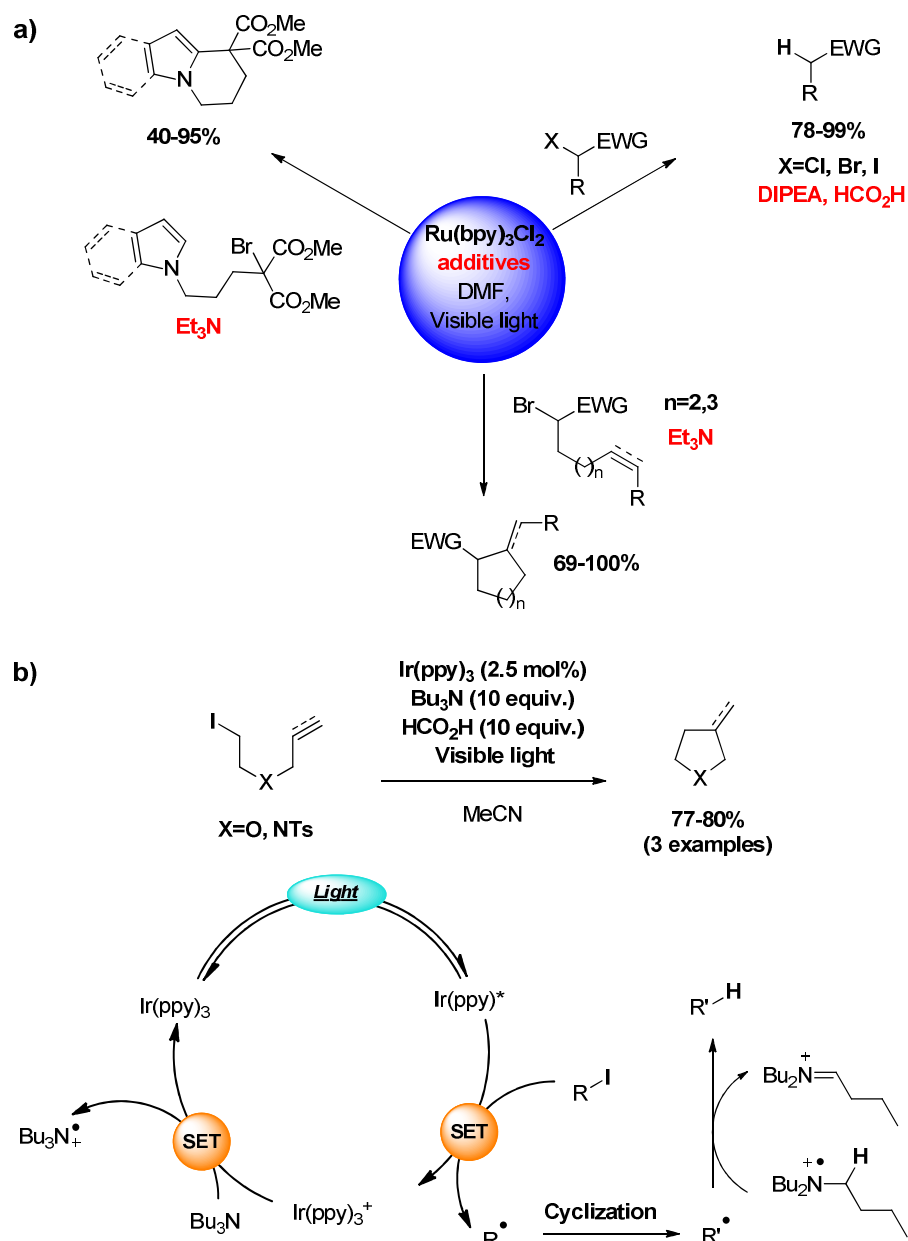
⁴³ J. M. R. Narayanam, J. W. Tucker and C. R. J. Stephenson, *J. Am. Chem. Soc.*, 2009, **131**, 8756–8757.

⁴⁴ (a) J. W. Tucker, J. D. Nguyen, J. M. R. Narayanam, S. W. Krabbe and C. R. J. Stephenson, *Chem. Commun.*, 2010, **46**, 4985–4987. (b) Nitin S. Dange, A. H. Jatoi, F. Robert and Y. Landais *Org. Lett.*, 2017, **19**, 3652–3655.

⁴⁵ J. W. Tucker, J. M. R. Narayanam, S. W. Krabbe and C. R. J. Stephenson, *Org. Lett.*, 2010, **12**, 368–371.

⁴⁶ (a) H. a. O. Hill, J. M. Pratt, M. P. O’Riordan, F. R. Williams and R. J. P. Williams, *J. Chem. Soc. Inorg. Phys. Theor.*, 1971, 1859–1862. (b) S. Rondinini, P. R. Mussini, P. Muttini and G. Sello, *Electrochim. Acta.*, 2001, **46**, 3245–3258. (c) P. Poizot, L. Laffont-Dantras and J. Simonet, *J. Electroanal. Chem.*, 2008, **624**, 52–58.

12 b)).⁴⁷ After light absorption, the iridium photocatalyst reduces the alkyl iodide to give the alkyl radical which directly cyclizes. The tributylamine regenerates the photocatalyst by SET, and the cyclized radical abstracts a hydrogen from the ammonium radical cation.



Scheme 12. Stephenson's photoreduction of halides

⁴⁷ J. D. Nguyen, E. M. D'Amato, J. M. R. Narayanam and Corey R. J. Stephenson, *Nature Chem.*, 2012, **4**, 854–859.

- **Photocatalyzed Barton-McCombie deoxygenation**

A famous reaction generating alkyl radicals is the Barton-McCombie deoxygenation reaction. Secondary or tertiary alcohols are converted to thiocarbonate, thiocarbamate or xanthate derivatives which are afterwards reduced by a tin-hydride reagent ($n\text{Bu}_3\text{SnH}$). During the process, the C-O bond of the modified alcohol undergoes fragmentation, to give an alkyl radical. After a hydrogen abstraction step from the tin-hydride reagent, the deoxygenated product and the reactive tin mediator ($n\text{Bu}_3\text{Sn}\cdot$) are obtained.⁴⁸ In order to avoid the use of tin reagents, some groups have tried a photocatalytic version. Similarly to the classical conditions of the Barton-McCombie deoxygenation, alcohols have to be activated as an ester, an oxalate or a thiocarbamate (**Scheme 13 a**)).

In 2013, inspired by the N-(acyloxy)phthalimides photocatalyzed decarboxylation of Okada,⁴⁹ Overman⁵⁰ reported the efficient deoxygenation of aliphatic tertiary alcohols by photoreduction of the corresponding N-(acyloxy)phthalimide oxalates derivatives in the presence of photocatalyst $\text{Ru}(\text{bpy})_3(\text{PF}_6)_2$, Hantzsch ester and $i\text{-Pr}_2\text{NEt.HBF}_4$ as a sacrificial electron donor and a H-atom donor respectively. The generated tertiary alkyl radicals could then be then engaged in Giese-type reactions (**Scheme 13 b**)). Although no example involving secondary or primary radicals were mentioned, Reiser *et al.* reported the photoreduction of 3,5-bis(trifluoromethyl)benzoate esters.⁵¹ Starting with the reduction of the photoexcited $[\text{Ir}(\text{ppy})_2(\text{dtbbpy})](\text{PF}_6)$ by DIPEA, benzyl, α -carbonyl and α -cyano esters were reduced by the $[\text{Ir}(\text{II})]$ complex to give the deoxygenated products in good yields (**Scheme 13 c**)). At the same time in our group, a procedure involving the reduction of *O*-thiocarbamates was developed.⁵² The high reductive potential of such derivatives (-1.56V to -1.73V vs SCE) required the use of the highly reducing photoexcited *fac*- $\text{Ir}(\text{ppy})_3$ photocatalyst ($E_{1/2}([\text{Ir}^+]/[\text{Ir}^*]) = -1.73\text{V vs SCE}$) and DIPEA as both an electron donor and a H-atom donor.

⁴⁸ D. H. R. Barton and S. W. McCombie, *J. Chem. Soc. [Perkin 1]*, 1975, 1574–1585.

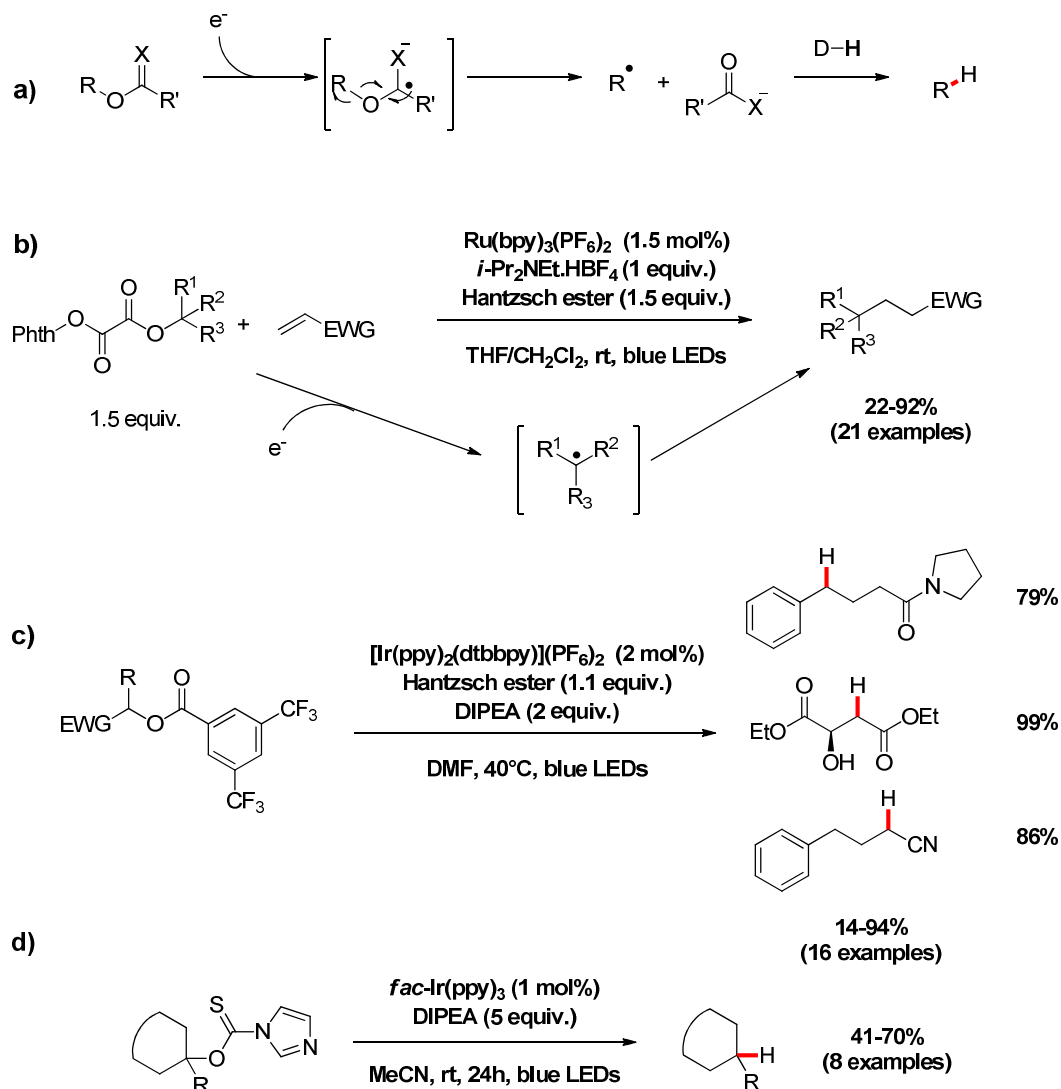
⁴⁹ (a) K. Okada, K. Okamoto, N. Morita, K. Okubo and M. Oda, *J. Am. Chem. Soc.*, 1991, **113**, 9401–9402. (b) K. Okada, K. Okubo, N. Morita, M. Oda, *Tetrahedron Lett.*, 1992, **33**, 7377–7380.

⁵⁰ G. L. Lackner, K. W. Quasdorf and L. E. Overman, *J. Am. Chem. Soc.*, 2013, **135**, 15342–15345.

⁵¹ D. Rackl, V. Kais, P. Kreitmeier and O. Reiser, *Beilstein J. Org. Chem.*, 2014, **10**, 2157–2165.

⁵² L. Chenneberg, A. Baralle, M. Daniel, L. Fensterbank, J.-P. Goddard and C. Ollivier, *Adv. Synth. Catal.*, 2014, **356**, 2756–2762.

Under these conditions, tertiary and secondary alcohols could be deoxygenated in moderate yields (**Scheme 13 d**)).



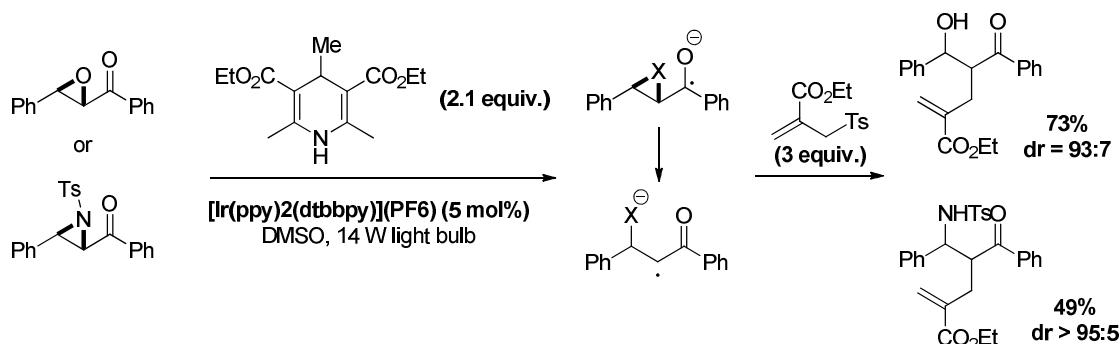
Scheme 13. Photoreductive Barton-McCombie type deoxygenation reactions.

- **Reduction of α -ketoepoxides and α -ketoaziridines**

Our group reported in 2011 the photoreduction of alpha-ketoepoxides and ketoaziridines⁵³ to generate an alpha carbonyl radical intermediate that can be trapped by allylsulfones. This transformation requires the use of $[\text{Ir}(\text{ppy})_2(\text{dtbbpy})](\text{PF}_6)$ that absorbs in

⁵³ M. H. Larraufie, R. Pellet, L. Fensterbank, J. P. Goddard, E. Lacôte, M. Malacria and C. Ollivier, *Angew. Chem. Int. Ed.*, 2011, **50**, 4463–4466.

the visible range and the Hantzsch ester methylated in position 4 in order to avoid the direct reduction by hydrogen abstraction and favor the allylation process (**Scheme 14**).



Scheme 14. Photoreduction of α -ketoepoxides and α -ketoaziridines

1.2.4.3 Photooxidative processes for the formation of alkyl radicals

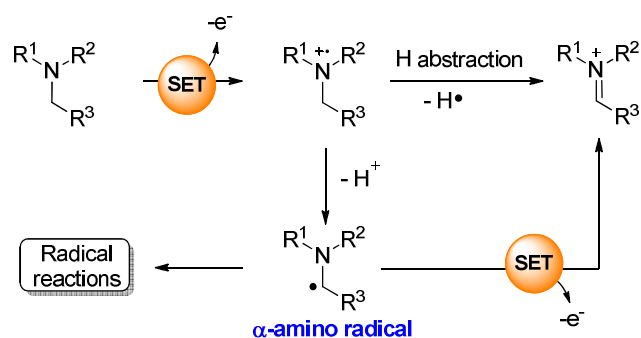
- **Processes involving oxidation of amines**

As previously observed, electron rich tertiary amines can be easily oxidized under photocatalytic conditions for the generation of alkyl radicals. An *N*-centered radical cation is generated which can evolve according two pathways. The first one previously detailed is an H-atom abstraction giving an iminium ion.⁵⁴ The second one consists of loss of a proton and generation of an α -amino radical⁵⁵ which can also be further oxidized to give the same iminium ion (**Scheme 15**).⁵⁶ Therefore, amines can react as electrophiles in the iminium form but also as nucleophiles in the α -amino radical form.

⁵⁴ J. P. Dinnocenzo and T. E. Banach, *J. Am. Chem. Soc.*, 1989, **111**, 8646–8653.

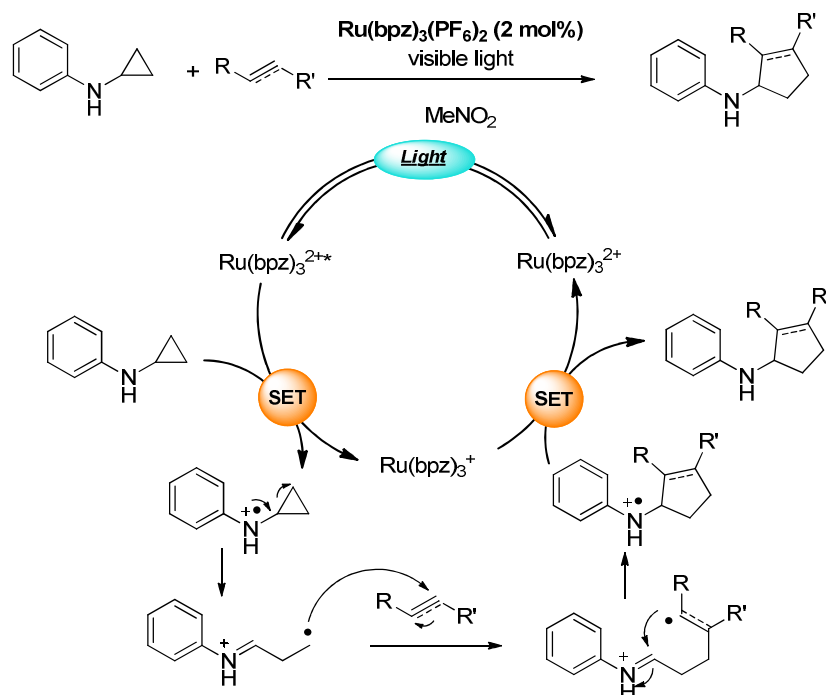
⁵⁵ V. D. Parker and M. Tilset, *J. Am. Chem. Soc.*, 1991, **113**, 8778–8781.

⁵⁶ (a) Y. L. Chow, W. C. Danen, S. F. Nelsen and D. H. Rosenblatt, *Chem. Rev.*, 1978, **78**, 243–274. F. D. Lewis, T. I. Ho and J. T. Simpson, *J. Am. Chem. Soc.*, 1982, **104**, 1924–1929. F. D. Lewis, *Acc. Chem. Res.*, 1986, **19**, 401–405.



Scheme 15. Evolution of *N*-centered radical cations

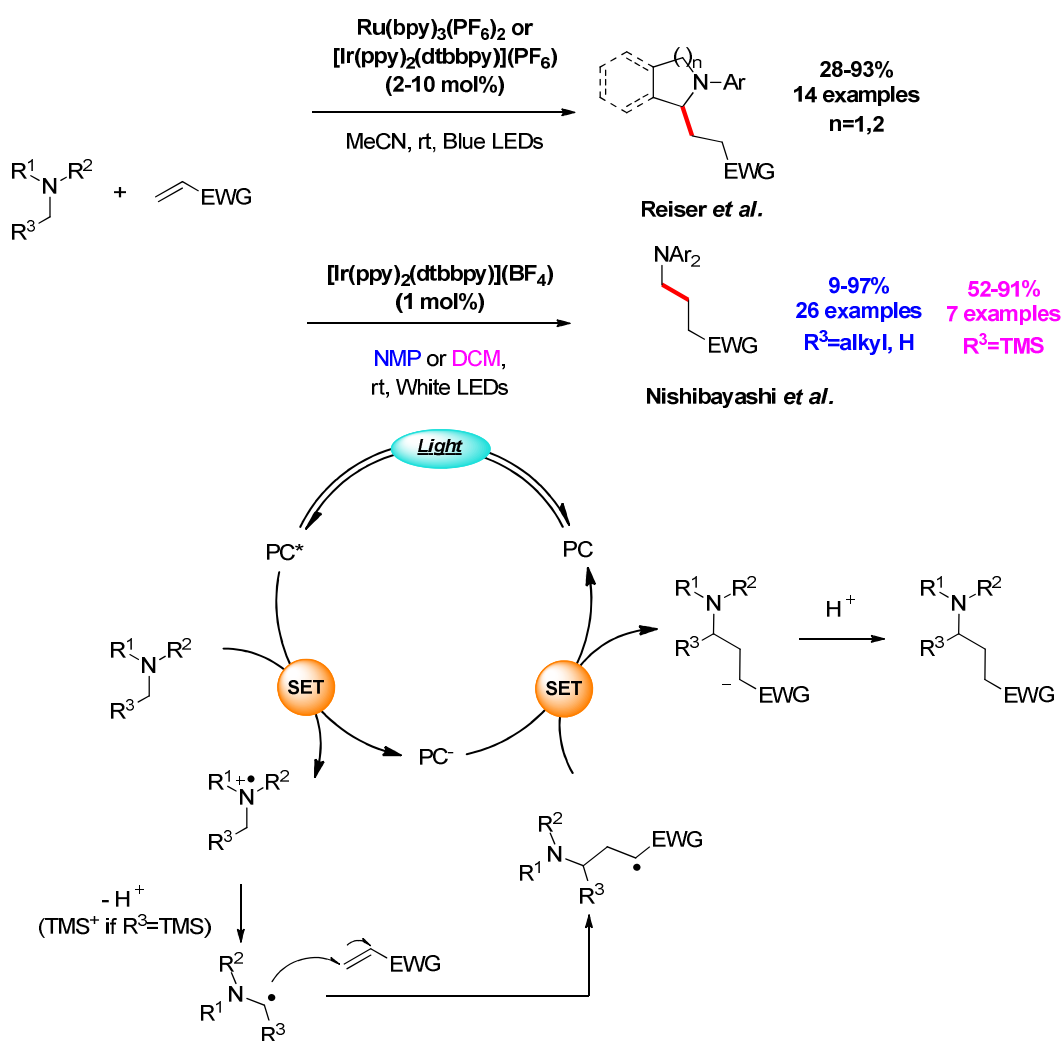
In 2012, Zheng and co-workers showed that an *N*-centered radical cation can evolve to the formation of carbon-carbon bonds. After oxidation of *N*-cyclopropylanilines, the cyclopropane ring opening led to an intermediate bearing an iminium moiety and a primary alkyl radical. The radical then adds to an alkene or an alkyne substituted by an aryl or an ester moiety.⁵⁷ The resulting stabilized radical cyclizes to the iminium to give the *N*-cyclopentyl (or *N*-cyclopentenyl) aniline (**Scheme 16**).



Scheme 16. Photocatalyzed intermolecular [3+2] cycloaddition of *N*-cyclopropylanilines

⁵⁷ (a) S. Maity, M. Zhu, R. S. Shinabery and N. Zheng, *Angew. Chem. Int. Ed.*, 2012, **51**, 222–226. (b) T. H. Nguyen, S. A. Morris and N. Zheng, *Adv. Synth. Catal.*, 2014, **356**, 2831–2837. (c) T. H. Nguyen, S. Maity and N. Zheng, *Beilstein J. Org. Chem.*, 2014, **10**, 975–980.

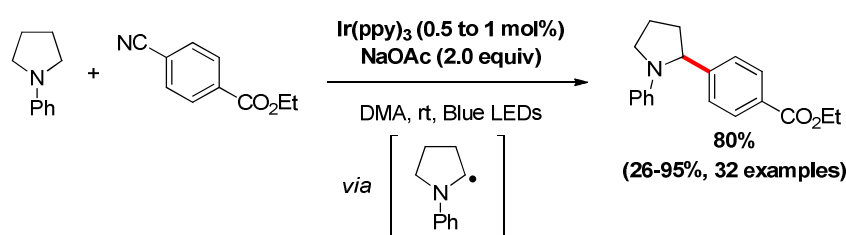
The same year, Reiser *et al.* reported the trapping of cyclic α -amino radicals by α,β -unsaturated carbonyl compounds.⁵⁸ Oxidation of the amine by the excited photocatalyst **PC*** leads to the formation of an α -stabilized carbon-centered radical after the loss of a proton. The addition of the radical to an α,β unsaturated acceptor gives the radical which is directly reduced by **PC⁻**. The resulting enolate is then protonated to give the final product (**Scheme 17**). At the same time, the group of Nishibayashi⁵⁹ realized the same process involving *N*-methylaniline or α -silylamine. In this last case, the aminyl radical evolves towards an alkyl radical by releasing a trimethylsilylium cation instead of a proton.



⁵⁸ P. Kohls, D. Jadhav, G. Pandey and O. Reiser, *Org. Lett.*, 2012, **14**, 672–675.

⁵⁹ (a) Y. Miyake, K. Nakajima and Y. Nishibayashi, *J. Am. Chem. Soc.*, 2012, **134**, 3338–3341. (b) Y. Miyake, Y. Ashida, K. Nakajima and Y. Nishibayashi, *Chem. Commun.*, 2012, **48**, 6966–6968.

In 2011, MacMillan mentioned a reaction between photogenerated α -amino radicals and benzonitrile.⁶⁰ The radicals were obtained by oxidation of *N*-alkyl anilines and added at the *ipso* position of the cyano arene releasing cyanide and the α -amino arene (**Scheme 18**). The reaction performed with the Ir(ppy)₃ photocatalyst was suitable for (non)-cyclic anilines and various cyano (hetero)arenes. Photoexcitation of the iridium photocatalyst leads to the reduction of the cyano arene. The [Ir^{IV}] intermediate then oxidizes the aniline, resulting in the formation of the α -amino radical which couples with the reduced arene. The newly formed anion provides the final formation of the product and cyanide.



Scheme 18. Photoredox amine α -arylation reaction

- **Oxidation of α -aminocarboxylates**

Anionic species are substrates of choice for oxidation reactions. MacMillan showed the ability of α -aminocarboxylates to undergo photooxidation, generating an α -amino radical by the loss of CO₂. As he showed before, the radicals were able to be coupled with dicyanobenzene in similar conditions.⁶¹ Even if the amine must be protected (Boc or Cbz) to avoid the oxidation of the nitrogen atom, secondary and tertiary amines could be engaged in the process because, these radicals' precursors are quite easy to oxidize ($E_{1/2}(\text{R-CO}_2^-/\text{R-CO}_2^\bullet) = +0.95 - +1.16$ V vs SCE).^{61,62} They were also engaged in vinylation reactions.⁶³ Oxidation of the carboxylate by photoexcited [Ir(dF(CF₃)ppy)₂(dtbbpy)](PF₆) catalyst gives the carbon-centered radical which is directly trapped by a vinylsulfone. After the C-SO₂Ph bond fragmentation, the sulfonyl radical ($E_{1/2}(\text{PhSO}_2^\bullet/\text{PhSO}_2\text{Na}) = +0.50$ V vs SCE)⁶⁴

⁶⁰ A. McNally, C. K. Prier and D. W. C. MacMillan, *Science*, 2011, **334**, 1114–1117.

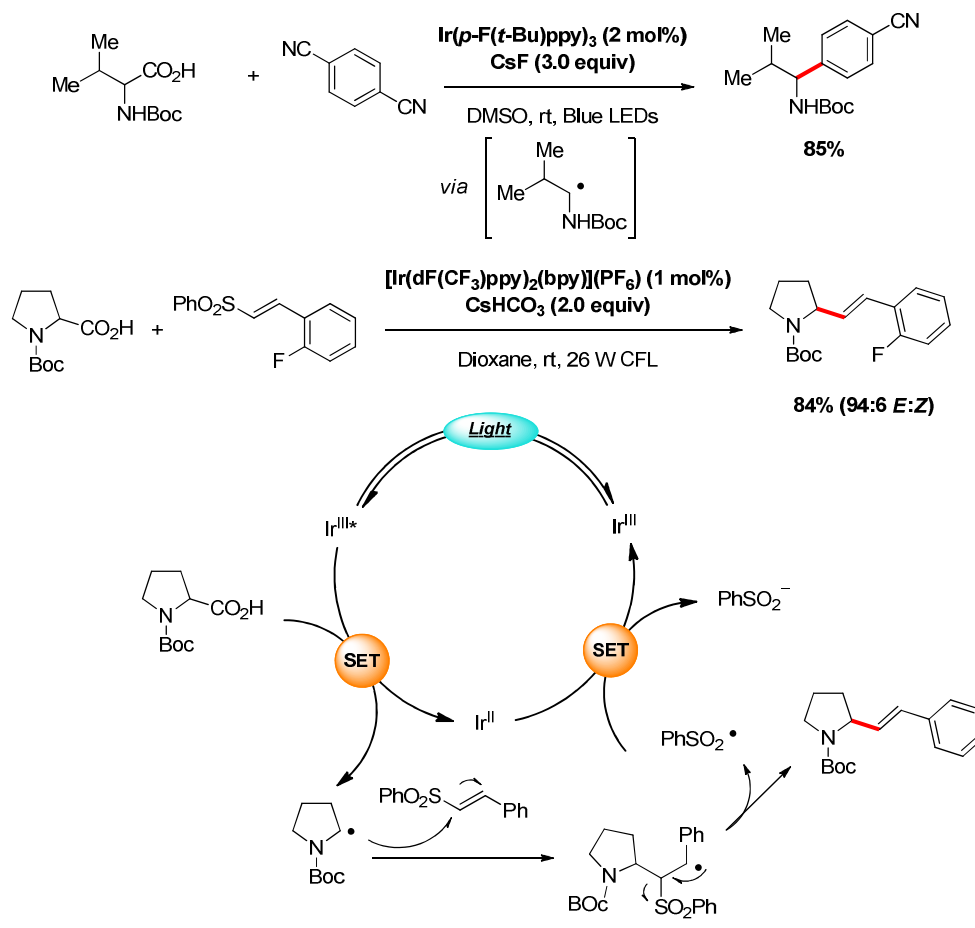
⁶¹ Z. Zuo and D. W. C. MacMillan, *J. Am. Chem. Soc.*, 2014, **136**, 5257–5260.

⁶² M. Galicia, F. J. J. Gonzalez, *Electrochem. Soc.* 2002, **149**, D46.

⁶³ A. Noble and D. W. C. MacMillan, *J. Am. Chem. Soc.*, 2014, **136**, 11602–11605.

⁶⁴ B. Persson, *Acta Chem. Scand.*, 1977, **31B**, 88.

participates to the regeneration of the photocatalyst *via* a SET with the Ir^{II} intermediate (Scheme 19).



Scheme 19. Photooxidation of α -aminocarboxylates

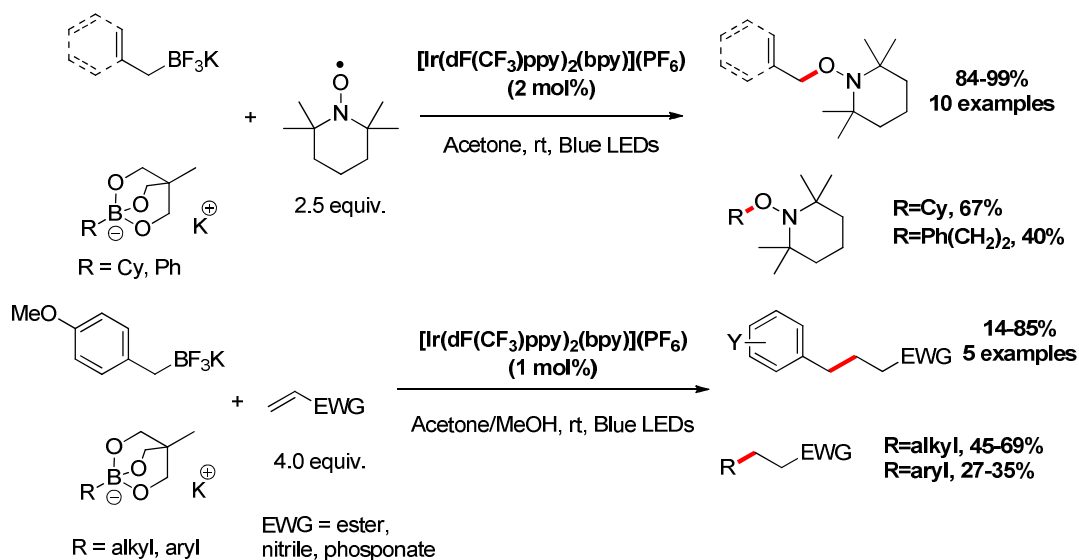
- **Oxidation of organoborates**

In the same line, alkyl trifluoroborates have proved to be suitable substrates to generate radicals upon oxidation.⁶⁵ Akita and Koike reported their work on the photooxidation of organoborates with the $[\text{Ir}(\text{dF}(\text{CF}_3)\text{ppy})_2(\text{bpy})](\text{PF}_6)$ catalyst.⁶⁶ In order to prove the photooxidation feasibility, they performed spin-trapping experiments with TEMPO and found that allyl, benzyl and tertiary alkyl trifluoroborates could form the corresponding alkyl-

⁶⁵ (a) Y. Nishigaichi, T. Orimi and A. Takuwa, *J. Organomet. Chem.*, 2009, **694**, 3837–3839. (b) G. Sorin, R. Martinez Mallorquin, Y. Contie, A. Baralle, M. Malacria, J.-P. Goddard and L. Fensterbank, *Angew. Chem. Int. Ed.*, 2010, **49**, 8721–8723. (c) G. A. Molander, V. Colombel and V. A. Braz, *Org. Lett.*, 2011, **13**, 1852–1855.

⁶⁶ Y. Yasu, T. Koike and M. Akita, *Adv. Synth. Catal.*, 2012, **354**, 3414–3420.

TEMPO adducts. However, secondary and primary alkyl trifluoroborates were not converted to the expected product. Only (triol)borates of 2-(hydroxymethyl)-2-methylpropane-1,3-diol which showed lower oxidation potentials and could provide TEMPO adducts in moderate yields (**Scheme 20**). Synthetic applications were also extended to Giese type reactions.

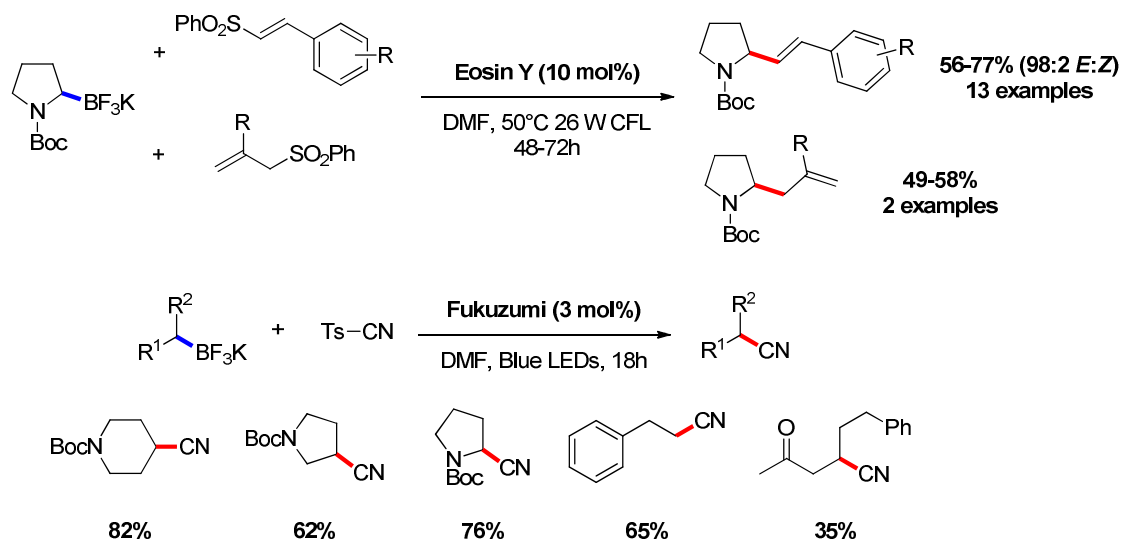


Scheme 20. Photooxidation of organoborates

Few years after, Molander and co-workers extended the synthetic applications of organotrifluoroborates.¹¹ They photooxidized α -pyrrolidinyltrifluoroborate ($E_{1/2}^{\text{ox}} = +0.78\text{V}$ vs SCE) with Eosin Y ($E_{1/2}^{\text{red}} = +0.83\text{V}$ vs SCE)⁶⁷ at 50°C. The generated α -amino radical was engaged in alkenylation reactions with vinyl sulfones and allylation reactions with allyl sulfones. Radical adducts were isolated in moderate to good yields (**Scheme 21**). Cyanation of primary and secondary alkyl trifluoroborates could be also performed by action of the highly oxidizing Fukuzumi's catalyst ($E_{1/2}^{\text{red}} = +2.06\text{V}$ vs SCE)⁶⁸ and tosylcyanide as radical acceptor. Secondary cyclic trifluoroborates gave the best yields while an unactivated primary aliphatic trifluoroborate provided the expected product in a low yield.

⁶⁷ C. K. Prier, D. A. Rankic and D. W. C. MacMillan, *Chem. Rev.*, 2013, **113**, 5322–5363.

⁶⁸ A. C. Benniston, A. Harriman, P. Li, J. P. Rostron, H. J. van Ramesdonk, M. M. Groeneveld, H. Zhang and J. W. Verhoeven, *J. Am. Chem. Soc.*, 2005, **127**, 16054–16064.



Scheme 21. Organic photooxidation of alkyl trifluoroborates

1.3 Conclusion

The photoredox catalysis has emerged as a powerful alternative method for the formation of radicals. The diversity of photocatalyst (ruthenium/iridium based complexes or organic dyes) with various redox potentials allows to promote single electron transfers selectively. Many reactions performed in classical conditions, could be realized in a photocatalytic version. The appeal of this field grows year after year and demonstrates its importance in the chemistry community and particularly for the development of a greener radical chemistry.

Chapter II

Merging photoredox and organometallic catalysis for cross-coupling reactions

2 Chapter II

Merging photoredox and organometallic catalysis for cross-coupling reactions

2.1 Context

Photoredox catalysis has shown its efficiency to accomplish radical reactions. Methods merging organocatalysis and photoredox catalysis have been also developed.^{14,41,42,93} Recently, photoredox catalysis has proved to be compatible with transition metal catalysis. In this type of catalysis, the photocatalyst is necessary to generate a radical and the organometallic catalyst performs the cross-coupling steps between an electrophile and the generated radical. Therefore, metal complexes able to trap radicals are catalysts of choice for such transformations.

2.2 Radical trapping by transition-metals

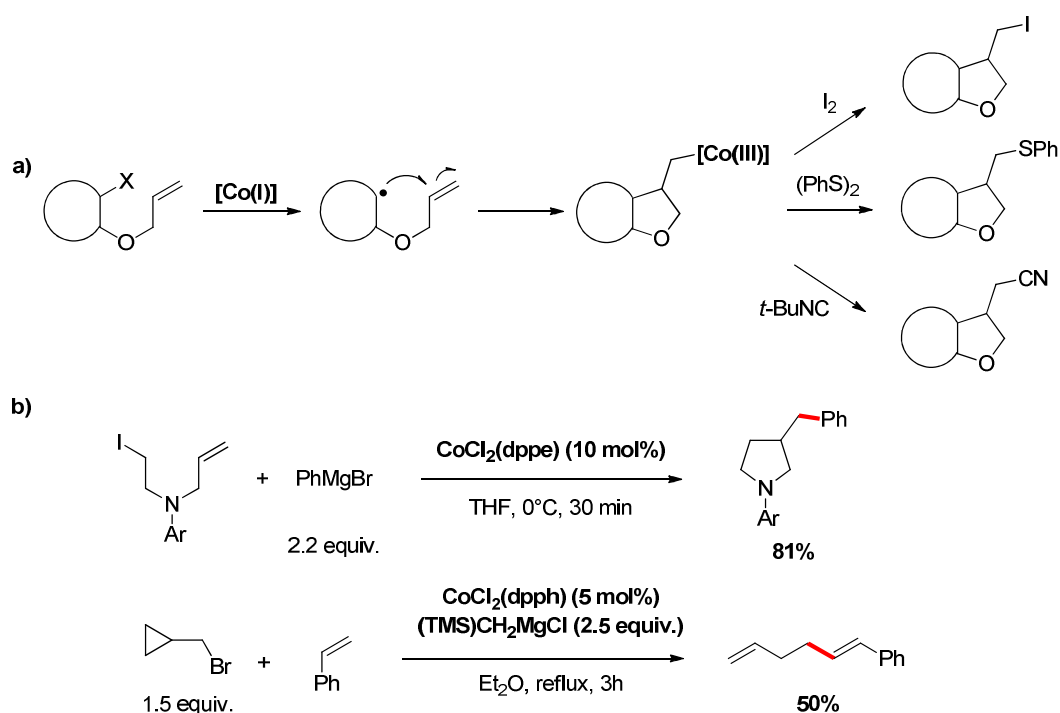
Transition metal catalyzed reactions have become essential tools for the elaboration of new molecular building blocks. For instance, palladium catalyzed cross-coupling reactions and C-H functionalization reactions are processes well-established and efficient. The mechanisms relying on two electron transfer steps are inherent to the nature of fifth period transition metal. However, concerning 3d transition metals, although they are known to perform oxidative addition in carbon-halogen or carbon-hydrogen bonds, they can also promote single electron transfer⁹⁴ and generate radicals. These ones can be further trapped by the metal and involved in organometallic processes.

⁹³ For examples of photoredox-organo dual catalysis: (a) D. S. Hamilton and D. A. Nicewicz, *J. Am. Chem. Soc.*, 2012, **134**, 18577–18580. (b) M. Neumann and K. Zeitler, *Org. Lett.*, 2012, **14**, 2658–2661. (c) D. A. DiRocco and T. Rovis, *J. Am. Chem. Soc.*, 2012, **134**, 8094–8097. (d) F. R. Petronijević, M. Nappi and D. W. C. MacMillan, *J. Am. Chem. Soc.*, 2013, **135**, 18323–18326. (e) M. A. Zeller, M. Riener and D. A. Nicewicz, *Org. Lett.*, 2014, **16**, 4810–4813.

⁹⁴ J. K. Kochi, *Acc. Chem. Res.*, 1974, **7**, 351–360.

- **Cobalt**

Some cobalt complexes showed to be able to reduce alkyl halides to alkyl radicals which could undergo cyclizations. The resulting radical intermediates lead the formation of an alkyl-[Co(III)] complex. Such species can be trapped by iodine, diphenyl disulfide, isonitrile⁹⁵ or can undergo cross-coupling reactions with Grignard reagents. Reduction of 5-hexenyl bromide or cyclopropylmethyl bromide lead to the formation of ring-closing or ring-opening products respectively,⁹⁶ suggesting the formation of alkyl radicals during the transformations (Scheme 22).



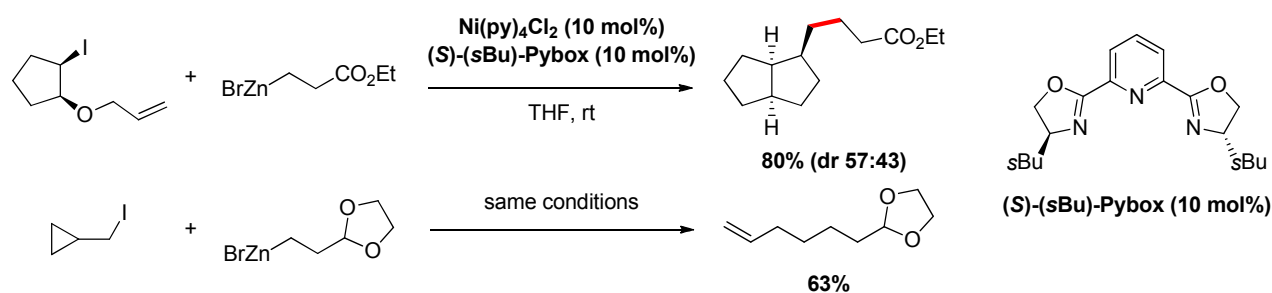
Scheme 22. Cobalt-mediated radical reactions

⁹⁵ (a) V. F. Patel and G. Pattenden, *Tetrahedron Lett.*, 1987, **28**, 1451–1454. (b) V. F. Patel and G. Pattenden, *J. Chem. Soc. Chem. Commun.*, 1987, 871–872. (c) V. F. Patel, G. Pattenden and D. M. Thompson, *J. Chem. Soc. [Perkin 1]*, 1990, 2729–2734. (d) A. Ali, D. C. Harrowven and G. Pattenden, *Tetrahedron Lett.*, 1992, **33**, 2851–2854.

⁹⁶ (a) K. Wakabayashi, H. Yorimitsu and K. Oshima, *J. Am. Chem. Soc.*, 2001, **123**, 5374–5375. (b) Y. Ikeda, T. Nakamura, H. Yorimitsu and K. Oshima, *J. Am. Chem. Soc.*, 2002, **124**, 6514–6515.

- **Nickel**

With the development of the Kumada-Corriu⁹⁷ reaction in the 70s, nickel catalysis has demonstrated impressive reactivities.⁹⁸ Like cobalt, a variety of nickel catalysts have revealed to be remarkably active in the formation of carbon-centered radicals. In the context of C(sp³)-C(sp³) cross coupling reactions between electrophiles and Grignard or organozinc reagents, several reports mentioned mechanisms involving radicals. Cardenas⁹⁹ accomplished the cross-coupling reactions between iodoalkanes and alkyl zinc halides. He observed that in the presence of a nickel catalyst with a Pybox ligand, a 5-hexenyl iodide type substrate underwent 5-*exo*-trig cyclization before the coupling step and cyclopropylmethyl iodide gave the ring-opening products (**Scheme 23**). From calculations, Cardenas supposed the formation of the radical by a reduction of the electrophile with an intermediate Ni(I) complex.



Scheme 23. Nickel-catalyzed Negishi cross-coupling reaction

Indeed, redox potentials of (terpyridyl)Ni^I(alkyl) complexes have been measured between -1.32 V and -1.44 V (vs Ag/Ag⁺ in THF),¹⁰⁰ allowing the reduction of alkyl halide to a carbon centered radical.¹⁰¹ Then the radical adds on a Ni(II) complex which after reductive elimination liberates the cross-coupling product (**Scheme 24**). Furthermore, methodologies

⁹⁷ (a) K. Tamao, K. Sumitani and M. Kumada, *J. Am. Chem. Soc.*, 1972, **94**, 4374–4376. (b) R. J. P. Corriu and J. P. Masse, *J. Chem. Soc. Chem. Commun.*, 1972, 144a–144a.

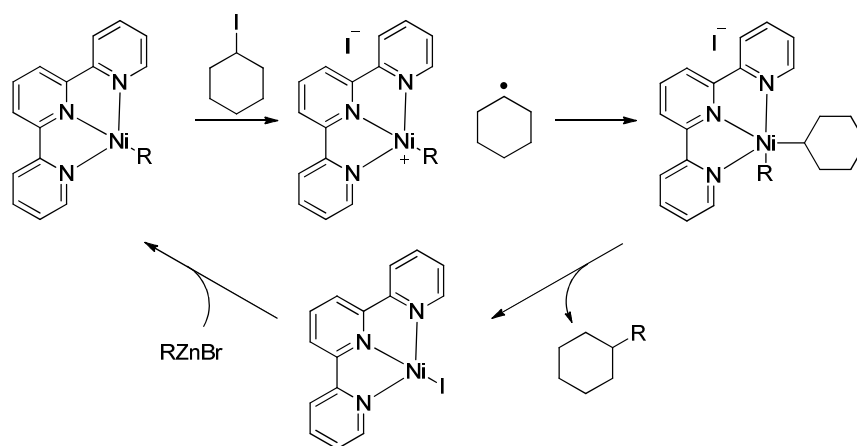
⁹⁸ For more details, see section 4.1.

⁹⁹ V. B. Phapale, E. Buñuel, M. García-Iglesias and D. J. Cárdenas, *Angew. Chem.*, 2007, **119**, 8946–8951.

¹⁰⁰ G. D. Jones, C. McFarland, T. J. Anderson and D. A. Vivic, *Chem. Commun.*, 2005, 4211–4213.

¹⁰¹ G. D. Jones, J. L. Martin, C. McFarland, O. R. Allen, R. E. Hall, A. D. Haley, R. J. Brandon, T. Konovalova, P. J. Desrochers, P. Pulay and D. A. Vivic, *J. Am. Chem. Soc.*, 2006, **128**, 13175–13183.

using others nucleophiles such as boronic acids, Grignard reagents or organostannanes,¹⁰² involved the formation of alkyl radicals in nickel catalysis.



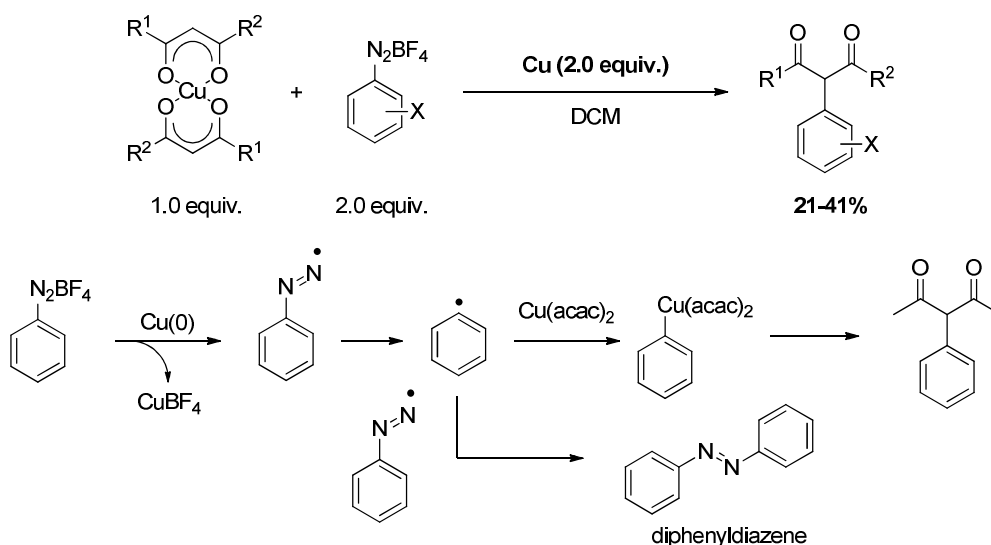
Scheme 24. Mechanism for Nickel-catalyzed alkyl-alkyl Negishi cross-coupling reactions

• Copper

Copper complexes also revealed efficient interaction with carbon centered radicals. Lloris *et al.* reported the arylation of β -diketones at the α position.¹⁰³ In the presence of copper powder, $\text{Cu}(\text{acac})_2$ type complexes and aryl diazonium salts could give the expected cross-coupling adducts in low to moderate yields. They proposed the reduction of the diazonium salts by copper(0) giving the aryl radical which adds on $\text{Cu}(\text{acac})_2$. The resulting $\text{Cu}(\text{III})$ intermediate provides the arylated product and $\text{Cu}(\text{acac})$ after reductive elimination (**Scheme 25**). As a side product, they observed the formation of diphenyldiazene. In their opinion, the product results from the radical coupling between a diazenyl radical and an aryl radical.

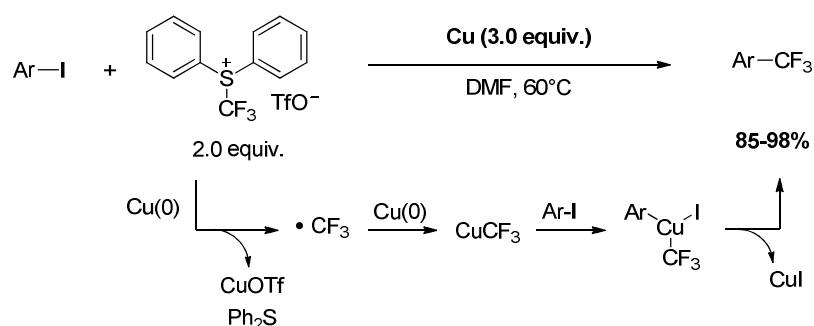
¹⁰² (a) J. Zhou and G. C. Fu, *J. Am. Chem. Soc.*, 2004, **126**, 1340–1341. (b) M. Guisán-Ceinos, R. Soler-Yanes, D. Collado-Sanz, V. B. Phapale, E. Buñuel and D. J. Cárdenas, *Chem. Eur. J.*, 2013, **19**, 8405–88410. (c) D. A. Powell, T. Maki and G. C. Fu, *J. Am. Chem. Soc.*, 2005, **127**, 510–511.

¹⁰³ M. E. Lorris, R. A. Abramovitch, J. Marquet and M. Moreno-Mañas, *Tetrahedron*, 1992, **48**, 6909–6916.



Scheme 25. Arylation of β -diketones

In 2001, Xiao demonstrated that (hetero)aryl iodides substrates were trifluoromethylated in the presence of diphenyl(trifluoromethyl)sulfonium triflate and copper(0).¹⁰⁴ NMR and mass spectrometry studies showed the *in-situ* formation of CuCF_3 . From a SET between Cu(0) and the sulfonium, the trifluoromethyl radical is generated and trapped by another atom of Cu(0) to generate the organocopper CuCF_3 which undergoes an oxidative addition of aryl iodide followed by a reductive elimination (**Scheme 26**).

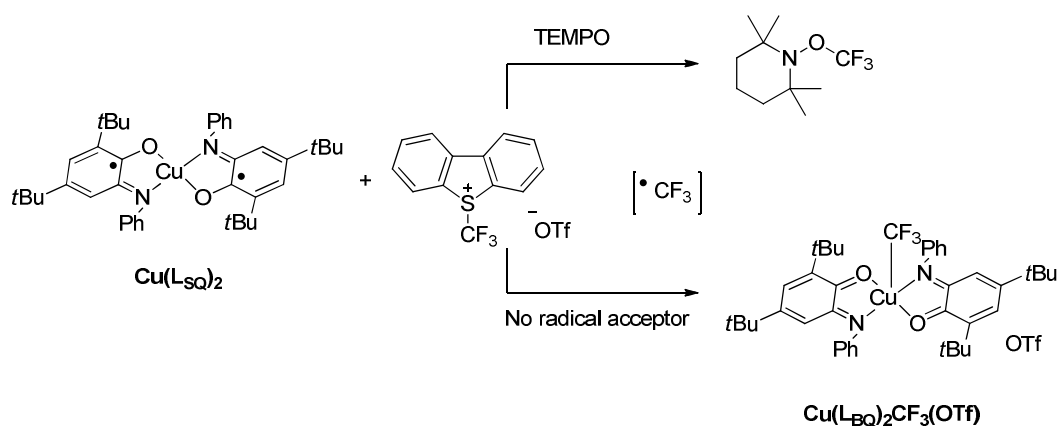


Scheme 26. Trifluoromethylation of iodo (hetero)arenes

In the same line, previous works in our group showed the formation of a well-defined copper complex displaying a Cu-CF_3 bond. Treating the $\text{Cu(L}_{\text{SQ}})_2$ (L_{SQ} = iminosemiquinone) by the

¹⁰⁴ C.-P. Zhang, Z.-L. Wang, Q.-Y. Chen, C.-T. Zhang, Y.-C. Gu and J.-C. Xiao, *Angew. Chem. Int. Ed.*, 2011, **50**, 1896–1900.

Umamoto reagent lead to the formation of a CF_3 radical which could be trapped by TEMPO.¹⁰⁵ The redox iminosemiquinone ligand can reduce the Umamoto reagent and generate the radical species. Without any radical acceptor in the reaction mixture, it was observed the formation of the $\text{Cu}(\text{L}_{\text{BQ}})_2\text{CF}_3(\text{OTf})$ complex (L_{BQ} = iminobenzoquinone) by radical addition on the copper. Association of UV-vis data, mass spectrometry values and 2D EPR experiments confirmed the atom sequence around the copper and the formation of the Cu-C bond (**Scheme 27**).¹⁰⁶ The isolated complex could be further engaged in a Chan-Lam coupling type reaction.¹⁰⁷



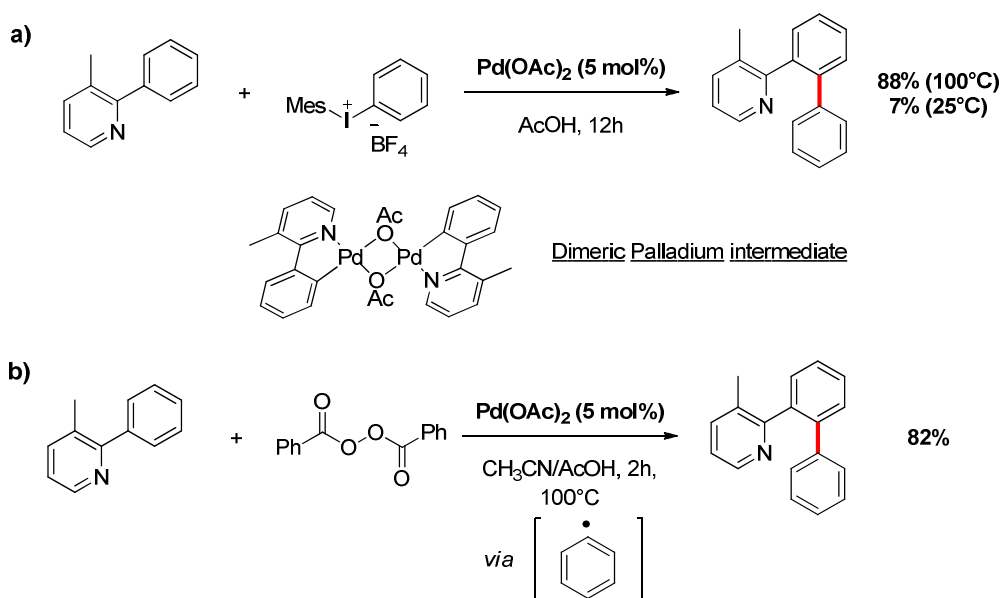
¹⁰⁵ J. Jacquet, E. Salanouve, M. Orio, H. Vezin, S. Blanchard, E. Derat, M. D.-E. Murr and L. Fensterbank, *Chem. Commun.*, 2014, **50**, 10394–10397.

¹⁰⁶ J. Jacquet, S. Blanchard, E. Derat, M. D.-E. Murr and L. Fensterbank, *Chem. Sci.*, 2016, **7**, 2030–2036.

¹⁰⁷ J. Jacquet, P. Chaumont, G. Gontard, M. Orio, H. Vezin, S. Blanchard, M. Desage-ElMurr and L. Fensterbank, *Angew. Chem. Int. Ed.*, 2016, **55**, 10712–10716.

2.3 Ruthenium and Palladium: Genesis of the photoredox/transition metal dual catalysis

The first example of photoredox/transition metal dual catalysis has been realized by the group of Sanford in 2011. Working on the palladium-catalyzed C-H functionalization of arylpyridine with diaryliodonium salts, Sanford showed the reaction to be temperature dependent. Lowering the reaction temperature from 100°C to 25°C decreased the yield dramatically (**Scheme 28 a**). This observation is related to the difficult oxidation step of the dimeric Pd(II) intermediate by the diaryliodonium salt to the Pd(IV) that triggers the reductive elimination.¹⁰⁸



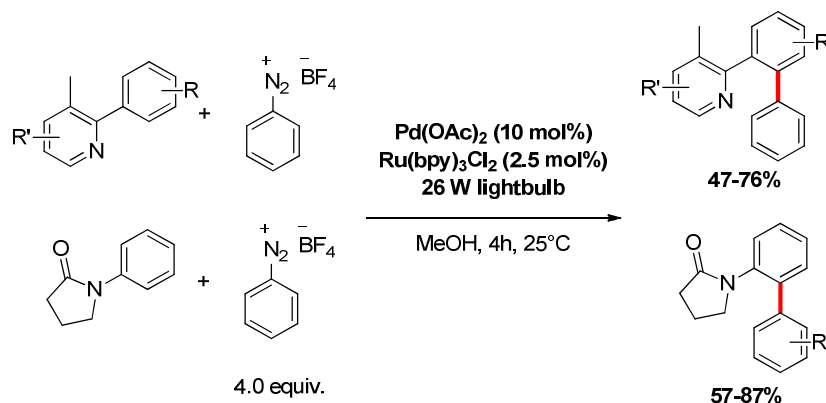
Scheme 28. Thermally activated C-H arylation of phenylpyridine

At the same time, Yu¹⁰⁹ showed that C-H functionalization of the same kind of substrates could be performed with benzoylperoxide (**Scheme 28 b**). At 100°C, the peroxide undergoes fragmentation and CO₂ extrusion to provide the phenyl radical which should react with the

¹⁰⁸ N. R. Deprez and M. S. Sanford, *J. Am. Chem. Soc.*, 2009, **131**, 11234–11241.

¹⁰⁹ W.-Y. Yu, W. N. Sit, Z. Zhou and A. S.-C. Chan, *Org. Lett.*, 2009, **11**, 3174–3177.

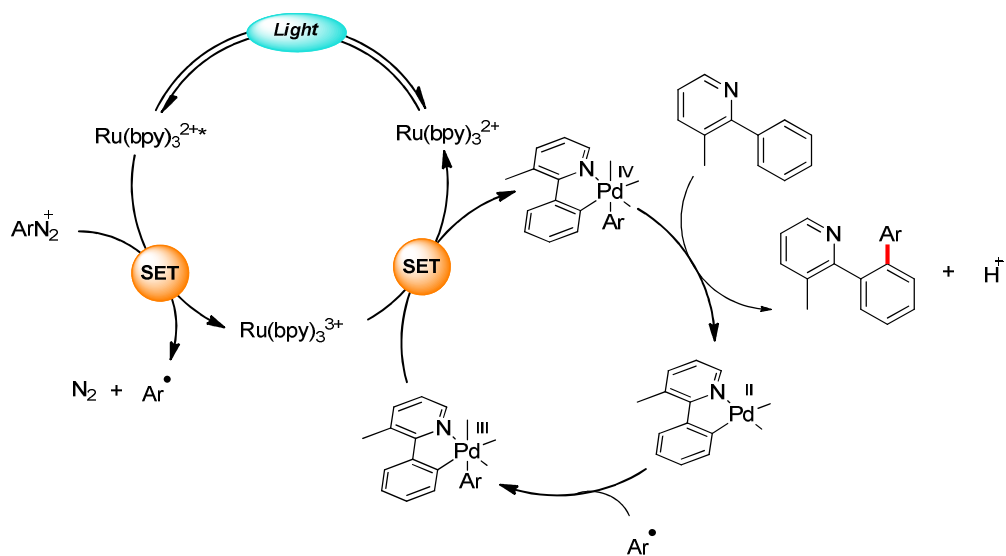
palladium complex intermediate. Based on these results, Sanford¹¹⁰ envisioned to generate an aryl radical by photoredox catalysis. As precursors of radicals aryl diazonium salts were selected due to their low reduction potential.³⁶ The diazonium salts were reduced by Ru(bpy)₃Cl₂ under visible-light irradiation at room temperature. The generated radical was then involved in palladium catalysis to give the C-H functionalized product. Phenylpyridines and phenylpyrrolidin-2-ones were obtained in moderate to good yields (**Scheme 29**).



Scheme 29. Photoredox/palladium C-H arylation catalysis

A possible catalytic cycle was then proposed. The photoexcited $[\text{Ru(bpy)}_3]^{2+*}$ complex reduces the diazonium salt to generate the aryl radical and the $[\text{Ru(bpy)}_3]^{3+}$ complex. Regarding the palladium catalytic cycle after C-H insertion, the aryl radical adds on the palladium(II) intermediate leading to a Pd(III) species. A SET with Ru(bpy)_3^{3+} regenerates the photocatalyst, and the obtained Pd(IV) undergoes reductive elimination to afford the arylated product and liberates the starting Pd(II) (**Scheme 30**).

¹¹⁰ D. Kalyani, K. B. McMurtrey, S. R. Neufeldt and M. S. Sanford, *J. Am. Chem. Soc.*, 2011, **133**, 18566–18569.



Scheme 30. Proposed mechanism for Photoredox/palladium C-H arylation catalysis

This mild approach for palladium catalyzed C-H bonds arylation is the first photoredox/transition metal dual catalytic process which demonstrates the feasibility of photoredox mediated cross-coupling reactions and pointed the way towards new synthetic opportunities.

2.4 Towards photoredox/transition-metal dual catalysis processes

Since the seminal work of Sanford, many photoredox/transition-metal dual catalysis processes have been developed. One of the most important features of this kind of catalysis is the opportunity offered by the photoredox transformations to modify the oxidation state of organometallic intermediates. This allows tuning the reactivity of the metallic centers for synthetic applications. Two tandem processes can be distinguished: – Catalytic reactions which do not involve the formation of radicals (except superoxide anion $[O_2]^\bullet$). In this case, the SET takes place only between the photocatalyst and the transition metal. – Reactions in which a photogenerated radical is trapped by an organometallic complex. In this case, a second electron transfer between the organometallic catalyst and the photocatalyst occurs to maintain the redox balance. Each process will be therefore named “Catalysis of Redox Steps” and “Catalysis of Downstream Steps” respectively (Figure 4).

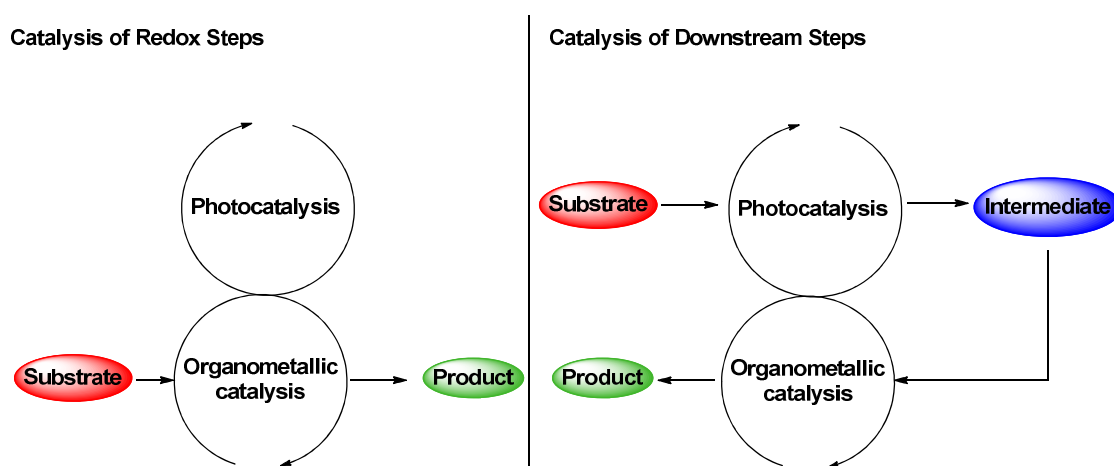


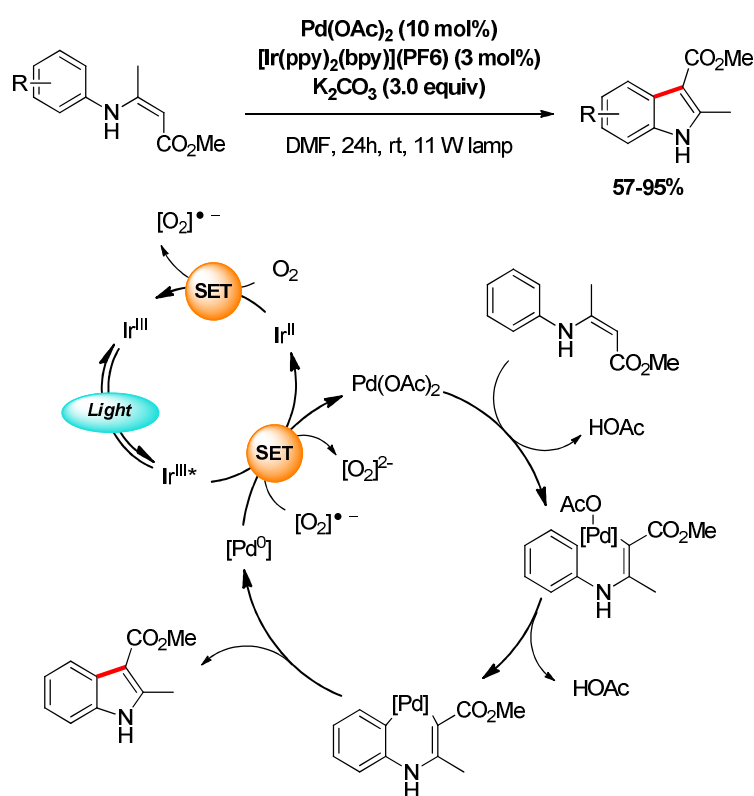
Figure 4. Modes of photoredox/transition metal catalysis

2.4.1 Processes without radical formation: Catalysis of Redox Steps

- C-H Functionalization

Among the photoredox/transition metal dual catalytic reactions reported in the literature, C-H functionalization has been particularly studied. Rueping and co-workers developed another approach to oxidative Heck Reaction so called Fujiwara-Moritani reaction

under photoredox conditions.¹¹¹ Based on an article of van Leeuwen¹¹² who reported the coupling reaction between anilidines and olefins with Pd(OAc)₂ as catalyst and benzoquinone as oxidant, they chose the photooxidizing catalyst [Ir(ppy)₂(bpy)](PF₆) to perform this catalytic process. Starting from (Z)-(phenylamino)but-2-enoate derivatives in the presence of Pd(OAc)₂ and potassium carbonate, they could obtain the formation of indoles in good to excellent yields. Control experiments showed that no reaction occurred under oxygen atmosphere. However, the presence of potassium superoxide proved to be essential. Based on these informations, the authors proposed a mechanism in which Pd(OAc)₂ did two consecutive C-H insertions. After reductive elimination, the indole is obtained and a Pd(0) complex re-oxidized simultaneously by superoxide and the photoexcited iridium complex. The Ir(II) photocatalyst transfers its excess of electron to a molecule of oxygen, regenerating the photocatalyst Ir(III) and providing a superoxide anion (**Scheme 31**).

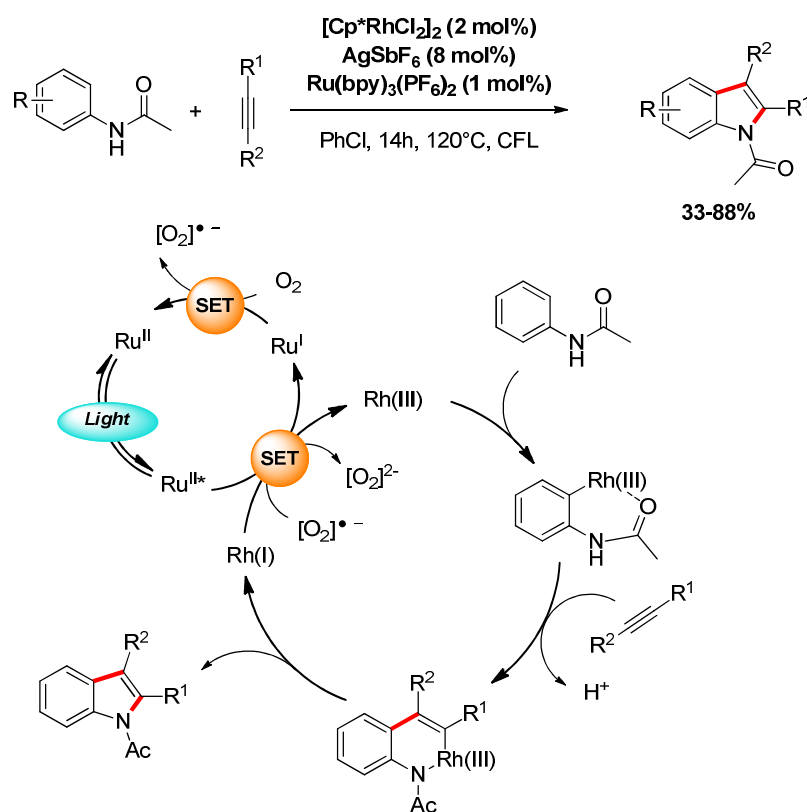


Scheme 31. Photocatalyzed Fujiwara-Moritani reaction

¹¹¹ J. Zoller, D. C. Fabry, M. A. Ronge and M. Rueping, *Angew. Chem. Int. Ed.*, 2014, **53**, 13264–13268.

¹¹² M. D. K. Boele, G. P. F. van Strijdonck, A. H. M. de Vries, P. C. J. Kamer, J. G. de Vries and P. W. N. M. van Leeuwen, *J. Am. Chem. Soc.*, 2002, **124**, 1586–1587.

In the same field, Rueping's group reported the photocatalyzed synthesis of indoles from acetanilides and alkynes. Inspired by the works of Fagnou,¹¹³ they found that the photocatalyst $\text{Ru}(\text{bpy})_3^{2+}$ under visible-light irradiation was a suitable photocatalytic oxidant instead of stoichiometric amount of $\text{Cu}(\text{OAc})_2$ to regenerate the active rhodium catalyst.¹¹⁴ Cationization of $[\text{Cp}^*\text{RhCl}_2]_2$ gives the active metalating agent¹¹⁵ which inserts in the C-H bond in *ortho* position of the acetanilide. After coordination of the alkyne to the rhodium, insertion of the triple bond results in the formation of a six-membered metallacycle intermediate. Then, a reductive elimination gives the *N*-acetyl indole and a Rh(I) complex is released. A similar re-oxidation with superoxide previously detailed with the palladium C-H functionalization may occur to end the catalytic cycle (Scheme 32).



Scheme 32. Combined Photoredox/Rhodium catalyzed C-H functionalization of acetanilides with alkynes

¹¹³ (a) D. R. Stuart, M. Bertrand-Laperle, K. M. N. Burgess and K. Fagnou, *J. Am. Chem. Soc.*, 2008, **130**, 16474–16475. (b) D. R. Stuart, P. Alsabeh, M. Kuhn and K. Fagnou, *J. Am. Chem. Soc.*, 2010, **132**, 18326–18339.

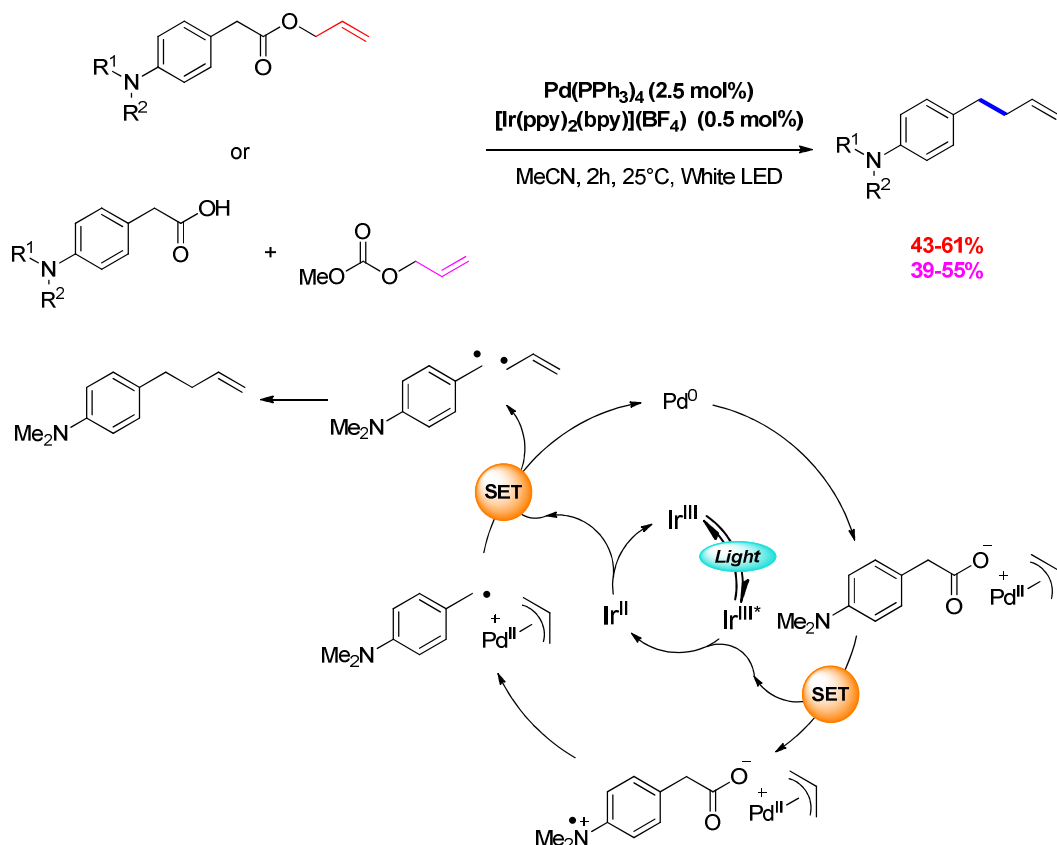
¹¹⁴ For more details see: D. C. Fabry and M. Rueping, *Acc. Chem. Res.*, 2016, **49**, 1969–1979; ref 69: Manuscript in preparation.

¹¹⁵ L. Li, W. W. Brennessel and W. D. Jones, *Organometallics*, 2009, **28**, 3492–3500.

- **Two successive SETs catalysis**

Others photoredox/transition-metal dual catalysis processes involving two SETs between both catalysts were developed. Each SET allows the organometallic catalyst to reach the specific oxidation state required for the catalysis. Tunge and co-workers reported a decarboxylative allylation of *para*-amino allyl 2-phenylacetate in the presence of Pd(PPh₃)₄ as transition metal catalyst and [Ir(ppy)₂(bpy)](BF₄) as photocatalyst.¹¹⁶ They could obtain *para*-homoallylaniline products in moderate yields. Alternatively starting the reaction from carboxylic acids and allyl methyl carbonate in stoichiometric amounts provided the products in the same range of yields. During the optimization, the authors noted the formation of a dibenzyl product suggesting the formation of a benzyl radical in the process. In addition, they observed the formation of a 1,5-hexadiene resulting from the presence of an allyl radical. So they suggested a plausible mechanism involving a benzyl-allyl radical coupling. They proposed the oxidative addition of the allyl ester to Pd(0) to form a Pd- π -allyl complex and a carboxylate anion (**Scheme 33**). The photoactivated iridium catalyst oxidizes the carboxylate which undergoes decarboxylation to furnish the benzyl radical. Thereafter, the Pd- π -allyl cationic complex is reduced by the Ir(II) intermediate to provide the allyl radical and regenerate both catalysts.

¹¹⁶ S. B. Lang, K. M. O'Nele and J. A. Tunge, *J. Am. Chem. Soc.*, 2014, **136**, 13606–13609.



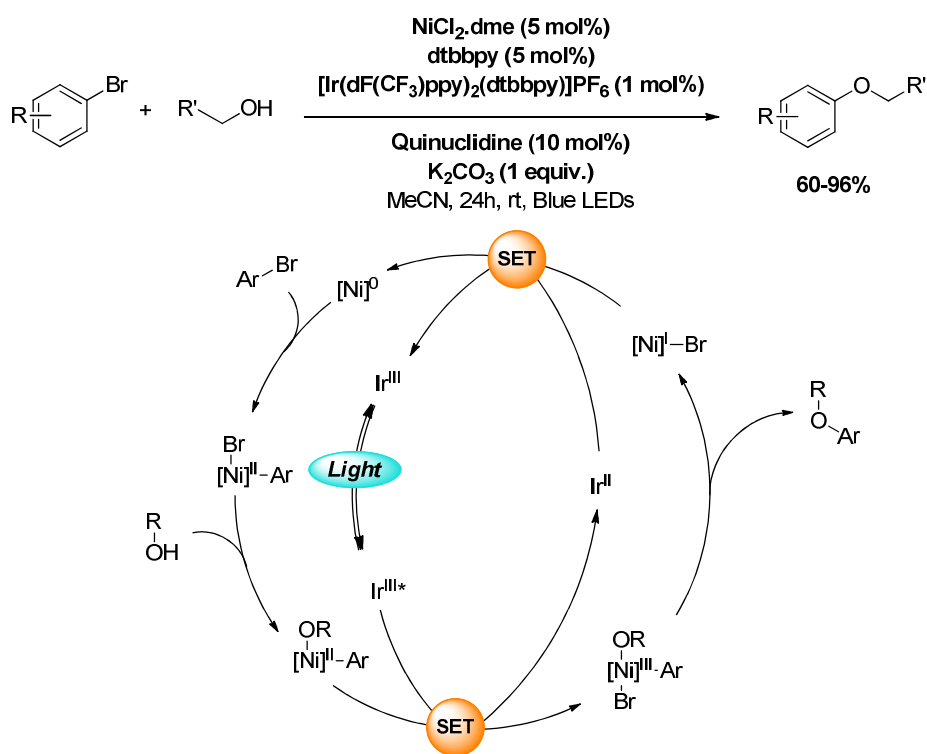
Scheme 33. Photocatalyzed decarboxylative allylation of phenylacetate derivatives

Nickel also proved to be a valuable candidate to photoredox/transition metal dual catalysis. MacMillan developed an efficient intermolecular cross-coupling reaction between aryl bromides and alcohols involving photoredox/nickel dual catalysis. Studies on the nickel catalysis revealed that the C-O bond formation using this metal is tricky. Reductive elimination of the C-Ni^{II}-O is endothermic¹¹⁷ and does not favor the C-O bond formation except for nickel metallacycles.¹¹⁸ However, reductive elimination from a nickel(III) intermediate was suspected to be much easier. In order to reach this oxidation state, the idea of this group was to use a photocatalyst to oxidize the [C-Ni^{II}-O] intermediate. Using NiCl₂.dme, a bipyridine type ligand and [Ir(dF(CF₃)ppy)₂(dtbbpy)]PF₆ as photocatalyst, they could obtain the expected aryl ether products in excellent yields (**Scheme 34**). Regarding the mechanism, they proposed an oxidative addition of the aryl bromide on the Ni(0)(dtbbpy)

¹¹⁷ S. A. Macgregor, G. W. Neave and C. Smith, *Faraday Discuss.*, 2003, **124**, 111–127.

¹¹⁸ (a) P. T. Matsunaga, G. L. Hillhouse and A. L. Rheingold, *J. Am. Chem. Soc.*, 1993, **115**, 2075–2077. (b) P. T. Matsunaga, J. C. Mavropoulos and G. L. Hillhouse, *Polyhedron*, 1995, **14**, 175–185. (c) R. Han and G. L. Hillhouse, *J. Am. Chem. Soc.*, 1997, **119**, 8135–8136.

active catalyst. A ligand exchange with the alcohol would then generate the Ni(II) aryl alkoxide. At this stage, the crucial oxidation to Ni(III) was carried out by the photoexcited iridium complex ($E_{1/2}(\text{Ni}^{\text{III}}/\text{Ni}^{\text{II}}) = +0.71\text{V}$ vs $\text{Ag}/\text{AgCl}^{119}$ and $E_{1/2}(\text{Ir}^{\text{III}*}/\text{Ir}^{\text{II}}) = +1.21\text{V}$ vs SCE). The Ni(III) aryl alkoxide complex then underwent reductive elimination to give the aryl ether and a Ni(I) complex reduced by the Ir(II) intermediate to regenerate both catalysts.



Scheme 34. Photoassisted nickel catalyzed C-O bond formation

¹¹⁹ A. Klein, A. Kaiser, W. Wielandt, F. Belaj, E. Wendel, H. Bertagnolli and S. Záliš, *Inorg. Chem.*, 2008, **47**, 11324–11333.

2.4.2 Processes with radical formation: Catalysis of Downstream Steps

Catalysis of downstream steps involves radical formation by photoredox catalysis. This chemical species adds on the organometallic transition metal, generating a reactive metallic intermediate which can undergo reductive elimination or participate to electrophilic activation of multiple bonds for instance.

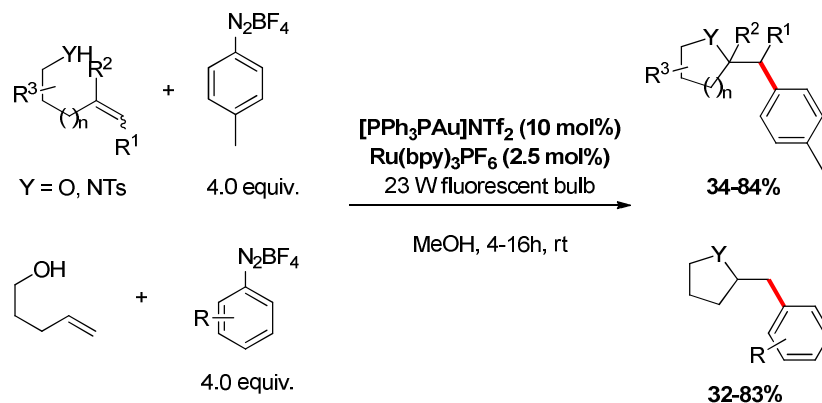
2.4.2.1 Gold mediated catalysis

Over the last years, gold catalysis has emerged as a powerful tool for the formation of cyclic systems, functionalization of alkenes, alkynes or allenes by nucleophilic addition reactions¹²⁰ and cross-coupling reactions. The latter involves a reductive elimination step from a Au(III) intermediate. In 2006, García and co-workers observed that benzyl and aryl radicals react with gold(I) complexes to afford organogold(III) species.¹²¹ This property has been exploited by Glorius to develop the first photoredox/gold dual catalysis.¹²² Aryldiazonium tetrafluoroborate salts were used as aryl radical precursors and Ru(bpy)₃(PF₆)₂ as photocatalyst under visible-light irradiation. The authors showed that the gold catalyst Ph₃AuNTf₂ was the most effective complex in methanol for tandem 5-*exo*-trig cyclization-arylation reactions of 4-penten-1-ol. The scope could be extended to 5-penten-1-ol and 5-penten-1-tosylamide. Various aryldiazoniums bearing substituents such as halogens, esters or methoxy groups led to the product formation of products in moderate to good yields (**Scheme 35**).

¹²⁰ For recent reviews on Gold catalysis see: (a) L. Fensterbank and M. Malacria, *Acc. Chem. Res.*, 2014, **47**, 953–965. (b) R. Dorel and A. M. Echavarren, *Chem. Rev.*, 2015, **115**, 9028–9072.

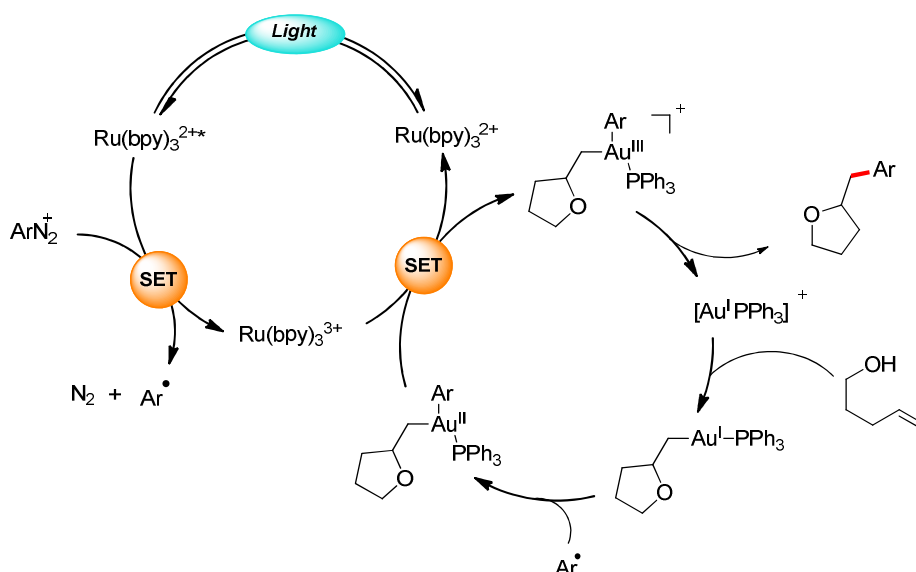
¹²¹ C. Aprile, M. Boronat, B. Ferrer, A. Corma and H. García, *J. Am. Chem. Soc.*, 2006, **128**, 8388–8389.

¹²² B. Sahoo, M. N. Hopkinson and F. Glorius, *J. Am. Chem. Soc.*, 2013, **135**, 5505–5508.



Scheme 35. Ru/Au catalyzed oxy/aminoarylation of alkenes

Regarding the mechanism, the starting cationic Au(I) coordinates to the alkene which gives a cyclic alkylgold(I) intermediate. The photoexcited Ru(II)* reduces the aryldiazonium to generate the aryl radical which adds on the alkylgold(I). The resulting Au(II) complex is then oxidized by Ru(III) to afford the key Au(III) intermediate. A reductive elimination step provides the final product and regenerates the initial Au(I) complex (**Scheme 36**).

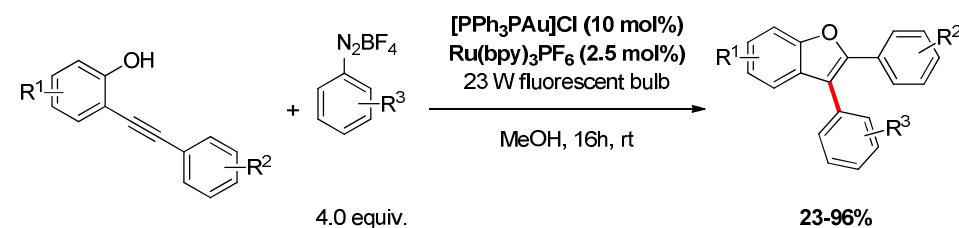


Scheme 36. Proposed mechanism for the Ru/Au dual catalysis

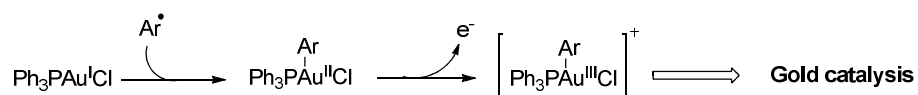
On the same line, our group realized a similar tandem process with *o*-alkynylphenols.¹²³ A neutral gold catalyst was used suggesting another possible pathway for the C-C bond

¹²³ Z. Xia, O. Khaled, V. Mouriès-Mansuy, C. Ollivier and L. Fensterbank, *J. Org. Chem.*, 2016, **81**, 7182–7190.

formation. The successive radical addition and oxidation steps would happen directly on the Ph_3PAuCl complex (**Scheme 37**). Then, the cationic Au(III) intermediate may promote the cyclization step by electrophilic activation of the triple bond and the reductive elimination leading to the C-C bond formation.



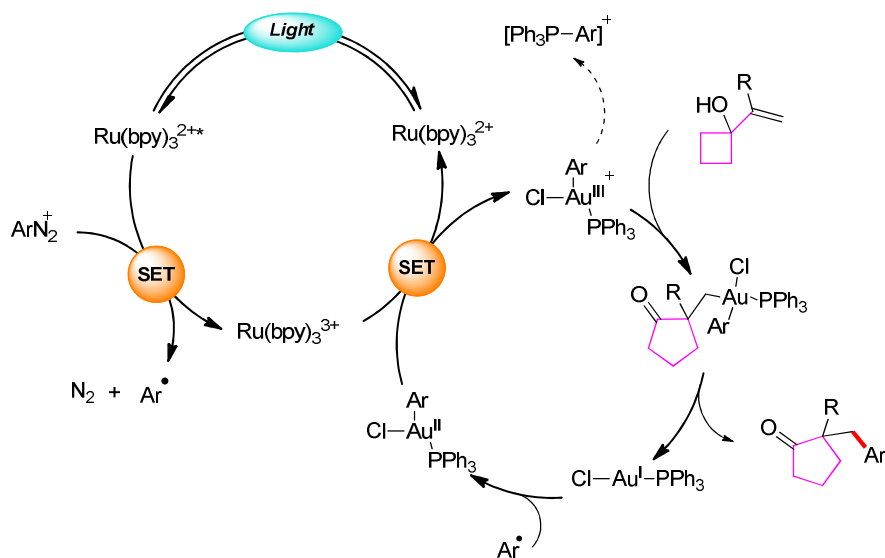
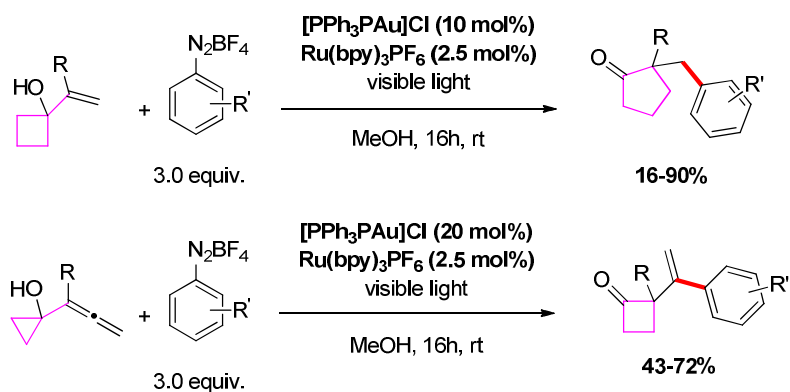
Other possible pathway



Scheme 37. Dual Photoredox/Gold catalysis arylation of *o*-alkynylphenols

This kind of pathway was first proposed by Toste for the arylation ring expansion cascade of alkenyl and allenyl cycloalkanols. Upon treatment with aryl diazonium salts, Ph_3PAuCl and $\text{Ru}(\text{bpy})_3(\text{PF}_6)_2$ as catalysts, aryl substituted cyclic ketones were obtained in low to good yields.¹²⁴ Regarding the mechanism (**Scheme 38**), the photoredox process is similar to the one proposed by Glorius, except that the neutral complex Ph_3PAuCl undergoes an addition of an aryl radical followed by oxidation with Ru(III). The resulting alkylgold(III) intermediate was proposed. Its formation was supported by the observation of $[\text{Ph}_3\text{P-Ph}]^+\text{BF}_4^-$ as a side product formed by reductive elimination. In the case of a fast coordination of the complex to the alkene or allene, the ring expansion may occur. Then, the reductive elimination affords the corresponding ketone and regenerates the starting Au(I) catalyst.

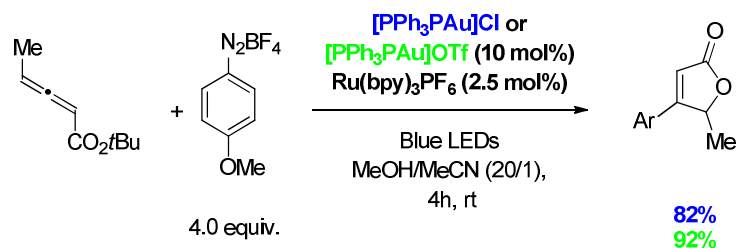
¹²⁴ X. Shu, M. Zhang, Y. He, H. Frei and F. D. Toste, *J. Am. Chem. Soc.*, 2014, **136**, 5844–5847.



Scheme 38. Photoredox/Gold catalyzed ring expansion-arylation reaction

Gold catalyzed transformation of allenes under photoredox conditions has also been reported by the group of Shin.¹²⁵ In the same way, allenoates could be converted to arylated furanone in the presence of a cationic gold complex, aryldiazonium salts and $\text{Ru}(\text{bpy})_3(\text{PF}_6)_2$. In the presence of a cationic gold(I) catalyst ($[\text{Ph}_3\text{PAu}]\text{OTf}$), allenoates are converted to a gold(I)-furanone intermediate. Then, the aryl radical addition and the oxidation step would generate the gold(III) complex which after reductive elimination liberates the arylated furanone and the starting gold(I) catalyst. (**Scheme 39**).

¹²⁵ D. V. Patil, H. Yun and S. Shin, *Adv. Synth. Catal.*, 2015, **357**, 2622–2628.



Scheme 39. Photoredox/Gold catalyzed cross-coupling of allenes with diazonium salts

The photoredox/gold dual catalysis has demonstrated its efficiency towards cross-coupling reactions with aryldiazonium salts. Moreover, the ability of gold to promote cyclizations or rearrangements and perform cross-coupling reactions depends mainly on the electrophilicity of the catalyst. Two mechanisms have been proposed depending on the nature of the starting gold catalyst (neutral or cationic).

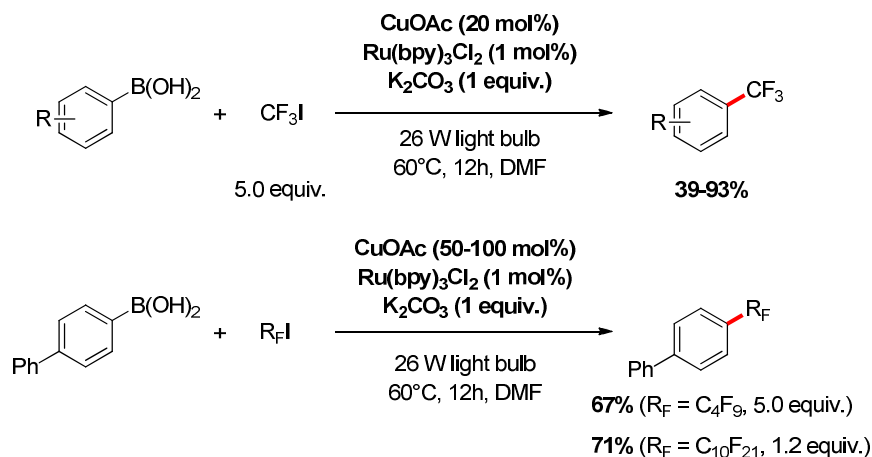
2.4.2.2 Copper-mediated catalysis

As mentioned in paragraph 2.2, copper is also an efficient radical trapping agent. After her pioneering works with palladium on dual catalysis, Sanford developed a copper-catalyzed trifluoromethylation of arylboronic acids. This known reaction usually required expensive trifluoromethylating agents or stoichiometric amounts of copper.¹²⁶ For these reasons, they choose CF_3I which can be reduced in the presence of $\text{Ru}(\text{bpy})_3(\text{PF}_6)_2$ as photoredox catalyst to a $\text{CF}_3\cdot$ radical,^{41,127} and a copper catalyst (20 mol% of $\text{Cu}(\text{OAc})$) to obtain the cross-coupling products.¹²⁸ Various aryl and heteroaryl (pyridine, furane, quinoline) boronic acids could be trifluoromethylated (**Scheme 40**). Electron-rich and electron-poor electrophiles were tolerated and converted to the expected products in moderate to excellent yields. In addition, perfluoroalkyl iodides were also suitable partners. However, with these materials, the loading of copper must be drastically increased to get satisfactory yields.

¹²⁶ (a) T. Liu and Q. Shen, *Org. Lett.*, 2011, **13**, 2342–2345. (b) J. Xu, D.-F. Luo, B. Xiao, Z.-J. Liu, T.-J. Gong, Y. Fu and L. Liu, *Chem. Commun.*, 2011, **47**, 4300. (c) C.-P. Zhang, J. Cai, C.-B. Zhou, X.-P. Wang, X. Zheng, Y.-C. Gu and J.-C. Xiao, *Chem. Commun.*, 2011, **47**, 9516.

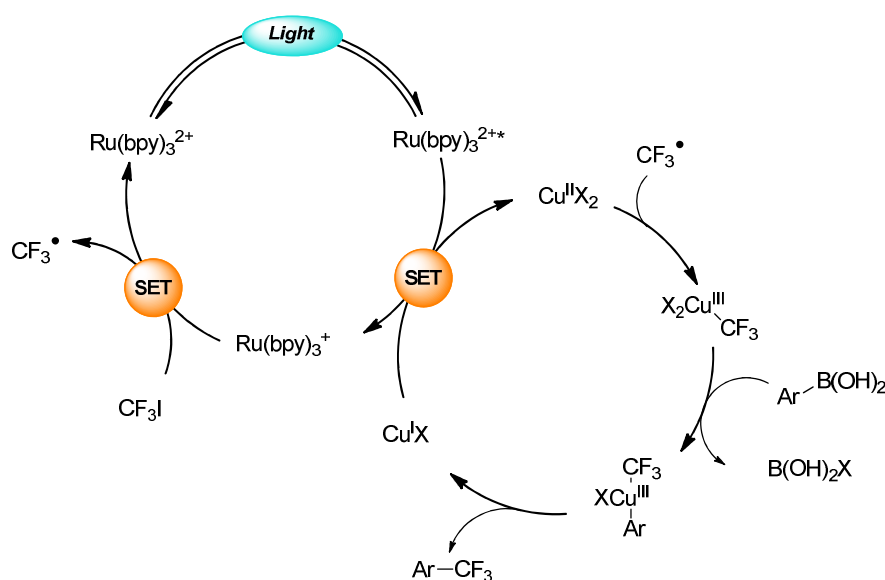
¹²⁷ P. V. Pham, D. A. Nagib and D. W. C. MacMillan, *Angew. Chem. Int. Ed.*, 2011, **50**, 6119–6122.

¹²⁸ Y. Ye, M. S. Sanford, *J. Am. Chem. Soc.*, 2012, **134**, 9034–9037.



Scheme 40. Photoredox/copper-catalyzed trifluoromethylation and perfluoroalkylation of boronic acids

Concerning the mechanism, the authors proposed a SET between the photoexcited Ru(II)* and Cu(OAc) to Ru(I) and Cu(II) complexes. The resulting Ru(I) then reduces CF₃I to produce the CF₃ radical which adds on the intermediate Cu(II). With the new complex Cu(III)-CF₃, the boronic acid may undergo transmetalation giving the transient complex [aryl-Cu(III)-CF₃]. After a reductive elimination, the adduct aryl-CF₃ is released and the starting Copper(I) salt is regenerated (**Scheme 41**).



Scheme 41. Possible mechanism for the Cu/Ru-catalyzed trifluoromethylation

2.5 Conclusion

The combination of photoredox catalysis and organometallic catalysis has shown to be a highly versatile approach for the construction of a wide range of molecular scaffolds. The overall methodology involves either only electron transfers between both catalysts, or with an additional radical trapping step by the organometallic catalyst. Various transition metals including palladium, gold and copper can be used to perform cyclizations or cross-coupling reactions via C-H or C-X bond activation. Nickel complexes have also widely participated to such type of transformations. These processes will be detailed in chapter four.

Chapter III

Oxidation of alkyl bis-catecholato silicates: a mild way for the formation of carbon centered radicals

3 Chapter III

Oxidation of alkyl bis-catecholato silicates: a mild way for the formation of carbon centered radicals

3.1 Definition of silicates

Silicon is the most abundant element by mass in earth's crust. Even if pure silicon (0) is widely used for its application in electronics, as semiconductor, it is commonly found combined with oxygens in minerals called "silicates" which contains the silicate ion $((\text{SiO}_4)^{4-})$ associated with metal oxides. However, in some minerals, the silicon-oxygen ratio is different than 1:4 due to the oligomerization of $((\text{SiO}_4)^{4-})$ monomers. In some extent, a silicon atom surrounded by 4 oxygen atoms is considered as a silicate. According to IUPAC nomenclature, an organic-containing silicate is a molecule with the general structure $(\text{RO})_a\text{Si}(\text{B})_b(\text{C})_c(\text{D})_d$, where R, B, C and D are organic moieties and $a+b+c+d = 4$.¹²⁹ However, since silicon can reach penta- and hexavalency with alkoxy or fluoride ligands, this definition is biased. Consequently, hypervalent silicon species bearing such groups are considered as silicates as well. Thus, pentacoordinate silicon species with 4 alkoxy ligands and 1 organic substituent are so called silicates (Figure 5).

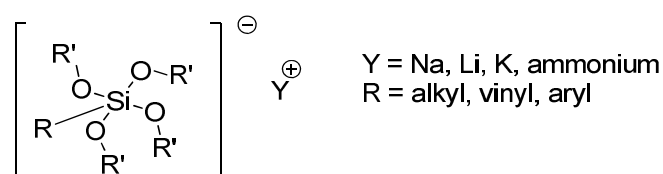


Figure 5. General representation of organic silicates

3.2 Oxidation of hypercoordinate silicon compounds

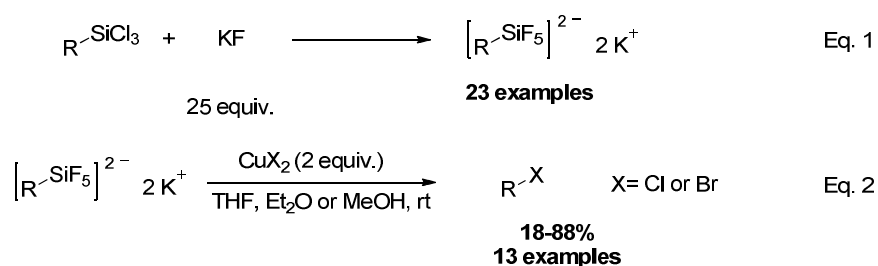
Hypercoordinated silicon compounds containing one, two or three alkyl residues have shown various reactivities for the formation of synthetic scaffolds. Indeed, these silicon

¹²⁹ <https://goldbook.iupac.org/html/O/OT07579.html>

derivative substrates have been especially engaged with nucleophiles,¹³⁰ used as Lewis acids¹³¹ for the activation of carbonyl compounds, or involved in Hiyama type cross-coupling reactions.¹³² Also, the *in situ* formation of such compounds led to the same kind of reactivity. Furthermore, anionic penta- and hexacoordinated silicon compounds display a negative charge which gives them a reductant feature which has been investigated

3.2.1 Metal mediated oxidation of organopentafluorosilicates

It is well established that the fluoride ion has the strongest affinity with silicon. Taking advantage of this property, the synthesis of hypercoordinated silicon compounds containing several fluorine atoms can be easily prepared by treatment of chlorosilane with a fluoride salt. Inspired by the work of Tansjö,¹³³ Kumada and co-workers¹³⁴ reported in 1982 the first efficient synthesis of organopentafluorosilicates. By treating a large panel of trichlorosilanes by potassium fluoride in aqueous conditions, they could synthesize a wide range of organopentafluorosilicates (**Scheme 42** Eq. 1).



Scheme 42. Synthesis and copper mediated oxidation of organopentafluorosilicates

¹³⁰ (a) A. Boudin, G. Cerveau, C. Chuit, R. J. P. Corriu and C. Reye, *Angew. Chem. Int. Ed. Engl.*, 1986, **25**, 473–474. (b) J. P. Corriu, C. Guerin, B. Henner and Q. Wang, *Organometallics*, 1991, **10**, 2297–2303. (c) C. Breliere, R. J. P. Corriu, G. Royo, W. W. C. Wong Chi Man and J. Zwecker, *Organometallics*, 1990, **9**, 2633–2635. (d) Voronkov, V.M Dyakov and S.V,Kirpichenko, *Journal of Organometallic Chemistry*, 1982, **233**, 1–147. (e) R. Müller, *Z. Chem.*, 1965, **99**, 1614.

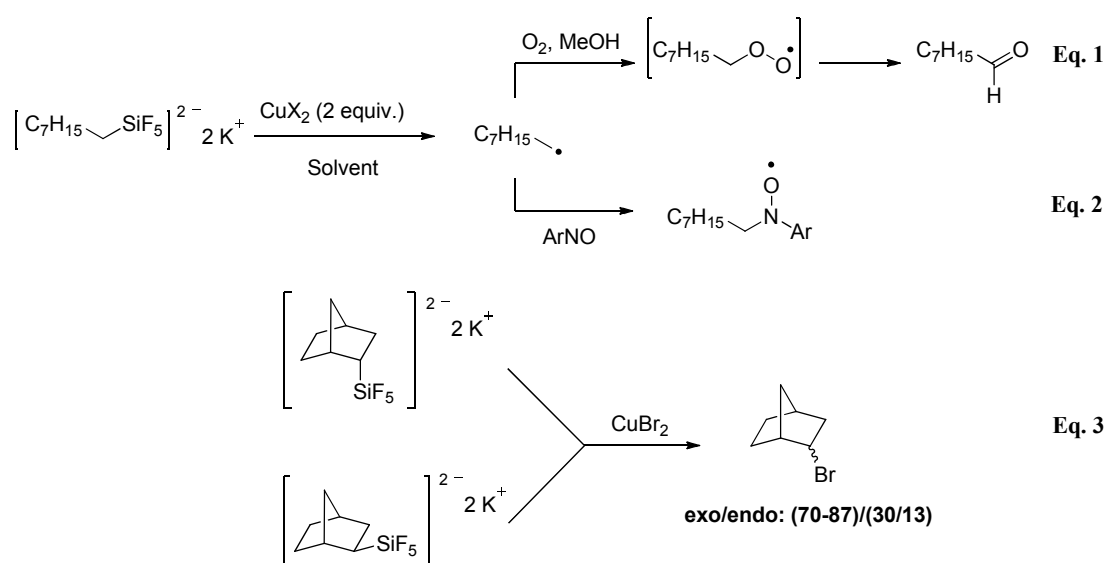
¹³¹ (a) G. Cerveau, C. Chuit, R. J. P. Corriu and C. Reye, *J. Organomet. Chem.*, 1987, **328**, C17–C20. (b) M. Kira, K. Sato and H. Sakurai, *J. Am. Chem. Soc.*, 1988, **110**, 4599–4602. (c) G. Majetich, A. Casares, D. Chapman and M. Behnke, *J. Org. Chem.*, 1986, **51**, 1745–1753.

¹³² (a) Y. Hatanaka and T. Hiyama, *J. Org. Chem.*, 1988, **53**, 918–920. (b) K. Hirabayashi, J. Kawashima, Y. Nishihara, A. Mori and T. Hiyama, *Org. Lett.*, 1999, **1**, 299–302. (c) S. E. Denmark and D. Wehrli, *Org. Lett.*, 2000, **2**, 565–568.

¹³³ L. Tansjö, *Acta Chem.Scand.*, 1961, **15**, 1583.

¹³⁴ K. Tamao, J. Yoshida, H. Yamamoto, T. Kakui, H. Matsumoto, M. Takahashi, A. Kurita, Murata and M. Kumada, *Organometallics*, 1982, **1**, 355–368.

Some of the synthesized silicates were engaged with stoichiometric amount of copper halide salts (CuCl_2 and CuBr_2). They showed that upon treatment in ether, THF or methanol, the alkylpentafluorosilicates were converted into the corresponding alkyl halides in low to good yields, depending on the nature of the starting copper salt (**Scheme 42** Eq. 2). Investigating the mechanism of the reaction, they evidenced of a radical pathway. When the reaction was performed with octylpentafluorosilicate and copper chloride in methanol under an oxygen atmosphere, they observed the formation of octanal. The octanylperoxy radical obtained from reaction of the octanyl radical with molecular oxygen, would produce octanal and octanol after dismutation (**Scheme 43** Eq. 1). Spin trapping experiments with nitrosobenzene derivatives revealed the formation of an *N*-oxyl radical confirmed by ESR (Eq. 2). Finally, treating pure *exo*- and *endo*-2-norbornylpentafluorosilicates with copper(II) bromide gave a mixture of *exo*- and *endo*-2-norbornyl bromide in an *exo/endo* ratio of (70-87)/(30-13) (Eq. 3). This epimerization suggests the formation of a planar radical intermediate. Moreover, the obtained ratios were similar to the literature on the formation of a 2-norbornyl radical.¹³⁵

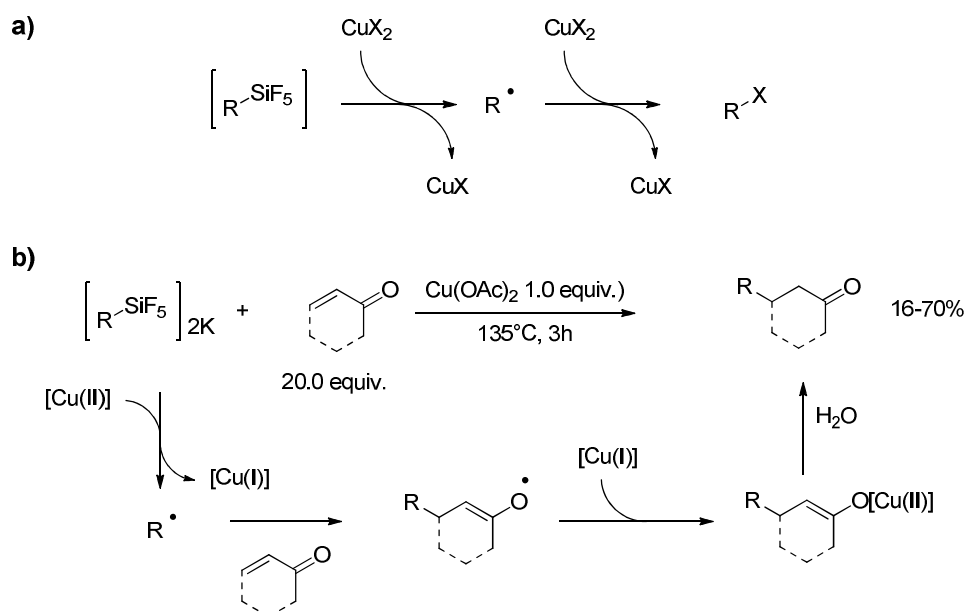


Scheme 43. Investigation on the mechanism of oxidation of organopentafluorosilicates

¹³⁵ (a) E. C. Kooyman and G. C. Vegter, *Tetrahedron*, 1958, **4**, 382–392. (b) F. D. Greene, C.-C. Chu and J. Walia, *J. Org. Chem.*, 1964, **29**, 1285–1289.

Finally, the proposed mechanism starts with a direct oxidation of the silicate by the copper(II) halide giving the radical and a copper(I). Another equivalent of copper(II) halide is required to generate the final alkyl halide (**Scheme 44 a**).

The methodology was then extended to radical conjugate addition processes. To limit the formation of alkyl halide, copper(II) acetate was used as oxidant. The radicals were involved in Giese-type reactions with various α,β unsaturated carbonyl compounds (**Scheme 44 b**).



Scheme 44. Mechanism of the oxidation of organopentafluorosilicates

Copper(II)-mediated oxidation of alkylpentafluorosilicates is the first process involving the formation of a carbon centered radical after fragmentation of the carbon-silicon bond of silicates. During the following twenty years, no other evidence about the oxidation of hypercoordinated silicon species was reported.

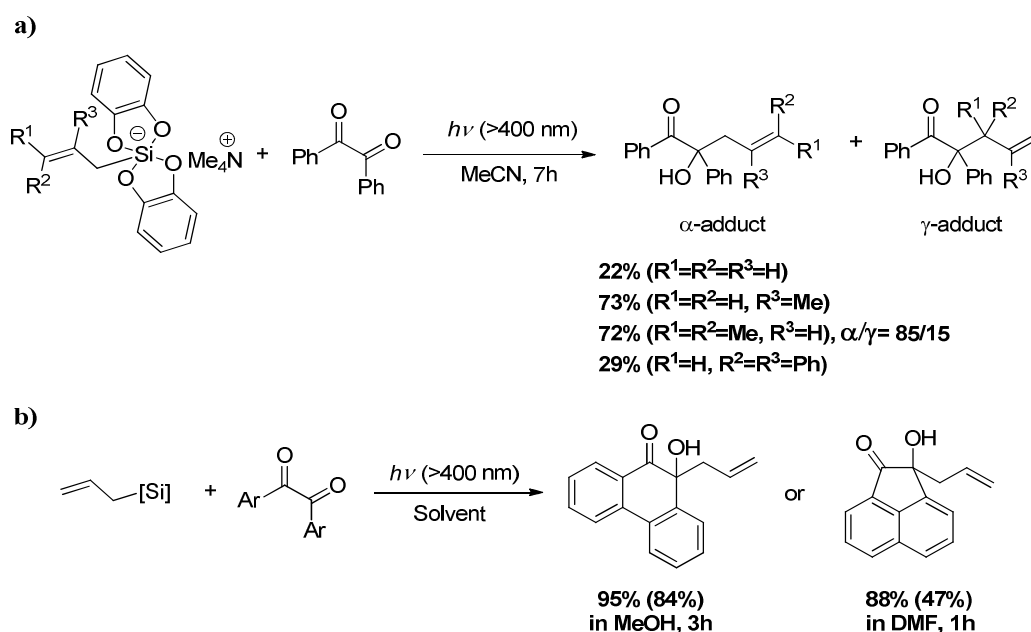
3.2.2 Photon-induced electron transfers with alkyl bis-catecholato silicates

Among the variety of hypercoordinated silicon compounds, the alkyl bis-catecholato silicates have shown interesting features for synthetic applications.^{131a,b,136} In 2005, Nishigaishi reported the first example of oxidation of such species.¹³⁷ When he engaged benzil or benzil derivatives with tetramethylammonium bis-catecholato allylsilicate

¹³⁶ (a) A. Hosomi, S. Kohra and Y. Tominaga, *J. Chem. Soc. Chem. Commun.*, 1987, 1517–1518. (b) A. Boudin, G. Cerveau, C. Chuit, R. J. P. Corriu and C. Reye, *Bull. Chem. Soc. Jpn.*, 1988, **61**, 101–106.

¹³⁷ Y. Nishigaishi, A. Suzuki, T. Saito and A. Takuwa, *Tetrahedron Lett.*, 2005, **46**, 5149–5151.

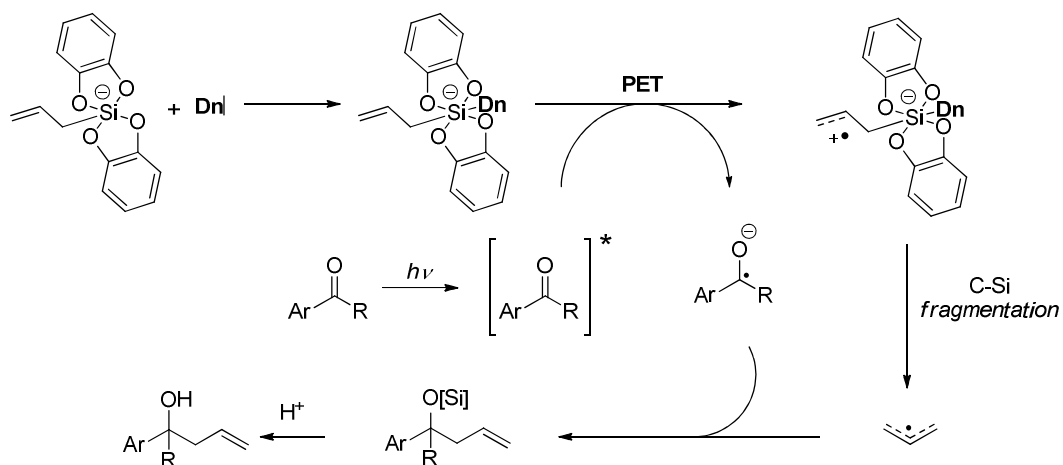
derivatives under light irradiation in acetonitrile, he could observe the formation of homoallylic alcohols in fair to good yields (**Scheme 45**). To rationalize the result, in the case of $R^1=R^2=Me$, $R^3=H$, he assumed that the major formation of the α -adduct comes from a Photo-induced Electron Transfer (PET) between the benzil and the bis-catecholato allylsilicate. To have a better mechanistic insight of the reaction, he performed solvent studies¹³⁸ and found that coordinating solvents such as DMF or methanol or additives (pyridine, imidazole, *n*-butylamine, DMF) drastically improved the yield of the reaction.



Scheme 45. Photo-induced Electron Transfer between allylsilicates and diketones

Regarding the mechanism, he proposed that the diketone absorbs the light and oxidizes the silicate to give a ketyl radical and the allyl radical cation. After fragmentation of the carbon-silicon bond, the allyl radical is released and the radical coupling with the diketone gives the homoallylic alcohol. Moreover, a donor molecule (MeOH, DMF) would generate a hexacoordinated silicon center which is more electron rich, increasing the reactivity of the silicate towards the oxidation step¹³⁸ (**Scheme 46**).

¹³⁸ Y. Nishigaichi, A. Suzuki and A. Takuwa, *Tetrahedron Lett.*, 2007, **48**, 211–214.



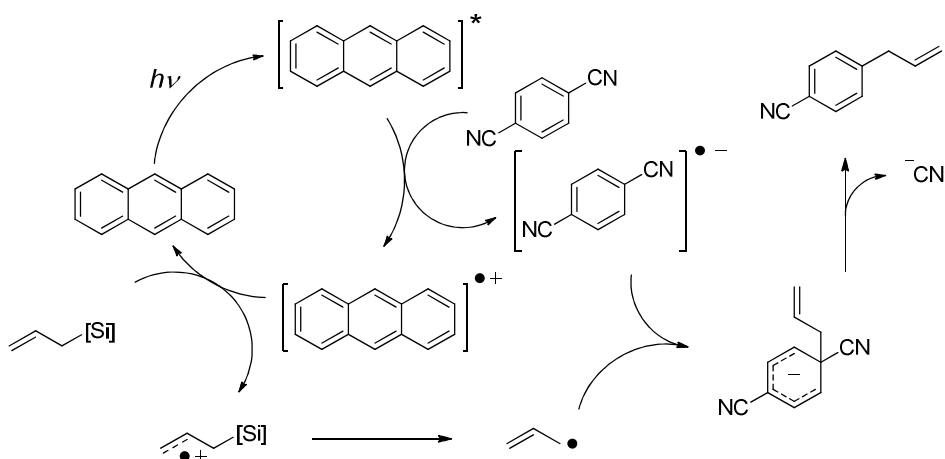
Scheme 46. Mechanism of photoallylation of the allyl bis-catecholato silicate

More recently, Nishigaichi also reported the oxidation of the allyl bis-catecholato silicate by anthracene under UV light irradiation and its reactivity towards dicyanoarenes in photosubstitution.¹³⁹ Considering the oxidation potential of allyl bis-catecholato silicate (+1.12V)¹³⁷ and the reduction potential of 1,4-dicyanobenzene (-1.53V)¹⁴⁰, he found that anthracene¹⁴¹ would be able to oxidize and reduce both partners respectively under UV light irradiation. He proposed that the photo-excited anthracene reduces the 1,4-dicyanobenzene by a Photon-induced Electron Transfer resulting in the formation of an aryl radical anion. The cationic anthracene would oxidize the silicate to provide the allyl radical. After a radical coupling and cyanide, the intermediate gives the final allylcyanobenzene (**Scheme 47**).

¹³⁹ D. Matsuoka and Y. Nishigaichi, *Chem. Lett.*, 2014, **43**, 559–561.

¹⁴⁰ A. A. Isse and A. Gennaro, *J. Phys. Chem. A*, 2004, **108**, 4180–4186.

¹⁴¹ M. Montalti, A. Credi, L. Prodi and M. T. Gandolfi, *Handbook of Photochemistry*, 3rd ed., Taylor & Francis, Boca Raton, 2006.



Scheme 47. Mechanism for allylation of dicyanoarenes

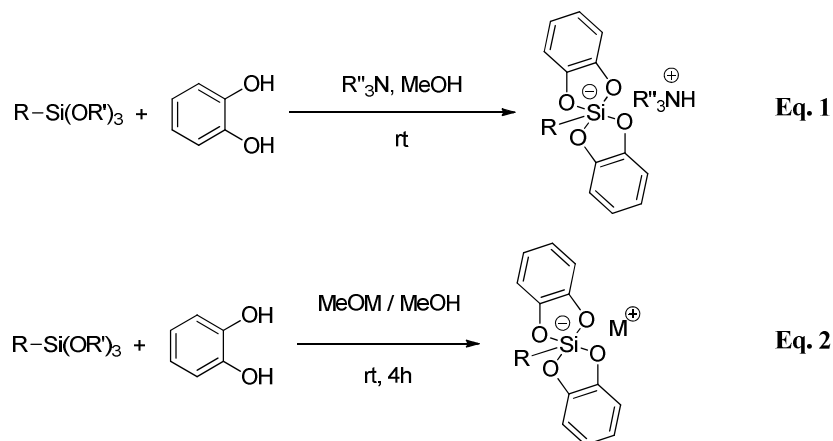
3.3 Alkyl bis-catecholato silicates in synthesis

3.3.1 Formation of alkyl bis-catecholato silicates

Pentacoordinated silicon species such as alkyl bis-catecholato silicates were first synthesized in the 60's by Cecil L. Frye¹⁴². When he treated an alkyl trialkoxysilane by catechol with a tertiary amine in methanol, he obtained the corresponding ammonium alkyl bis-catecholato silicates. Among the bases used for the synthesis, he also demonstrated that pyridine or quaternary ammonium hydroxide were also effective (**Scheme 48** Eq.1). At the end of the 80's Corriu,^{136b,143} inspired by the work of Frye, reported the synthesis of alkaline alkyl bis-catecholato silicates. Instead of using amines as base he proposed to use methanolic solution of sodium or potassium methoxide to get the corresponding sodium and potassium silicates (**Scheme 48** Eq.2).

¹⁴² C. L. Frye, *J. Am. Chem. Soc.*, 1964, **86**, 3170–3171.

¹⁴³ G. Cerveau, C. Chuit, R. J. P. Corriu, L. Gerbier, C. Reye, J.-L. Aubagnac, B. El Amrani, *Int. J. Mass Spectrom. Ion Phys.* 1988, **82**, 259.



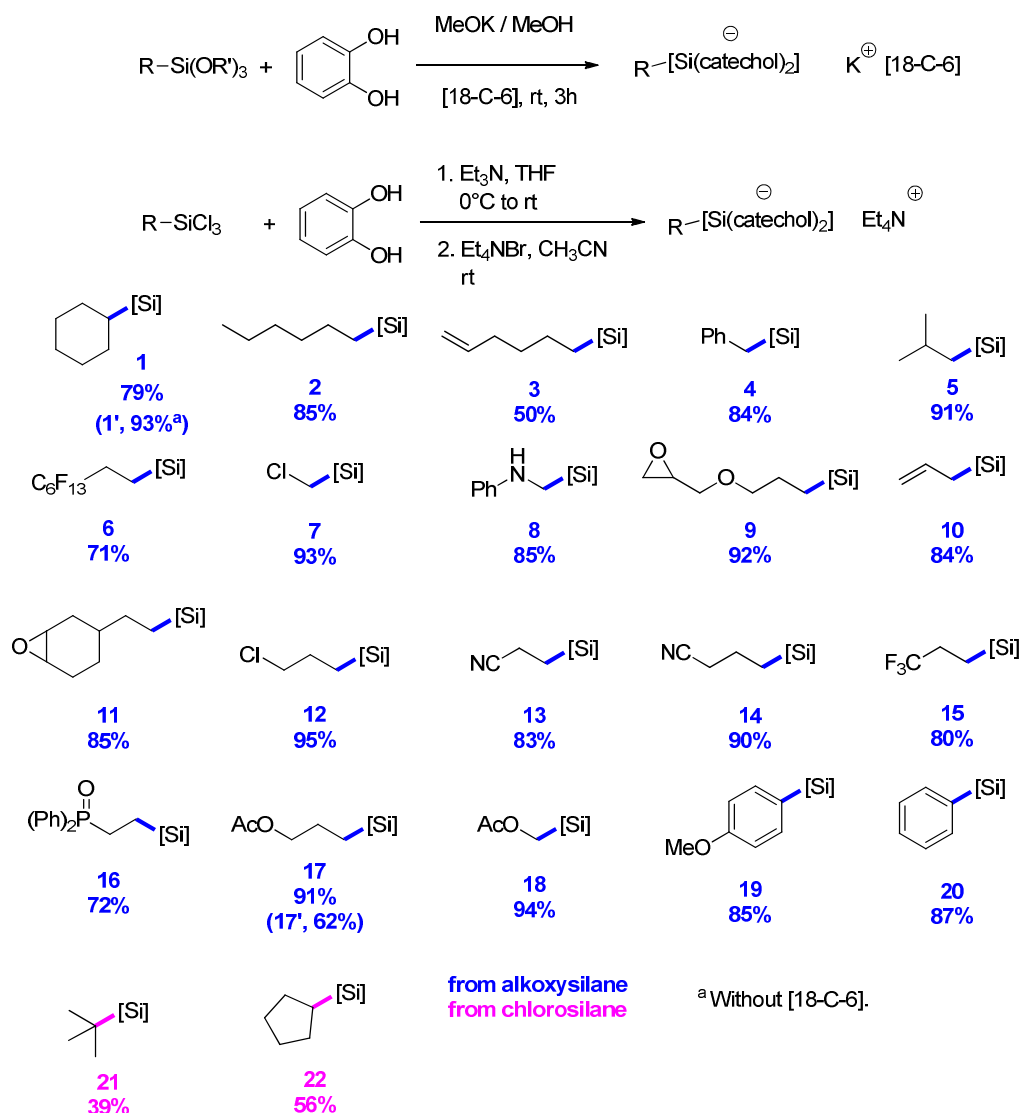
Scheme 48. First synthesis of alkyl bis-catecholato silicates

In our laboratory, we decided to apply these methods with modifications. Indeed, we found that the potassium version of these silicates is not stable. In less than one week, we observed a slow decomposition of the silicates. In order to stabilize them, we envisioned to add a [18-C-6] crown ether to intensify the hypervalent bond by charge separation^{144a} (**Scheme 49**). With this modification, we avoided the introduction of water in the solid and we managed to synthesize a wide range of primary (**2-18**), secondary (**1**, **1'** and **22**), tertiary (**21**) and aryl (**19-20**) silicates and store them on the bench for months.^{32a,144}

About the ammonium version, we decided to develop a straightforward synthesis of tetraalkylammonium silicates. So, starting from trichlorosilane, catechol and a tertiary amine in THF, the triethylammonium silicates were obtained. Then a metathesis performed with tetraethylammonium bromide in acetonitrile gave the tetraethylammonium silicates (**21** and **22**).

With this easy synthetic approach, primary, secondary and tertiary alkylsilicates as well as arylsilicates were obtained in moderate to excellent yields.

¹⁴⁴ (a) V. Corcé, L.-M. Chamoreau, E. Derat, J.-P. Goddard, C. Ollivier and L. Fensterbank *Angew.Chem. Int.Ed.* 2015, **54**, 11414–11418. (b) C.Lévêque, L. Chénneberg, V. Corcé, J.-P. Goddard, C. Ollivier and L. Fensterbank, *Org. Chem. Front.*, 2016, **3**, 462-465.



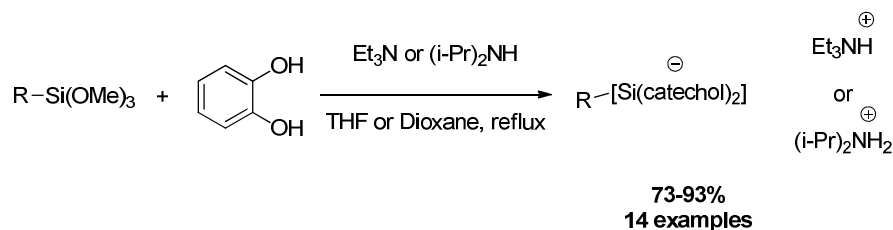
Scheme 49. Modified synthesis of alkyl bis-catecholato silicates and scope synthesis

All the silicates can be categorized into 4 groups: the activated silicates, secondary silicates, primary silicates and aryl silicates. Tertiary, benzyl and allylsilicates and silicates substituted in α position by a hetero atom will be all considered as activated silicates.

It has to be noted that the group of Molander reported the synthesis of ammonium silicates without performing any metathesis step.¹⁴⁵ The alkoxy silanes were treated by catechol and triethylamine or diisopropylamine in THF or dioxane according to the Frye's

¹⁴⁵ M Jouffroy, D N. Primer and G A. Molander, *J. Am. Chem. Soc.*, 2016, **138**, 475-478.

procedure (**Scheme 50**). They were able to get primary and secondary alkyl silicates in good yields but with questionable stabilities.



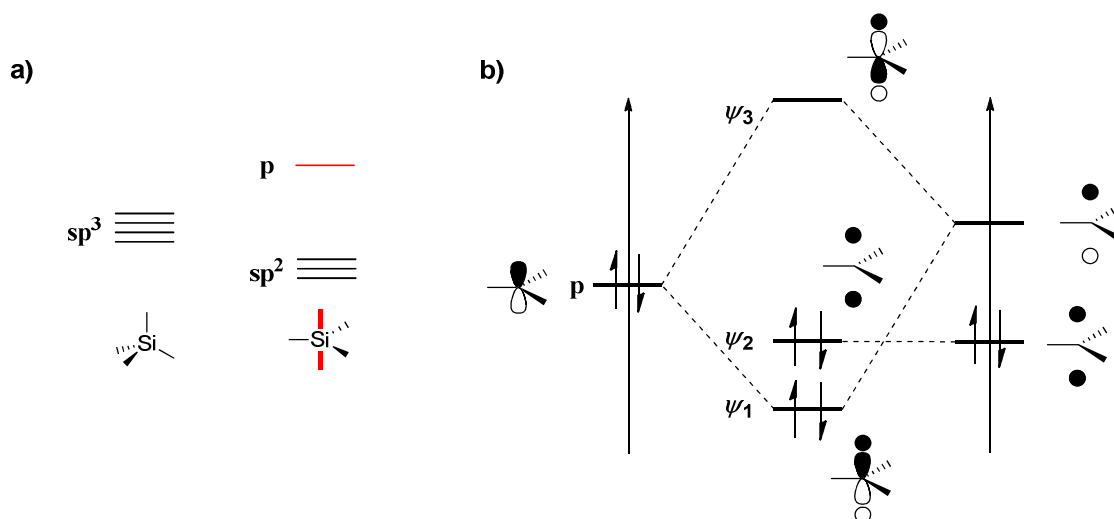
Scheme 50. Molander's Ammonium silicates synthesis

3.3.2 Structural analysis and properties

3.3.2.1 Hypercoordination of the silicon atom in alkyl bis-catecholato silicates

Like the element carbon, silicon is tetracoordinated in a tetrahedral geometry respecting the octet rule. Nevertheless, silicon can extend its coordination to 5 and 6 with a trigonal bipyramidal or pyramidal square base structure, and octahedral structure respectively around the silicon. We will not consider the hexacoordinated silicon species in this part.

In the case of a pentacoordinated silicon atom, a p orbital is engaged in a hypervalent three-center four-electron (3c-4e) bonding giving the hypervalent bonds. Indeed, on a tetrahedral geometry, 4 hybridized sp orbitals of the silicon interact with the ligands. If the silicon atom is pentavalent 3 sp orbitals interact with three ligands while a non-hybridized p orbital interacts with two ligands (**Scheme 51 a**). The combination of three atomic orbitals (two s orbitals from the ligand and a p orbital from the central atom) creates three molecular orbitals: a bonding (ψ_1), a nonbonding (ψ_2) and an antibonding orbital (ψ_3). The HOMO of the system (ψ_2) has an electron density localized on the ligand while a node is on the central atom (**Scheme 51 b**). On an empirically qualitative aspect, the formation of hypervalent bonds occurs if a strong electronic affinity between the donor atom and the ligand exists. For this reason, hypercoordinated silicon species containing Si-O or Si-F bonds are frequently encountered.



Scheme 51. a) Hybridization of silicon orbitals. b) Molecular orbital diagram of 3c-4e interaction.

The [18-C-6] potassium alkyl bis-catecholato silicates was crystallized and analyzed by X-ray diffraction. We observed that the stability of these silicates depends on the interaction with the potassium. Even if the crown ether, modify de near environment of the potassium, the bond lengths of the Si-O and Si-C are not importantly modified (Table 1). The effect is more noticeable for the C-Si-O and O-Si-O angles. According to the values, the potassium cyclohexyl bis-catecholato silicate crystallize in a trigonal bipyramidal structure whereas the [18-C-6] cyclohexyl bis-catecholato silicate (**1**) is almost in a pyramidal square base structure.

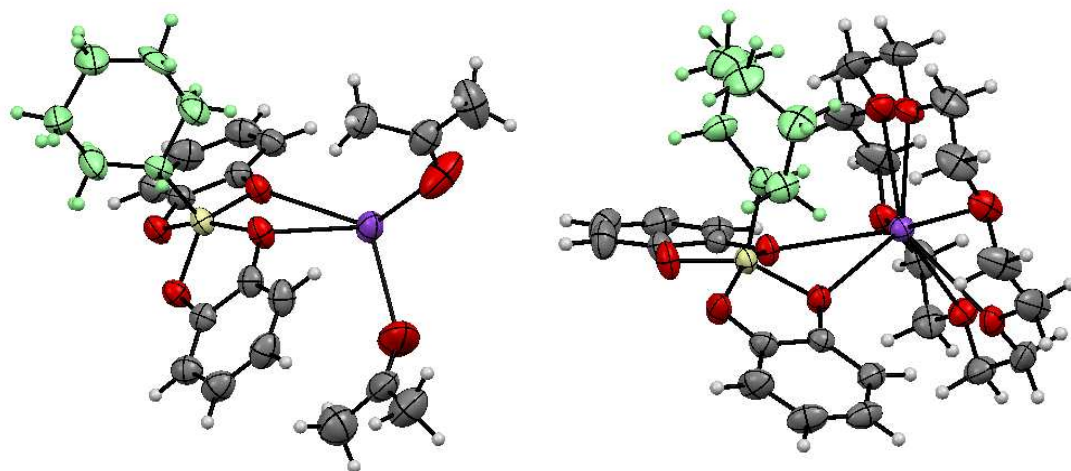
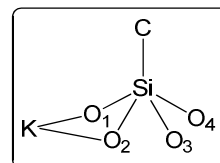


Figure 6. Crystal structures of potassium cyclohexyl bis-catecholato silicates with acetone (left **1'**) and [18-C-6] (right **1**)

Table 1. Crystallographic data around the silicon for the cyclohexyl silicates

Silicate	d_{C-Si} (Å)	d_{O-Si} (Å)	α_{C-Si-O} (°)	α_{O-Si-O} (°)
With acetone	1.880	O ₁ : 1.778 O ₂ : 1.737 O ₃ : 1.776 O ₄ : 1.735	O ₁ : 93.48 O ₂ : 116.35 O ₃ : 105.75 O ₄ : 105.98	O ₁ -O ₃ : 160.64 O ₂ -O ₄ : 137.40
With [18-C-6]	1.883	O ₁ : 1.749 O ₂ : 1.769 O ₃ : 1.743 O ₄ : 1.743	O ₁ : 103.61 O ₂ : 103.61 O ₃ : 106.88 O ₄ : 106.88	O ₁ -O ₃ : 149.51 O ₂ -O ₄ : 149.51



3.3.2.2 Redox properties

Even if the redox potential is a thermodynamic value and does not give any information about the kinetic of the reaction, it is important to know in photocatalysis the redox properties of the substrates. Indeed, these data inform us about the feasibility of a considered reaction. Some electrochemical experiments were realized on all the synthesized silicates. Activated silicates showed to be the easiest to oxidize ($E^{\text{ox}} = +0,34 \text{ } +0,72 \text{ V vs SCE}$) followed by the secondary silicates ($E^{\text{ox}} = +0,69 \text{ } +0,76 \text{ V vs SCE}$), primary silicates ($E^{\text{ox}} = +0,74 \text{ } +0,90 \text{ V vs SCE}$) and the aryl silicates ($E^{\text{ox}} > +0,88\text{V vs SCE}$) (**Figure 7**). If we envisage that the silicates may undergo homolytic fragmentation of the C-Si bond to provide the carbon centered radicals, the stability of the radicals seem linked to the oxidation facility of the corresponding silicates.

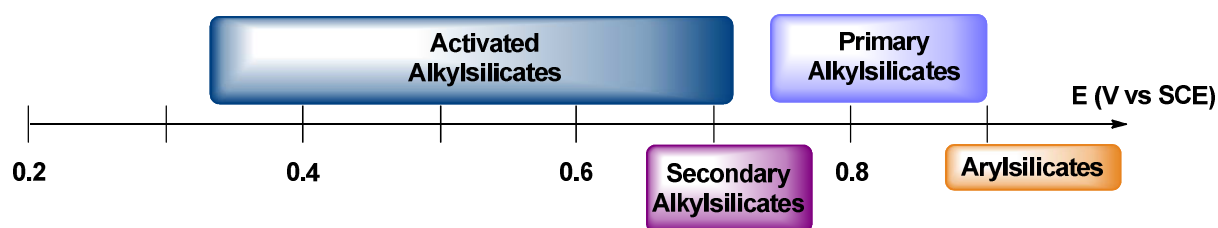


Figure 7. Scale of the oxidation potential of the silicates

Regarding the oxidation process, DFT calculations revealed that the oxidation likely occurs on a catechol ring of the silicates. The resulting catechol radical is then highly delocalized and so stabilized. Prokof'ev and co-workers¹⁴⁶ showed by ESR experiments of penta-coordinated bis-(3,6-ditertbutylcatecholato) silicates derivatives that the radical of this species is especially localized on the four oxygen atoms (Figure 8). The presence of the *tert*-butyl group on the catechol ring was chosen to increase the kinetic stability of the radicals and to simplify the ESR spectrum. Nevertheless, in their case and ours, the radical may also be delocalized on both rings, increasing the number of mesomeric form and so the stability of the radical. Moreover, the calculations revealed that the BDE of the C-Si bond becomes low

¹⁴⁶ A.I. Prokof'ev, T.I. Prokof'eva, I.S. Belostotskaya, N.N. Bubnov, S.P. Solodovnikov, V.V. Ershov, M.I. Kabachnik *Tetrahedron*, 1979, **35**, 24712482

enough to observe the homolytic fragmentation (Table 2) and give the free radical by an irreversible radical substitution on the silicon of the phenoxyl radical.

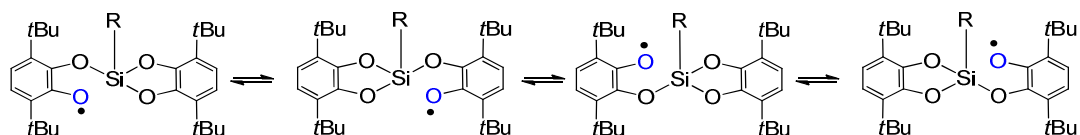


Figure 8. Valence tautomerism of bis-(3,6-ditertbutylcatecholato) silicate radicals

Table 2. Calculated BDE of C-Si bond (before/after oxidation)

Carbon chain	C-Si BDE* (kcal/mol)
n-hexyl	88.8/ 23.8
cyclohexyl	86.0/ 20.3
benzyl	79.8/ 13.8
PhNHCH ₂	86.3/ 17.0
phenyl	104.1/ 37.5

Even though these silicates are easy to oxidize, the difference of redox potentials is not well rationalized. Since the oxidation is considered to occur on the catechol ring, the oxidation potential must be only depending on the electron density on the catechol which must be the same for all the silicates. Indeed, no electron withdrawing or donating group was added on the ligand. Considering an orbital approach, the oxidation process takes out an electron of the HOMO of the silicate localized on the catechol rings. The higher is the energy level of the HOMO the lower is the oxidation potential. Actually, the HOMO-1 is representative of the C-Si bond. In term of energy, if the HOMO-1 energy level increases, the one of the HOMO increases also. In consequence, different kind of alkyl group would not have the same effect on the oxidation potential of the silicates. In addition, Nishigaishi reported that coordinating solvent would facilitate the oxidation of the silicates.¹³⁸ Coordination of the DMF to the silicon is therefore possible. Probably a combination of both effects would drastically modify the oxidation potential of the silicates.

3.4 Studies on photooxidation of alkyl bis-catecholato silicates

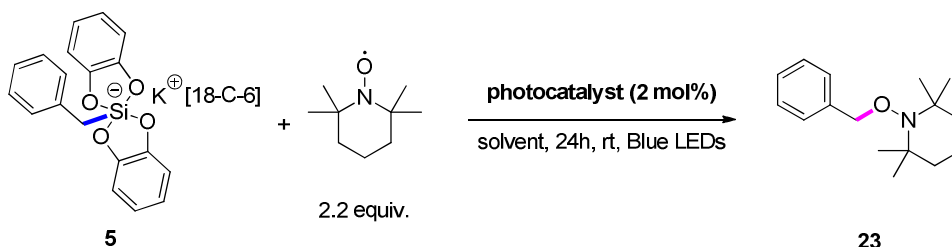
Bis-catecholato silicates offer many advantages in terms of preparation and stability. They also display interesting low oxidation potentials (~0.3 – 0.9V vs SCE). The very mild and more sustainable conditions, offered by photoredox catalysis, were strongly appealing. We have realized some investigations about the generation of radicals by photooxidation of alkyl bis-catecholato silicates.^{144a}

3.4.1 Photooxidation by polypyridine transition metal photocatalysts

Prior to engage the [18-C-6] potassium alkyl bis-catecholato silicates in radical carbon-carbon bond forming reactions, the generation of alkyl radicals was proved by spin-trapping experiment with TEMPO. It is known that TEMPO is a good radical scavenger that quickly reacts with carbon centered radicals.¹⁴⁷ To get a representative result, benzylsilicate**5** was chosen due to its low oxidation potential. It was found that the benzylsilicate reacts with TEMPO (2.2 equivalent) in the presence of 2 mol% of Ir[(dF(CF₃)ppy)₂(bpy)](PF₆) in DMF for 24 hours under light irradiation (477 nm) at room temperature to afford the benzyl-TEMPO adduct **23** in 95% yield (**Table 3**). This result demonstrates that the benzylsilicate is an excellent precursor of a benzyl radical under visible-light photooxidative conditions.

¹⁴⁷ V. W. Bowry and K. U. Ingold, *J. Am. Chem. Soc.*, 1992, **114**, 4992–4996.

Table 3. Optimization of photooxidation of benzylsilicate and spin-trapping experiments with TEMPO



Entry	Photocatalyst	Solvent	Yield ^a
1	Ru(bpy) ₃ (PF ₆) ₂	Acetone	34%
2	Ir[(dF(CF ₃)ppy) ₂ (dtbbpy)](PF ₆)	Acetone	34%
3	Ir[(dF(CF ₃)ppy) ₂ (bpy)](PF ₆)	Acetone	38%
4	Ru(bpy) ₃ (PF ₆) ₂	Acetonitrile	25%
5	Ir[(dF(CF ₃)ppy) ₂ (dtbbpy)](PF ₆)	Acetonitrile	20%
6	Ir[(dF(CF ₃)ppy) ₂ (bpy)](PF ₆)	Acetonitrile	23%
7	Ru(bpy) ₃ (PF ₆) ₂	MeOH	52%
8	Ir[(dF(CF ₃)ppy) ₂ (dtbbpy)](PF ₆)	MeOH	86%
9	Ir[(dF(CF ₃)ppy) ₂ (bpy)](PF ₆)	MeOH	77%
10	Ru(bpy) ₃ (PF ₆) ₂	DMF	90%
11	Ir[(dF(CF ₃)ppy) ₂ (dtbbpy)](PF ₆)	DMF	95%
12	Ir[(dF(CF ₃)ppy) ₂ (bpy)](PF ₆)	DMF	95%

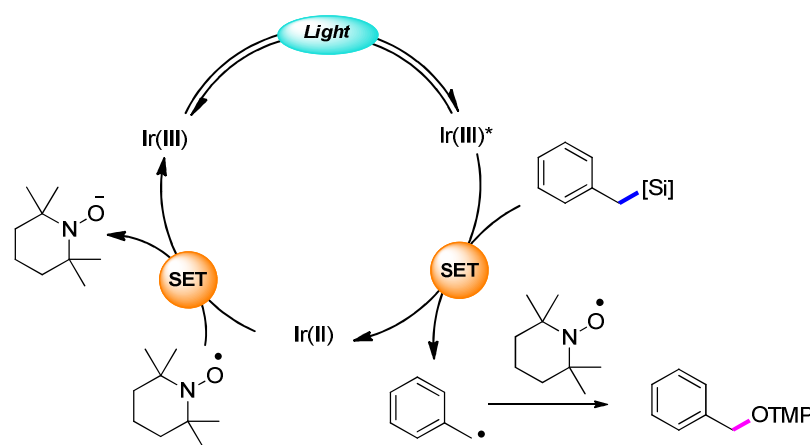
^a NMR yields, butadiene sulfone was used as internal standard.

All the screened photocatalysts were competent for the photooxidation of the benzylsilicate including Ru(bpy)₃(PF₆)₂, Ir[(dF(CF₃)ppy)₂(dtbbpy)](PF₆) and Ir[(dF(CF₃)ppy)₂(bpy)](PF₆). This last photocatalyst was chosen for the next studies. This photocatalyst showed a redox potential at the excited state ($E^\circ(\text{Ir(III)}^*/\text{Ir(II)}) = + 1.21\text{V vs SCE}$) appropriated to oxidize the benzylsilicate ($E^\circ(\text{Bn-[Si]}^-/\text{Bn}^\cdot) = + 0.61\text{V vs SCE}$) and liberate the TEMPO adduct with an excellent 95% yield. Indeed, fluorescence experiments demonstrated that the luminescence of the photocatalyst is quenched by the silicate. However, it is also known that TEMPO is also a luminescence quenching agent⁶⁶ of this iridium photocatalyst, which can provide the N-oxoammonium cation ($E^\circ(\text{TEMPO}^+/\text{TEMPO}) \approx +1.00\text{V vs SCE in water}^{148}$). However,

¹⁴⁸ J. L. Hodgson, M. Namazian, S. E. Bottle and M. L. Coote, *J. Phys. Chem. A*, 2007, **111**, 13595–13605.

comparing the oxidation potentials of TEMPO and benzylsilicate **23**, it is reasonable to admit that the excited photocatalyst directly react with the silicate instead of TEMPO. About the influence of the solvent, we observed the same trend reported by Nishigaichi.¹³⁸ Solvent with a strong donor effect (DMF and methanol) gave better yields of benzyl-TEMPO adduct than acetone or acetonitrile which are weak donating solvents.

In summary and based on the work of Akita on photooxidation of alkyl trifluoroborates,⁶⁶ it was proposed that benzylsilicate is oxidized by the excited Ir(III)*. The benzyl radical is directly trapped by the TEMPO and the Ir(II) intermediate transfers an electron to another equivalent of TEMPO (**Scheme 52**).

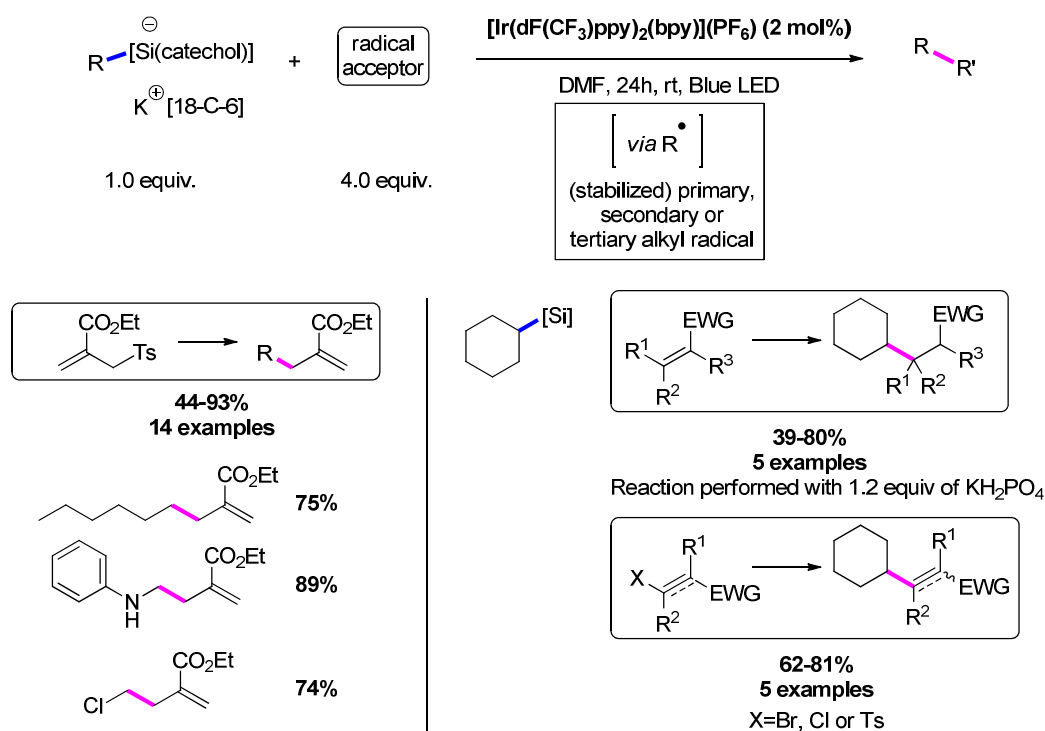


Scheme 52. Mechanism of formation of benzyl-TEMPO adduct under photooxidative conditions

To explore the reactivity of silicates as carbon centered radical precursors, the synthesized [18-C-6] potassium alkyl bis-catecholato silicates were engaged in radical allylation reactions with allylsulfone **27**.¹⁴⁹ With the previously optimized photooxidative conditions, all categories of silicates (stabilized or not) were tested. The corresponding allylated compounds were isolated in moderate to good yields (**Scheme 53**). The methodology was then extended to various radical acceptors. The scope of the reaction proved to be quite large from primary to tertiary silicates. Particularly, we can mention the generation of primary non-activated radical, a new example of aminomethylation and this never reported

¹⁴⁹ (a) C.-P. Chuang, *Tetrahedron*, 1991, **47**, 5425–5436. (b) M. H. Larraufie, R. Pellet, L. Fensterbank, J. P. Goddard, E. Lacôte, M. Malacria, C. Ollivier, *Angew. Chem. Int. Ed.*, 2011, **50**, 4463–4466.

chloromethylation. The cyclohexyl silicate could be engaged in Giese-type reactions, alkenylation and alkynylation reactions, giving the radical adducts in moderate to good yields.



Scheme 53. Examples of intermolecular radical additions

3.4.2 To a metal free oxidation

On the basis of this work, we envisioned to develop a metal free oxidation of silicates for eco-compatible reasons. We also compared their reactivities with the respective alkyl trifluoroborates.

3.4.2.1 Stoichiometric oxidation

Inspired by the work of Kumada on stoichiometric oxidation of pentafluorosilicates,¹³⁴ our group reported studies on copper(II)-mediated oxidation of alkyl trifluoroborates,¹⁵⁰ a

¹⁵⁰ G. Sorin, R. Martinez Mallorquin, Y. Contie, A. Baralle, M. Malacria, J.-P. Foddard and L. Fensterbank, *Angew. Chem. Int. Ed.*, 2010, **49**, 8721–8723.

previously known reaction¹⁵¹ but not exploited in radical chemistry. Post functionalization of the resulting radicals was achieved by TEMPO spin trapping, allylation¹⁵² or conjugate addition reactions.

Our purpose was to avoid the use of metallic oxidants by replacing with pure organic oxidants. We previously found that the Dess-Martin periodinane (DMP) could efficiently oxidize trifluoroborates in Et₂O.¹⁵⁰ So we considered Et₂O as an optimized solvent for the oxidation of trifluoroborates with non-metallic oxidants. Owing to the facile oxidation of alkyl bis-catecholato silicates in DMF with iridium photocatalyst, we also performed the study in this solvent. Among the organic oxidants, tritylium tetrafluoroborate, an underexplored oxidant,¹⁵³ was tested first with a series of alkyl trifluoroborates and alkyl bis-catecholato silicates.¹⁵⁴ For the reasons previously mentioned,^{147,150} we engaged respectively benzyltrifluoroborate and the benzylsilicate in spin-trapping experiments with TEMPO. We observed that a good yield of TEMPO adduct was obtained in Et₂O for the oxidation of benzyltrifluoroborate and DMF did not appear as the best solvent, while benzylsilicate did not react efficiently with the tritylium in both solvents (Table 4).

We also considered the Ledwith-Weitz aminium salt as organic oxidant for both radical precursors. The use of this radical cation oxidant as a SET oxidative agent (oxidation potential: + 1.06V vs SCE)¹⁵⁵ had never been tested. The reactions were performed in DMF and Et₂O as well. For benzyltrifluoroborate and benzylsilicate, the benzyl-TEMPO adduct was not obtained in satisfactory yield. However, DMF had a surprising effect on the reaction and the expected product was isolated in 69% and 86% yield respectively. The low yields obtained in Et₂O for benzylsilicate might be due to their low solubility in this solvent. The difference of yield obtained with both oxidants is not obvious to rationalize.

¹⁵¹ C. Cazorla, E. Métay, B. Andrioletti and M. Lemaire, *Tetrahedron Lett.*, 2009, **50**, 6855–6857.

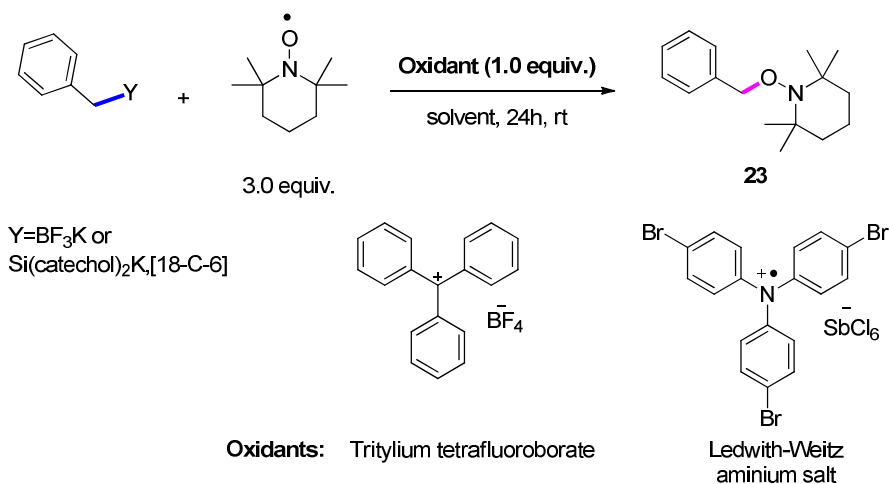
¹⁵² Y. Nishigaichi, T. Orimi and A. Takuwa, *J. Organomet. Chem.*, 2009, **694**, 3837–3839.

¹⁵³ (a) M. Daniel, L. Fensterbank, J.-P. Goddard and C. Ollivier, *Org. Chem. Front.*, 2014, **1**, 551–555. (b) Z. Xie, L. Liu, W. Chen, H. Zheng, Q. Xu, H. Yuan and H. Lou, *Angew. Chem. Int. Ed.*, 2014, **53**, 3904–3908.

¹⁵⁴ L. Chenneberg, C. Lévéque, V. Corcé, A. Baralle, J.-P. Goddard, C. Ollivier, L. Fensterbank, *Synlett*, **2016**, 27, 731–735.

¹⁵⁵ (a) A. C. Herath, J. Y. Becker, *J. Electroanal. Chem.*, 2008, **98**, 619–620. (b) K. H. G. Brinkhaus, E. Steckhan, Schmidt, W. *Acta Chem. Scand., Ser. B* **1983**, 37, 499. (c) Wend, R.; Steckhan, E. *Electrochim. Acta* **1983**, 42, 2027. For a recent use, see: (d) Drew, S. L.; Lawrence, A. L.; Sherburn, M. S. *Angew. Chem. Int. Ed.* **2013**, 52, 4221.

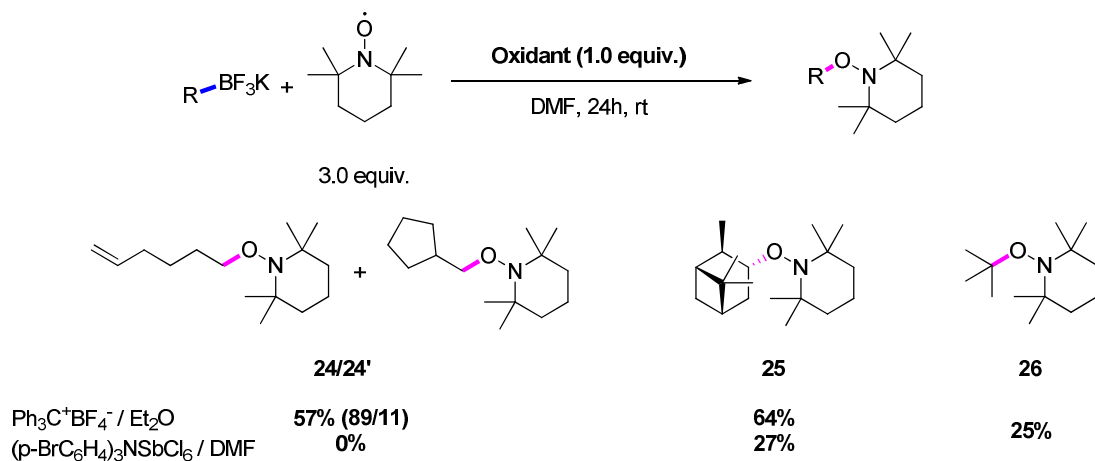
Table 4. Spin-trapping experiments with organic oxidants



Benzyl precursor	Oxidant	Solvent	Yield
Bn-BF ₃ K	Ph ₃ CBF ₄	Et ₂ O	65%
Bn-Si(catechol) ₂ K [18-C-6]	Ph ₃ CBF ₄	Et ₂ O	16%
Bn-BF ₃ K	Ph ₃ CBF ₄	DMF	35%
Bn-Si(catechol) ₂ K [18-C-6]	Ph ₃ CBF ₄	DMF	10%
Bn-BF ₃ K	Ar ₃ N.SbCl ₆	Et ₂ O	2%
Bn-Si(catechol) ₂ K [18-C-6]	Ar ₃ N.SbCl ₆	Et ₂ O	16%
Bn-BF₃K	Ar₃N.SbCl₆	DMF	69%
Bn-Si(catechol)₂K [18-C-6]	Ar₃N.SbCl₆	DMF	86%

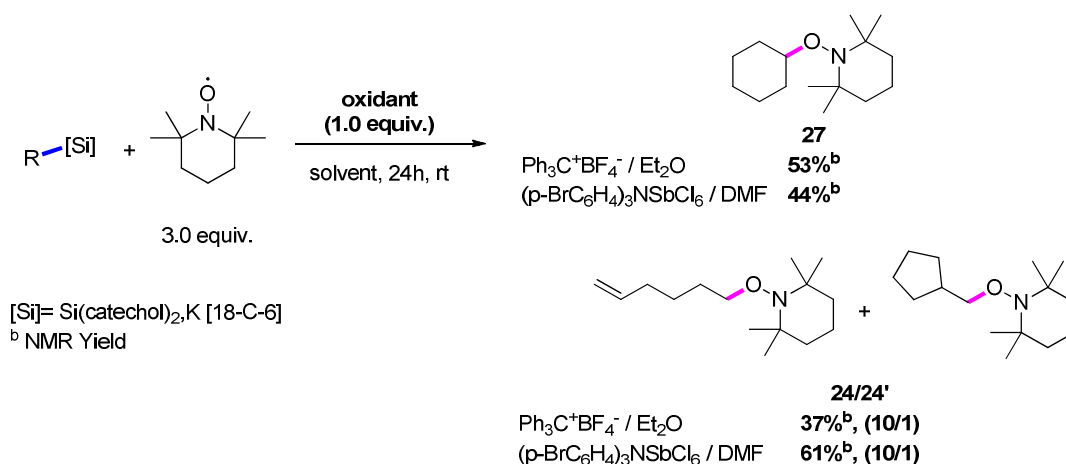
Less stabilized trifluoroborates and silicates were further engaged in the optimized conditions to see the synthetic opportunities of these oxidants. Good yields were obtained with the secondary (**25**) and primary series (**24/24'**) of alkyl trifluoroborates using Et₂O and tritylium conditions (**Scheme 54**). Only *tert*-butyl precursor gave low yield of product **26**,

(25%) presumably for steric reasons. Only 27% yield of **25** with the secondary substrate and no TEMPO adduct in the primary alkyl for the aminium salt oxidation version.



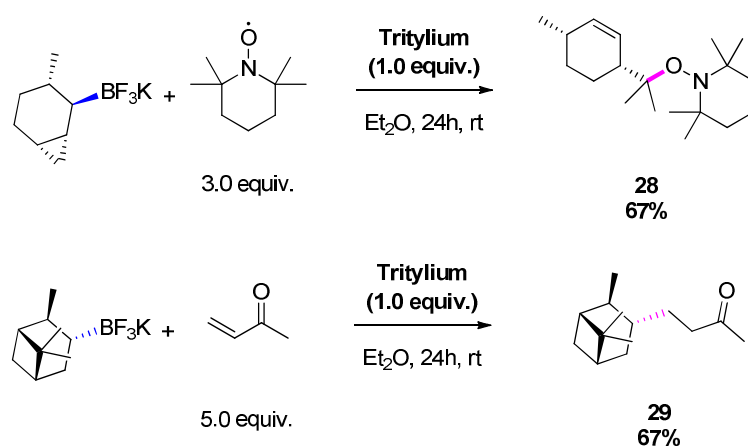
Scheme 54. Oxidation of organotrifluoroborates by organic reagents

5-Hexenyl (**3**) and cyclohexyl silicates (**1**) were involved in this process. The aminium salt proved to be ractive in DMF for secondary and primary alkyl substrates giving, 44% of **27** and 61% of 24/24' respectively (**Scheme 55**). Tritylium can also be used as a reliable oxidant for the silicates. In fact, tritylium conditions gave also a moderate yield of 53% for **27**. In the case of the 5-hexenyl silicate, a mixture of linear (**24**) and cyclized products (**24'**) with a ratio of 10:1 was observed demonstrating once again the radical character of these transformations.



Scheme 55. Screening of stoichiometric oxidation of silicates

Then we were able to oxidize the potassium ((1S,2R,3S,6S)-3-methylbicyclo[4.1.0]heptan-2-yl)trifluoroborate salt leading the generation of secondary radical, the trifluoroborate salt subsequently underwent a ring opening of the cyclopropane to give **28** (Scheme 56). This time, the tertiary radical was trapped in good yield (67%). Interestingly, the tritylium in diethyl ether conditions proved to be also compatible with conjugate addition since the methyl vinyl ketone (MVK) adduct **29** was also isolated in satisfactory yield (63%). No reaction was observed with silicates. Even if we succeed to oxidize moderately the alkyl bis-catecholato silicates with stoichiometric organic oxidants, the next step was to improve these conditions to a catalytic version. The solution was to use an organic photocatalyst.



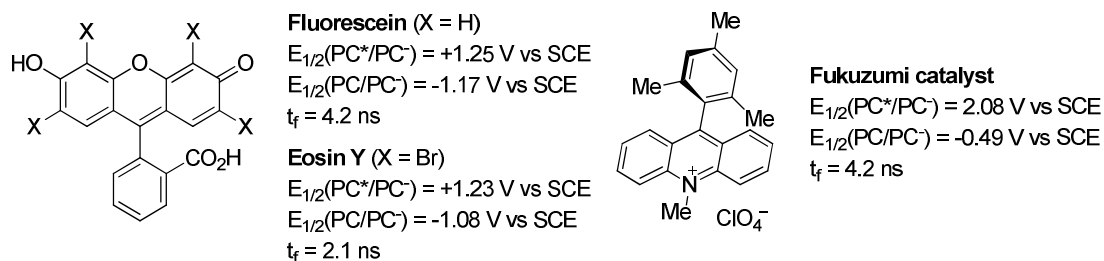
Scheme 56. Generation of tertiary radical and conjugate addition

3.4.2.2 Organic dyes as photooxidant

Organic dyes have already attested their efficiency in photoredox processes.¹⁵⁶ We envisioned using some dyes for which the redox potentials (excited state reduced photocatalyst) match with those of silicates and TEMPO. Fluorescein, Eosin Y and Fukuzumi catalyst (9-Mesityl-10-methylacridinium perchlorate) were first selected. The main drawback of these photocatalysts is their short excited state lifetime (< 6 ns) (Scheme 57). The

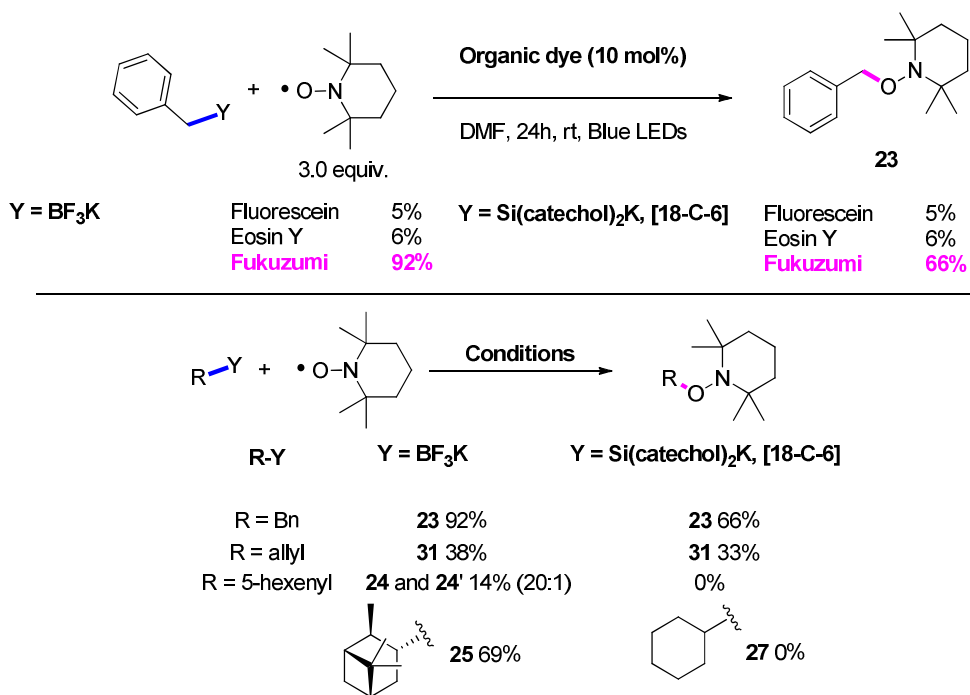
¹⁵⁶ For selective reports on organic dyes as photocatalyst see: (a) D. P. Hari, T. Hering and B. König, *Org. Lett.*, 2012, **14**, 5334–5337. (b) Y. C. Teo, Y. Pan and C. H. Tan, *ChemCatChem*, 2013, **5**, 235–240. (c) D. Leow, *Org. Lett.*, 2014, **16**, 5812–5815. (d) S. P. Pitre, C. D. McTiernan, H. Ismaili and J. C. Scaiano, *ACS Catal.*, 2014, **4**, 2530–2535. (e) P. D. Morse and D. A. Nicewicz, *Chem. Sci.*, 2014, **6**, 270–274. (f) A. Graml, I. Ghosh and B. König, *J. Org. Chem.*, 2017, **82**, 3552–3560.

experiments were performed with benzyltrifluoroborate and benzylsilicate to see the viability of the methodology and its applications in other radical processes.



Scheme 57. Selected organic dyes for the photooxidation of silicates

We choose DMF as solvent and a 10 mol% of photocatalyst loading to start the study. Fluorescein and Eosin Y showed to be not convenient photocatalyst. Only small amount of benzyl-TEMPO adduct was obtained when the reaction was performed with benzyltrifluoroborate. Fukuzumi catalyst allowed us to get the expected product with benzyltrifluoroborate and benzylsilicate in 92% and 66% yield respectively (**Scheme 58**). We then considered this catalyst for further substrates. In this photooxidative conditions, allyl, 5-hexenyl and cyclohexyl type substrates were tested. For both kinds of substrates, the same trend was observed: the less stabilized is the radical, the lower is the yield. However, the yields were rather better for trifluoroborates than for silicates, especially for the primary and secondary radical precursors.

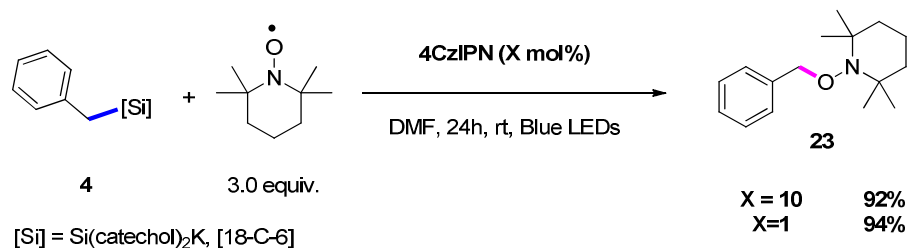


Scheme 58. Photooxidation of silicates and trifluoroborates with organic photocatalysts

At this stage, the metal-free photooxidation of silicates showed to be possible but not highly efficient. These photocatalysts may suffer from a short excited state lifetime. Even if the thermodynamic data enable the reaction, the kinetic of the oxidation step is probably too slow compared to the other deexcitation pathways of the excited state. In 2012, Adachi et al. described a family of carbazolyl dicyanobenzenes as light-harvesters for organic light-emitting diodes.^{25c} Among them, 1,2,3,5-tetrakis-(carbazol-yl)-4,6-dicyanobenzene (4CzIPN) displayed promising photophysical properties for photoredox catalysis: a high photoluminescence quantum yield (94.6%) and a long life-time in the excited state (5.1 μ s) which is a really huge value for an organic photosensitizer.

The group of Zhang²⁶ calculated the redox parameters of this chromophore. Thanks to photophysical analysis and electrochemical studies, they found the following values: $E_{1/2}(*4CzIPN/[4CzIPN]) = +1.35$ V and $E_{1/2}(4CzIPN/[4CzIPN]^-) = -1.21$ V vs. SCE. Taking account of all the photophysical and thermodynamical data, we were optimistic about the photooxidation of the silicates.

In the same conditions as before, we were pleased to see the formation of the benzyl-TEMPO adduct in 92% yield using 4CzIPN as photocatalyst. Moreover, decreasing the photocatalyst loading to 1 mol% showed the same efficiency (**Scheme 59**).

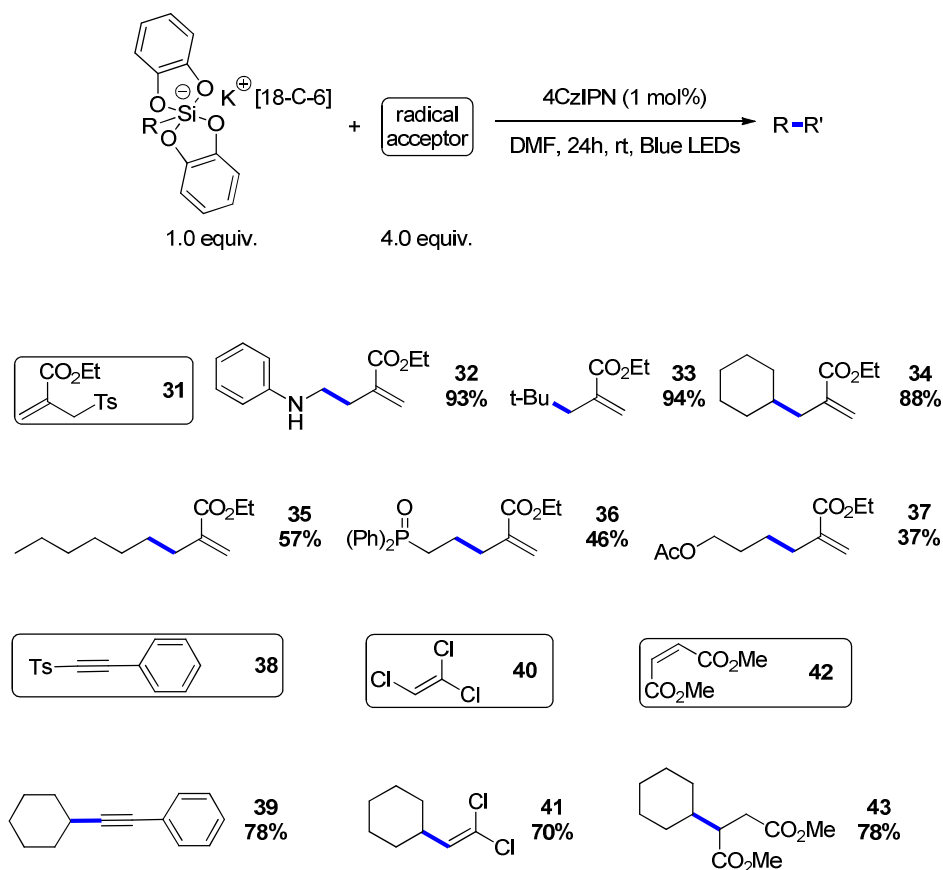


Scheme 59. Spin-trapping experiments with 4CzIPN as photocatalyst

In order to explore the potential of this dye, various alkyl silicates were engaged in a series of radical addition reactions (**Scheme 60**). The first selected radical acceptor was the activated allylsulfone **31** which previously proved to be a convenient radical trap.^{144a,149} Allylation adducts were obtained in excellent yields for stabilized radicals (α -aminyl and tertiary) and secondary radicals (**32-34**), and in moderate yields for primary radicals (**35-37**). Interestingly, 2-(diphenylphosphineoxide)ethylsilicate gave allylation adduct (**36**), without fragmentation of the Ph_2PO radical.¹⁵⁷ The kinetic rate of β -fragmentation is probably lower than the addition of the carbon-centered radical on the double bond of the acceptor. Cyclohexylsilicate (**1**) was further chosen as radical precursor for alkynylation **39**,¹⁵⁸ vinylation¹⁵⁸ **41** and Giese-type reaction **43**. In each case, the expected product was obtained in good yield.

¹⁵⁷ (a) D. Leca, L. Fensterbank, E. Lacôte and M. Malacria, *Angew. Chem., Int. Ed.*, 2004, **43**, 4220. (b) G. Ouvry, B. Quiclet-Sire and S. Z. Zard, *Angew. Chem., Int. Ed.*, 2006, **45**, 5002.

¹⁵⁸ A.-P. Schaffner, V. Darmency and P. Renaud, *Angew. Chem., Int. Ed.*, 2006, **45**, 5847.



Scheme 60. Radical addition reaction catalyzed by 4CzIPN

3.5 Conclusion

Ammonium and [18-C-6] potassium alkyl bis-catecholato silicates can be synthesized quantitatively and efficiently. Oxidation of such species led to the formation of (non)-stabilized carbon-centered radicals which can be trapped by acceptors. Stoichiometric organic oxidants demonstrated to be a valuable oxidant, but photocatalysts (metal based or organic) are more performing for the generation of the radicals. It is the first evidence for the generation of non-stabilized alkyl radicals by photooxidation. Development of new synthetic combining photooxidation of silicates and transition metals catalysis can be therefore envisioned to develop other types of cross-coupling processes.

Chapter IV

Combining photooxidation of alkyl bis-catecholato silicates and Nickel catalysis: functionalization of electrophiles

4 Chapter IV

Combining photooxidation of alkyl bis-catecholato silicates and Nickel catalysis: functionalization of electrophiles

Nickel is the first element of group 10, above palladium, platinum and darmstadtium. Named after the goblin-like sprite of Germanic mythology *Nickel*, this element has been extremely used for its corrosion resistance when it is employed in alloys. Also, nickel's compounds are involved in electrochemical processes, especially in rechargeable cells. Unfortunately, evidence of allergic reactions and toxicity made the use of nickel restricted. Despite its presumed hazards for health, nickel has found applications in efficient catalytic industrial processes (oil, pharmaceutical, food), and has recently received significant development in organic synthesis for cross-coupling reactions.

4.1 Progress in Nickel catalysis

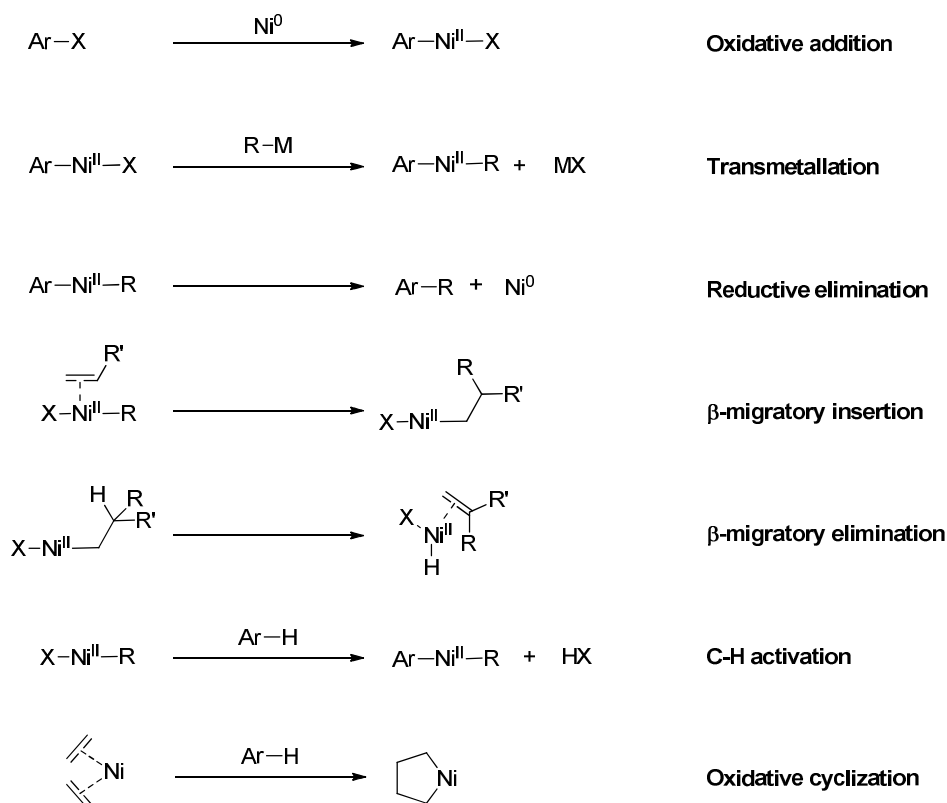
As a fourth-period transition metal, nickel is able to do SET processes (2.2) like its neighbor, cobalt and copper. Also, located just above palladium, it has similar reactivity and can promote the same elementary steps such as oxidative addition, reductive elimination or C-H activation (**Scheme 61**). In contrary to Hiyama, Sonogashira, Stille or Suzuki coupling and Heck reaction where a palladium catalyst is almost always used, nickel proved to be an alternative to palladium to Negishi cross-coupling reactions. Moreover, nickel is much cheaper (4.5 \$/mmol) than palladium (6.200 \$/mmol)¹⁵⁹ which makes it more attractive for economic reasons. Due to its specific properties, nickel has proven to be an efficient catalyst involved in various transformations¹⁶⁰ thanks to the large oxidation states accessible (**Table 5**).

¹⁵⁹ <http://www.chemicool.com/elements/> (Consulted in July 2017)

¹⁶⁰ S. Z. Tasker, E. A. Standley and T. F. Jamison, *Nature*, 2014, **509**, 299–309.

Table 5. Comparison of characteristics of nickel and palladium

	Nickel	Palladium
Oxidation states	-1 0 +1 +2 +3 +4	0 +1 +2 +3 +4
Atomic radius	135 pm	140 pm
Electronegativity	1.91	2.20
	Harder	Softer
	Facile oxidative addition	Facile reductive elimination
	β -migratory insertion	β -migratory elimination
	Radical pathways more accessible	

**Scheme 61.** Examples of elementary organometallic reaction steps with nickel complex

Nickel is an electron-rich element which can easily undergo oxidation to give nickel(II) oxides.¹⁶¹ Indeed, the most common oxidation state of nickel is +2, which is an important

¹⁶¹ T. T. Tsou and J. K. Kochi, *J. Am. Chem. Soc.*, 1979, **101**, 6319–6332.

oxidation state in cross-coupling reactions. It has been shown that oxidation states from +1 to +4 are also accessible.^{102,162} This ability of nickel allows different kinds of reactivities and radical pathways. Thus, catalytic cycle involving 1, 2, 3 or 4 different oxidation states are possible. Thanks to these properties, new approaches for the formation of the C-C bond have been envisaged and the studies are still going on.

One major progress in nickel catalysis has been brought recently by the work of Weix. In 2010, he reported the cross-electrophile coupling of aryl halides with alkyl halides.¹⁶³ Instead of using an organometallic nucleophile with an electrophile like in the common cross-coupling reactions, his group succeeded to perform the cross-coupling reaction of two electrophiles using a nickel catalyst and a reductant in a stoichiometric amount. In situ formation of a Ni(0) complex with 4,4'-di-*tert*-butyl-2,2'-bipyridine and 1,2-bis(diphenylphosphino)benzene as ligands led to the cross-coupling products bearing various functional groups on both partners like boronic esters, carbamates or esters for instance (**Scheme 62**). In order to render the process catalytic, they found that a Mn(0) was required as a reductant.



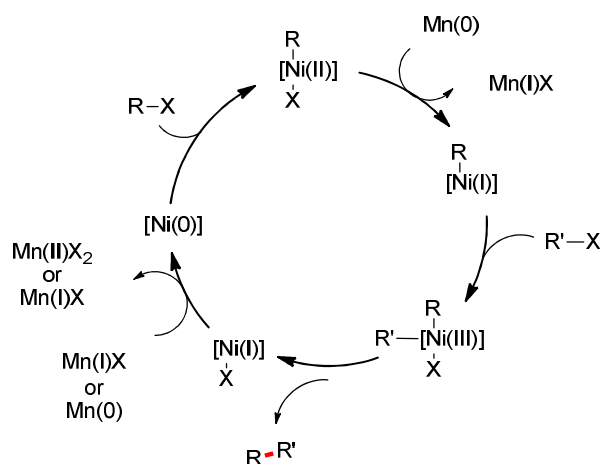
Scheme 62. Nickel-catalyzed cross-electrophile coupling of aryl halides and alkyl halides

They observed that starting the reaction with Ni(COD)₂, as a nickel(0) precatalyst, gave the expected products with similar yields. They proposed that the active catalytic species is a Ni(0) complex which undergoes oxidative addition with an organic halide (R-X) to form an intermediate R[Ni(II)]X (**Scheme 63**). After a reduction step by an equivalent of manganese, the generated complex R[Ni(I)] reacts with another organic halide

¹⁶² (a) J. Hanss and H.-J. Krüger, *Angew. Chem. Int. Ed.*, 1998, **37**, 360–363. (b) G. E. Martinez, C. Ocampo, Y. J. Park and A. R. Fout, *J. Am. Chem. Soc.*, 2016, **138**, 4290–4293. (c) E. Chong, J. W. Kampf, A. Ariafard, A. J. Canty and M. S. Sanford, *J. Am. Chem. Soc.*, 2017, **139**, 6058–6061.

¹⁶³ D. A. Everson, R. Shrestha and D. J. Weix, *J. Am. Chem. Soc.*, 2010, **132**, 920–921.

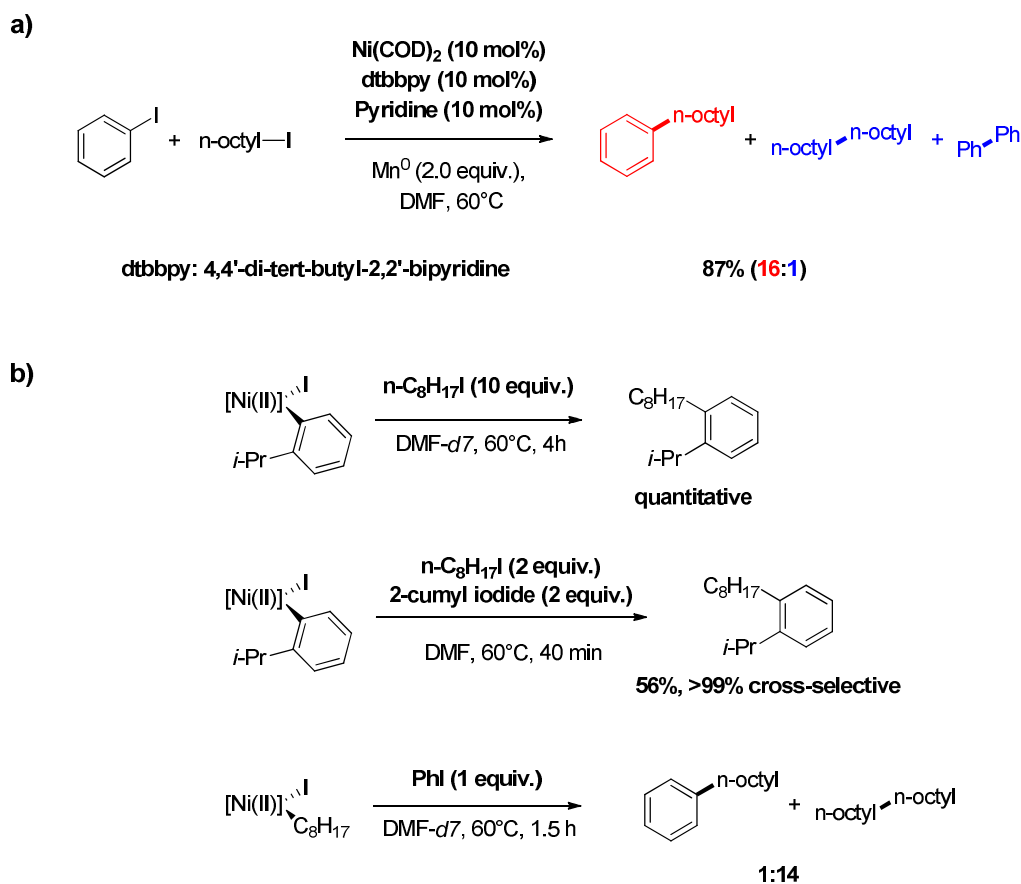
to give the highly reactive intermediate $RR'[\text{Ni(III)}]\text{X}$. The reductive elimination liberates the product and a Ni(I) complex was reduced by manganese to regenerate the Ni(0) catalyst.



Scheme 63. Proposed mechanism of the nickel catalyzed cross-electrophile coupling

In order to get a better insight of the mechanism of the reaction, Weix and co-worker did a series of experiments.¹⁶⁴ The study focused on the coupling of aryl iodides and alkyl iodides. At first, they measured the quantities of products formed during the reaction involving phenyl iodide and n-octyl iodide, with a Ni(0) catalyst and manganese as a reductant. They observed the formation of the expected product and two homocoupling products as dimers of each electrophile, with a ratio of 16:1 (cross-coupling/homo-coupling) clearly in favor of the cross-electrophile coupling reaction (**Scheme 64a**). Further experiments revealed that the first oxidative addition occurs between the Ni(0) catalyst and the aryl iodide. Indeed, treating a preformed $\text{Ar}[\text{Ni(II)}]\text{I}$ with a large excess of alkyl iodide or both electrophiles gave only the cross-coupling product. Moreover, from an *in situ* generated $\text{alkyl}[\text{Ni(II)}]\text{I}$, an addition of phenyl iodide resulted mostly in the formation of the alkyl-alkyl dimer (**Scheme 64 b**). Therefore, the first step was considered as the oxidative addition with the aryl iodide.

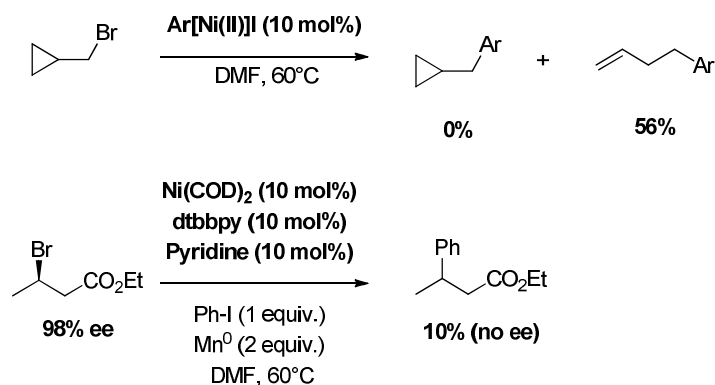
¹⁶⁴ S. Biswas and D. J. Weix, *J. Am. Chem. Soc.*, 2013, **135**, 16192–16197.



Scheme 64. First oxidation step determination

Regarding the next steps of the mechanism, they envisioned the formation of radicals. Radical clock experiments proved the generation of radicals: when cyclopropylmethyl bromide was used as alkyl electrophile, only the homoallyl product was obtained and performing the reaction with an enantiopure alkyl bromide provided a racemic mixture of cross-coupling products (**Scheme 65**). Both results are consistent with the formation of an alkyl radical after the oxidative addition step of the aryl halide. This nickel-mediated radical formation may occur before the addition of the radical on the same nickel center. As a proof, they used 5-hexenyl iodide because the 5-hexenyl radical is known to cyclize slower ($k = 2.3 \times 10^5$) than the ring-opening of the cyclopropylmethyl radical ($k = 7 \times 10^7$).^{6a} A mixture of cyclized (**A**) and linear (**B**) products should be observed. Variation of the concentration of the catalyst changed the ratio of cyclized and linear products (**Figure 9**) which is contrary to the idea of a direct radical formation \square radical trapping by the same nickel center. Indeed, if the radical formation and the radical addition happen on the same nickel center, the ratio must be

unchanged, whatever the concentration. But, in the case of a high concentration, the radical should not have time to cyclize and should be directly trapped by a nickel center (the same or not).



Scheme 65. Radical clock experiments

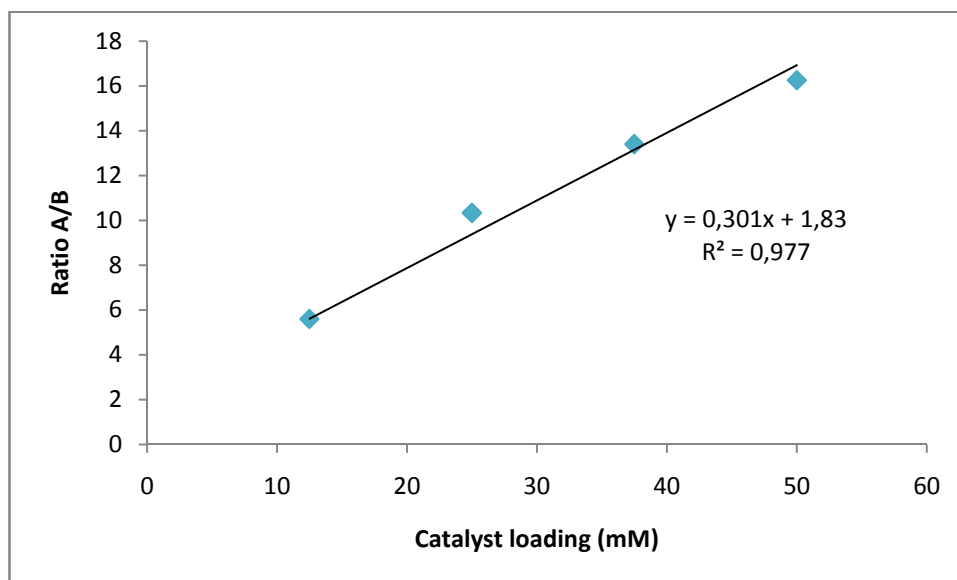
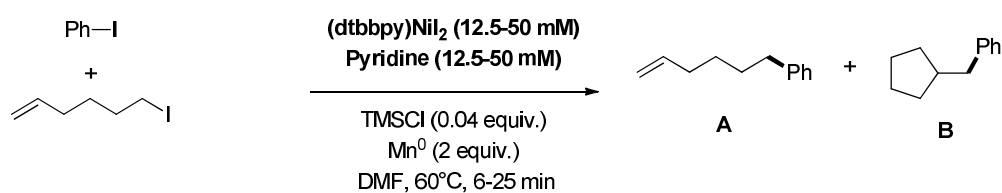
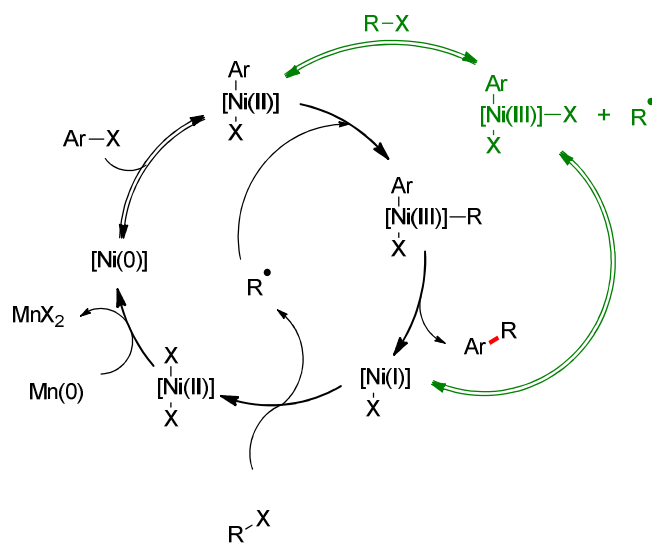


Figure 9. Evolution of cyclized/linear products depending on the concentration of nickel catalyst

With all these results, they proposed a mechanism starting from the oxidative addition of the aryl halide to the Ni(0) catalyst (**Scheme 66**). The intermediate Ar[Ni(II)]X would then react with an alkyl radical to give Ar[Ni(III)]RX. After reductive elimination, the cross-coupling product is liberated with [Ni(I)]X which may react by SET with the alkyl halide giving the alkyl radical. They excluded in this step the formation of aryl radical which are less stable than alkyl radical. The resulting nickel complex [Ni(II)]X₂ is then reduced by manganese to regenerate the starting catalyst. In addition, a **self-initiation pathway** was proposed. The intermediate Ar[Ni(II)]X can react with the alkyl halide to give the alkyl radical and the complex Ar[Ni(III)]X₂ which is in equilibrium with [Ni(I)]X and the aryl halide.

The nickel catalyzed cross-electrophile coupling reaction was then extended to aryl-aryl,¹⁶⁵ vinyl-alkyl,¹⁶⁶ allyl-alkyl¹⁶⁷ and alkyl-alkyl¹⁶⁸ coupling reactions. The ability of radical species to react with nickel intermediates and formation of carbon-carbon bonds has been exploited afterward in photoredox catalysis.



Scheme 66. Proposed mechanism for cross-electrophile coupling of an aryl halide with an alkyl halide

¹⁶⁵ (a) J. A. Buonomo, D. A. Everson and D. J. Weix, *Synthesis*, 2013, **45**, 3099–3102. (b) L. K. G. Ackerman, M. M. Lovell and D. J. Weix, *Nature*, 2015, **524**, 454–457.

¹⁶⁶ K. A. Johnson, S. Biswas and D. J. Weix, *Chem. – Eur. J.*, 2016, **22**, 7399–7402.

¹⁶⁷ (a) L. L. Anka-Lufford, M. R. Prinsell and D. J. Weix, *J. Org. Chem.*, 2012, **77**, 9989–10000. (b) J. A. Caputo, M. Naodovic and D. J. Weix, *Synlett*, 2015, **26**, 323–326.

¹⁶⁸ M. R. Prinsell, D. A. Everson and D. J. Weix, *Chem. Commun.*, 2010, **46**, 5743–5745.

4.2 Development of visible-light photoredox/nickel dual catalysis

With the dynamic initiated by Sanford¹¹⁰ on photoredox/transition metal dual catalysis and the work of Weix on nickel catalysis, the idea of merging photoredox catalysis and nickel arose with two distinct reports from Molander¹⁶⁹ in one hand and MacMillan and Doyle¹⁷⁰ in the other hand.

4.2.1 Pioneer works

- **Benzyltrifluoroborates in photoredox/nickel dual catalysis**

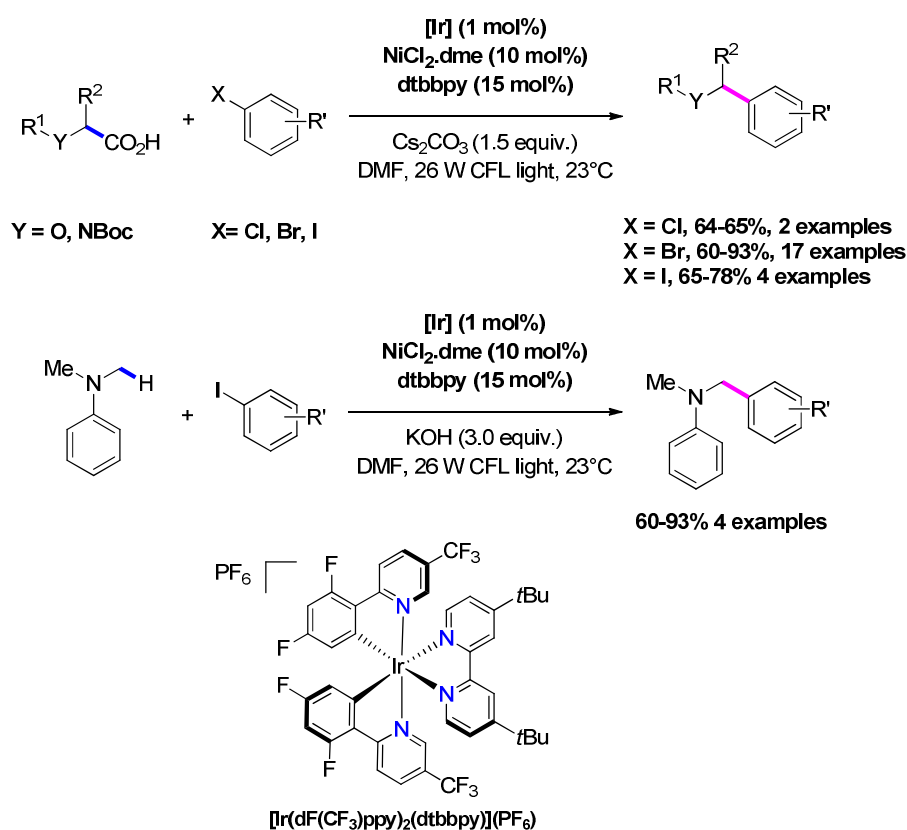
The work of Molander was inspired by the report of Akita⁶⁶ who demonstrated the photooxidation of alkyl trifluoroborates to generate stabilized alkyl radicals in the presence of $[\text{Ir}(\text{dF}(\text{CF}_3)\text{ppy})_2\text{bpy}](\text{PF}_6)$ as photocatalyst under blue light irradiation. His idea was to engage the formed radical in a nickel catalytic process. Among the alkyl trifluoroborates, the benzyl precursor was selected due to its lowest oxidation potential ($E_{1/2}^{\text{ox}} = +1.13\text{V}$ vs SCE in MeCN). In the presence of 2 mol% of the iridium photocatalyst, 3 mol% of $\text{Ni}(\text{COD})_2$ and 4,4'-di-*tert*-butyl-2,2'-bipyridine (as the ligand) they managed to couple the benzyl radical with (hetero)aryl bromide derivatives in moderate to excellent yields (**Scheme 67**). The reaction could be performed with benzyltrifluoroborates bearing electron donating or electron withdrawing groups with high yields. Various aryl bromides could be coupled with excellent yields. Moreover, bromo- pyridine, pyrimidine, indole, quinoline and thiophene have proved to be also suitable substrates.

¹⁶⁹ J.C. Tellis, D. N. Primer and G. A. Molander, *Science*, 2014, **345**, 433436.

¹⁷⁰ Z. Zuo, D. T. Ahneman, L. Chu, J. A. Terrett, A. G. Doyle and D. W. C. MacMillan, *Science*, 2014, **345**, 437-440.

- **α -amino radicals in photoredox/nickel dual catalysis**

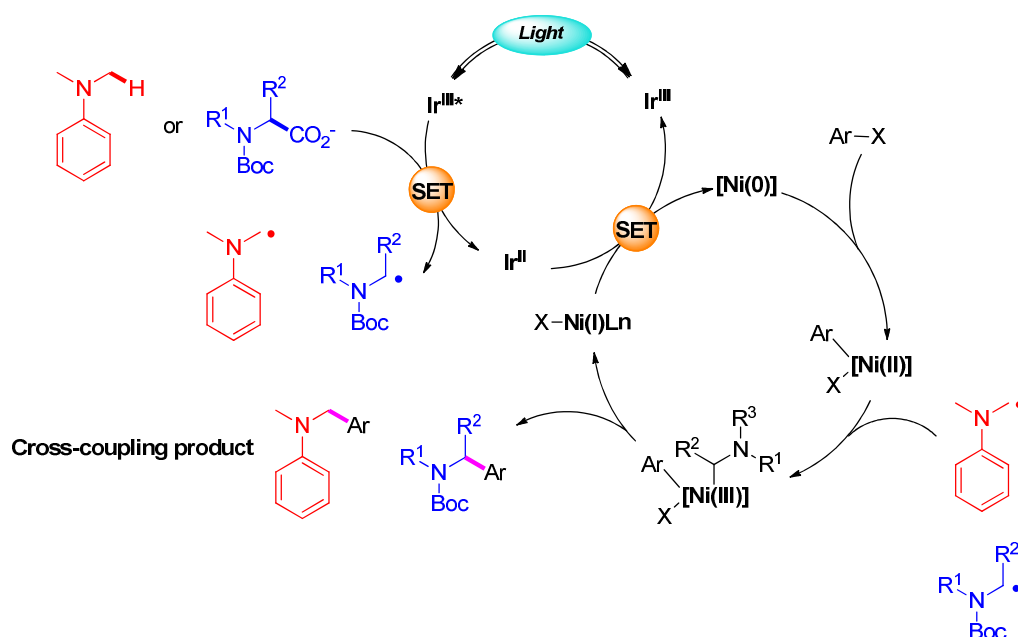
At the same time, MacMillan and Doyle reported a similar approach with the participation of α -amino radicals. These radicals were obtained by photooxidation of α -amino carboxylic acids in the presence of cesium carbonate^{61,63} or by photooxidation of dimethylaniline.⁶⁰ Both radicals were coupled with aryl halides through a nickel catalysis. The radicals were obtained by a photooxidative process with $[\text{Ir}(\text{dF}(\text{CF}_3)\text{ppy})_2(\text{dtbbpy})](\text{PF}_6)$ as photocatalyst and the cross-coupling reactions realized with $\text{NiCl}_2\cdot\text{dme}$ as precatalyst and 4,4'-di-*tert*-butyl-2,2'-bipyridine as ligand. Chloro, bromo and iodo arenes, and heteroaryl bromides could be cross-coupled with cyclic α -amino carboxylates with good yields (**Scheme 69**). As efficiently, non-cyclic α -amino and α -anilino radicals were engaged with aryl bromides.



Scheme 69. Photoredox cross-coupling of α -amino radicals with aryl halides

The authors proposed the same mechanism as Molander (**Scheme 70**). They envisaged the reduction of the $[\text{Ni}(\text{II})]$ complex by two SET event to give the $[\text{Ni}(0)]$ active catalyst.

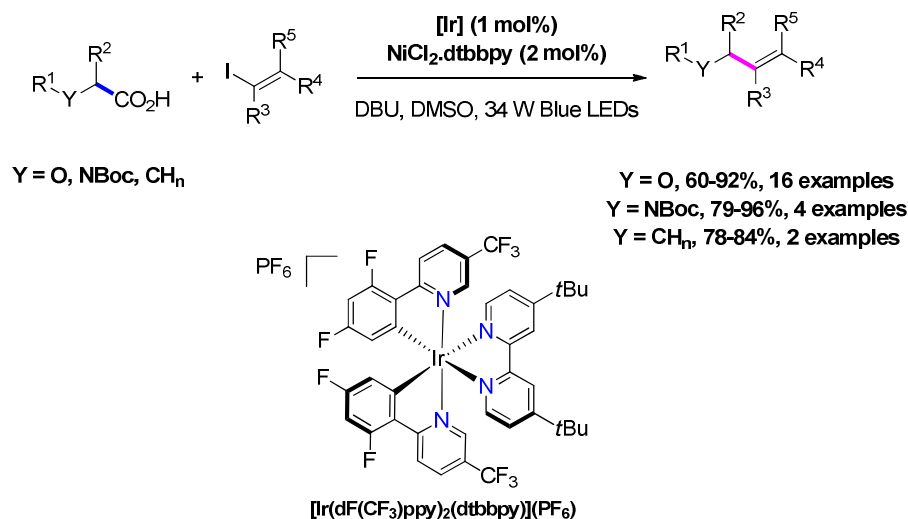
This complex may undergo oxidative addition with the aryl halide to form the $\text{Ar}[\text{Ni}(\text{II})]\text{X}$ intermediate. Oxidation of the carboxylate ($E_{1/2}(\text{R}-\text{CO}_2^-/\text{R}-\text{CO}_2\cdot) = +0.95 - +1.16\text{V}$ vs SCE) or dimethyl aniline ($E_{1/2}(\text{PhNMe}_2/\text{PhN}^+\cdot\text{Me}_2) = +0.71$ vs SCE) by the photoexcited Ir(III) ($E_{1/2}^{\text{red}}(\text{Ir}^{\text{III}*}/\text{Ir}^{\text{II}}) = +1.21\text{V}$ vs SCE in MeCN) leads to the corresponding α -amino radical which adds on the nickel complex to form the intermediate $\text{Ar}[\text{Ni}(\text{III})]\text{RX}$. After reductive elimination, the benzylamine and complex $[\text{Ni}(\text{I})]\text{X}$ are obtained. A final SET with the Ir(II) regenerates both catalysts.



Scheme 70. Proposed mechanism of photoredox/nickel dual catalysis α -amino arylation

This photoredox/nickel dual catalysis was then extended to the coupling of α -oxy carboxylic acids with vinyl iodide as electrophile. The α -oxy carboxylates are as easy as the α -amino carboxylate ($E_{1/2}^{\text{ox}} = +1.08\text{V}$ vs SCE in MeCN)¹⁷¹ to be photooxidized and so able to provide α -oxy radicals after decarboxylation which can be engaged in dual-catalysis. Following the same mechanism, allyl ethers were obtained in good yields with only 1 mol% of iridium photocatalyst and 2 mol% of nickel catalyst. It is interesting to mention that the process showed to be stereoconvergent. No erosion of the *E:Z* ratio was observed during the process. Moreover, α -amino and simple alkyl carboxylic acids could be engaged in a similar dual catalysis (**Scheme 71**).

¹⁷¹ A. Noble, S. J. McCarver and D. W. C. MacMillan, *J. Am. Chem. Soc.*, 2015, **137**, 624–627.



Scheme 71. Decarboxylative cross-coupling of carboxylic acids with vinyl Iodides

4.2.2 Advances on photoredox/nickel dual catalysis

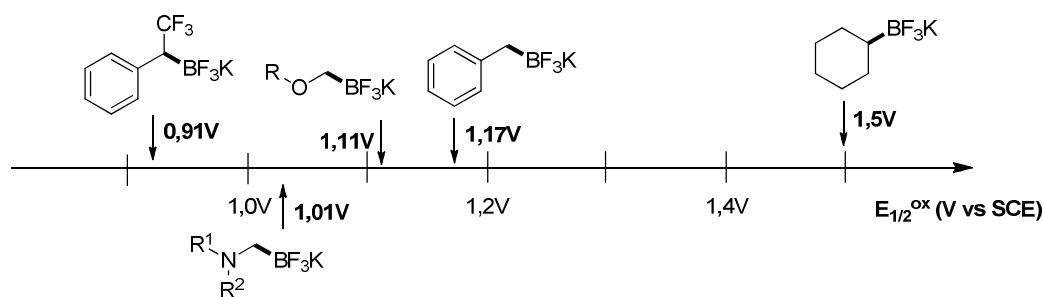
- **Tuning of alkyl trifluoroborates**

About the alkyl trifluoroborates, only activated radical precursors could be engaged. The limitation of the process is due to the photooxidation step. Indeed, generation of unstabilized radicals from trifluoroborates is tricky, caused by the high oxidative potential of such species. Nevertheless, good yields of cross-coupling products can be obtained once the generated radical is stabilized such as secondary,¹⁷² benzyl¹⁷³ and α -amino or oxy¹⁷⁴ radicals are valuable entities for such coupling reactions. In order to promote, the formation of the radicals. The oxidation potential can be decreased from 1.50V vs SCE for the secondary trifluoroborates to 0.91V for (2,2,2-trifluoroethyl)benzene trifluoroborates (**Scheme 72**).

¹⁷² (a) D. N. Primer, I. Karakaya, J. C. Tellis and G. A. Molander, *J. Am. Chem. Soc.*, 2015, **137**, 2195–2198. (b) J. C. Tellis, J. Amani and G. A. Molander, *Org. Lett.*, 2016, **18**, 2994–2997.

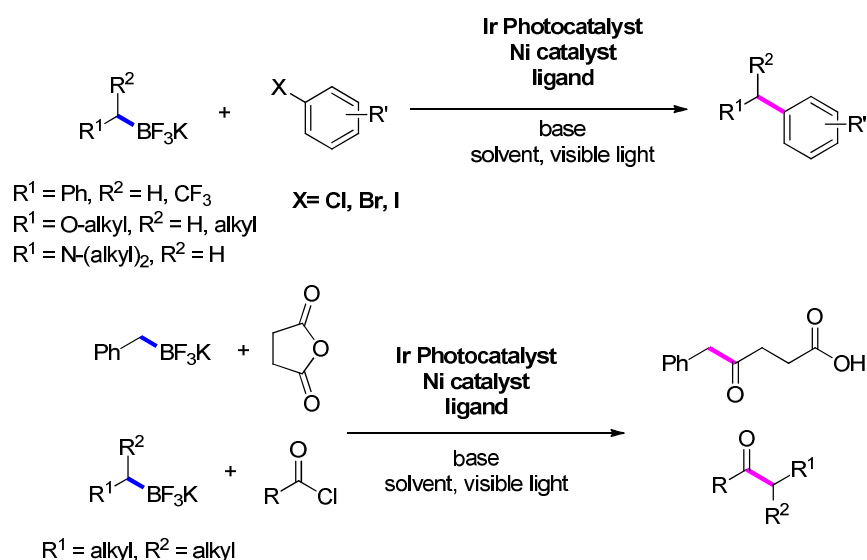
¹⁷³ D. Ryu, D. N. Primer, J. C. Tellis and G. A. Molander, *Chem. - Eur. J.*, 2016, **22**, 120–123.

¹⁷⁴ (a) M. ElKhatib, R. A. M. Serafim and G. A. Molander, *Angew. Chem. Int. Ed.*, 2016, **55**, 254–258. (b) I. Karakaya, D. N. Primer and G. A. Molander, *Org. Lett.*, 2015, **17**, 3294–3297. (c) K. Matsui and G. A. Molander, *Org. Lett.*, 2017, **19**, 436–439.



Scheme 72. Scale of organotrifluoroborates oxidation potential

Concerning the electrophiles, aryl and heteroaryl halides were the most suitable substrates (**Scheme 73**). Recently, acid derivatives such as acyl chloride¹⁷⁵ and anhydride¹⁷⁶ also revealed to be potent coupling partners. Non-activated primary alkyl trifluoroborates did not afford cross-coupling product so far, that is one of the drawbacks of such radical precursors.



Scheme 73. Organotrifluoroborates in photoredox/nickel dual catalysis

¹⁷⁵ J. Amani and G. A. Molander, *J. Org. Chem.*, 2017, **82**, 1856–1863

¹⁷⁶ E. E. Stache, T. Rovis and A. G. Doyle, *Angew. Chem. Int. Ed.*, 2017, **56**, 3679–3683.

- **Decarboxylative processes**

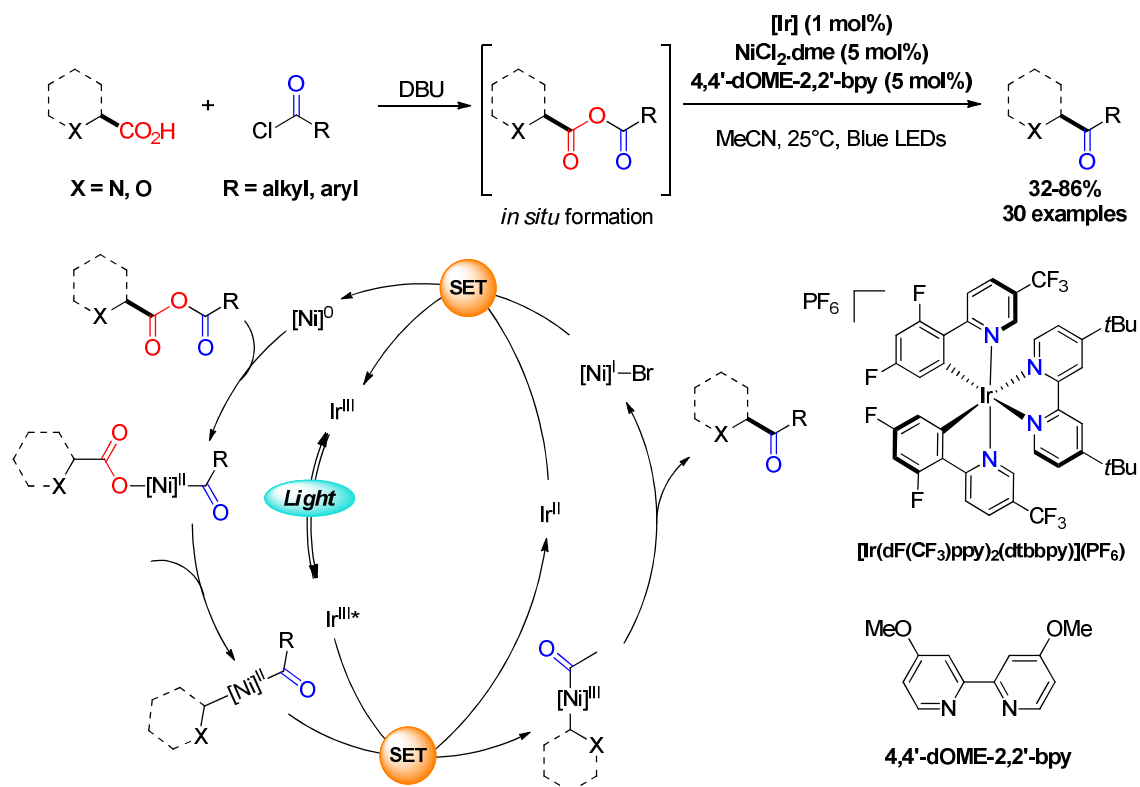
MacMillan demonstrated all the potential of his methodology based on the generation of alkyl radicals by photooxidation of carboxylic acids followed by decarboxylation. Among the substrates susceptible to undergo CO₂ extrusion, α -amino acids,¹⁷⁰ anhydrides,¹⁷⁷ keto acids¹⁷⁸ and oxalates¹⁷⁹ revealed to be excellent radical precursors.

After in situ formations of anhydride, from a carboxylic acid and an acyl chloride, a Ni(0) complex can do an insertion in a C-O bond. The resulting intermediate RCO₂[Ni(II)]C(O)R' is oxidized by a photoexcited iridium photocatalyst to a Ni(III) complex. After CO₂ extrusion, the new Ni(III) complex undergoes reductive elimination to give a ketone. The last Ni(I) complex does a SET with the Ir(II) complex in order to regenerate both catalysts were restored by SET between the releasing Ni(I) complex and the Ir(II) photocatalyst (**Scheme 74**). Among the carboxylic acids, cyclic and linear α -amino acids were tolerated in the reported conditions, as well as acyl chloride bearing ester, nitrile or ether moieties.

¹⁷⁷ C. “Chip” Le and D. W. C. MacMillan, *J. Am. Chem. Soc.*, 2015, **137**, 11938–11941.

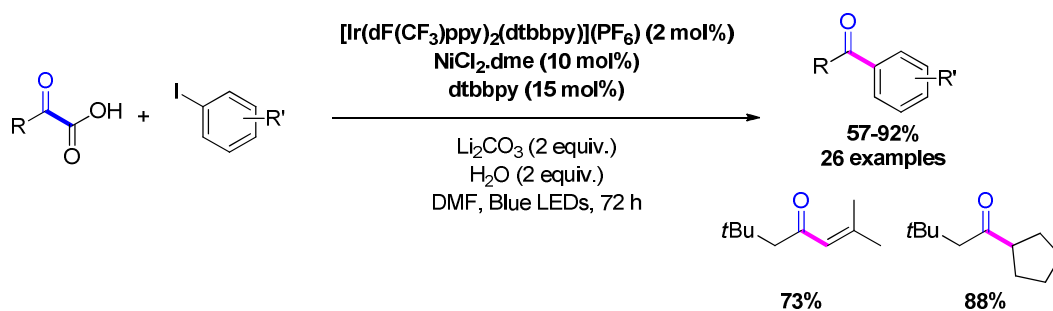
¹⁷⁸ L. Chu, J. M. Lipshultz and D. W. C. MacMillan, *Angew. Chem. Int. Ed.*, 2015, **54**, 7929–7933.

¹⁷⁹ X. Zhang and D. W. C. MacMillan, *J. Am. Chem. Soc.*, 2016, **138**, 13862–13865.



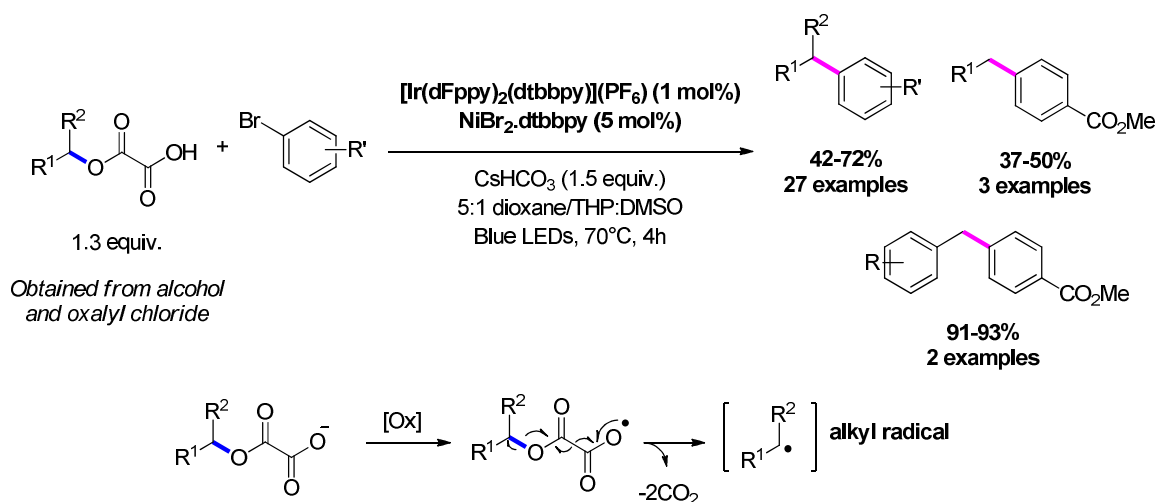
Scheme 74. Nickel-catalyzed ketone formation via decarboxylation of anhydrides

On the same line, they developed a methodology for the cross-coupling of aryl bromides/iodides with keto acids to provide aryl ketones. Aryl electrophiles bearing electron withdrawing groups or electron donating groups afforded the expected products in good yields. Aliphatic and aryl keto acids were also valuable coupling partners. Interestingly, vinyl bromides and secondary alkyl bromides could be engaged in the process (**Scheme 75**). The authors proposed a photooxidation of the keto carboxylate which after loss of CO_2 provides the acyl radical. The postulated mechanism is then similar to those reported above (**Scheme 70**) except the nature of the generated radical.



Scheme 75. Photoredox/Nickel-catalyzed decarboxylation of keto-acids

Another kind of decarboxylative process was performed from oxalates. Indeed, secondary alkyl radicals could be obtained from photooxidative decarboxylation of oxalates, pre-formed by the reaction between secondary alcohols and oxalyl chloride (**Scheme 76**). The radicals were coupled with aryl bromides in the presence of a nickel(II) catalyst following the methodology already exposed. Various electrophiles bearing electron donating or electron withdrawing groups could be engaged in moderate yields, as well as heteroaryl bromides. Interestingly, benzyl alcohols gave good yields but these ones dramatically dropped when non-activated primary alcohols were tested.



Scheme 76. Photoredox/nickel catalyzed cross-coupling reactions from oxalates

- **Formation of radicals by atom abstraction**

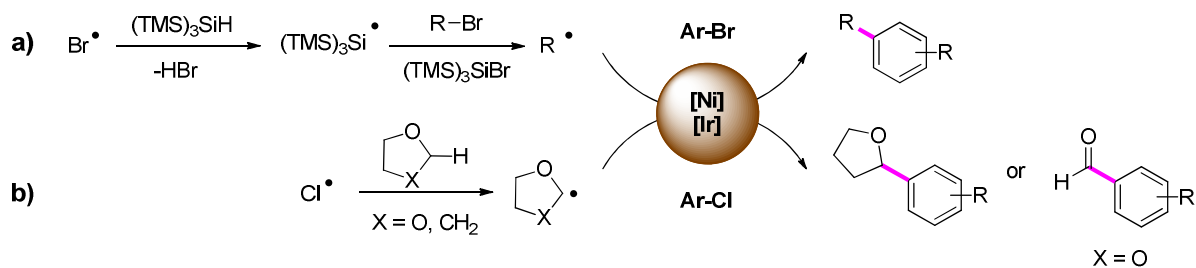
Once the nickel catalyst undergoes oxidative addition of RX to give the intermediate R[Ni(II)]X and a radical R'• adds upon it to furnish the transient complex RR'[Ni(III)]X. The way to generate the carbon-centered radical is, therefore an essential point. The direct oxidation of radical precursors proved to be effective toward these dual/catalytic processes. Recently, the formation of radicals by atom abstraction further involved in this kind of synthetic approach has been reported. MacMillan and co-workers could realize the cross-coupling reaction of alkyl bromides with aryl bromides.¹⁸⁰ This type of reaction previously reported by Weix could be performed at room temperature by using as radical mediator TTMSSH (**Scheme 77 a**). The authors proposed the formation of a bromine radical in the process which can abstract a hydrogen atom to the TTMSSH. Then, the silyl radical abstracts the bromine of the alkyl bromide and liberates the reactive alkyl radical.

The group of Doyle proposed a hydrogen atom abstraction by a chlorine radical. In their system, the cross-coupling was achieved between an aryl chloride and an α -oxy radical (**Scheme 77 b**). They proposed that a chlorine radical can be formed from the intermediate Ar[Ni(III)]Cl. Actually, after oxidative addition, the Ar[Ni(II)]Cl is oxidized by the photoexcited catalyst. Then, the intermediate Ar[Ni(III)]Cl would release the chlorine radical which abstract a hydrogen to the solvent (THF¹⁸¹ or dioxolane¹⁸²). The generated carbon-centered radical reacts in the same manner as above to give the cross-coupling product. In the case of dioxolane, treatment of the product by HCl provided benzaldehyde derivatives.

¹⁸⁰ P. Zhang, C. “Chip” Le and D. W. C. MacMillan, *J. Am. Chem. Soc.*, 2016, **138**, 8084–8087.

¹⁸¹ B. J. Shields and A. G. Doyle, *J. Am. Chem. Soc.*, 2016, **138**, 12719–12722.

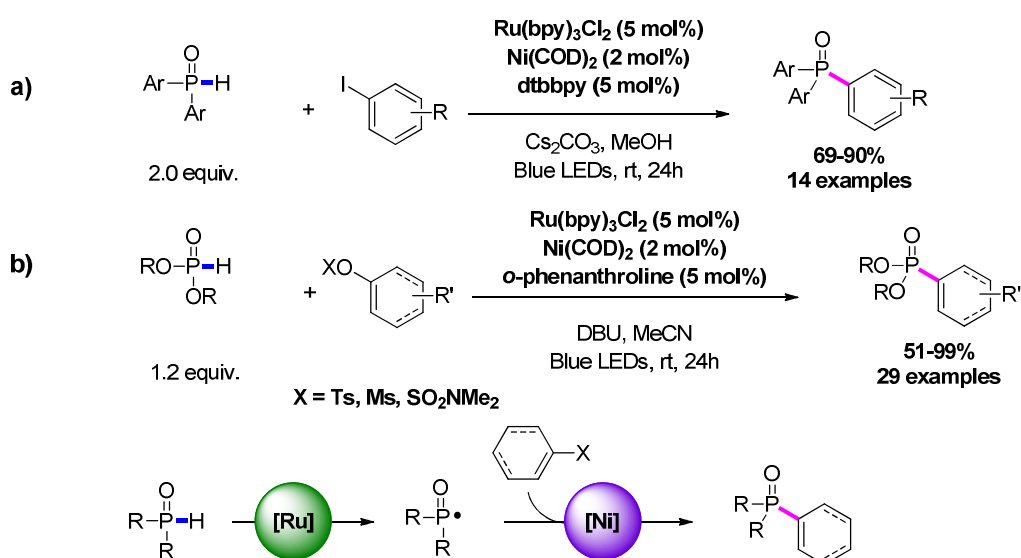
¹⁸² M. K. Nielsen, B. J. Shields, J. Liu, M. J. Williams, M. J. Zacuto and A. G. Doyle, *Angew. Chem.*, 2017, **129**, 7297–7300.



Scheme 77. Photoredox/nickel dual catalysis with the generation of radicals by atom abstraction

- **Formation of C-P/C-S bonds**

Radicals are not only carbon-centered. The formation of C-X bonds by photoredox/nickel dual catalysis has been also envisioned. In 2015, the group of Xiao reported an efficient method for the C-P bond formation under mild conditions. Thanks to a ruthenium photocatalyst and an *in-situ* formed nickel catalyst, they could realize the cross-coupling reaction between (hetero)aryl iodides and phosphine oxides in high yields. The authors proposed the same catalytic cycles as above except that a phosphinyl radical is at stake. This radical is obtained by a base-assisted photooxidation of the phosphinous acid (**Scheme 78**). More recently, another group engaged phosphonates as radical precursors and aryl/alkenyl tosylate, mesylate or sulfamate as electrophiles.



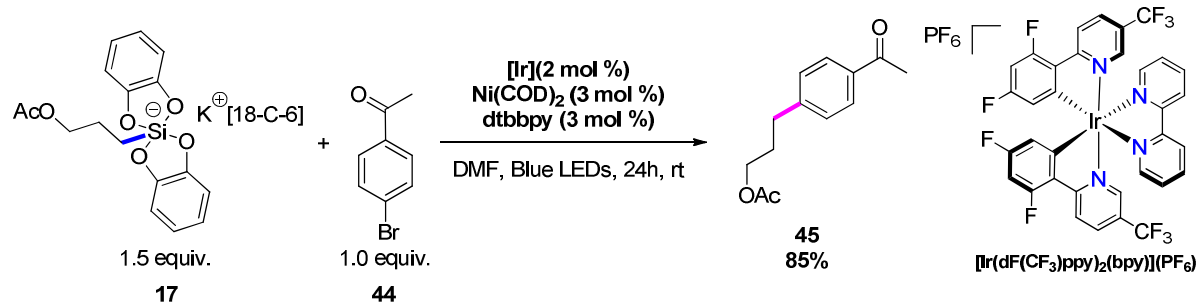
Scheme 78. Photoredox/nickel dual-catalyzed C-P bond formation

Thiyl radicals showed to be reactive intermediates in radical chain reactions.¹⁸³ Johannes and co-workers demonstrated that these radicals can be involved in photoredox mediated and nickel-catalyzed cross coupling reactions with (hetero)aryl iodides. Thiophenol, alkyl and benzyl thiols could be coupled with electrophiles bearing electron donating and electron withdrawing groups in good to excellent yields (**Scheme 79**). In their case, a NiCl₂.dme was used as precatalyst with 4,4'-di-*tert*-butyl- 2,2'-bipyridine as ligand. In addition, NiCl₂.dppe as catalyst gave also the expected products. However, no reaction was observed with a Ni(0) precatalyst under an inert atmosphere or not. The authors considered that the mechanism of the reaction would be different than those proposed before. The photoexcited iridium catalyst oxidizes the thiol which after deprotonation provides the thiyl radical. Redox potentials for NiCl₂.dppe/NiCl.dppe and NiCl.dppe/Ni(0)dppe are respectively -0,88V vs SCE and -1.41V vs SCE in DMF/THF (4:1). A reduction step of the NiCl₂.dppe by Ir(II) ($E(\text{Ir}^{\text{III}}/\text{Ir}^{\text{II}}) = -1.37\text{V vs SCE in MeCN}$) was therefore considered as an initiation step. According to the authors, the same step would be possible with NiCl₂.dtbbpy. The resulting active complex [Ni(I)]Cl would react with the thiyl radical to generate the intermediate RS[Ni(II)]Cl. Another reduction step from Ir(II) may give the complex RS[Ni(I)] which would undergo oxidative addition with an aryl iodide. After reductive elimination, the RS[Ni(III)]X was converted to the active nickel complex, and the thioether was obtained.

¹⁸³ (a) K. S. Feldman, A. L. Romanelli, R. E. Ruckle and R. F. Miller, *J. Am. Chem. Soc.*, 1988, **110**, 3300–3302. (b) K. S. Feldman and K. Schildknecht, *J. Org. Chem.*, 1994, **59**, 1129–1134. (c) K. S. Feldman, A. K. K. Vong, *Tetrahedron Lett.*, 1990, **31**, 823–826. (d) K. Miura, K. Fugami, K. Oshima and K. Utimoto, *Tetrahedron Lett.*, 1988, **29**, 5135–5138. (e) S. Kim, S. Lee, *Tetrahedron Lett.*, 1991, **32**, 6575–6578.

various aryl electrophiles.^{144b} We found that 2 mol% of photocatalyst and 3 mol% of nickel catalyst under blue light irradiation, gave the cross-coupling product **45** between the acetoxypylsilicate **17** and 4'-bromoacetophenone **44** (Table 6). Control experiments showed that each reagent is necessary for the reaction as well as the light irradiation. Moreover, the reaction was performed with the acetoxypylsilicate **17'** without the crown-ether (entry 6). No effect of the chelating agent was observed on the yield of the reaction.

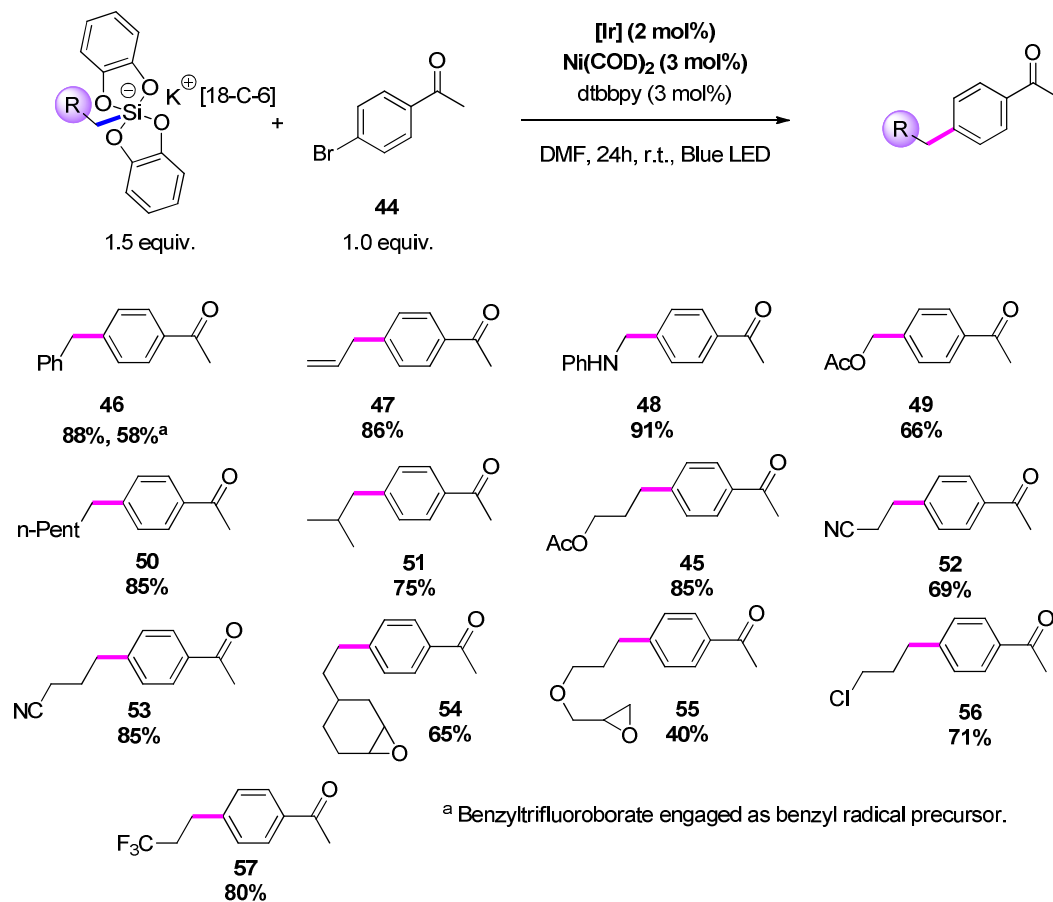
Table 6. Control experiments and influence of the crown ether



Entry	Conditions	Yield
1	Standard conditions	85%
2	No [Ir]	0%
3	No $\text{Ni}(\text{COD})_2$	0%
4	No ligand	0%
5	No light	0%
6	Silicate without [18-C-6]	86%

We then limited our studies to primary [18-C-6] potassium alkyl bis-catecholato silicates. First of all, the silicates were screened with 4'-bromoacetophenone as electrophile (Scheme 80). Silicate precursors of stabilized benzyl, allyl and α -amino radicals gave excellent yields of cross-coupling products **46**, **47**, **48** with 88%, 86% and 91% yields respectively. A lower yield was obtained with the acetoxymethylsilicate **49**. Synthetically more attracting, non-stabilized radicals could also be involved furnishing the corresponding coupling products. Aliphatic silicates such as hexyl or isobutyl silicate gave product **47** and **51** in good yields. The reaction conditions were tolerated by various silicates bearing functional groups such as an ester **45** and **49**, a nitrile **52** and **53**, an oxirane **54** and **55** or a

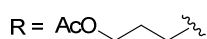
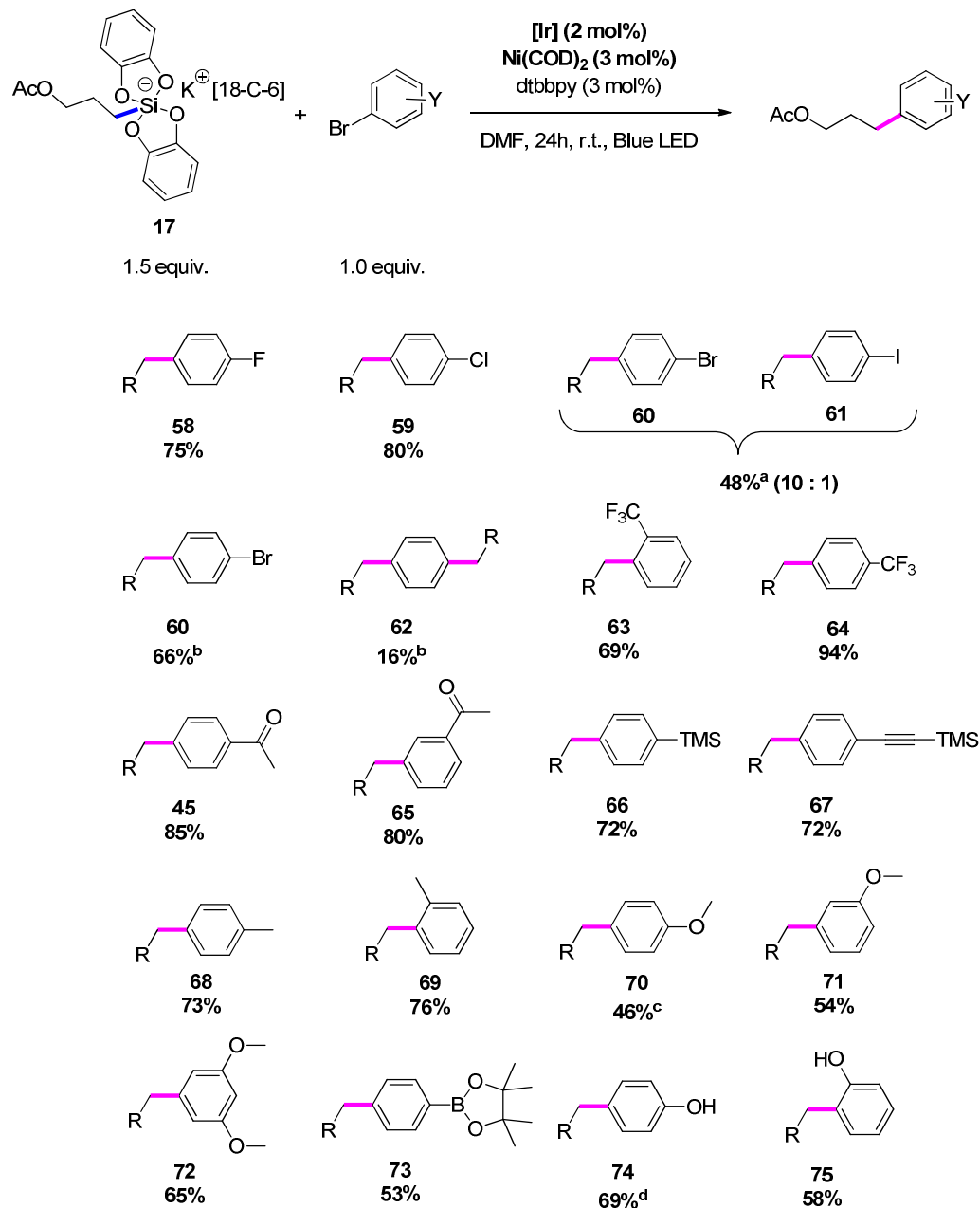
halogen **56** and **57**. A comparison of reactivity was made with the benzyltrifluoroborate in our conditions. It was found a better reactivity of the benzylsilicate.



Scheme 80. Cross-coupling reactions of alkyl silicates with 4'-bromoacetophenone

Using the same conditions, a series of arylbromides with various substituents was engaged with acetoxypropylsilicate **17** (**Scheme 81**). We first studied the selectivity towards the substitution of halogen atoms on the aryl ring. Bromobenzenes substituted at the *para* position with other halogens were screened. Fluoro and chloro substituted bromobenzenes were converted to the cross-coupling product **58** and **59** in good yields. The reaction is highly selective as no substitution of the fluorine or chlorine atom was observed. However, when the reaction was started with 1-bromo-4-iodobenzene, a mixture of products **60** and **61** was obtained in moderate yield in a ratio 10:1. The functionalization of the iodo position was

preferred over the bromo position. Indeed, oxidative addition is more likely at the C-I bond¹⁸⁴ that explains the selectivity observed. 1,4-Dibromobenzene gave largely the mono-functionalized product **60** and the di-functionalized product **62** in low yield.



^a Starting from 1-bromo-4-iodobenzene

^b Starting from 1,4-dibromobenzene

^c Starting from 4-iodoanisole

^d Pinacole borane directly oxidized before purification (H_2O_2 , NaOH for 30 min at 0°C)

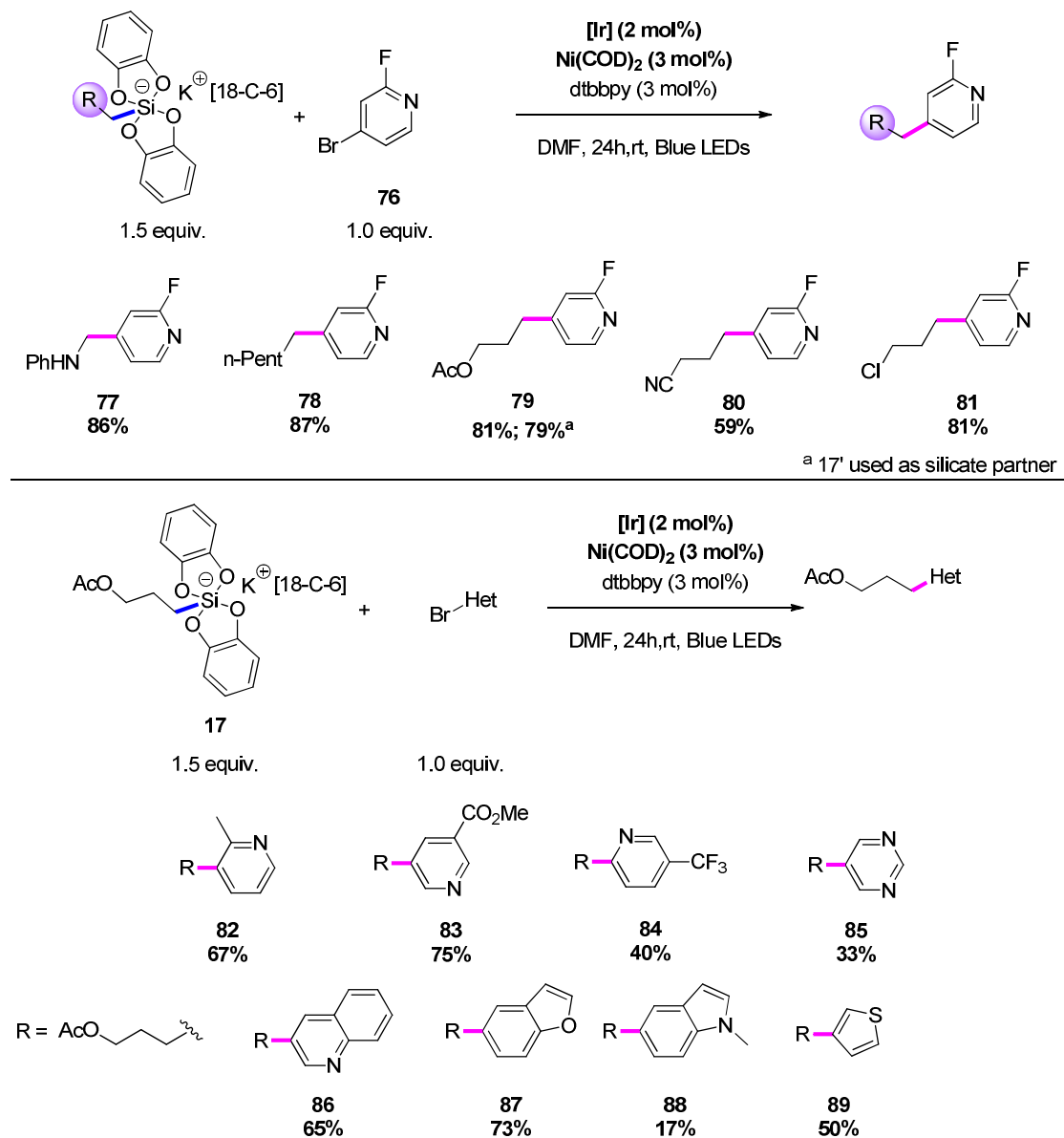
Scheme 81. Cross-coupling reactions of silicate **17** with various aryl bromides

¹⁸⁴ J. F. Hartwig, *Organotransition Metal Chemistry: From Bonding to Catalysis*, University Science Books, Sausalito, 2009.

This cross-coupling methodology was very efficient for substrates bearing electron withdrawing groups such as trifluoromethyl **63** and **64** or acetyl **45** and **65** moieties at the *ortho*, *meta* or *para* position. We further investigated electron enriched aryl substrates. Electrophiles substituted by slightly donor groups such as methyl **68** and **69** or trimethylsilyl **66** and **67**, were converted in good yields. Various bromoanisoles were then engaged in the reaction conditions. Cross-coupling products were obtained for *meta*-bromoanisoles **71** and **72** in moderate yields. However, only the starting material was recovered with *ortho*-bromoanisole and *para*-bromoanisole. Using 1-bromo-4-iodoanisole instead afforded the expected adduct **70** in moderate yield (46%). These results highlight again the importance of the oxidative addition in the process. Aryl bromides substituted by strongly donor groups are not reactive enough. In this case, the corresponding iodo compound should be privileged.

Remarkably, a pinacol boronate function could also be tolerated under these conditions as illustrated by the formation of **73** that could be utilized for further coupling reactions. Since pinacol boronates are sensitive to acidic conditions and to purification by silica column chromatography, a direct oxidation to the phenol was performed (NaOH, H₂O₂). Higher yields were obtained in phenol product **74** (69% *vs* 53% for **73**). A similar procedure was applied to give product **75**.

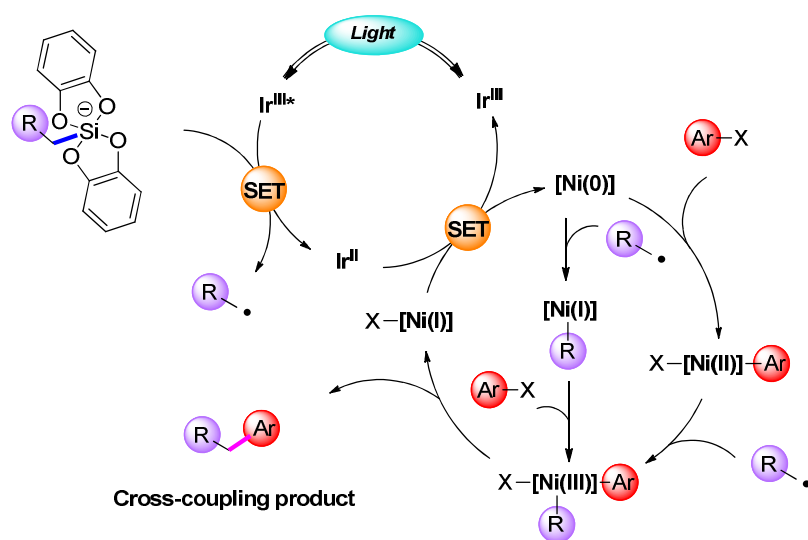
This transformation was then extended to heterocyclic bromides. 2-Fluoro-4-bromopyridine was selected as electrophile in the same catalytic conditions and coupled with silicates (**Scheme 82**). A small library of new alkyl-fluoropyridines was obtained **77-81** in satisfactory yields (59-86%). As before, silicate **17'** without the crown-ether gave adduct **79** in a similar yield (79% *vs* 81%). Other heteroaryl bromide derivatives were screened. Pyridyl systems proved to be compatible with these cross-coupling reaction conditions. Methylpyridine **82**, trifluoromethylpyridine **84** and methylnicotinate **83** adducts were obtained in 40-75% yields. Others heterolytic systems such as pyrimidine, quinoline, indole, benzofuran and thiophene were converted to the corresponding cross-coupling products **85-89** in low to fair yields.



Scheme 82. Cross-coupling reactions of silicates with various heteroaryl bromides

To rationalize this work, we proposed catalytic cycles based on our results and we took inspiration from the previous works on such processes (**Scheme 83**). Excitation of the photoredox iridium catalyst produces a long-lived oxidant photoexcited state ($E_{1/2}(\text{Ir}^{\text{III}*}/\text{Ir}^{\text{II}}) = +1.32 \text{ V vs SCE in MeCN}$). The latter undergoes a SET with the alkyl silicates ($E_{1/2}^{\text{ox}} = +0.34 \text{ V to } +0.87 \text{ V vs SCE in DMF}$)¹⁴⁴ generating a primary alkyl radical which interacts with a Ni species. All the reports converge toward a Ni(III) intermediate which releases the cross-coupling product after a reductive elimination step and a Ni(I) further reduced to Ni(0) by SET from the Ir(II) photocatalyst. The remaining question concerns the formation of the key

Ni(III) complex which would be the result of two successive steps: oxidative addition of the aryl halide and addition of the radical on the nickel. The order of the steps is still not elucidated. Some computations on benzyltrifluoroborates suggest a complex mechanism with a thermodynamically favored radical addition whether to a Ni(0) or a Ni(II).¹⁸⁵ According to the report, both pathways involving first the oxidative addition of ArX to the Ni(0) followed by the radical addition or the opposite can occur. Some of our results (**59-62**) showed nevertheless the importance of the oxidative addition step.



Scheme 83. Proposed mechanism of the photoredox/nickel dual catalysis using silicates

Of note, the group of Molander developed a similar methodology involving ammonium alkyl bis-catecholato silicates. They used Ru(bpy)₃(PF₆)₂ as photocatalyst and a nickel(II) precatalyst. As we did, they could engage a wide range of silicates with various aryl and heteroaryl bromides.¹⁸⁶

¹⁸⁵ O. Gutierrez, J. C. Tellis, D. N. Primer, G. A. Molander and M. C. Kozlowski, *J.Am.Chem.Soc.*, 2015, **137**, 4896–4899.

¹⁸⁶ M. Jouffroy, D. N. Primer and G. A. Molander, *J.Am.Chem.Soc.*, 2016, **138**, 475–478.

4.3.2 Toward a green dual catalytic system

We demonstrated first the ability of potassium ([18-C-6]) bis-catecholato silicates of being good precursors of alkyl radicals for cross-coupling reactions. We also proved that photooxidation of such species can be mediated by as well ruthenium or iridium polypyridine complex or more interestingly by organic dyes and especially by 4CzIPN. Zhang *et al.* reported²⁶ the first examples of the use of 4CzIPN as photocatalyst in photoredox/nickel dual-catalyzed cross-coupling reactions of aminocarboxylates and benzyltrifluoroborates with arylbromides. Similarly, we planned to extend this mixed organic photoredox/metallic dual-catalysis to alkyl silicates and compare its efficiency to our previous conditions.^{32a} Thus, we selected acetoxypropylsilicate (1.5 equiv.) **17** and 4'-bromoacetophenone **44** as cross-coupling partners (Table 7). We were expecting to find Ni(COD)₂ as a workable nickel source but no product formation was observed after 24 hours (entry 1). Switching to NiCl₂.dme as a precatalyst (3 mol%) with 4CzIPN (2 mol%) and 4,4'-di-*tert*-butyl- 2,2'-bipyridine, these new conditions provided the cross-coupling product **45** in 77% yield. We were able to decrease the catalysts loading to 2 mol% of the nickel and 1 mol% of photocatalyst for a 83% yield of the expected product (Entry 4). Unfortunately, decreasing the amount of alkyl silicate affected the yield of the reaction (Entry 5).

Table 7. Screening of reaction conditions for organic photoredox/nickel dual-catalyzed cross-coupling of acetoxypropylsilicate and 4'-bromoacetophenone



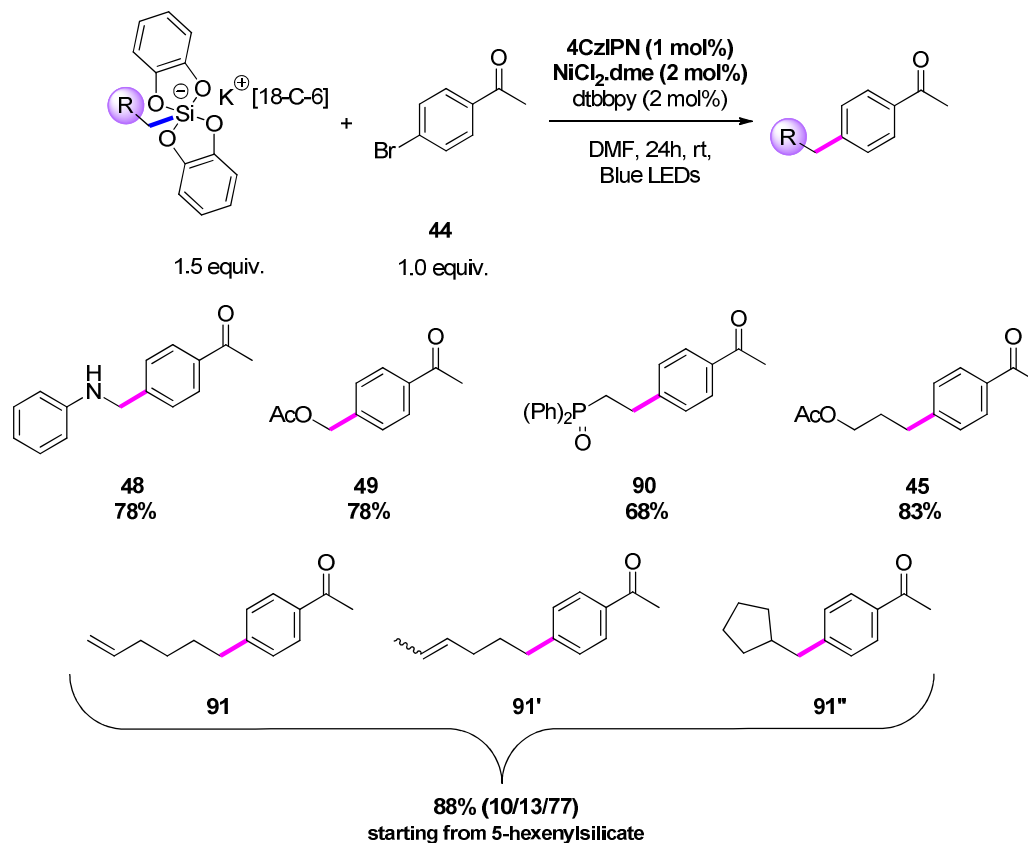
Entry	Silicate (nb equiv.)	4CzIPN loading (mol%)	Nickel source/loading (mol%)	Yield (%)
1	1.5	2	Ni(COD) ₂ , 3	0%
2	1.5	2	NiCl ₂ .dme, 3	77% ^a
3	1.5	2	NiCl ₂ .dme, 5	81% ^a
4	1.5	1	NiCl ₂ .dme, 2	79% ^a , 83% ^b
5	1.2	1	NiCl ₂ .dme, 2	57% ^a

^aNMR yield. ^b Isolated yield

At first, the compatibility of several types of alkyl silicates was explored with 4'-bromoacetophenone (**Scheme 84**). As previously reported conditions, α -amino and α -oxo alkyl silicates provided the products **48** and **49** in good yields. When the chloromethyl silicate was used as radical precursor, no product formation was observed. Aliphatic silicates bearing a phosphine oxide, an ester or an alkene function were as well tolerated. Concerning the phosphine oxide silicate **16**, and as previously mentioned no product resulting from the generation of a P-centered radical was observed. 5-Hexenyl silicate gave rise a mixture of products **91**, **91'** and **91''** in a 10/13/77 ratio and 88% overall yield. Here, the intermediate 5-hexenyl radical would directly react to provide products **91** and **91'** resulting from post-isomerization of **91**.¹⁸⁷ Interestingly, the formation of the major product **91''** is attributed to a 5-*exo*-trig cyclization of the radical prior to the addition to the nickel intermediate in the

¹⁸⁷ (a) R. G. Miller, P. A. Pinke, R. D. Stauffer, H. J. Golden and D. J. Baker, *J. Am. Chem. Soc.*, 1974, **96**, 4211–4220. (b) F. Weber, A. Schmidt, P. Roëse, M. Fischer, O. Burghaus and G. Hilt, *Org. Lett.*, 2015, **17**, 2952–2955.

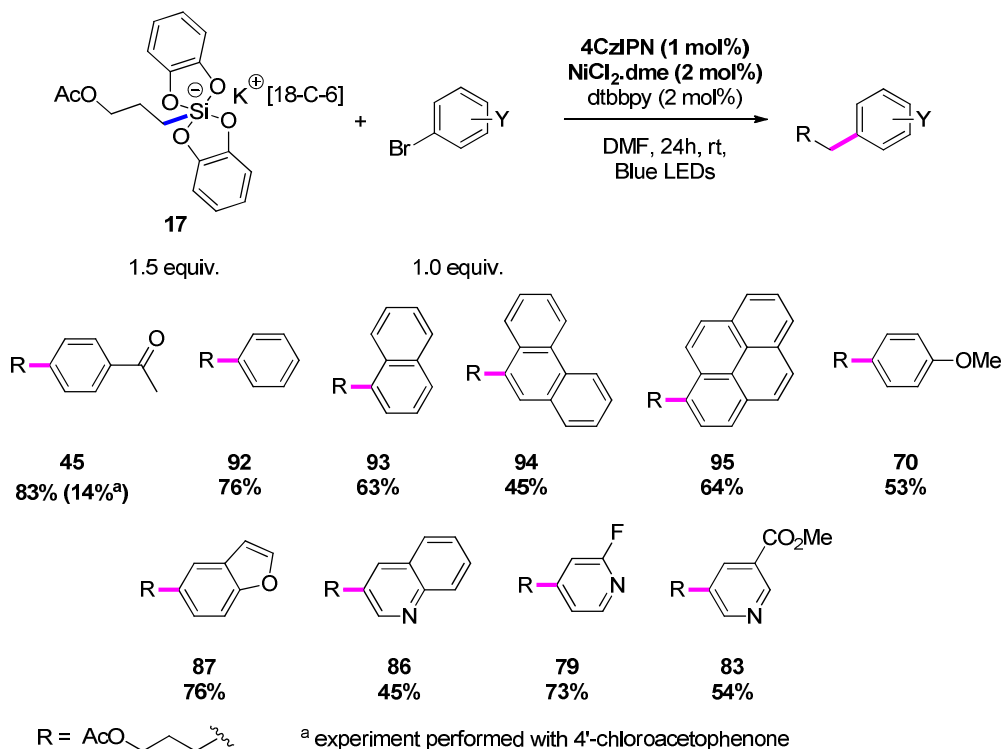
coupling process. This last result highlights once again the radical character of the transformation.



Scheme 84. Screening of alkyl silicates for organic photoredox/nickel dual catalysis with **44**

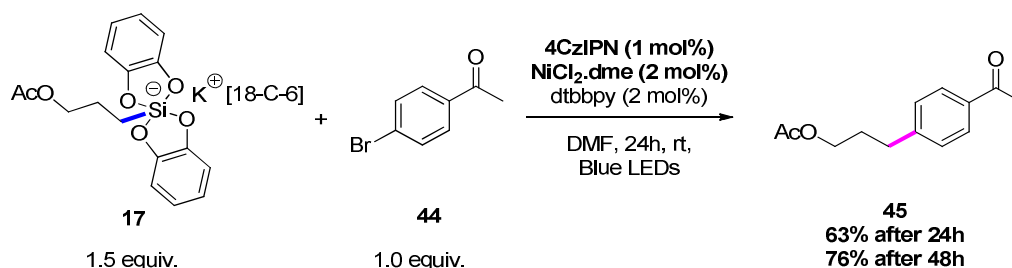
Again, we screened several aryl and heteroaryl bromides with acetoxypopylsilicate **17** (**Scheme 85**). A better yield was observed for the electron neutral substrate **92** and the electron poor electrophile **45** than for *para*-bromoanisole **96**. Polyaromatic substrates also gave the expected products **93-95** in moderate yields. In these cases, the polyarylated bromides may act as quencher of luminescence of the photocatalyst through an energy transfer. The oxidative process would be then in competition. Moreover, when 4'-chloroacetophenone was engaged, the yield of cross-coupling adduct decreased dramatically (from 83% to 14% of **45**). This highlights the importance of the oxidative addition step, in accordance with the postulated mechanism. Heteroaryl bromides can also act as electrophilic

partners. Pyridines **79** and **83**, quinoline **86** or benzofuran derivatives **87** provided coupling products in moderate to good yields.



Scheme 85. Screening of (hetero)aryl bromides for organic photoredox/nickel dual catalysis with **17**

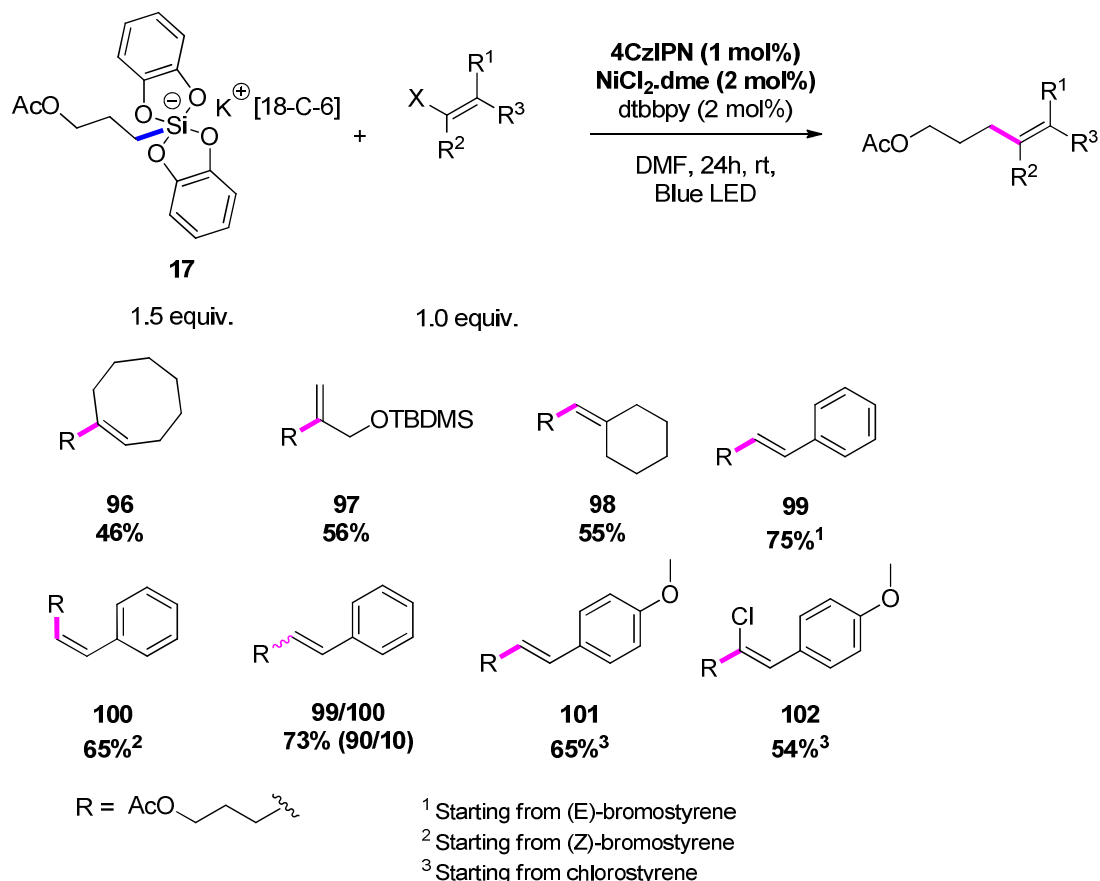
In order to illustrate the efficiency of 4CzIPN as a photocatalyst for this type of dual catalysis, a scale-up experiment was accomplished using acetoxypropylsilicate **17** and 4'-bromoacetophenone **44**. The reaction was performed on 3 mmol by using the usual experimental conditions except for the reaction time. Indeed, after 24 hours of reaction, only 63% yield of **45** was obtained, which could be further improved to 76% by increasing the reaction time to 48 hours (**Scheme 86**).



Scheme 86. Scale-up reaction

We then considered extending this methodology to alkenyl halides. These ones were already reported to be valuable electrophiles in such processes¹⁷¹ and particularly with silicates.¹⁸⁸ Therefore, we engaged alkenyl bromides with acetoxypropylsilicate **17** under these modified conditions. Unactivated alkenyl bromides were converted to their corresponding products in moderate yields **96-98**. Using activated alkenyl halides such as styryl bromide, styryl chloride and β -gem-dichlorostyrene gave fair to good yields of coupling products **99-102** (**Scheme 87**). The β -gem-dichlorostyrene derivative gave only the (*Z*)-mono functionalized product **100** in moderate yield after 48 hours. Starting from pure (*E*) or (*Z*) β -bromostyrene, we observed a complete retention of the double bond geometry during the transformation **99**, **100** and **101**. A commercial mixture with an 85/15 *E/Z* ratio showed the same behavior with a 90/10 ratio of products **99** and **100**.

¹⁸⁸ N. R. Patel, C. B. Kelly, M. J. Jouffroy and G.A Molander, *Org. Lett.*, 2016, **18**, 764–767.



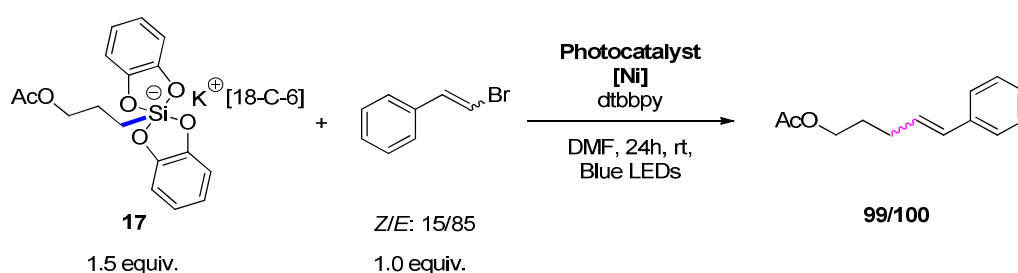
Scheme 87. Reaction of silicates with alkenyl halides

It was interesting to compare this finding with the metallic photocatalysts Ru(bpy)₃(PF₆)₂ and [Ir(dF(CF₃)ppy)₂(bpy)](PF₆) (Table 8). Previously reported conditions^{144b,188} led to the expected products in 75% (*E/Z*: 85/15) yield with the ruthenium photocatalyst (entry 2) and 90% (*E/Z*: 67/33) with the iridium photocatalyst (entry 3). In order to verify that the reaction does not follow a pure radical vinylation mechanism involving an addition-β-elimination tandem, the reaction was performed without nickel catalyst but only traces of products were observed. This result rules out the exclusive radical pathway. In addition, isomerization of β-bromostyrene in the presence of a photosensitizer has been already reported.¹⁸⁹ Control experiments were realized in the absence of the nickel catalyst and silicate and showed that the bromide slightly isomerized in the presence of 4CzIPN (*E/Z*: 65/35) (entry 5) compared to an *E/Z* ratio of 40/60 with the iridium complex (entry 7). The bromide atom has brought a

¹⁸⁹ (a) Y.-P. Zhao, L.-Y. Yang and R. S. H. Liu, *Green Chem.*, 2009, **11**, 837–842. (b) K. Singh, S. J. Staig and J. D. Weaver, *J. Am. Chem. Soc.*, 2014, **136**, 5275–5278.

heavy atom effect and so an easy access to the triplet state¹⁹⁰ which then promotes the isomerization. The photoexcited Ru(bpy)₃^{2+*} did not provide any isomerization of the styryl bromide, probably due to its lower energy triplet state (entry 6). Therefore we can assume that the 4CzIPN can act as photosensitizer of styryl derivatives but the photooxidation is faster than the photoisomerisation, opening opportunities for stereoselective alkenyl-alkyl cross-coupling reactions.

Table 8. Comparison of experimental conditions for photoredox/nickel dual-catalysis with β -bromostyrene



Entry	Photocatalyst (mol%)	Nickel source (mol%)	Yield (E/Z)
1	4CzIPN (1)	NiCl ₂ .dme (2) ^a	73% ^b (90/10)
2	Ru(bpy) ₃ (PF ₆) ₂ (2)	NiCl ₂ .dme (3) ^a	75% ^b (85/15)
3	[Ir(dF(CF ₃)ppy) ₂ (bpy)](PF ₆) (2)	Ni(COD) ₂ (3) ^a	93% ^b (67/33)
4	4CzIPN (1)	No nickel	<5% ^b
5	4CzIPN (1)	No nickel	S.M. ^{b,c} (65/35)
6	Ru(bpy) ₃ (PF ₆) ₂ (2)	No nickel	S.M. ^{b,c} (85/15)
7	[Ir(dF(CF ₃)ppy) ₂ (bpy)](PF ₆) (2)	No nickel	S.M. ^{b,c} (40/60)

In conclusion, this organic dye has proved its efficiency in photoredox/nickel dual catalysis with alkyl silicates. Other works reported later the use of the 4CzIPN with alkyl silicates for the functionalization of imines,¹⁹¹ borylated bromoarenes,^{32b} and also with benzyltrifluoroborates.^{32c}

¹⁹⁰ For a review on molecular photochemistry, see: N. J. Turro, V. Ramamurthy and J. C. Scaiano, *Modern Molecular Photochemistry*, University Science Books, Sausalito CA, 1991.

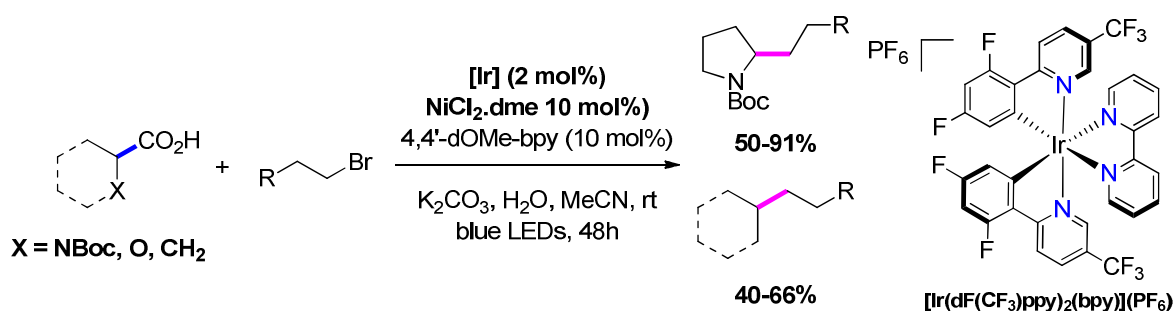
¹⁹¹ N. R. Patel, C. B. Kelly, A. P. Siegenfeld and G. A. Molander, *ACS Catal.*, 2017, **7**, 1766–1770.

4.4 Alkyl bis-catecholato silicates in photoredox/nickel dual catalysis: formation of C(sp³)-C(sp³) bonds

Alkyl bis-catecholato silicates have demonstrated to be powerful substrates for the generation of primary alkyl radicals which can be involved in radical addition reactions and nickel-catalyzed C(sp³)-C(sp²) bonds formation. The remaining challenge is to develop a catalytic version for the C(sp³)-C(sp³) bonds formation.

4.4.1 C(sp³)-C(sp³) cross-coupling reactions involving alkyl carboxylates

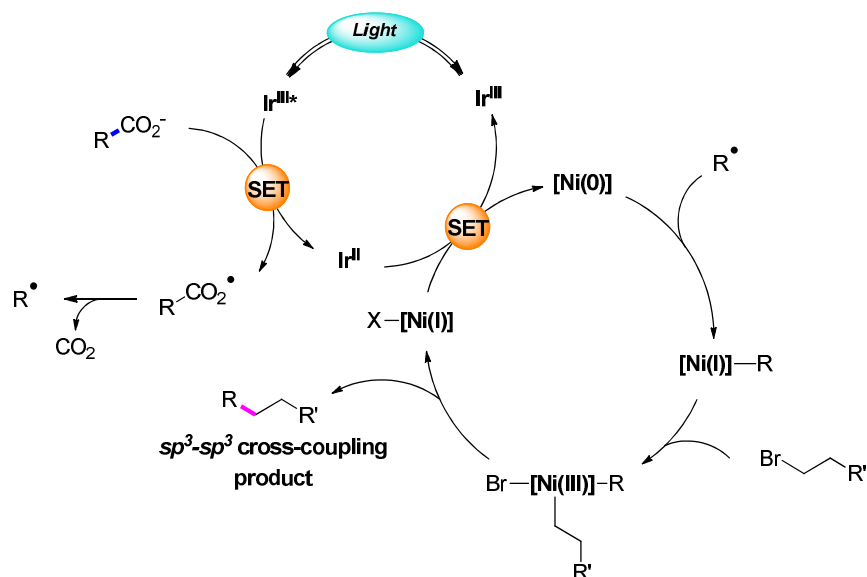
In 2016, the group of MacMillan reported new reaction conditions for cross-coupling reactions between alkyl carboxylates and alkyl bromides.¹⁹² The reported methodology involves the use of [Ir(dF(CF₃)ppy)₂(dtbbpy)](PF₆) as oxidizing photocatalyst, NiCl₂.dme as nickel source and 4,4'-dimethoxy-2,2'-bipyridine (4,4'-dOMe-bpy) as ligand. The carboxylates obtained by reaction of the corresponding carboxylic acids with potassium carbonate reacted with various alkyl bromides under these conditions. Decarboxylation of α-amino or α-oxo carboxylates gave stabilized alkyl radicals which could be coupled with primary or secondary alkyl bromides in good yields (**Scheme 88**). The reaction conditions were tolerated by electrophiles bearing a free alcohol, carbonyl or oxirane function. In addition, unactivated primary and secondary carboxylic acids were engaged in the process, giving the coupling products in moderate yields.



Scheme 88. Dual photoredox/nickel catalyzed sp^3 - sp^3 coupling reaction between alkyl carboxylates and alkyl bromides

¹⁹² C. P. Johnston, R. T. Smith, S. Allmendinger and D. W. C. MacMillan, *Nature*, 2016, **536**, 322–325.

The authors proposed an usual mechanism for this transformation (**Scheme 89**). The excited iridium photocatalyst oxidizes the carboxylate. After CO₂ extrusion, the generated radical adds on the Ni(0) catalyst to form the Ni(I) species. Oxidative addition with the alkyl bromide leads to a Ni(III) intermediate. A reductive elimination step would give the desired product and another Ni(I). A final SET from Ir(II) to Ni(I) regenerates both catalysts to complete a single turnover.



Scheme 89. Proposed mechanism for the cross-coupling of carboxylates with alkyl bromides

4.4.2 Silicates as nucleophilic partners

When MacMillan and co-workers reported their advances on C(sp³)-C(sp³) cross-coupling photoredox/nickel dual catalysis, we were developing our own catalytic system involving alkyl bis-catecholato silicates.¹⁹³

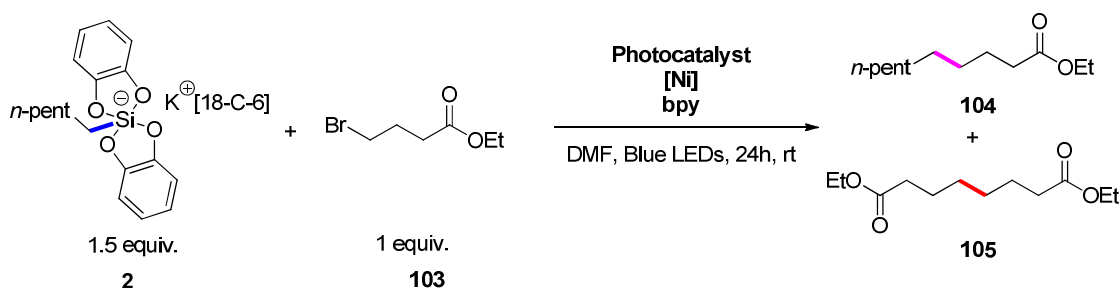
4.4.2.1 Optimization of the cross-coupling reaction

We started our studies on the coupling of [18-C-6] *n*-hexylsilicate **2** with ethyl 4-bromobutyrate **103**. The catalytic system was composed with 2 mol% of [Ir(dF(CF₃)ppy)₂(bpy)](PF₆) as photocatalyst and 5 mol% of Ni(COD)₂ and 2,2'-bipyridine to

¹⁹³ C. Lévêque, V. Corcé, L. Cheneberg, C. Ollivier and L. Fensterbank, *Eur. J. Org. Chem.* **2017**, 2118–2121.

produce the organometallic catalyst. After 24 hours in DMF under light irradiation with 1.2 equivalents of silicate and 1 equivalent of the electrophile **103**, we were pleased to see the formation of cross-coupling product **104** in 29% yield (Table 9 entry 4). Contrary to MacMillan's results, we observed the dimerization product of the electrophile **105** in 52% yield. This byproduct has been previously reported by Weix and co-workers during their studies on the nickel-catalyzed dimerization of alkyl halides.¹⁹⁴ They used the same conditions as for the aryl-alkyl electrophilic cross-coupling reactions.^{163,164} Based on their mechanism, they proposed (**Scheme 66**) the alkyl halide may furnish an alkyl radical. Therefore two kinds of radicals would be in competition in the reaction mixture. Then, the aim was to improve the reaction conditions in order to avoid the formation of the homocoupling product and favor the cross-coupling adduct. Increasing the photocatalyst loading to 5 mol% slightly improved the **104/105** ratio (entry 1). Switching to other photocatalysts (Ru(bpy)₃PF₆ and 4CzIPN) did not give better results (entry 2 and 3). However, starting with 1.5 equivalents of silicates gave the best ratio of products **104/105** 42/38 (entry 6) whereas changing the number of equivalents of the silicate (to 2 equiv.) (entry 7) or using a nickel(II) precatalyst proved to be less effective (entry 8).

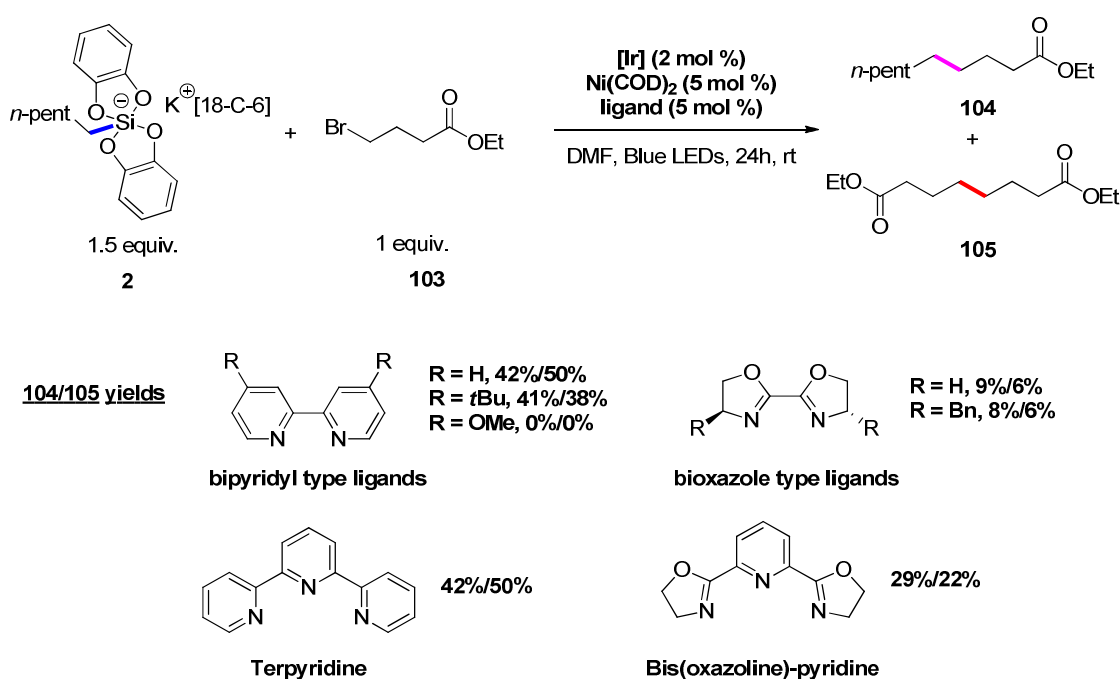
Table 9. Optimization of the reaction conditions



Entry	Silicate (equiv.)	Photocatalyst (mol%)	Ni source (5 mol%)	Yield (104/105)
1	1.2	[Ir] (5)	Ni(COD) ₂	34/38
2	1.2	Ru(bpy) ₃ (PF ₆) (5)	Ni(COD) ₂	22/36
3	1.2	4CzIPN (5)	Ni(COD) ₂	22/25
4	1.2	[Ir] (2)	Ni(COD) ₂	29/52
5	1.5	[Ir] (2)	Ni(COD) ₂	42/50
6	1.5	[Ir] (5)	Ni(COD) ₂	43/38
7	2	[Ir] (5)	Ni(COD) ₂	44/42
8	1.5	[Ir] (5)	NiCl ₂ .dme	26/30

¹⁹⁴ M. R. Prinsell, D. A. Everson, D. J. Weix, *Chem. Commun.*, 2010, **46**, 5743–5745.

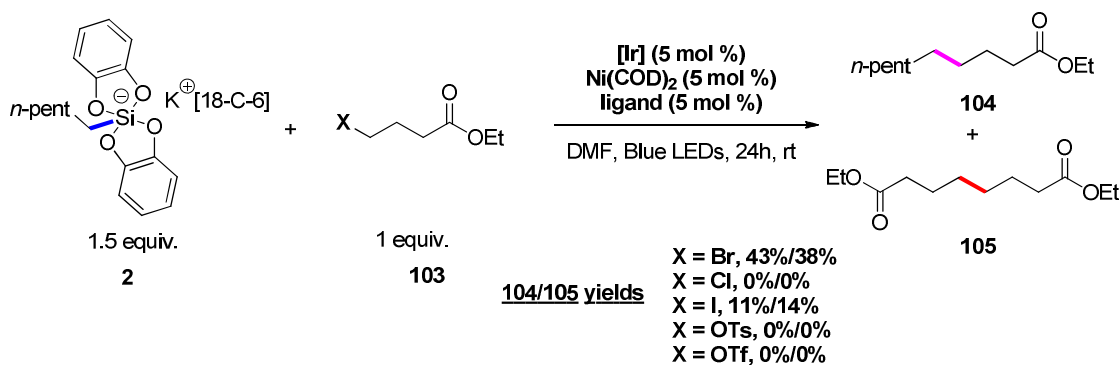
The nature of the ligand was analyzed. Indeed, the efficiency of the process has been proved to be dependent of the ligand.^{192,195} Several bidentate ligands were screened (**Scheme 90**). Modified bipyridyl type ligands did not enhance the yield of cross-coupling product **104** and limit the formation of adduct **105**. In particular, the ligand 4,4'-dOMe-bpy revealed to be ineffective. Bioxazole derivatives were also engaged as ligand but again, the reaction was less productive. Tridentate ligands were also tested. Terpyridine proved to be an effective ligand leading to **104** in 42% yield but did not avoid the dimerization (50% of **105**). 2,6-Bis(oxazoline)-pyridine (pybox) gave both products in lower yields.



Scheme 90. Screening of ligands

The electrophile partner was also modified (**Scheme 91**). Ethyl 4-chlorobutyrate was not converted as well as the tosyl derivative while the iodo analogous afforded both products in poor yields. The triflate derivative was also tested but showed to react with the solvent DMF.

¹⁹⁵ F. Lima, M. A. Kabeshov, D. N. Tran, C. Battilocchio, J. Sedelmeier, G. Sedelmeier, B. Schenkel, S. V. Ley, *Angew. Chem. Int. Ed.*, 2016, **55**, 14085–14089.



Scheme 91. Screening of electrophiles

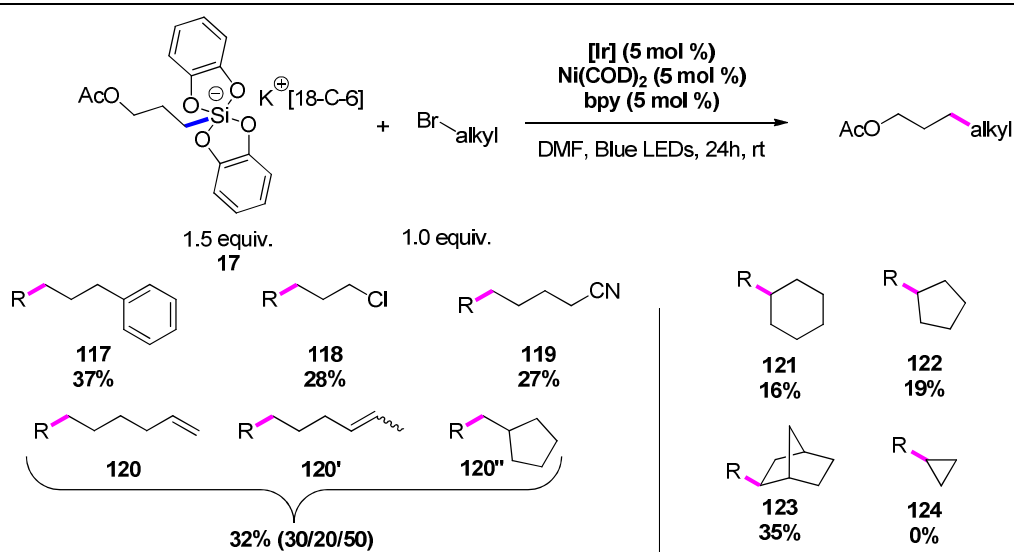
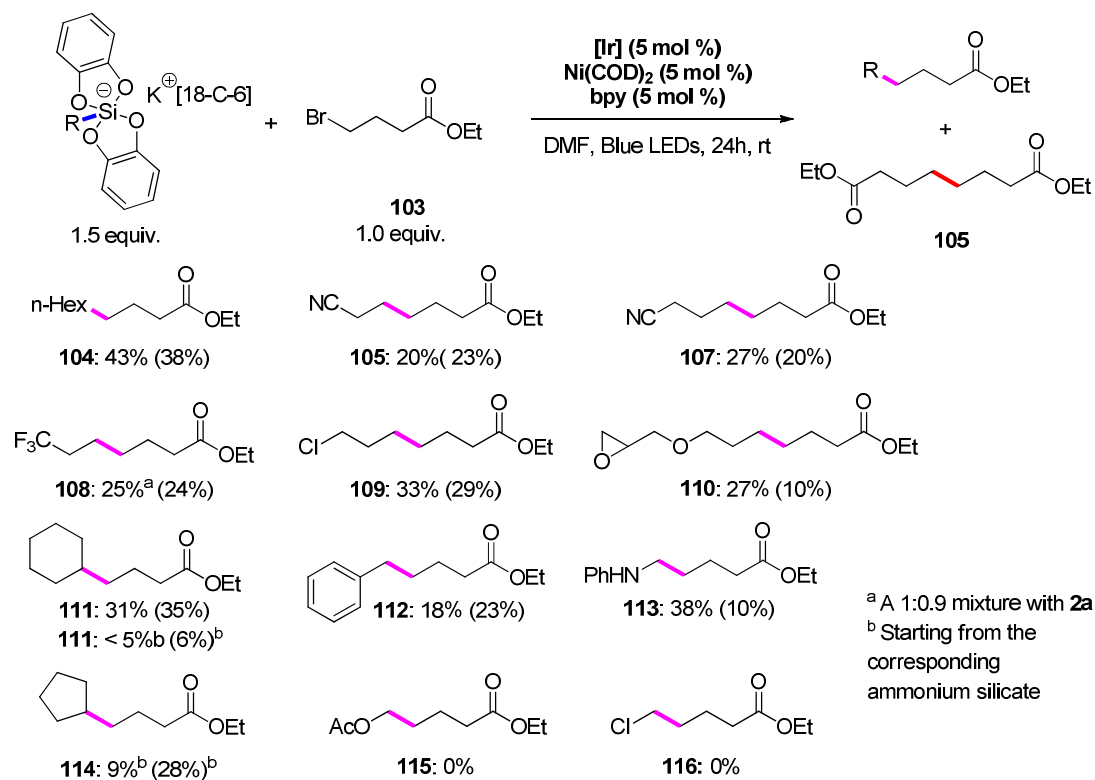
Under the optimized reaction conditions, we envisioned that the formation of the desired product **104** might be promoted at lower concentration. Thus, we performed the cross-coupling reaction with slow addition of ethyl 4-bromobutyrate **103**. The electrophile was added over 18 hours thanks to a syringe pump. Unfortunately, the homocoupling and the cross-coupling products were obtained in similar yields.

4.4.2.2 Scope of the reaction and limitations

After optimisation, various silicates were engaged in our reaction conditions. As for the aryl-alkyl cross-coupling reactions, silicates bearing a nitrile group **106** and **107**, a halogen **108** and **109** or an oxirane **110** could be coupled with compound **103** (**Scheme 92**). Activated silicates such as benzyl or anilinomethyl silicates afforded the cross-coupling products **112** and **113**. Conversely, acetoxymethyl and chloromethyl silicates did not provide any coupling product **115** and **116**. Secondary cyclohexyl silicate showed also to be reactive leading to **111**. With triethylammonium cyclohexyl and cyclopentyl silicates, the reaction revealed to be poorly effective to give **111** and **114** and so, the yields of cross-coupling products were low to moderate. It should be noted that the formation of the homocoupling product observed in the optimization study, was obtained in each case with yields close to those of the cross-coupling product. It suggests that the formation of both products is simultaneous, and so two catalytic pathways are occurring at the same time with possibly a nickel intermediate involved in both processes. Finally, we also engaged different bromides with acetoxypropylsilicate **17**. Primary **117-120** and secondary alkyl bromides (**121-123** reacted more or less efficiently (27–37 and 16–35%, respectively). 5-Hexenyl bromide provided a mixture of direct $\text{C}(\text{sp}^3)\text{-C}(\text{sp}^3)$ cross-

coupling products **120/120'** together with a tandem *5-exo-trig*/cross-coupling product **120''**. The latter presumably indicates the generation of the 5-hexenyl radical and its further interception by the nickel complex to enter the cross-coupling catalytic cycle. This radical generation from the alkyl bromide partner may also be at the origin of the homocoupling product.

We succeed to extend the photoredox/nickel dual catalysis process with alkyl silicates and electrophiles to the formation of C(sp³)-C(sp³) bonds. Unfortunately, the yields of cross-coupling products are low to moderate due to the formation of the homocoupling product. Based on the reports on the nickel electrophilic cross-coupling reaction and photoredox/nickel catalysis, we could not propose a mechanism taking account of the formation of each product. This mechanism poses intriguing questions and required to be more investigated.



Scheme 92. Screening of alkylsilicates and alkyl bromides for the photoredox/nickel C(sp³)-C(sp³) cross-coupling reactions

4.5 Extension to other catalytic systems

The efficiency of alkyl bis-catecholato silicates to generate alkyl radicals is now well established. We expected to engage these precursors in other catalytic systems.

4.5.1 Concept of non-innocent ligands

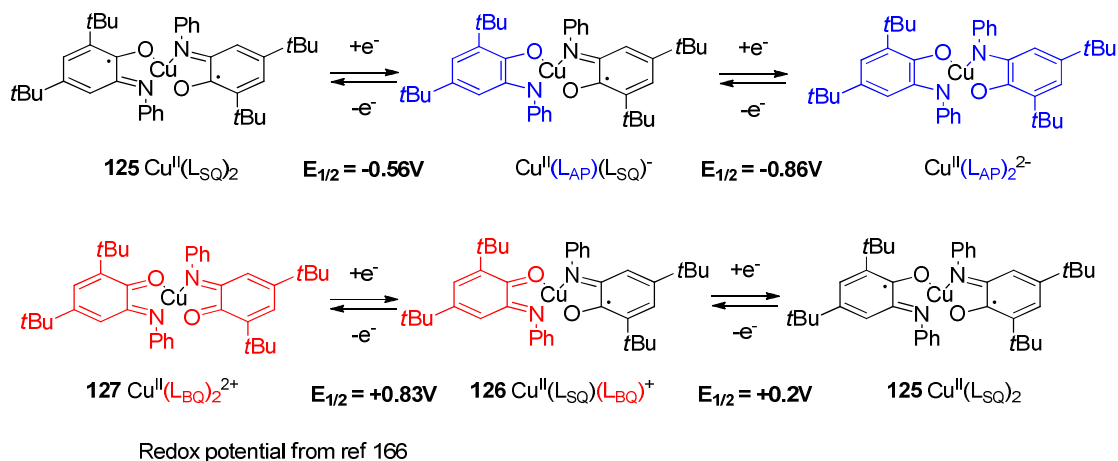
In our group and in the context of the Ph.D. thesis of Jérémy Jacquet,¹⁹⁶ it has been demonstrated that some non-innocent ligands can catalyze redox processes through the generation of radicals. In 1966, Jørgensen defined the concept of innocent ligand: ‘*ligands are innocent when they allow oxidation state of the central atoms to be defined*’.¹⁹⁷ For instance, ligands in palladium-catalyzed cross-coupling reactions are innocent. In each step of the catalysis, the oxidation state of the metal is well-defined. At the opposite, iridium and ruthenium complexes in photoredox catalysis are catalyst with non-innocent ligands because they are metal-ligand coupled redox system. In addition, some complexes exist with almost pure ligand centered redox processes. This is the case of the bis-iminosemiquinonato copper complex $\text{Cu}(\text{L}_{\text{SQ}})_2$ **125**, which displays a Cu(II) and two iminosemiquinonate radical ligands (**Scheme 93**).

This complex can undergo two successive single electron reductions leading to the formation of the bis-anionic bis-aminophenolate copper(II) complex $\text{Cu}(\text{L}_{\text{AP}})_2^{2-}$, or two successive single electron oxidations to give the bis-cationic bis-iminobenzoquinone copper(II) complex $\text{Cu}(\text{L}_{\text{BQ}})_2^{2+}$ **127** (**Scheme 93**).¹⁹⁸ This ability of single electron redox processes can be exploited to generate radicals by SET between one of the copper species and a radical precursor.

¹⁹⁶ For the PhD manuscript see: Catalyse coopérative avec les ligands rédox non-innocents : processus radicalaires et organométalliques, Jérémy Jacquet, Université Pierre et Marie Curie, 2016.

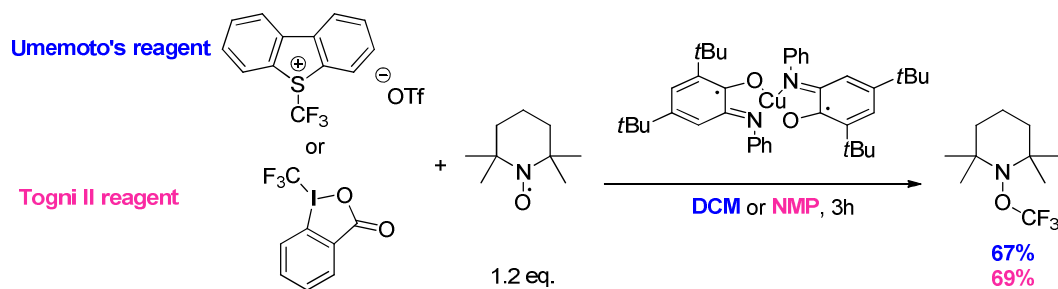
¹⁹⁷ C. K. Jørgensen, *Coord. Chem. Rev.*, 1966, **1**, 164–178.

¹⁹⁸ P. Chaudhuri, C. Nazari Veani, E. Bill, E. Bothe, T. Weyhermüller, K. Wieghardt, *J. Am. Chem. Soc.*, 2001, **123**, 2213–2223.



Scheme 93. Redox properties of $\text{Cu}(\text{L}_{\text{SQ}})_2$

It was found that complex $\text{Cu}(\text{L}_{\text{SQ}})_2$ **125** can reduce electrophilic CF_3 sources to produce radicals. Spin-trapping experiments with TEMPO and stoichiometric amounts of the trifluoromethylating agent and the copper complex were realized (**Scheme 94**). In DCM after 3 hours, the adduct CF_3 -TEMPO can be obtained in 67% yield from the Umemoto's reagent. The same product was obtained after 3 hours in 69% yield from the Togni II reagent in NMP.¹⁹⁹

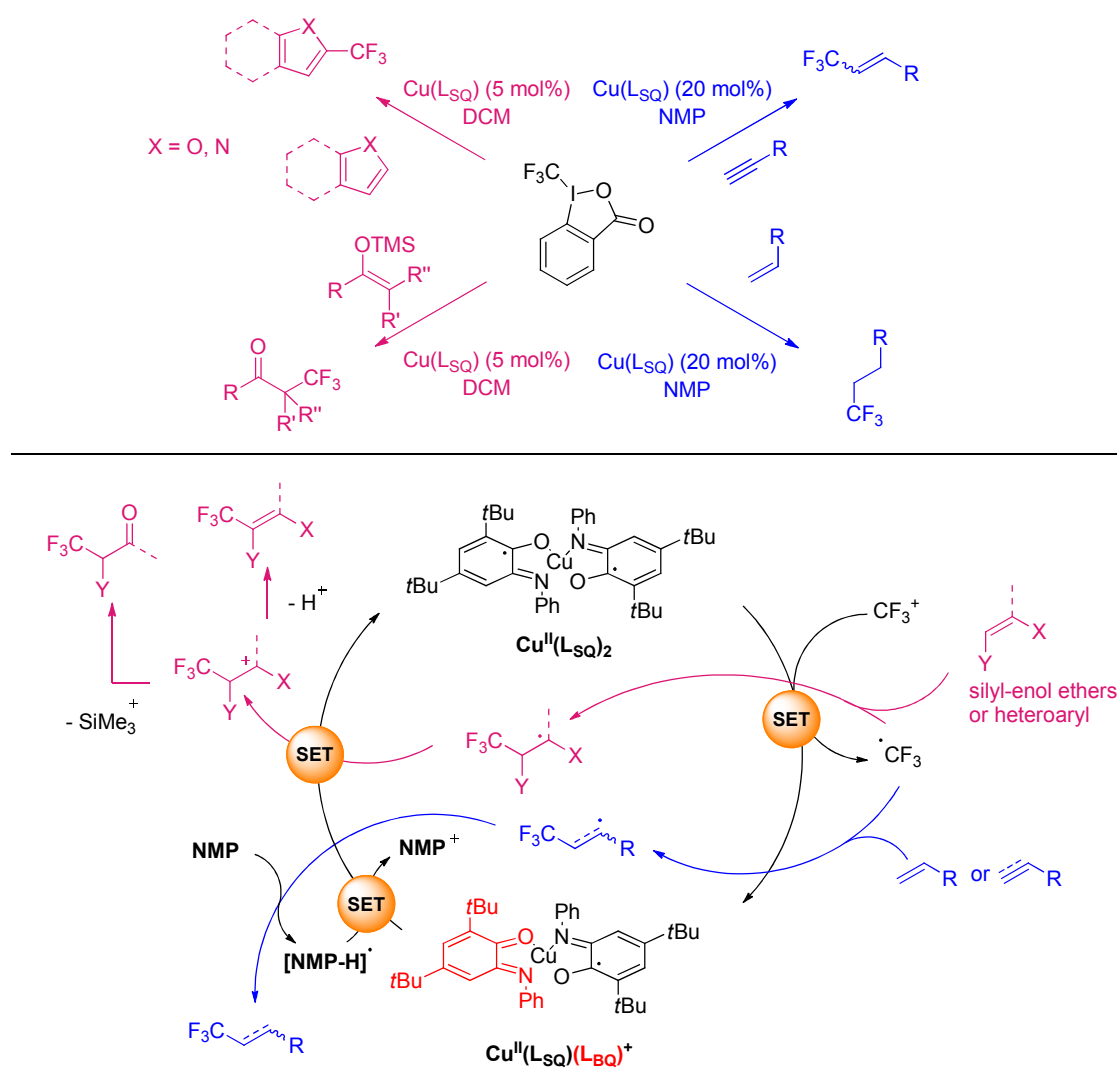


Scheme 94. Spin-trapping of $\text{CF}_3\cdot$ radical experiments with TEMPO

The evidence of the trifluoromethyl radical formation established, radical addition experiments were performed with a catalytic loading of copper complex **125**. The trifluoromethyl radical generated by reduction of the Togni II reagent could be trapped by alkenes or alkynes in NMP, as well as silyl-enol ethers or electron-rich heteroaryls such as pyrroles, indoles or furans in DCM. It was proposed that complex **125** would reduce the

¹⁹⁹ J. Jacquet, S. Blanchard, E. Derat, M. Desage-El Murr and L. Fensterbank, *Chem. Sci.*, 2016, **7**, 2030–2036.

Togni II reagent to produce the trifluoromethyl radical and the complex $\text{Cu}(\text{L}_{\text{SQ}})(\text{L}_{\text{BQ}})^+$ **126**. In NMP, the radical adds on the alkene or alkyne to generate an alkyl radical or a vinyl radical respectively. After a hydrogen abstraction on the NMP, the product is formed and the radical [NMP-H] realizes a SET with complex **126** to regenerate the catalyst (**Scheme 95**). In DCM, the trifluoromethyl radical adds on the silyl-enol ether or the heteroaryl and provides an alkyl radical which directly reacts with complex **126** to regenerate the catalyst. Then, the cation evolves either by loss of SiMe_3^+ generating an α - CF_3 carbonyl, or by loss of H^+ providing the CF_3 -substituted heteroaryl at the C2 position.

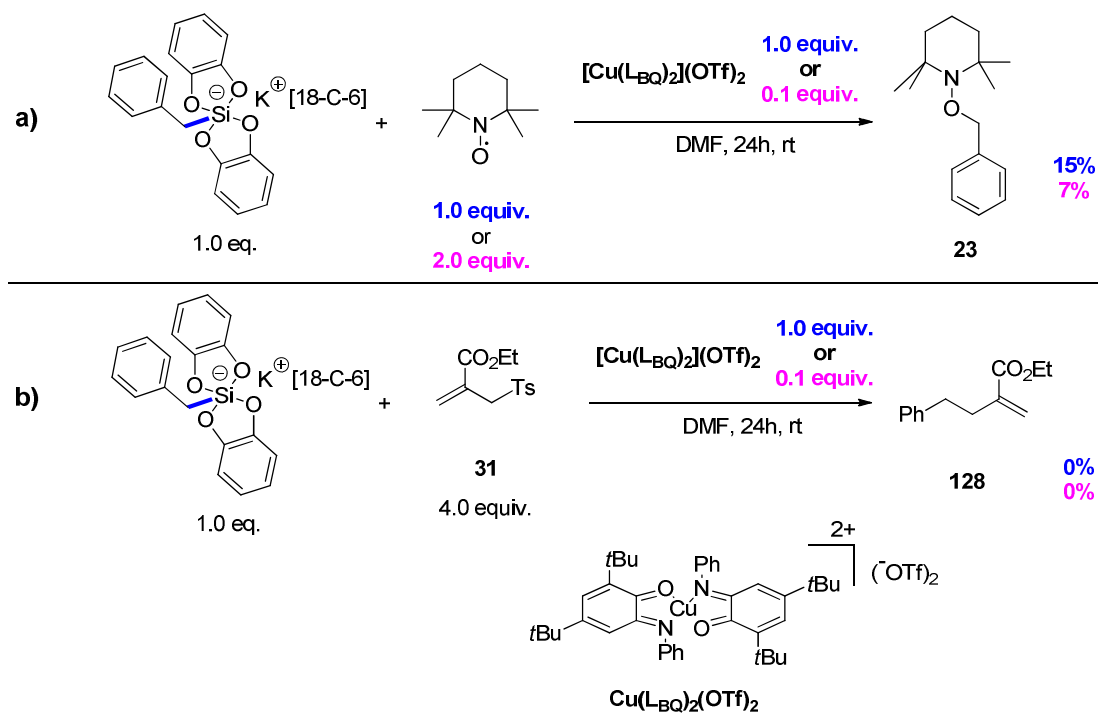


Scheme 95. Copper catalyzed radical trifluoromethylation reactions, and mechanisms

Inspired by these catalytic processes, we envisioned to develop a copper-mediated catalytic oxidation of alkyl bis-catecholato silicates.

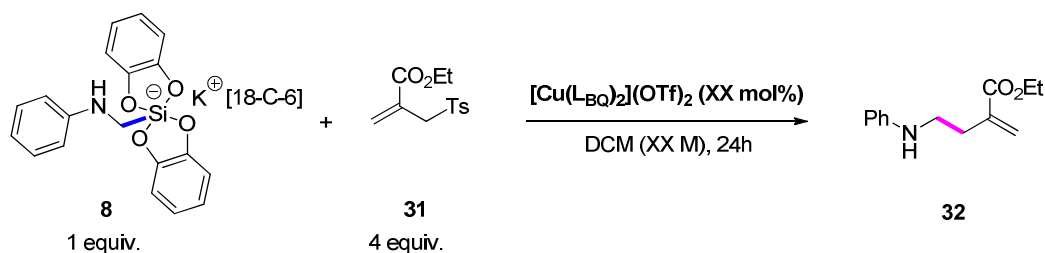
4.5.2 Preliminary results

We first considered two properties of the alkyl bis-catecholato silicates to perform the oxidation. In one hand, these substrates are easy to oxidize given that the range of oxidation potential is +0.34-+0.90 V vs SCE in DMF. On the other hand, the oxidation process is more efficient in DMF than other solvents. With these two parameters, we expected to realize efficiently the oxidation with the complex $\text{Cu}(\text{L}_{\text{BQ}})_2(\text{OTf})_2$ ($E_{1/2} = +0.83\text{V}$ vs SCE in DCM). In addition, these types of copper complexes showed efficient in NMP,¹⁹⁹ which displays a similar polarity to DMF. So for this reason, we opted for this last solvent. We first looked at the possible formation of alkyl radicals from the corresponding bis-catecholato silicates by oxidation with the copper complex **127**. Benzylsilicate **4** was engaged in spin-trapping experiments with TEMPO in the presence of a stoichiometric amount of complex **127**. The benzyl TEMPO adduct**23** was isolated in 15% yield after 24 hours in DMF (**Scheme 96**). The same reaction was also performed with 10 mol% of catalyst and two equivalents of TEMPO. In this case, only 7% yield of the product was obtained. We also tested allylsulfone **31** as radical scavenger. However, with a catalytic loading or a stoichiometric amount of copper complex **127**, we never observed the formation of product **128**.



Scheme 96. Copper mediated trapping experiments of benzyl radical

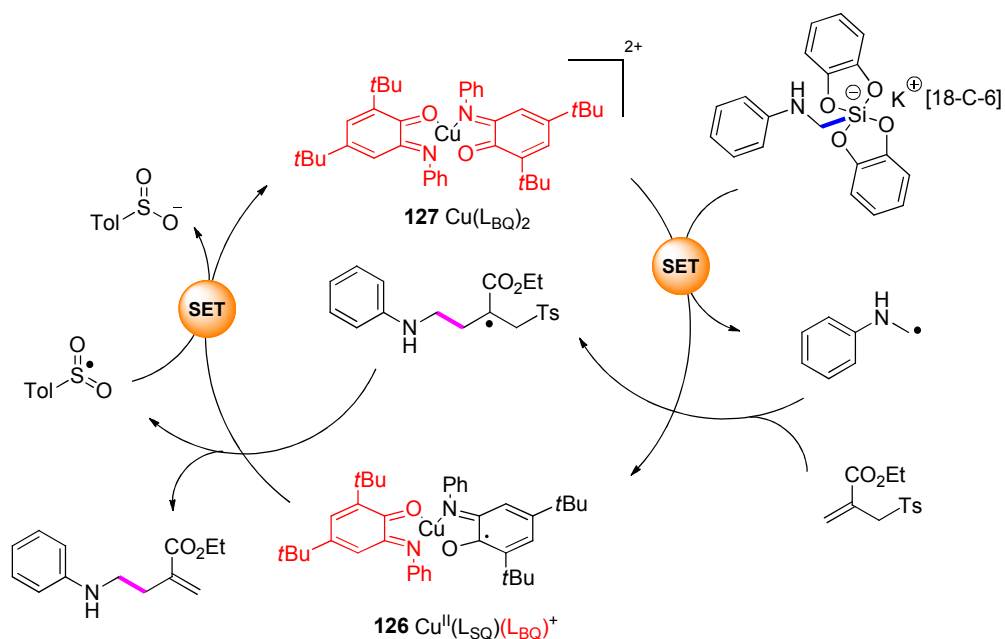
We next switched to DCM which proved to be also efficient with this family of copper complexes.¹⁹⁹ Anilinomethyl silicate **8** was selected due to its lowest oxidation potential ($E_{\text{ox}} = +0.34$ V vs SCE in DMF), in order to render the reaction as thermodynamically favorable as possible. In this case, we did not engage the silicate with TEMPO because it should lead to an unstable hemiaminal. Allylsulfone **31** was used as radical acceptor with 10 mol% of complex **127** to give product **32** in 52% yield after 24 hours of reaction (**Table 10**, entry 1). Several parameters of the reaction were modified to optimize the system. The catalyst loading was first analyzed. Decreasing the amount of copper complex from 10 mol% to 5 mol% dropped dramatically the yield (12%) of the reaction and the worst case was observed with 2 mol% (entry 4 and 5). We then considered the influence of the concentration. Dividing or multiplying by two, the concentration had not significant impact on the yield (entry 2 and 3). Increasing the number of equivalents of acceptor from 4 to 6 improved the yield to 66% (entry 6).

Table 10. Optimization of copper mediated oxidation of anilinomethylsilicate

Entry	Concentration	Loading [Cu]	Yield
1	0.1M	10 mol%	52%
2	0.05M	10 mol%	48%
3	0.2M	10 mol%	56%
4	0.1M	5 mol%	12%
5	0.1M	2 mol%	6%
6	0.1M	10 mol%	66% ^a

^a 6 equivalents of allylsulfone **27** used.

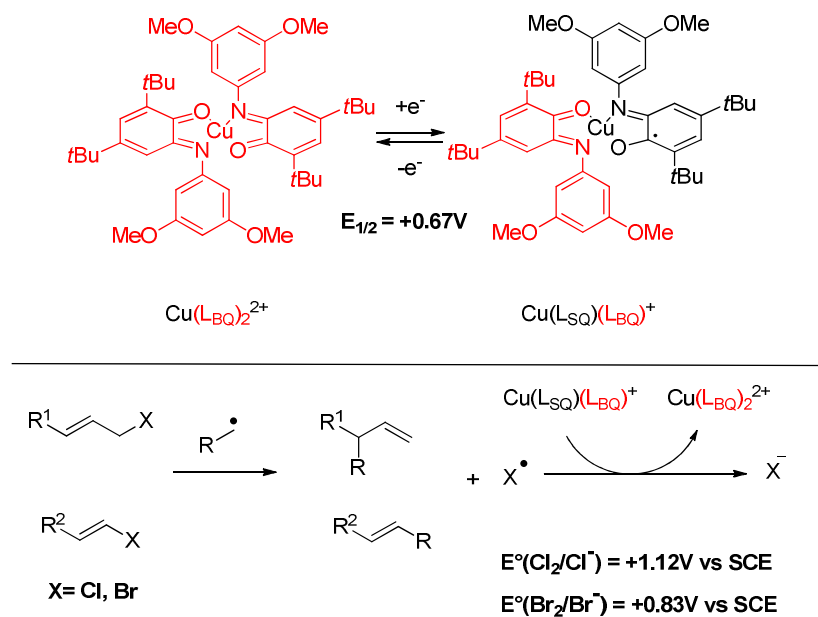
About the mechanism of the reaction, copper catalyst **127** would oxidize silicate **8** and provide the anilinoethyl radical and complex **126**. After addition of the radical on the acceptor followed by fragmentation of the C-S bond, product **32** would be obtained with a tosyl radical. This one might oxidize complex **126** regenerating the catalyst **127** with the formation of a sulfinate anion (**Scheme 97**). However, analysis of the redox potentials of these species involved in the last step reveals that the electron transfer is not thermodynamically favored ($E_{1/2}(\text{PhSO}_2\cdot/\text{PhSO}_2\text{Na}) = +0.50\text{V}$ vs SCE and $E_{1/2}(\text{Cu}(\text{L}_{\text{BQ}})_2^{2+}/\text{Cu}(\text{L}_{\text{BQ}})(\text{L}_{\text{SQ}})^+) = +0.83\text{V}$ vs SCE).



Scheme 97. Envisioned mechanism for the copper-mediated oxidation of silicates

Synthetic modifications of the catalyst to tune the redox potential and improve the reactivity of the system would be a promising solution. Indeed, copper bis-iminosemiquinonate complex with modified aniline moieties have been reported.²⁰⁰ Second oxidation of $\text{Cu}(\text{L}_{\text{SQ}})_2$ analogous with methoxy substituents in the 3- and 5- positions of aniline group was measured at +0.68V vs SCE in DCM. Another possibility would be to use other acceptors which lead to the formation of a stronger oxidizing radical intermediate such as allyl/vinyl chlorides or allyl/vinyl bromides providing a chlorine or bromine radical (**Scheme 98**).

²⁰⁰ C. Mukherjee, U. Pieper, E. Bothe, V. Bachler, E. Bill, T. Weyhermüller and P. Chaudhuri, *Inorg. Chem.*, 2008, **47**, 8943–8956.



Scheme 98. Possible modifications to optimize the oxidation of silicates with non-innocent ligands complexes.

4.6 Conclusion

The alkyl radicals generated by photooxidation of alkyl bis-catecholato silicates could be engaged in dual-catalytic processes involving photoredox/nickel dual catalysis. Thanks to the nickel catalysis, formation of C(sp²)-C(sp³) bonds from alkyl silicates and substituted aryl or heteroaryls could be realized with an iridium based photocatalyst. A dual-catalytic system was also developed with 4CzIPN, an organic dye as photocatalyst. These new reaction conditions showed to be as efficient compared with those previously exposed. Moreover, the methodology was extended to the formation of alkyl substituted alkenes. Finally, a dual-catalytic process for the C(sp³)-C(sp³) bonds formation was developed with a limited efficiency due to the formation of a homocoupling adduct as side product. Finally, the ability of alkyl bis-catecholato silicates to undergo radical formation upon oxidation may also be extended to other catalytic processes such as the use of copper complexes with non-innocent ligands which require more investigations.

Experimental Section

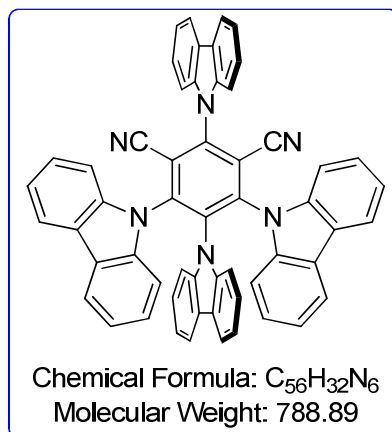
5 Experimental Section

5.1 General informations

Unless otherwise noted, reactions were carried out under an argon atmosphere in oven-dried glassware. THF and diethyl ether were distilled over sodium/benzophenone, triethylamine over potassium hydroxide. Catechol was purchased from commercial source and purified by crystallization from toluene followed by sublimation. Reagents and chemicals were purchased from commercial sources and used as received. Substrates without synthetic procedure detailed were purchased from commercial sources and used as received. Infrared (IR) spectra were recorded on a Bruker Tensor 27 (ATR diamond) spectrophotometer. Melting points were determined on a melting point apparatus SMP3 (Stuart scientific) and are uncorrected. ^1H , ^{19}F , ^{31}P and ^{13}C NMR spectra were recorded at room temperature at 400, 377, 162 and 100 MHz respectively, on a Bruker AVANCE 400 spectrometer. ^{29}Si NMR spectra were recorded at 119 MHz on a Bruker AVANCE III 600 spectrometer. Chemical shifts (δ) are reported in ppm and coupling constants (J) are given in Hertz (Hz). Abbreviations used for peak multiplicity are: s (singlet); bs (broad singlet); d (doublet); t (triplet); q (quartet); quint (quintet); sept (septet); m (multiplet). Thin layer chromatographies (TLC) were performed on Merck silica gel 60 F 254 and revealed with a UV lamp ($\lambda = 254 \text{ nm}$) and KMnO_4 staining. Flash Column Chromatographies were conducted on silica Geduran[®] Si 60 Å (40 – 63 μm). High resolution mass spectrometries were performed on a micro TOF (ESI).

5.2 Synthesis of photocatalysts

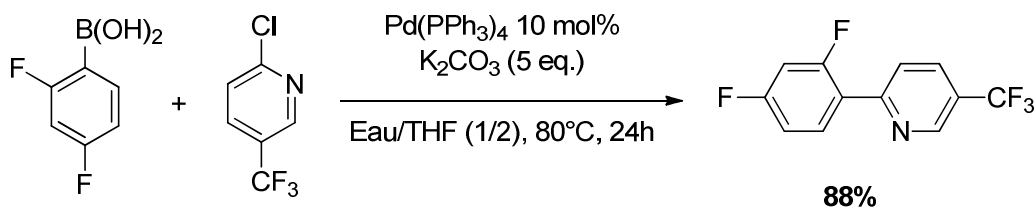
Synthesis of 4CzIPN



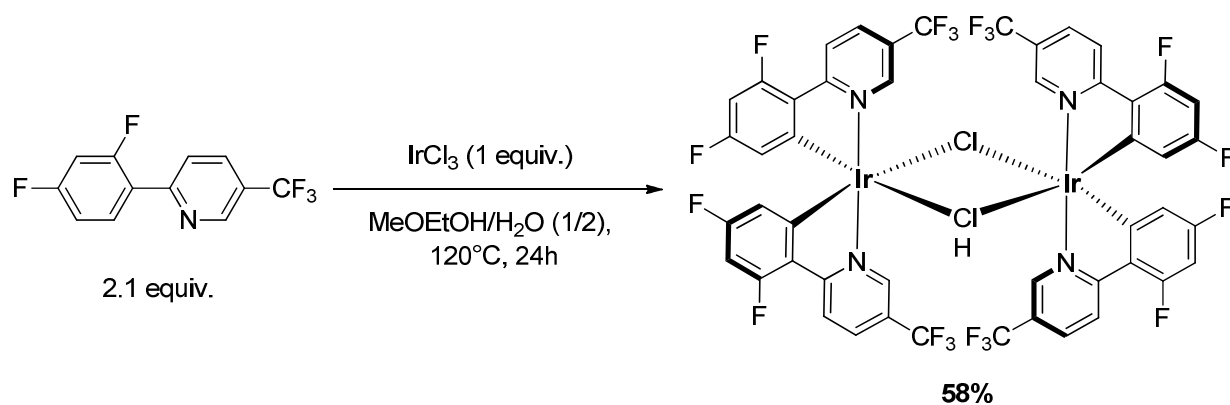
The 4CzIPN has been synthesized following a previous reported procedure.^[7] To a 100 mL round-bottom-flask was added NaH (60% in mineral oil) (15 mmol, 600 mg). THF (40 mL) was added followed by the slow addition of carbazole (10 mmol, 1.67 g). After 30 min of stirring at room temperature the tetrafluoroisophtalonitrile (2 mmol, 400 mg) was added and the mixture was stirred at room temperature for 20 hours. A yellow precipitate progressively appeared. Water (1 mL) was added to neutralize the excess of NaH and the mixture was evaporated to give a yellow solid. The solid was successively washed with water and ethanol. The crude product was dissolved in the minimum of DCM and crystallized by addition of pentane to give the pure **4CzIPN** (1.13g, 71% yield). The spectroscopic data are in agreement with those reported in the literature.

¹H NMR (400 MHz, $CDCl_3$): δ 8.35 (dt, $J = 7.7, 1.0$ Hz, 2H), 8.19 (d, $J = 8.3$ Hz, 2H), 7.87 – 7.84 (m, 4H), 7.76 – 7.72 (m, 6H), 7.55 – 7.44 (m, 6H), 7.12 (dtd, $J = 17.9, 7.3, 1.3$ Hz, 8H), 6.83 – 6.79 (m, 2H), 6.72 – 6.68 (m, 2H). **¹³C NMR** (100 MHz, $CDCl_3$): δ 145.4 (2 C), 144.8 (2 C), 140.1 (2 C), 138.3 (4 C), 137.1 (2 C), 134.9 (2 C), 127.1 (2 C), 125.9 (4 C), 125.1 (2 C), 124.9 (2 C), 124.7 (2 C), 124.0 (2 C), 122.5 (2 C), 122.1 (4 C), 121.5 (2 C), 121.1 (2 C), 120.6 (4 C), 119.8 (2 C), 116.5 (2 C), 111.8 (2 C), 110.1 (4 C), 109.6 (2 C), 109.6 (2 C).

Synthesis of Ir[(dF(CF₃)ppy)₂(bpy)](PF₆)



The ligand 2-(2,4-difluorophenyl)-5-(trifluoromethyl)pyridine was prepared following a previously reported procedure.²⁰¹



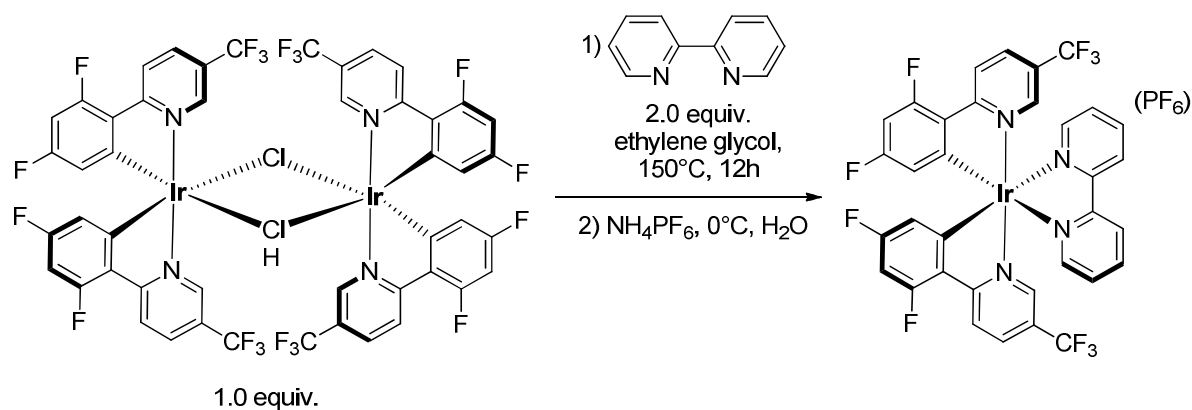
To a 50 mL round-bottom flask equipped with a magnetic stir bar was added 2-(2,4-difluorophenyl)-5-(trifluoromethyl)pyridine (400 mg, 1.50 mmol) and IrCl₃ hydrate (209 mg, 0.70 mmol). The flask was equipped with a cold water condenser and evacuated and purged with argon three times. A degassed mixture of methoxyethanol/water (2/1) (12 mL) was added and the resulting mixture stirred at 120°C for 20 h, during which time a yellow precipitate was observed to form. After cooling to rt, 10 mL of water were added and the precipitate was collected by vacuum filtration. The solid was washed with water (2x20 mL) and hexanes (~30 mL) to afford iridium μ -Cl-dimer (58%).

The spectroscopic data are in agreement with those reported in the literature.²⁰²

²⁰¹ A. Beeby, S. Bettington, I. J. S. Fairlamb, A. E. Goeta, A. R. Kapdi, E. H. Niemelä and A. L. Thompson, *New J. Chem.*, 2004, **28**, 600-605.

²⁰² M. Nonoyama, *Bull. Chem. Soc. Jpn.*, 1974, **47**, 767-768.

$^1\text{H NMR}$ (400 MHz, CDCl_3): δ 9.52 (s, 1H), 8.46 (dd, $J = 8.8, 3.1$ Hz, 1H), 8.05 (d, $J = 8.3$ Hz, 1H), 6.50 – 6.36 (m, 1H), 5.08 (d, $J = 8.9$ Hz, 1H).



To a 25 mL round-bottom flask equipped with a magnetic stir bar was added iridium dimer (302 mg, 0.2 mmol) and 2,2'-bipyridine (66 mg, 0.42 mmol). The flask was attached to a reflux condenser and the flask were placed under an inert atmosphere by three evacuation/purge cycles. The reaction components were dissolved in degassed ethylene glycol (13 mL) and heated with stirring at 150 °C for 16 h. Upon cooling to rt, the reaction mixture was diluted with water (120 mL) and transferred to a separatory funnel. The aqueous phase was washed three times with hexanes (3x 60 mL), then drained into an erlenmeyer flask and heated to 85 °C for 15 min to remove residual hexanes. Upon cooling to rt, an aqueous solution of NH_4PF_6 (2g in 20 mL) was added and the mixture cooled at 0°C, resulting in the formation of a fine yellow precipitate that was isolated by vacuum filtration and then washed with H_2O (20 mL) and hexanes (15 mL). The solid was dried under high vacuum to remove residual H_2O and hexane to give $\text{Ir}[(\text{dF}(\text{CF}_3)\text{ppy})_2(\text{bpy})](\text{PF}_6)$ (323 mg, 80%).

The spectroscopic data are in agreement with those reported in the literature.²⁰³

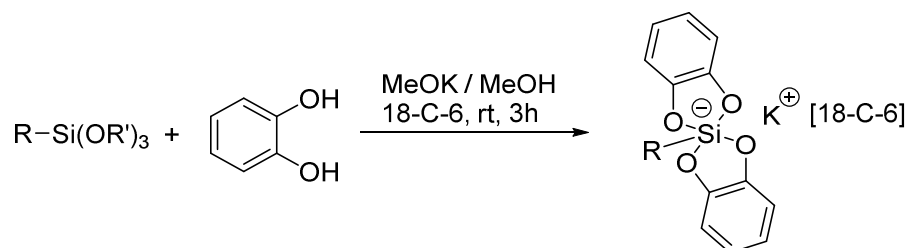
$^1\text{H NMR}$ (400 MHz, $\text{MeCN-}d_3$): δ 8.66 (dt, $J = 8.1, 1.1$ Hz, 1H), 8.60 (ddd, $J = 8.8, 2.0, 0.8$ Hz, 1H), 8.36–8.26 (m, 2H), 8.14 (ddd, $J = 5.5, 1.6, 0.8$ Hz, 1H), 7.75 (dt, $J = 1.9, 0.9$ Hz, 1H), 7.69 (ddd, $J = 7.7, 5.5, 1.3$ Hz, 1H), 6.88 (ddd, $J = 12.8, 9.4, 2.3$ Hz, 1H). $^{13}\text{CNMR}$ (100

²⁰³ D. Hanss, J. C. Freys, G. Bernardinelli, O. S. Wenger, *Eur. J. Inorg. Chem.*, 2009, 4850–4859.

MHz, MeCN-*d*3): δ 168.56 (d, $J = 6.8$ Hz), 165.76 (dd, $J = 208.1, 13.0$ Hz), 163.17 (dd, $J = 211.8, 12.9$ Hz), 156.6, 155.8 (d, $J = 7.2$ Hz), 152.5, 146.9 (d, $J = 4.8$ Hz), 141.4, 138.0 (d, $J = 3.5$ Hz), 130.0, 127.9 (d, $J = 4.9$ Hz), 126.4 (q, $J = 34.5$), 126.3, 125.0 (d, $J = 21.0$ Hz), 124.4, 121.7, 115.6 (dd, $J = 18.0, 3.1$ Hz), 100.4 (t, $J = 27.1$ Hz). ¹⁹F NMR (376.5 MHz, MeCN-*d*3): δ -63.6 (s, 6F), -72.7 (d, $J = 707.5$ Hz, 6F), -104.7 (d, $J = 12.0$ Hz, 4F), -108.0 (d, $J = 12.0$ Hz, 4F).

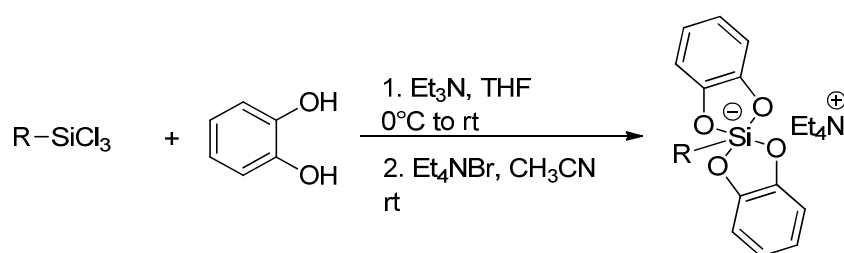
5.3 Synthesis of silicates

General procedure A for [18-C-6] potassium silicate synthesis



To a stirred solution of catechol (2 eq.) in dry methanol (0.25 M) was added 18-C-6 (1 eq.). After dissolution of the crown ether, the trialkoxy organosilane (1 eq.) was added, followed by a solution of potassium methoxide in methanol (1 eq.). The reaction mixture was stirred for 3 hours and the solvent was removed under reduced pressure. The residue was dissolved in the minimum volume of acetone and diethyl ether was added until a cloudy solution was obtained (scrapping on the edge of the flask could be done to induce crystallization). The flask was placed at -20°C overnight. The crystals were collected by filtration, washed with diethyl ether and dried under vacuum to afford [18-C-6] potassium silicate.

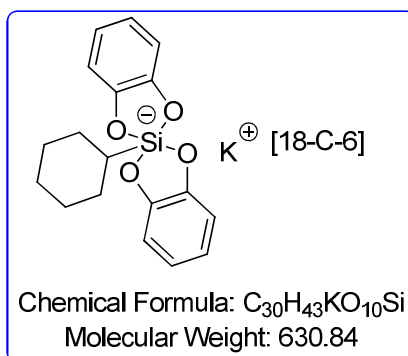
General procedure B for tetraethylammonium silicate synthesis



To a stirred solution of catechol (2 eq.) in dry THF (0.1 M) was added triethylamine (4 eq.). The reaction mixture was cooled to 0°C with an ice bath and the organotrichlorosilane (1 eq.) was added dropwise. The mixture was stirred for an hour at 0°C and an additional hour at room temperature. The triethylamine hydrochloride salt was filtered off and the filtrate was evaporated under reduced pressure. The residue was taken up in acetonitrile (0.3 M) and

tetraethylammonium bromide (1 eq.) was added. The mixture was stirred for an hour and the solvent was evaporated under reduced pressure. The solid was taken up in water, filtered, washed with water and dried under high vacuum to afford the tetraethylammonium silicate.

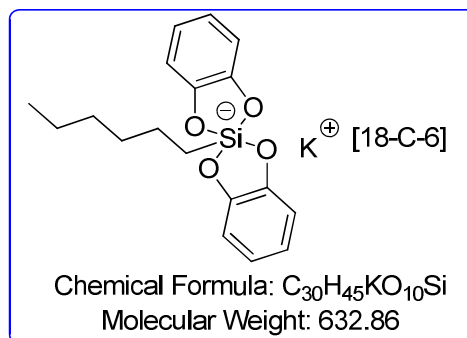
Potassium [18-Crown-6] bis(catecholato)-cyclohexylsilicate (**1**)



Following the general procedure A with cyclohexyltriethoxysilane (2.5 mmol, 0.5 mL), catechol (5.0 mmol, 550.6 mg), 18-Crown-6 (2.5 mmol, 660 mg) and potassium methoxide (2.5 mmol, 700 μ L of a 3.56 M solution in methanol) in 10 mL of dry methanol at room temperature. The crude product was purified according the general procedure to afford **1** (1.23 g, 78%) as a white solid.

1H NMR (400 MHz, Methanol-*d*₄): δ 6.72 – 6.60 (m, 4H), 6.57 – 6.49 (m, 4H), 3.53 (s, 24H), 1.69 – 1.48 (m, 5H), 1.34 – 1.02 (m, 5H), 0.84 (tt, $J = 12.2, 3.1$ Hz, 1H). **^{13}C NMR** (100 MHz, Methanol-*d*₄): δ 151.5 (4 C), 119.0 (4 C), 111.2 (4 C), 71.2 (12 C), 31.4, 29.6 (2 C), 29.4 (2 C), 28.3. **^{29}Si NMR** (119 MHz, Methanol-*d*₄): δ -77.93. **HRMS** calc. For $[C_{18}H_{19}O_4Si]^+$ 327.1058; found 327.1047. **M.p.** 220°C. **IR** (neat): 2900, 2844, 1486, 1454, 1351, 1267, 1100, 1011, 963, 893, 816, 739, 593 cm^{-1} .

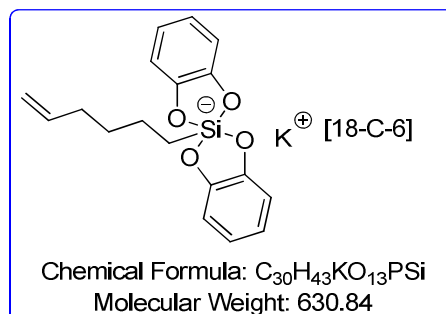
Potassium [18-Crown-6] bis(catecholato)-hexylsilicate (2)



Following the general procedure A with hexyltriethoxysilane (5.0 mmol, 1.0 mL), catechol (10.0 mmol, 1.10 g), 18-Crown-6 (5.0 mmol, 1.32 g) and potassium methoxide (2.5 mmol, 1.4 mL of a 3.56 M solution in methanol) in 20 mL of dry methanol at room temperature. The crude product was purified according to the general procedure to afford **2** (2.5 g, 80%) as a white solid.

1H NMR (400 MHz, Methanol-*d*₄): δ 8.29 – 8.17 (m, 4H), 8.15– 8.04 (m, 4H), 5.09 (s, 24H), 2.91 – 2.82 (m, 2H), 2.79 – 2.66 (m, 6H), 2.36 (t, $J = 6.9$ Hz, 3H), 2.27 – 2.16 (m, 2H). ^{13}C NMR (100 MHz, Methanol-*d*₄): δ 151.1 (4 C), 119.2 (4 C), 111.4 (4 C), 71.2 (12 C), 34.2, 32.9, 25.4, 23.6, 18.5, 14.5. ^{29}Si NMR (119 MHz, Methanol-*d*₄): δ -75.6. HRMS calc. for $[C_{18}H_{21}O_4Si]^-$ 329.1215; found 329.1218. M.p. 208°C. IR (neat): 2915, 2869, 1488, 1454, 1350, 1298, 1246, 1104, 1013, 949, 911, 893, 866, 818, 751, 738, 586 cm^{-1} .

Potassium [18-Crown-6] bis(catecholato)-hex-5-enylsilicate (3)

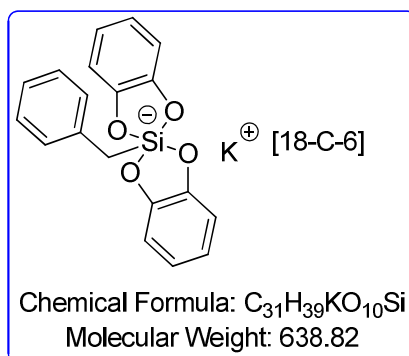


Following the general procedure A with hexenyltrimethoxysilane (2.5 mmol, 511 mg), catechol (5 mmol, 550.6 mg), 18-Crown-6 (2.5 mmol, 660 mg) and potassium methoxide (2.5

mmol, 700 μ L of a 3.56 M solution in methanol) in 10 mL of dry methanol. The crude product was purified according the general procedure to afford **3** (800 mg, 50%) as a white solid.

^1H NMR (400 MHz, Methanol-*d*4): δ 6.71 – 6.62 (m, 4H), 6.58 – 6.52 (m, 4H), 5.69 (ddt, J = 17.0, 10.2, 6.7 Hz, 1H), 4.89 – 4.82 (m, 1H), 4.80 – 4.75 (m, 1H), 3.54 (s, 24H), 1.96 – 1.85 (m, 2H), 1.39 – 1.20 (m, 4H), 0.71 – 0.62 (m, 2H). **^{13}C NMR** (100MHz, Methanol-*d*4): δ 151.1 (4 C), 140.5, 119.2 (4 C), 114.1, 111.4 (4 C), 71.2 (12 C), 34.8, 33.9, 25.1, 18.3. **^{29}Si NMR** (119 MHz, Methanol-*d*4): δ -75.7. **HRMS** calc. for $[\text{C}_{18}\text{H}_{19}\text{O}_4\text{Si}]^-$ 327.1058; found 327.1051. **M.p.** 196°C. **IR** (neat): 3063, 2898, 1598, 1485, 1452, 1350, 1283, 1267, 1246, 1102, 1010, 963, 816, 739, 587 cm^{-1} .

Potassium [18-Crown-6] bis(catecholato)-benzylsilicate (**4**)

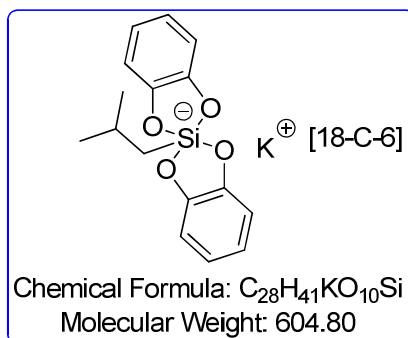


Following the general procedure A with benzyltriethoxysilane (2.5 mmol, 642 μ L), catechol (5 mmol, 550.6 mg), 18-Crown-6 (2.5 mmol, 660 mg) and potassium methoxide (2.5 mmol, 700 μ L of a 3.56 M solution in methanol) in 10 mL of dry methanol. The crude product was purified according the general procedure to afford **4** (1.35 g, 84%) as a white solid.

^1H NMR (400 MHz, Methanol-*d*4): δ 7.09 – 6.75 (m, 5H), 6.66– 6.60 (m, 4H), 6.56 – 6.49 (m, 4H), 3.55 (s, 24H), 2.14 (s, 2H). **^{13}C NMR** (100 MHz, Methanol-*d*4): δ 150.9 (4 C), 142.8, 129.8 (2 C), 128.2 (2 C), 123.9, 119.3 (4 C), 111.5 (4 C), 71.3 (12 C), 27.9. **^{29}Si NMR** (119 MHz, Methanol-*d*4): δ -80.90. **HRMS** calc. For $[\text{C}_{19}\text{H}_{15}\text{O}_4\text{Si}]^-$ 335.0745; found

335.0734. **M.p.** 192°C. **IR** (neat): 3017, 2891, 1485, 1352, 1247, 1225, 1204, 1103, 1011, 952, 886, 823,774, 735, 699, 652, 587 cm^{-1} .

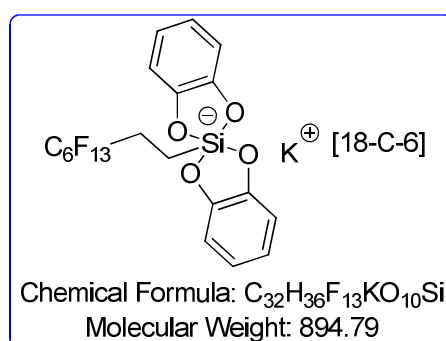
Potassium [18-Crown-6] bis(catecholato)-isobutylsilicate (5)



Following the general procedure A with isobutyltrimethoxysilane (2.5 mmol, 482 μL), catechol (5 mmol, 550.6 mg), 18-Crown-6 (2.5 mmol, 660 mg) and potassium methoxide (2.5 mmol, 700 μL of a 3.56 M solution in methanol) in 10 mL of dry methanol. The crude product was purified according the general procedure to afford **5** (1.39 g, 91%) as a white solid.

^1H NMR (400 MHz, Methanol- d_4): δ 6.73 – 6.65(m, 4H), 6.60 – 6.52 (m, 4H), 3.57 (s, 24H), 1.80 (dp, $J = 13.2, 6.6$ Hz, 1H), 0.82 (d, $J = 6.6$ Hz, 6H), 0.67 (d, $J = 6.8$ Hz, 2H). **^{13}C NMR** (100 MHz, Methanol- d_4): δ 151.1 (4 C), 119.2 (4C), 111.5 (4 C), 71.3 (12 C), 29.4, 26.8 (2 C), 25.7. **^{29}Si NMR** (119 MHz, Methanol- d_4): δ - 76.14. **HRMS** calc. for $[\text{C}_{16}\text{H}_{17}\text{O}_4\text{Si}]^-$ 301.0902; found 301.0913. **M.p.** 206°C. **IR**(neat): 3033, 2891, 2866, 1595, 1486, 1362, 1351, 1244, 1101, 1009, 963,900, 892, 835, 815, 745, 732, 713, 589 cm^{-1} .

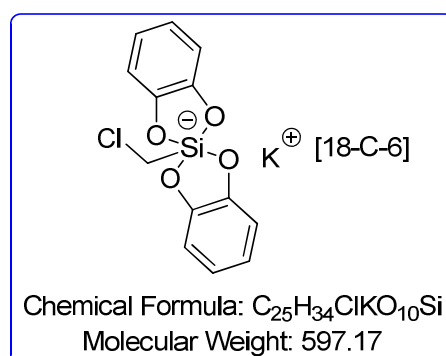
Potassium [18-Crown-6] bis(catecholato)-1H, 1H, 2H, 2H-perfluorooctylsilicate (6)



Following the general procedure A with 1H, 1H, 2H, 2H - perfluorooctyltriethoxysilane (2.5 mmol, 950 μ L), catechol (5 mmol, 550.6 mg), 18-Crown-6 (2.5 mmol, 660 mg) and potassium methoxide (2.5 mmol, 700 μ L of a 3.56 M solution in methanol) in 10 mL of dry methanol. The crude product was purified according the general procedure to afford **6** (1.6 g, 71%) as a white solid.

$^1\text{H NMR}$ (400 MHz, Methanol-*d*₄): δ 6.75 – 6.68(m, 4H), 6.62 – 6.56 (m, 4H), 3.56 (s, 24H), 2.26 – 1.90 (m, 2H), 0.90 – 0.73 (m, 2H). $^{13}\text{C NMR}$ (100 MHz, Methanol-*d*₄): δ 150.7 (4 C), 119.6 (4C), 111.6 (4 C), 71.3 (12 C), 27.7 (t), 7.0. $^{19}\text{Si NMR}$ (376 MHz, Methanol-*d*₄): δ –82.43 (tt, $J = 10.3, 2.7$ Hz, 3F), –117.03 – –117.59 (m, 2F), –122.81 – –123.09 (m, 2F), –123.67 – –124.06 (m, 2F), –124.32 – –124.87 (m, 2F), –126.78 – –127.54 (m, 2F). $^{29}\text{Si NMR}$ (119 MHz, Methanol-*d*₄): δ –78.51. **HRMS** calc. for $[C_{20}H_{12}F_{13}O_4Si]^-$ 591.0303; found 591.0326. **M.p.** 182 – 186°C. **IR** (neat): 2890, 1599, 1487, 1352, 1246, 1209, 1191, 1142, 1105, 1012, 953, 884, 825, 769, 736, 700, 647, 596 cm^{-1} .

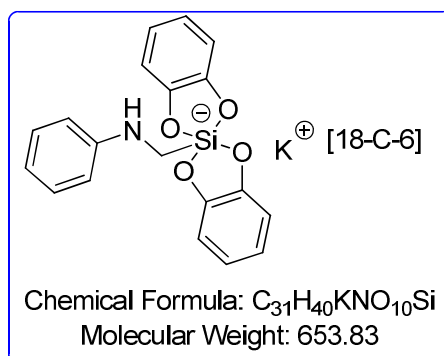
Potassium [18-Crown-6] bis(catecholato)-3-chloropropylsilicate (7)



Following the general procedure A with chloromethyltrimethoxysilane (2.5 mmol, 377 μL), catechol (5 mmol, 550.6 mg), 18-Crown-6 (2.5 mmol, 660 mg) and potassium methoxide (2.5 mmol, 700 μL of a 3.56 M solution in methanol) in 10 mL of dry methanol. The crude product was purified according the general procedure to afford **7** (1.4 g, 93%) as a white solid.

$^1\text{H NMR}$ (600 MHz, Methanol- d_4): δ 6.78 – 6.67 (m, 4H), 6.65– 6.45 (m, 4H), 3.56 (s, 24H), 2.80 (s, 2H). $^{13}\text{C NMR}$ (151 MHz, Methanol- d_4): δ 150.8 (4 C), 119.6 (4 C), 111.6 (4 C), 71.3 (12 C), 31.3. $^{29}\text{Si NMR}$ (119 MHz, Methanol- d_4): δ -85.57. **HRMS** calc. for $[\text{C}_{13}\text{H}_{10}\text{ClO}_4\text{Si}]^-$ 293.0042; found 293.0051. **M.p.** 132 – 135 $^\circ\text{C}$ C. **IR** (neat): 3043, 2893, 1598, 1485, 1351, 1243, 1101, 1011, 964, 824, 742, 732, 695, 637, 589 cm^{-1} .

Potassium [18-Crown-6] bis(catecholato)-anilinomethylsilicate (**8**)

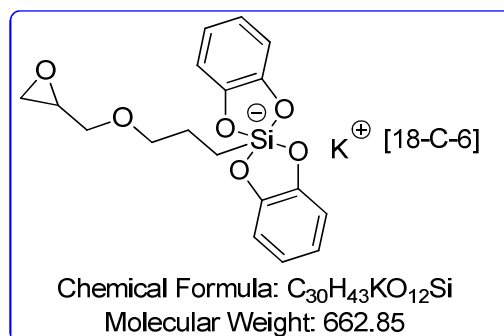


Following the general procedure A with N-((trimethoxysilyl)methyl)aniline (2.5 mmol, 597 μL), catechol (5.0 mmol, 550.6 mg), 18-Crown-6 (2.5 mmol, 666 mg) and potassium methoxide (2.5 mmol, 700 μL of a 3.56 M solution in methanol) in 10 mL of dry methanol at room temperature. The crude product was purified according the general procedure to afford **8** (1.42 g, 87%) as a white solid.

$^1\text{H NMR}$ (400 MHz, Methanol- d_4): δ 7.27 – 6.90 (m, 2H), 6.87 – 6.71 (m, 4H), 6.70 – 6.54 (m, 4H), 6.55 – 6.39 (m, 3H), 3.56 (s, 24H), 2.52 (s, 2H), NH manquant. $^{13}\text{C NMR}$ (100 MHz, Methanol- d_4): δ 152.2, 150.8 (4 C), 129.8 (2 C), 119.7 (4 C), 117.0, 113.4 (2 C), 111.9 (4 C), 71.3 (12 C), 34.1. $^{29}\text{Si NMR}$ (119 MHz, Methanol- d_4): δ -50.08 and -81.36. **HRMS** calc. for

$[\text{C}_{19}\text{H}_{16}\text{NO}_4\text{Si}]^-$ 350.0854; found 350.0851. **M.p.** $>250^\circ\text{C}$. **IR** (neat): 3393, 3043, 2897, 1599, 1487, 1352, 1246, 1106, 1013, 964, 834, 741, 692, 586 cm^{-1} .

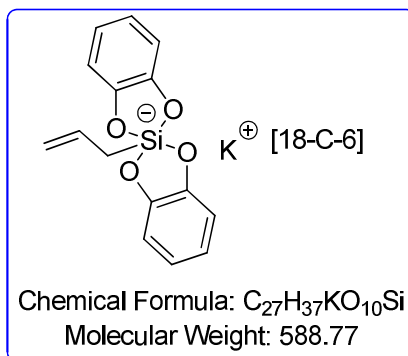
Potassium [18-Crown-6] bis(catecholato)-(3-glycidyoxypropyl)silicate (9)



Following the general procedure A with (3-glycidyoxypropyl)triethoxysilane (2.5 mmol, 552 μL), catechol (5 mmol, 550.6 mg), 18-Crown-6 (2.5 mmol, 660 mg) and potassium methoxide (2.5 mmol, 700 μL of a 3.56 M solution in methanol) in 10 mL of dry methanol. The crude product was purified according the general procedure to afford **9** (1.53 g, 92%) as a white solid.

^1H NMR (400 MHz, Methanol- d_4): δ 6.74 – 6.61 (m, 4H), 6.61– 6.49 (m, 4H), 3.57 (s, 24H), 3.53 (dd, $J = 11.6, 3.1$ Hz, 1H), 3.40 – 3.32 (m, 2H), 3.20 (dd, $J = 11.6, 6.0$ Hz, 1H), 3.03 – 2.96 (m, 1H), 2.68 (dd, $J = 5.1, 4.2$ Hz, 1H), 2.49 (dd, $J = 5.1, 2.7$ Hz, 1H), 1.71 – 1.53 (m, 2H), 0.71 – 0.60 (m, 2H). **^{13}C NMR** (100 MHz, Methanol- d_4): δ 151.0 (4 C), 119.3 (4 C), 111.5 (4 C), 75.6, 72.4, 71.3 (12 C), 51.8, 44.9, 25.6, 13.9. **^{29}Si NMR** (119 MHz, Methanol- d_4): δ -76.13. **HRMS** calc. for $[\text{C}_{18}\text{H}_{19}\text{O}_6\text{Si}]^-$ 359.0956; found 359.0954. **M.p.** 180°C . **IR** (neat): 3038, 2898, 1593, 1486, 1460, 1348, 1281, 1242, 1188, 1105, 1009, 966, 838, 818, 760, 592 cm^{-1} .

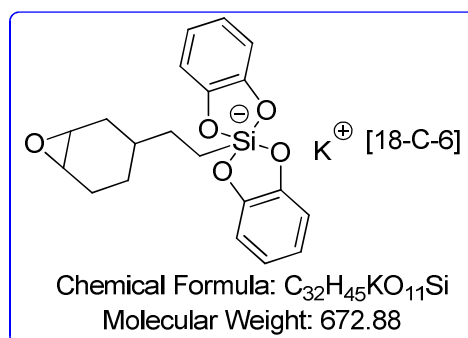
Potassium [18-Crown-6] bis(catecholato)-allylsilicate (**10**)



Following the general procedure A with allyltriethoxysilane (2.5 mmol, 538 μ L), catechol (5 mmol, 550.6 mg), 18-Crown-6 (2.5 mmol, 660 mg) and potassium methoxide (2.5 mmol, 700 μ L of a 3.56 M solution in methanol) in 10 mL of dry methanol at -20°C . The crude product was purified according the general procedure to afford **10** (1.25 g, 84%) as a white solid.

¹H NMR (400 MHz, Methanol-*d*₄): δ 6.69 – 6.65 (m, 4H), 6.59 – 6.53 (m, 4H), 5.77 (ddt, $J = 16.9, 10.0, 8.0$ Hz, 1H), 4.65 (ddt, $J = 17.0, 2.8, 1.5$ Hz, 1H), 4.50 (ddt, $J = 10.0, 2.5, 1.2$ Hz, 1H), 3.56 (s, 24H), 1.64 (dt, $J = 8.0, 1.4$ Hz, 2H). **¹³C NMR** (100 MHz, Methanol-*d*₄): δ 151.0 (4 C), 137.9, 119.3 (4 C), 111.8, 111.5 (4 C), 71.3 (12 C), 26.2. **²⁹Si NMR** (119 MHz, Methanol-*d*₄): δ -80.24. **HRMS** calc. For [C₁₅H₁₃O₄Si]⁻ 285.0589; found 285.0585. **M.p.** 167 – 169 $^{\circ}\text{C}$. **IR** (neat): 3035, 2892, 2870, 1486, 1350, 1240, 1166, 1100, 1009, 964, 888, 819, 746, 732, 689, 603, 588 cm^{-1} .

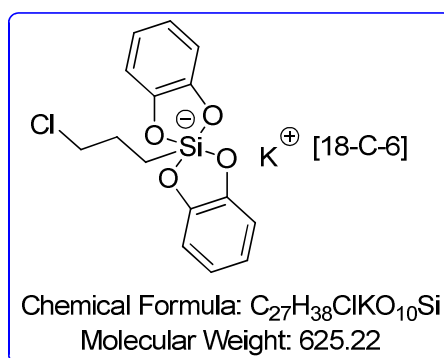
Potassium [18-Crown-6] bis(catecholato)-[2-(7-oxabicyclo[4.1.0]hept-3-yl)ethyl]silicate (**11**)



Following the general procedure A with [2-(7-oxabicyclo[4.1.0]hept-3yl)ethyl]trimethoxysilane (2.5 mmol, 578 μ L, mixture of diastereoisomers), catechol (5 mmol, 550.6 mg), 18-Crown-6 (2.5 mmol, 660 mg) and potassium methoxide (2.5 mmol, 700 μ L of a 3.56 M solution in methanol) in 10 mL of dry methanol. The crude product was purified according the general procedure to afford **11** (1.53 g, 85%, mixture of diastereoisomers) as a white solid.

^1H NMR (400 MHz, Methanol-*d*₄): δ 6.81 – 6.63 (m, 4H), 6.61 – 6.50 (m, 4H), 3.58 (s, 24H), 3.13 – 2.99 (m, 2H), 2.08 – 1.84 (m, 2H), 1.75 – 1.53 (m, 1H), 1.47 – 1.34 (m, 1H), 1.34 – 1.11 (m, 4H), 1.12 – 0.97 (m, 1H), 0.95 – 0.70 (m, 1H), 0.71 – 0.60 (m, 2H). **^{13}C NMR** (100 MHz, Methanol-*d*₄): δ 151.1 (4 C), 119.2 (4 C), 111.5 (4 C), 71.2 (12 C), 54.6, 54.1, 53.6, 53.4, 36.2, 33.5, 32.5, 32.5, 31.7, 31.7, 27.5, 26.4, 25.3, 24.4, 15.4, 15.1. **^{29}Si NMR** (119 MHz, Methanol-*d*₄): δ -75.75. **HRMS** calc. for $[\text{C}_{20}\text{H}_{21}\text{O}_5\text{Si}]^-$ 369.1164; found 369.1176. **M.p.** 197°C. **IR** (neat): 2895, 1588, 1485, 1453, 1350, 1246, 1228, 1096, 1012, 949, 821, 743, 657, 585 cm^{-1} .

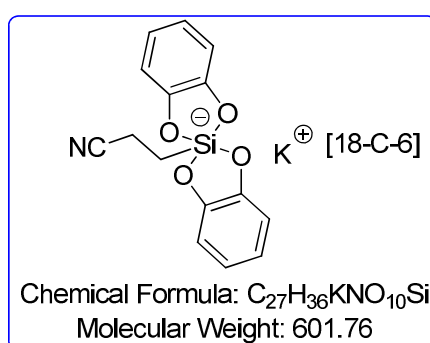
Potassium [18-Crown-6] bis(catecholato)-3-chloropropylsilicate (**12**)



Following the general procedure A with 3-chloropropyltrimethoxysilane (5 mmol, 910 μ L), catechol (10 mmol, 1.10 g), 18-Crown-6 (5 mmol, 1.32 g) and potassium methoxide (5 mmol, 1.4 mL of a 3.56 M solution in methanol) in 20 mL of dry methanol. The crude product was purified according the general procedure to afford **12** (2.96 g, 95%) as a white solid.

¹H NMR (600 MHz, Methanol-*d*₄): δ 6.68 (dd, *J* = 5.6, 3.4 Hz, 4H), 6.56 (dd, *J* = 5.6, 3.4 Hz, 4H), 3.53 (s, 24H), 3.37 (t, *J* = 7.2 Hz, 2H), 1.80 – 1.69 (m, 2H), 0.79 – 0.69 (m, 2H). **¹³C NMR** (151 MHz, Methanol-*d*₄): δ 150.9 (4 C), 119.4 (4 C), 111.5 (4 C), 71.2 (12 C), 48.8, 29.6, 15.8. **²⁹Si NMR** (119 MHz, Methanol-*d*₄): δ -76.9. **HRMS** calc. for [C₁₅H₁₄ClO₄Si]⁻ 321.0355; found 321.0367. **M.p.** 147.7°C. **IR** (neat): 3044, 2894, 2872, 1598, 1485, 1351, 1243, 1104, 952, 817, 741 cm⁻¹.

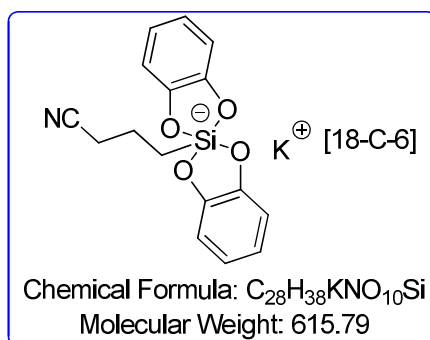
Potassium [18-Crown-6] bis(catecholato)-2-cyanoethylsilicate (**13**)



Following the general procedure A with 2-cyanoethyltriethoxysilane (2.5 mmol, 555 μL), catechol (5 mmol, 550.6 mg), 18-Crown-6 (2.5 mmol, 660 mg) and potassium methoxide (2.5 mmol, 700 μL of a 3.56 M solution in methanol) in 10 mL of dry methanol. The crude product was purified according the general procedure to afford **13** (1.25 g, 83%) as a white solid.

¹H NMR (400 MHz, Methanol-*d*₄): δ 6.80 – 6.66 (m, 4H), 6.63 – 6.55 (m, 4H), 3.54 (s, 24H), 2.32 – 2.24 (m, 2H), 1.04 – 0.95 (m, 2H). **¹³C NMR** (100 MHz, Methanol-*d*₄): δ 150.6 (4 C), 123.4, 119.7 (4 C), 111.7 (4 C), 71.2(12 C), 14.5, 13.0. **²⁹Si NMR** (119 MHz, Methanol-*d*₄): δ -80.17. **HRMS** calc. for [C₁₅H₁₂NO₄Si]⁻ 298.0541; found 298.0530. **M.p.** 141°C. **IR** (neat): 3038, 2890, 2823, 2360, 2341, 2248, 1597, 1486, 1349, 1263, 1246, 1181, 1104, 1011, 963, 825, 738, 703, 669, 589 cm⁻¹.

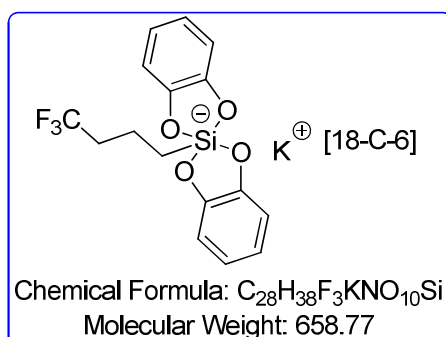
Potassium [18-Crown-6] bis(catecholato)-3-cyanopropylsilicate (14)



Following the general procedure A with 3-cyanopropyltriethoxysilane (5 mmol, 1.16 mL), catechol (10 mmol, 1.10 g), 18-Crown-6 (5 mmol, 1.32 g) and potassium methoxide (5 mmol, 1.4 mL of a 3.56 M solution in methanol) in 20 mL of dry methanol. The crude product was purified according the general procedure to afford **14** (2.76 g, 90%) as a white solid.

1H NMR (600 MHz, Methanol- d_4): δ 6.69 (dd, $J = 5.6, 3.5$ Hz, 4H), 6.57 (dd, $J = 5.7, 3.4$ Hz, 4H), 3.54 (s, 24H), 2.29 (t, $J = 7.2$ Hz, 2H), 1.69 – 1.60 (m, 2H), 0.82 – 0.75 (m, 2H). ^{13}C NMR (151 MHz, Methanol- d_4): δ 150.9 (4 C), 121.6, 119.5 (4 C), 111.6 (4 C), 71.2 (12 C), 22.5, 20.2, 17.6. ^{29}Si NMR (119 MHz, Methanol- d_4): δ -77.6. HRMS calc. for $[C_{16}H_{14}NO_4Si]^-$ 312.0698; found 312.0699. M.p. 167.6°C. IR (neat): 3039, 2952, 2870, 2236, 1702, 1599, 1484, 1353, 1245, 1227, 1098, 1011, 953, 820, 737 cm^{-1}

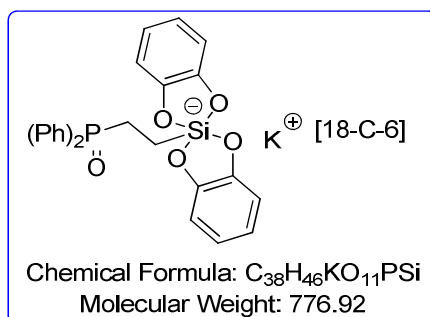
Potassium [18-Crown-6] bis(catecholato)-3,3,3-trifluoropropylsilicate (15)



Following the general procedure A with 3,3,3-trifluoropropyltrimethoxysilane (5 mmol, 956 μL), catechol (10 mmol, 1.10 g), 18-Crown-6 (5 mmol, 1.32 g) and potassium methoxide (5 mmol, 1.4 mL of a 3.56 M solution in methanol) in 20 mL of dry methanol. The crude product was purified according the general procedure to afford **15** (2.56 g, 80%) as a white solid.

$^1\text{H NMR}$ (600 MHz, Methanol- d_4): δ 6.70 (dd, $J = 5.6, 3.5$ Hz, 4H), 6.59 (dd, $J = 5.7, 3.4$ Hz, 4H), 3.54 (s, 24H), 2.06 – 1.95 (m, 2H), 0.83 – 0.76 (m, 2H). $^{13}\text{C NMR}$ (151 MHz, Methanol- d_4): δ 150.8 (4 C), 130.6 (q, $J = 275.6$ Hz), 119.6 (4 C), 111.6 (4 C), 71.2 (12 C), 30.5 (q, $J = 28.6$ Hz), 9.6. $^{19}\text{F NMR}$ (376 MHz, Methanol- d_4): δ -70.5 (t, $J = 11.1$ Hz). $^{29}\text{Si NMR}$ (119 MHz, Methanol- d_4): δ -78.6. **HRMS** calc. for $[\text{C}_{15}\text{H}_{12}\text{F}_3\text{O}_4\text{Si}]^-$ 341.0462; found 341.0460. **M.p.** 177.7°C. **IR** (neat): 3040, 2907, 2871, 1597, 1485, 1353, 1245, 1201, 1098, 1057, 820, 739 cm^{-1} .

Potassium [18-Crown-6] bis(catecholato)-2-(diphenylphosphineoxide)ethylsilicate (16)

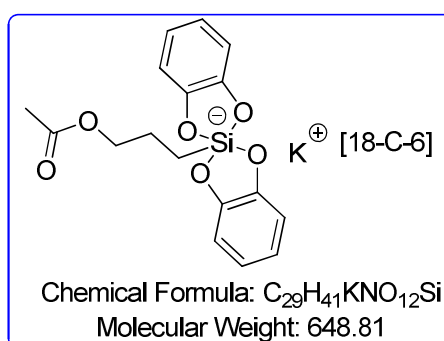


Following the general procedure A with 2-(diphenylphosphine oxide)ethylsilane (2.5 mmol, 981 mg), catechol (5 mmol, 550.6 mg), 18-Crown-6 (2.5 mmol, 660 mg) and potassiummethoxide (2.5 mmol, 700 μL of a 3.56 M solution in methanol) in 10 mL of dry methanol at room temperature. The crude product was purified according the general procedure to afford **16** (1.41 g, 72%) as a white solid.

$^1\text{H NMR}$ (400 MHz, Methanol- d_4): δ 7.57 – 7.47 (m, 6H), 7.42 – 7.39 (m, 4H), 6.71 – 6.70 (m, 4H), 6.60 – 6.59 (m, 4H), 3.52 (s, 24H), 2.38 – 2.33 (m, 2H), 0.83 – 0.79 (m, 2H). $^{13}\text{C NMR}$ (100 MHz, Methanol- d_4): δ 150.8 (4 C), 133.3 (d, $J = 97.5$ Hz, 2 C), 133.0 (d, $J = 2.6$

Hz, 2 C), 131.8 (d, $J = 9.3$ Hz, 4 C), 129.8 (d, $J = 11.6$ Hz, 4 C), 119.6 (4 C), 111.7 (4 C), 71.2 (12 C), 25.1 (d, $J = 70.4$ Hz), 8.2 (d, $J = 7.3$ Hz, 2 C). ^{31}P NMR (162 MHz, Methanol- d_4): δ 40.12. ^{29}Si NMR (119 MHz, Methanol- d_4): δ -78.10 (d, $J = 34.8$ Hz). HRMS calc. for $[\text{C}_{26}\text{H}_{22}\text{O}_5\text{PSi}]^-$ 473.0980; found 473.0964. M.p. 229°C. IR (neat): 2990, 2895, 1482, 1238, 1103, 826, 734, 723 cm^{-1} .

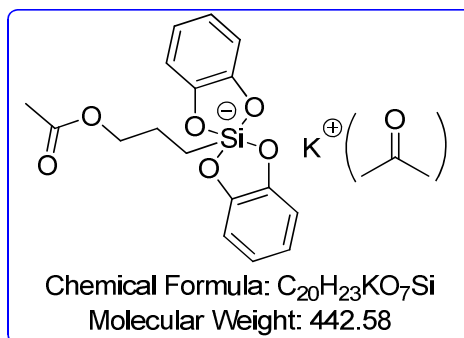
Potassium [18-Crown-6] bis(catecholato)-acetoxypropylsilicate (17)



Following the general procedure A with 3-acetoxypropyltrimethoxysilane (2.5 mmol, 523 μL), catechol (5 mmol, 550.6 mg), 18-Crown-6 (2.5 mmol, 660 mg) and potassium methoxide (2.5 mmol, 700 μL of a 3.56 M solution in methanol) in 10 mL of dry methanol at room temperature. The crude product was purified according the general procedure to afford **17** (1.35 g, 83%) as a white solid.

^1H NMR (400 MHz, Methanol- d_4): δ 6.68 (dd, $J = 5.6, 3.5$ Hz, 4H), 6.56 (dd, $J = 5.6, 3.5$ Hz, 4H), 3.88 (t, $J = 7.0$ Hz, 2H), 1.92 (s, 3H), 1.66 – 1.56 (m, 2H), 0.70 – 0.65 (m, 2H). ^{13}C NMR (101 MHz, Methanol- d_4): δ 173.1, 150.9 (4 C), 119.3 (4 C), 111.5 (4 C), 71.2 (12 C), 68.6, 24.9, 20.8, 13.9. ^{29}Si NMR (119 MHz, Methanol- d_4): δ -76.6. HRMS calc. for $[\text{C}_{17}\text{H}_{17}\text{O}_6\text{Si}]^-$ 345.0800; found 345.0813. M.p. 160°C. IR (neat): 3016, 2950, 2882, 1735, 1597, 1486, 1351, 1242, 1105, 955, 819, 749, 725 cm^{-1} .

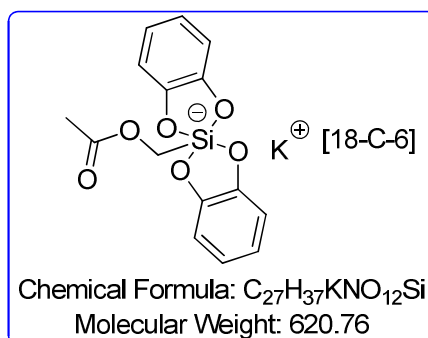
Potassium bis(catecholato)-acetoxypropylsilicate (**17'**)



Following the general procedure A with acetoxypropyl trimethoxysilane (5 mmol, 1.05 mL), catechol (10 mmol, 1.10 g) and potassium methoxide (5 mmol, 1.4 mL of a 3.56 M solution in methanol) in 20 mL of dry methanol. The crude product was purified according to the general procedure to afford **17'** (1.55 g, 70%*) as a white solid.

1H NMR (400 MHz, Methanol- d_4): δ 6.68 (dd, $J = 5.6, 3.5$ Hz, 4H), 6.56 (dd, $J = 5.6, 3.5$ Hz, 4H), 3.88 (t, $J = 7.0$ Hz, 2H), 2.15 (s, 6H), 1.92 (s, 3H), 1.66 – 1.56 (m, 2H), 0.7 – 0.65 (m, 2H). ^{13}C NMR (101 MHz, Methanol- d_4): δ 173.3, 150.8 (4 C), 119.4 (4 C), 111.5 (4 C), 68.6, 24.9, 20.8, 13.7. HRMS calc. for $[C_{17}H_{17}O_6Si]^-$ 345.0800; found 345.0813. M.p. 160°C. IR (neat): 3016, 2950, 2882, 1735, 1597, 1486, 1351, 1242, 1105, 955, 819, 749, 725 cm^{-1} .
*Silicate without [18-Crown-6] crystallizes with a molecule of acetone.

Potassium [18-Crown-6] bis(catecholato)-acetoxymethylsilicate (**18**)

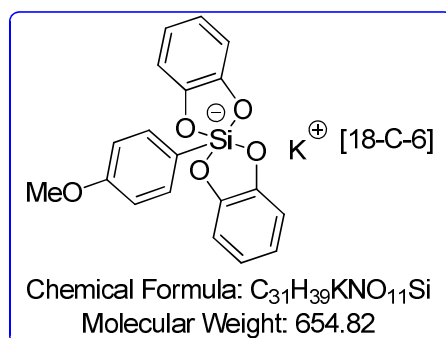


Following the general procedure A with 3-acetoxypropyltrimethoxysilane (2.5 mmol, 590 μ L), catechol (5 mmol, 550.6 mg), 18-Crown-6 (2.5 mmol, 660 mg) and

potassiummethoxide (2.5 mmol, 700 μ L of a 3.56 M solution in methanol) in 10 mL of dry methanol at room temperature. The crude product was purified according the general procedure to afford **18** (1.36 g, 87%) as a white solid.

$^1\text{H NMR}$ (600 MHz, Methanol- d_4): δ 6.68 (dd, $J = 5.6, 3.4$ Hz, 4H), 6.57 (dd, $J = 5.8, 3.5$ Hz, 4H), 3.82 (s, 2H), 3.53 (s, 24H), 1.83 (s, 3H). $^{13}\text{C NMR}$ (151 MHz, Methanol- d_4): δ 174.1, 150.9 (4 C), 119.5 (4 C), 111.7 (4C), 71.2 (12 C), 58.1, 20.7. $^{29}\text{Si NMR}$ (119 MHz, Methanol- d_4): δ -85.8 (t, $J = 5.7$ Hz). **HRMS** calc. for $[\text{C}_{15}\text{H}_{13}\text{O}_6\text{Si}]^-$ 317.0487; found 317.0495. **M.p.** 110°C. **IR** (neat): 3028, 2901, 2868, 1719, 1599, 1487, 1348, 1243, 1102, 963, 830, 737 cm^{-1} .

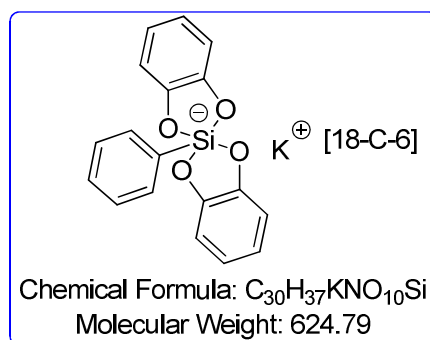
Potassium [18-Crown-6] bis(catecholato)-4-methoxyphenylsilicate (**19**)



Following the general procedure A with 4-methoxyphenyltriethoxysilane (2.5 mmol, 656 μ L), catechol (5 mmol, 550.6 mg), 18-Crown-6 (2.5 mmol, 660 mg) and potassium methoxide (2.5 mmol, 700 μ L of a 3.56 M solution in methanol) in 10 mL of dry methanol. The crude product was purified according the general procedure to afford **19** (1.4 g, 85%) as a white solid.

$^1\text{H NMR}$ (400 MHz, Methanol- d_4): δ 7.53 (d, $J = 8.8$ Hz, 2H), 6.90 – 6.66 (m, 6H), 6.62 – 6.45 (m, 4H), 3.69 (s, 3H), 3.52 (s, 24H). $^{13}\text{C NMR}$ (100 MHz, Methanol- d_4): δ 161.4, 151.1 (4 C), 137.6 (2 C), 132.8, 119.4 (4 C), 113.6 (2 C), 111.6 (4 C), 71.2 (12 C), 55.3. $^{29}\text{Si NMR}$ (119 MHz, Methanol- d_4): δ -87.50. **HRMS** calc. for $[\text{C}_{19}\text{H}_{15}\text{O}_5\text{Si}]^-$ 351.0694; found 351.0700. **M.p.** >250°C. **IR** (neat): 3044, 2906, 2871, 1591, 1488, 1450, 1349, 1245, 1183, 1095, 1037, 1013, 948, 822, 795, 730, 698, 596 cm^{-1} .

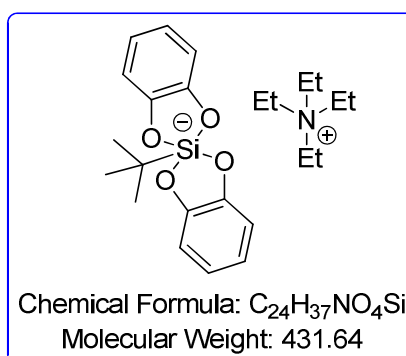
Potassium [18-Crown-6] bis(catecholato)-phenylsilicate (**20**)



Following the general procedure A, method A with phenyltrimethoxysilane (2.5 mmol, 466 μ L), catechol (5 mmol, 550.6 mg), 18-Crown-6 (2.5 mmol, 660 mg) and potassium methoxide (2.5 mmol, 700 μ L of a 3.56 M solution in methanol) in 10 mL of dry methanol. The crude product was purified according the general procedure to afford **20** (1.36 g, 87%) as a white solid.

1H NMR (400 MHz, Methanol- d_4): δ 7.65 – 7.54 (m, 2H), 7.25 – 7.08 (m, 3H), 6.86 – 6.72 (m, 4H), 6.65 – 6.54 (m, 4H), 3.51 (s, 24H). ^{13}C NMR (100 MHz, Methanol- d_4): δ 151.1 (4 C), 141.7, 135.6 (2 C), 129.1, 127.9 (2 C), 119.5 (4 C), 111.6 (4 C), 71.2 (12 C). ^{29}Si NMR (119 MHz, Methanol- d_4): δ -87.83. HRMS calc. for $[C_{18}H_{13}O_4Si]^-$ 321.0589; found 321.0577. **M.p.** 224°C. **IR** (neat): 3054, 2902, 2871, 1710, 1598, 1485, 1349, 1241, 1099, 1012, 959, 816, 738, 707, 598 cm^{-1} .

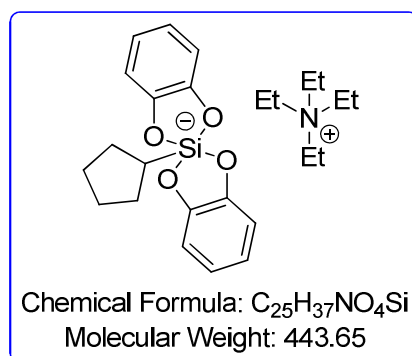
Tetraethylammoniumbis(catecholato)-tertbutylsilicate (**21**)



Following the general procedure B with tert-butyltrichlorosilane (10 mmol, 1.91g), catechol (20 mmol, 2.20 g), triethylamine (40 mmol, 1.4 mL) and tetraethylammonium bromide (10 mmol, 2.10 g) in 100 mL of dry THF. The crude product was purified according to the general procedure to afford **21** (1.54 g, 39%) as a white solid.

¹H NMR (600 MHz, Acetonitrile-*d*₃): δ 6.61 – 6.54 (m, 4H), 6.51 – 6.45 (m, 4H), 3.09 (q, *J* = 7.3 Hz, 8H), 1.23 – 1.09 (m, 12H), 0.77 (s, 9H). **¹³C NMR** (150 MHz, Acetonitrile-*d*₃): δ 152.6 (4 C), 118.1 (4 C), 110.2 (4 C), 53.0 (t, *J* = 3 Hz, 4 C), 29.6 (3 C), 24.0, 7.6 (4 C). **²⁹Si NMR** (119 MHz, Acetonitrile-*d*₃): δ -76.21. **HRMS** calc. for [C₁₆H₁₇O₄Si]⁻ 301.0902; found 301.0891. **M.p.** >250°C. **IR** (neat): 2980, 2951, 2928, 2840, 1596, 1485, 1393, 1361, 1246, 1174, 1100, 1012, 1000, 890, 815, 738, 696, 626, 595 cm⁻¹.

Tetraethylammonium bis(catecholato)-cyclopentylsilicate (**22**)



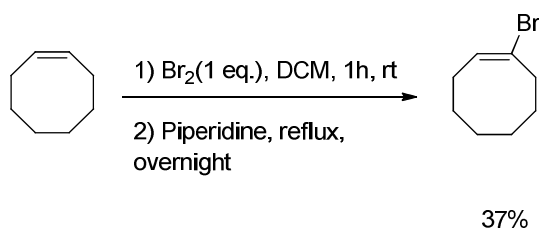
Following the general procedure B with cyclopentyltrichlorosilane (5 mmol, 830 μL), catechol (10 mmol, 1.1 g), Et₃N (20 mmol, 2.79 mL) in 50 mL of dry THF. The counter anion metathesis was performed with Et₄NBr (5 mmol, 1.05 g) in 20 mL of acetonitrile. The crude product was purified according to the general procedure to afford **22** (1.25 g, 56%) as a white solid.

¹H NMR (600 MHz, DMSO-*d*₆): δ 6.55 – 6.48 (m, 4H), 6.46 – 6.40 (m, 4H), 3.17 (q, *J* = 7.3 Hz, 8H), 1.50 – 1.42 (m, 2H), 1.39 – 1.27 (m, 4H), 1.27 – 1.19 (m, 2H), 1.17 – 1.09 (m, 12H), 0.86 (tt, *J* = 10.1, 7.8 Hz, 1H). **¹³C NMR** (150 MHz, DMSO-*d*₆): δ 150.9 (4 C), 116.9 (4 C), 109.2 (4 C), 51.4 (t, *J* = 3 Hz, 4 C), 29.8, 28.6 (2 C), 25.9 (2 C), 7.0 (4 C). **²⁹Si NMR** (119 MHz, DMSO-*d*₆): δ -75.61. **HRMS** calc. for [C₁₇H₁₇O₄Si]⁻ 313.0902; found 313.0912.

M.p.>250°C. **IR** (neat): 2979, 2861, 1591, 1484, 1358, 1246, 1222, 1172, 1097, 1012, 997, 884, 822, 734, 651, 585 cm⁻¹.

5.4 Synthesis of electrophiles

1-Bromocyclooctene

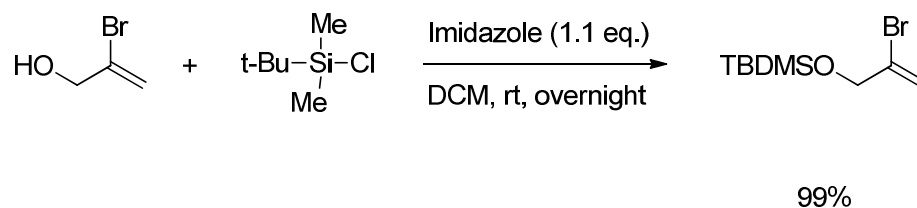


To a 50 mL round-bottom-flask was added cyclooctene (31.5 mmol, 3.5 g) and 7 mL of DCM. At 0°C was added dropwis bromine (31.5 mmol, 1.65 g) and the mixture stirred 1 hour at room temperature. The solvent was removed under reduced pressure to give 1,2-dibromocyclooctane. The compound was added in 14 mL of piperidine without purification. The mixture was heated at reflux temperature and stirred overnight. The solution was filtrated and the solid washed with pentane. The organic phase was then washed with HCl (1M, 2x70 mL), saturated NaHCO₃ (2x70 mL) and brine (100 mL), and dried over magnesium sulphate. The solvent was removed under reduced pressure to give 1-bromocyclooctene (3.15g, 37%).

The spectroscopic data are in agreement with those reported in the literature.¹⁸⁸

¹H NMR (400 MHz, CDCl₃): δ 6.03 (t, *J* = 8.5, 1H), 2.63 – 2.59(m, 2H), 2.13 – 2.07 (m, 2H), 1.64 – 1.62 (m, 2H), 1.55 – 1.50 (m, 6H). **¹³C NMR** (100 MHz, CDCl₃): δ131.8, 125.0, 35.3, 30.0, 28.8, 27.6, 26.6, 25.6.

((2-Bromoallyl)oxy)(tert-butyl)dimethylsilane

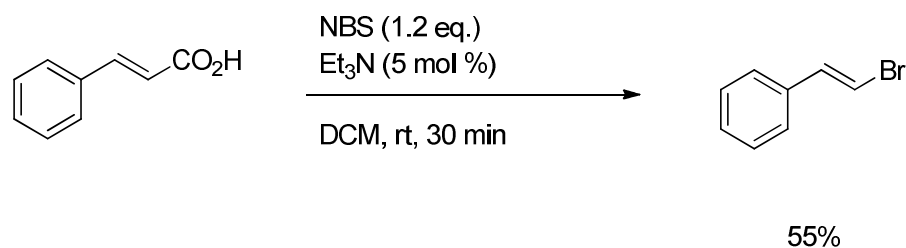


To a 50 mL round-bottom-flask was added *tert*-butyldimethylsilyl chloride (5.25 mmol, 791 mg), 2-bromoallyl alcohol (5 mmol, 685 mg) and 25 mL of DCM. After 15 minutes of stirring, imidazole (5.25 mmol, 374 mg) was added and the mixture stirred overnight. The mixture was filtrated over a pad of silica and eluted with Et₂O. The solvent was removed under reduced pressure to give ((2-bromoallyl)oxy)(*tert*-butyl)dimethylsilane (1.25 g, 99%).

The spectroscopic data are in agreement with those reported in the literature.²⁰⁴

¹H NMR (400 MHz, CDCl₃): δ5.85 (d, *J* = 1.8 Hz, 1H), 5.43 (d, *J* = 1.6 Hz, 1H), 4.11– 4.10 (m, 2H), 0.82 (s, 9H), 0.00 (s, 6H). **¹³C NMR** (100 MHz, CDCl₃): δ132.0, 114.8, 67.6, 25.9 (3 C), 18.5, -5.2 (2 C). **IR** (neat): 2958, 2854, 1637, 1463, 124, 1085, 838, 774 cm⁻¹.

(*E*)-(2-bromovinyl)benzene



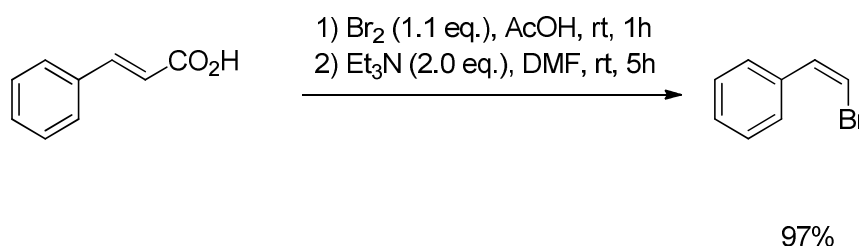
To a solution of cinnamic acid (10 mmol, 1.48 g) in methylene chloride triethylamine (0.5 mmol, 70 μL) was added at room temperature and stirred for five minutes. *N*-bromosuccinimide (12.0 mmol, 2.13 g) was added in one portion and the mixture stirred for 30 minutes. The solvent was removed under reduced pressure. The crude was purified by flash column chromatography (pentane) to afford (*E*)-(2-bromovinyl)benzene (1.06 g, 99%).

²⁰⁴ M. Charpenay, A. Boudhar, C. Hulot, G. Blond and J. Suffert, *Tetrahedron*, 2013, **69**, 7568–7591.

The spectroscopic data are in agreement with those reported in the literature.²⁰⁵

¹H NMR (400 MHz, CDCl₃): δ 7.35 – 7.30 (m, 5H), 7.13 (d, *J* = 14.0 Hz, 1H), 6.79 (d, *J* = 14.0 Hz, 1H). **¹³C NMR** (100 MHz, CDCl₃): δ 137.3, 136.0, 128.9 (2 C), 128.4, 126.2 (2 C), 106.6.

(Z)-(2-bromovinyl)benzene



To a solution of cinnamic acid (50 mmol, 8.9 mmol) in AcOH (25 mL) was added bromine (55 mL, 2.85 mL) at rt. When the solution turns yellow the reaction is over. The mixture was quenched with an aqueous solution of sodium thiosulfate (1 M, 25 mL). The precipitate was filtered and washed with water. The dibromo intermediate compound was directly engaged in a solution of triethylamine (100 mmol, 5.8 mL) in DMF at 0°C. The resulting mixture was warmed to room temperature and stirred for 5 h. The reaction was quenched by addition of water, the two phases were separated and the aqueous phase was extracted with pentane (2x40 mL). The combined organic layers were washed with water (50 mL), then dried over anhydrous magnesium sulfate and concentrated under reduced pressure to afford the (Z)-(2-bromovinyl)benzene (15 g, 97%).

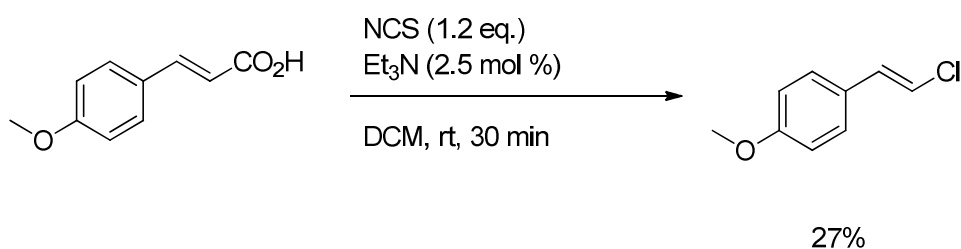
The spectroscopic data are in agreement with those reported in the literature.²⁰⁶

¹H NMR (400 MHz, CDCl₃): δ 7.83– 7.80 (m, 2H), 7.52– 7.4 (m, 3H), 7.15 (d, *J* = 8.1 Hz, 1H), 6.52 (d, *J* = 8.1 Hz, 1H). **¹³C NMR** (100 MHz, CDCl₃): δ 137.3, 136.0, 128.9 (2 C), 128.4, 126.2 (2 C), 106.6.

²⁰⁵D. R. Williams, M. W. Fultz, T. E. Christos and J. S. Carter, *Tetrahedron Lett.*, 2010, **51**, 121–124.

²⁰⁶D. Müller, A. Alexakis, *Chem. Eur. J.*, 2013, **19**, 15226 – 15239.

(2-Chlorovinyl)benzene



To a solution of (*E*)-3-(4-methoxyphenyl)acrylic acid (20 mmol, 3.56g) in DCM (70 mL) was added triethylamine (5 mmol, 0.7 mL). The mixture was stirred at room temperature for 5 minutes and NCS (24 mmol, 3.2 g) was added and the solution stirred overnight. The solvent was removed under reduced pressure. The crude was purified by flash column chromatography (pentane/AcOEt: 95/5) to afford (2-chlorovinyl)benzene (933 mg, 27%). A mixture of isomer was obtained (ratio *Z/E* 5:95).

The spectroscopic data are in agreement with those reported in the literature.¹⁸⁸

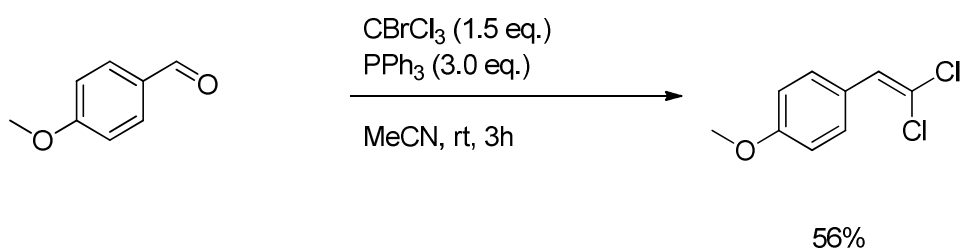
(*E*) isomer:

¹H NMR (400 MHz, CDCl₃): δ7.11 (d, *J* = 8.6 Hz, 2H), 6.74 (d, *J* = 8.6 Hz, 2H), 6.65 (d, *J* = 13.6 Hz, 1H), 6.38 (d, *J* = 13.6 Hz, 1H), 3.69 (s, 3H). ¹³C NMR (100 MHz, CDCl₃): δ159.7, 132.8, 127.7, 127.5 (2 C), 116.5, 114.3 (2 C), 55.4.

(*Z*) isomer:

¹H NMR (400 MHz, CDCl₃): δ7.55 (d, *J* = 8.7 Hz, 2H), 6.80 (d, *J* = 8.9 Hz, 2H), 6.45 (d, *J* = 8.1 Hz, 1H), 6.04 (d, *J* = 8.1 Hz, 1H), 3.71 (s, 3H). ¹³C NMR (100 MHz, CDCl₃): δ159.5, 130.8 (2 C), 128.7, 127.0, 115.5, 113.8 (2 C), 55.4.

1-(2,2-dichlorovinyl)-4-methoxybenzene



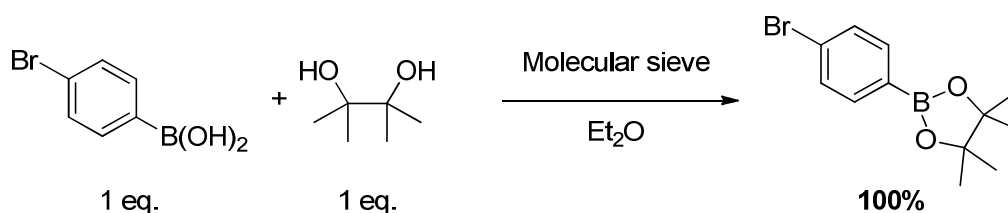
To a 250 mL round-bottom-flask was added the *para*-anisaldehyde (5 mmol, 0.607 mL) and 40 mL of MeCN. The reaction mixture was cooled with an ice bath to 0°C and BrCCl₃ (7.5 mmol, 0.740 mL) was added, followed by addition of a solution of triphenylphosphine (15 mmol, 3.95 g) in the minimum of MeCN. The reaction mixture was stirred at room temperature for 3 hours and the solvent was removed under reduced pressure to afford the crude product. The residue was dissolved in 80 mL of pentane and the organic phase was washed with water (80 mL), brine (80 mL) and dried over MgSO₄. The solvent was removed under reduced pressure and the residue filtered on a pad of silica eluted with pentane, giving the pure material (559 mg, 55%).

The spectroscopic data are in agreement with those reported in the literature.²⁰⁷

¹H NMR (400 MHz, CDCl₃): δ7.50 (d, *J* = 8.8 Hz, 2H), 6.90 (d, *J* = 8.8 Hz, 2H), 6.79 (s, 1H), 3.83 (s, 3H). ¹³C NMR (100 MHz, CDCl₃): δ159.7, 130.2 (2 C), 128.2, 126.1, 118.9, 114.0 (2 C), 55.4.

²⁰⁷M. R. Heinrich, O. Blank, D. Ullrich, M. Kirschstein, *J. Org. Chem.*, 2007, **72**, 9609 – 9616.

Synthesis of 2-(4-bromophenyl)-4,4,5,5-tetramethyl-1,3,2-dioxaborolane

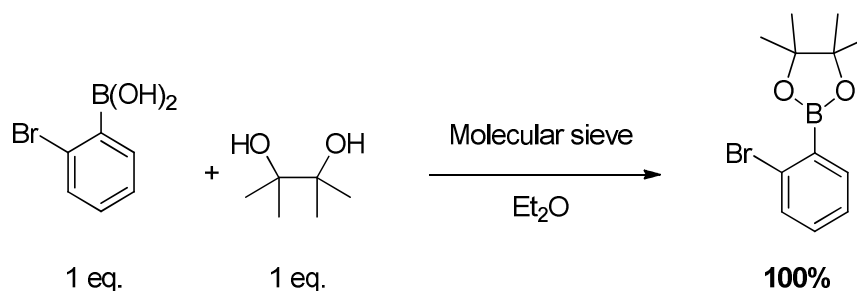


To a 50 mL Schlenk was added (4-bromophenyl)boronic acid (5 mmol, 1.04 g), pinacol (5 mmol, 591 mg), 750 mg of activated molecular sieve (3Å). Under argon was added 12 mL of distilled Et₂O and the solution stirred 20 hours at room temperature. The mixture was filtrated over a pad of celite and the solvent removed under reduced pressure to give the pure product (1.43g, 100%).

The spectroscopic data are in agreement with those reported in the literature.²⁰⁸

¹H NMR (400 MHz, CDCl₃): δ7.67 – 7.64 (m, 2H), 7.52 – 7.49 (m, 2H), 1.34 (s, 12H). ¹³C NMR (100 MHz, CDCl₃): δ136.4 (2 C), 131.1 (2 C), 126.2, 84.2 (2 C), 25.0 (4 C). One missing signal in ¹³C NMR. ¹¹B NMR (128 MHz, CDCl₃): δ30.76.

Synthesis of 2-(2-bromophenyl)-4,4,5,5-tetramethyl-1,3,2-dioxaborolane



To a 50 mL Schlenk was added (2-bromophenyl)boronic acid (3 mmol, 600 mg), pinacol (3 mmol, 355 mg), 450 mg of activated molecular sieve (3Å). Under argon was added 8 mL of distilled Et₂O and the solution stirred 20 hours at room temperature. The mixture was

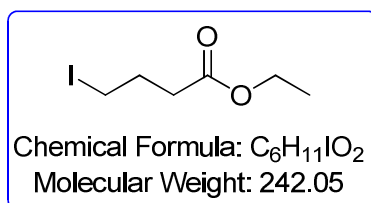
²⁰⁸ F.Mo, Y. Jiang, D. Qiu, Y. Zhang and J. Wang, *Angew. Chem. Int. Ed.*, 2010, **49**, 1846–1849.

filtrated over a pad of celite and the solvent removed under reduced pressure to give the pure product (950 mg, 100%).

The spectroscopic data are in agreement with those reported in the literature.²⁰⁹

¹H NMR (400 MHz, CDCl₃): δ7.62 – 7.60 (m, 1H), 7.55 – 7.52 (m, 1H), 7.30 – 7.22 (m, 2H), 1.38 (s, 12H). **¹³C NMR** (100 MHz, CDCl₃): δ136.5, 132.8, 132.0, 128.2, 126.4, 84.5 (2 C), 25.0 (4 C). **¹¹B NMR** (128 MHz, CDCl₃): δ30.86.

Synthesis of ethyl 4-iodobutyrate

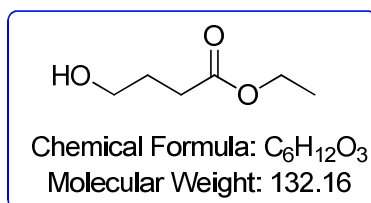


To a 100 mL round-bottom-flask was added ethyl 4-bromobutyrate (10.5 mmol, 1.5 mL) and 40 mL of acetone. Sodium iodide (21 mmol, 3.14 g) was added to the solution and the mixture heated to reflux for 2 hours. The reaction mixture was filtered and the solvent removed under reduced pressure. The residue was dissolved in 40 mL of Et₂O and the organic phase was washed with water (40 mL), brine (40 mL) and dried over MgSO₄. The solvent was removed under reduced pressure and the residue dissolved in DCM (15 mL).

¹H NMR (400 MHz, CDCl₃): δ4.10 (q, *J* = 7.1 Hz, 2H), 3.21 (t, *J* = 6.8 Hz, 2H), 2.40 (t, *J* = 7.2 Hz, 1H), 2.09 (p, *J* = 7.0 Hz, 1H) (s, 1H), 3.83 (s, 3H).

²⁰⁹ H. L. Li, Y. Kuninobu and M. Kanai, *Angew. Chem. Int. Ed.*, 2017, 56, 1495–1499.

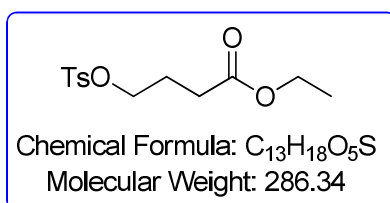
Synthesis of ethyl 4-hydroxybutanoate



To a 50 mL round-bottom-flask was added butyrolactone (40 mmol, 3.44 g) and 9 mL of distilled methanol. To the mixture was slowly added a solution of potassium hydroxide (40 mmol, 2.24 g) in the minimum of methanol. After 4 hours of reaction, the solvent was removed under reduced pressure. The resulting white solid was washed with AcOEt and pentane. The solid was dissolved in DMF (25 mL) and bromoethane (40 mmol, 4.5 mL) was added to the solution. The mixture was stirred overnight at room temperature and then diluted with water (75 mL). The aqueous phase was extracted with AcOEt (3x50 mL). The combined organic phase were washed with water (2x50mL), NaHCO₃ (2x50 mL and brine (2x50 mL), and dried with magnesium sulfate. The solvent was removed under reduced pressure to give the product (4.2 g, 79%).

¹H NMR (400 MHz, CDCl₃): δ4.11 (q, *J* = 7.1 Hz, 2H), 3.65 (t, *J* = 6.2 Hz, 2H), 2.40 (t, *J* = 7.2 Hz, 2H), 1.85 (tt, *J* = 7.2, 6.1 Hz, 2H), 1.23 (t, *J* = 7.1 Hz, 3H).

Synthesis of ethyl 4-(tosyloxy)butanoate



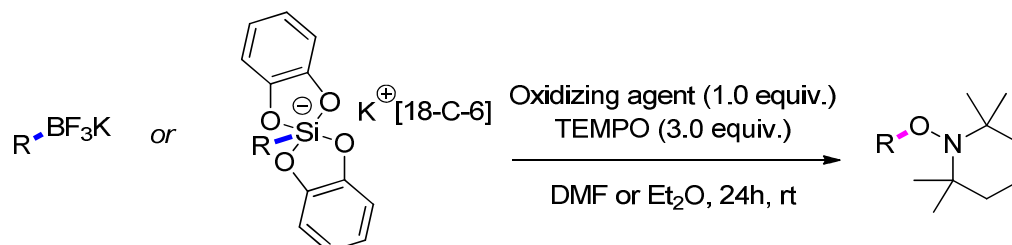
To a 100 mL round-bottom-flask was added ethyl 4-hydroxybutanoate (7.6 mmol, 1.01 g), pyridine (3 mL) and 30 mL of distilled DCM. At 0°C was slowly added tosyl chloride (7.6 mmol, 2.43 g). The resulting yellow mixture was stirred overnight. The solution was washed with a saturated solution of CuSO₄. The aqueous phase was extracted with DCM (2x30 mL) and the combined organic phases dried magnesium sulfate. The solvent was removed under

reduced pressure and the residue filtrated over a pad of celite to give the product (1.29 g, 59%).

¹H NMR (400 MHz, CDCl₃): δ7.78 – 7.75 (m, 2H), 7.35 – 7.31 (m, 2H), 4.11 – 4.04 (m, 4H), 2.43 (s, 3H), 2.35 (t, *J* = 7.2 Hz, 2H), 1.99 – 1.91 (m, 2H), 1.21 (t, *J* = 7.1 Hz, 3H). **¹³C NMR** (100 MHz, CDCl₃): δ172.4, 144.9, 133.1, 130.0 (2 C), 128.0 (2 C), 69.5, 60.6, 30.0, 24.3, 21.7, 14.2.

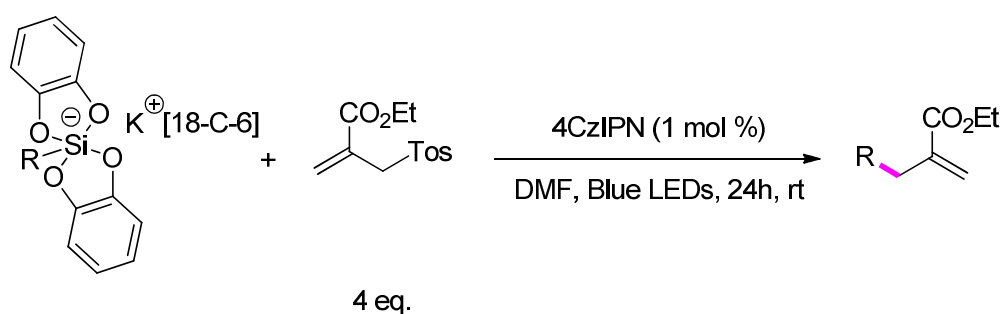
5.5 Radical additions reactions

General procedure C for stoichiometric oxidation of organotrifluoroborate and organobis(catecholato) silicate.



To a Schlenk flask was added the appropriate trifluoroborate salt or silicate salt (0.3 mmol), the oxidizing agent (0.3 mmol) and TEMPO (0.9 mmol, 1 41 mg). The Schlenk flask was sealed with a rubber septum, and evacuated/purged with vacuum/argon three times. Degassed DMF or diethyl ether (3 mL) was introduced followed by two freeze-pump-thaw cycles. The reaction mixture was stirred at room temperature for 24h under an argon atmosphere. The reaction mixture was diluted with diethyl ether (50 mL), washed with water (2 times), brine (2 times), dried over $MgSO_4$ and evaporated under reduced pressure. The reaction residue was purified by flash column chromatography on silica gel.

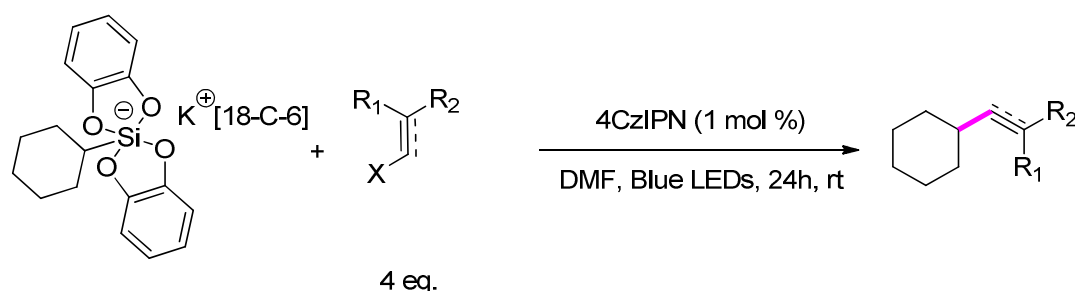
General procedure D for addition of silicates to allylsulfone



To a Schlenk flask was added the appropriate silicate (1 eq., 0.3 mmol), allyl sulfone (4 eq., 1.2 mmol, 322 mg) and 4CzIPN (1 mol %, 3 μ mol, 2.4 mg). Degassed DMF was added (3 mL) and the reaction mixture was irradiated with blue LED (477 nm) at room temperature for 24h under an argon atmosphere. The reaction mixture was diluted with diethyl ether (50 mL),

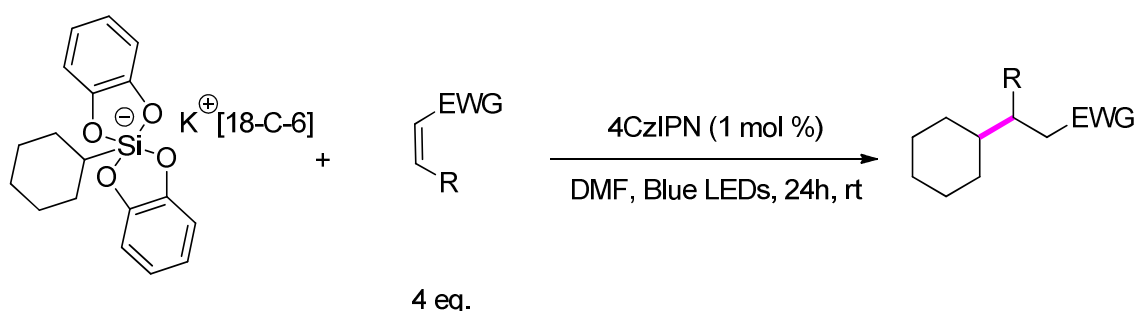
washed with saturated aqueous NaHCO_3 (2 times), brine (2 times), dried over MgSO_4 and evaporated under reduced pressure. The crude product was purified by flash column chromatography to afford the adduct.

General procedure E for vinylation and alkynylation reactions of cyclohexylsilicate 1



To a Schlenk flask was added potassium [18-C-6] bis(catecholato) cyclohexylsilicate (1 eq., 0.3 mmol, 189.3 mg), 4CzIPN (1 mol %, 3 μmol , 2.4 mg) and the desired acceptor (4 eq., 1.2 mmol) (liquid alkenes were added with the solvent). Degassed DMF was added (3 mL). The reaction mixture was irradiated with blue LED (477 nm) for 24 hours. The reaction mixture was diluted with diethyl ether (50 mL), washed with saturated aqueous NaHCO_3 (2 times), brine (2 times), dried over MgSO_4 and evaporated under reduced pressure. The crude product was purified by flash column chromatography to afford the adduct.

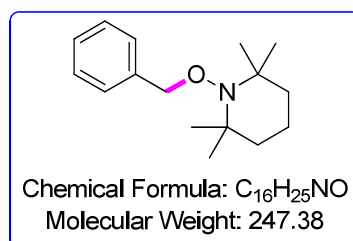
General procedure F for addition of cyclohexylsilicate 1 to activated alkenes



To a Schlenk flask was added potassium [18-C-6] bis(catecholato) cyclohexylsilicate 1d (1 eq., 0.3 mmol, 189.3 mg), KH_2PO_4 (1.2 eq., 0.36 mmol, 49 mg), 4CzIPN (1 mol %, 3 μmol , 2.4 mg) and the desired alkene 3 (4 eq., 1.2 mmol) (liquid alkenes were added with the

solvent). Degassed DMF was added (3 mL). The reaction mixture was irradiated with blue LED (477 nm) for 24 hours. The reaction mixture was diluted with diethyl ether (50 mL), washed with saturated aqueous NaHCO₃ (2 times), brine (2 times), dried over MgSO₄ and evaporated under reduced pressure. The crude product was purified by flash column chromatography to afford the 1,4 adduct.

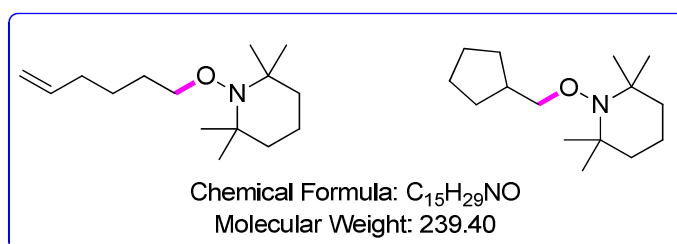
1-(Benzyloxy)-2,2,6,6-tetramethylpiperidine (23)



Following general procedure C with potassium benzyl trifluoroborate (0.3 mmol, 59 mg) and triphenylcarbenium tetrafluoroborate (0.3 mmol, 99 mg) in diethyl ether. The crude product was purified by flash column chromatography (pentane/diethyl ether, 99/1) to afford **23** as a colorless oil (48 mg, 65%). The spectroscopic data are in agreement with those reported in the literature.¹⁵⁰

¹H NMR (400 MHz, CDCl₃): δ 7.26– 7.11 (m, 5H), 4.71 (s, 2H), 1.50 – 1.21 (m, 6H), 1.14 (s, 6H), 1.04 (s, 6H). ¹³C NMR (100 MHz, CDCl₃): δ 138.3, 128.2 (2 C), 127.4 (2 C), 127.3, 78.7, 60.0 (2 C), 39.7 (2 C), 33.1 (2 C), 20.3 (2 C), 17.1.

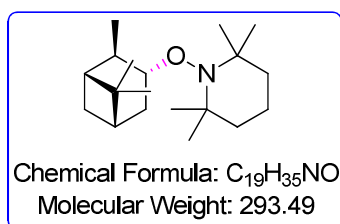
1-(Hex-5-en-1-yloxy)-2,2,6,6-tetramethylpiperidine (24) and 1-(cyclopentylmethoxy)-2,2,6,6-tetramethylpiperidine (24')



Following general procedure C with potassium 5-hexenyl-1-trifluoroborate (0.3 mmol, 57 mg) triphenylcarbenium tetrafluoroborate (0.3 mmol, 99 mg) in diethyl ether. The crude product was purified by flash column chromatography (pentane) to afford a mixture of **24** and **24'** as a colorless oil (41 mg, 57%) in a 89/11 ratio. The spectroscopic data are in agreement with those reported in the literature.¹⁵⁰

¹H NMR for **24** (400 MHz, CDCl₃): δ 5.82 (m, 1H), 5.01 (m, 1H), 4.94 (m, 1H), 3.72 (t, *J* = 6.1 Hz, 2H), 2.07 (q, *J* = 7.2 Hz, 2H), 1.14 (s, 6H), 1.04 (s, 6H). Characteristic signal for **24'**: 3.64 (d, *J* = 6.8 Hz, 2H). ¹³C NMR for **24** (100 MHz, CDCl₃): δ 139.1, 114.5, 80.8, 59.9, 59.8, 39.7 (2 C), 34.0, 33.2 (2 C), 28.4, 25.9, 20.3 (2 C), 17.3. Characteristic signal for **24'**: 76.7.

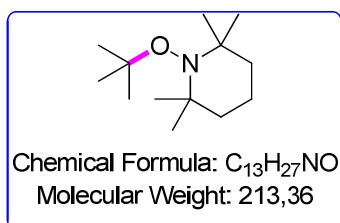
2,2,6,6-Tetramethyl-1-(((1R,2R,3R,5S)-2,6,6-trimethylbicyclo[3.1.1]heptan-3-yl)oxy)piperidine (25)



Following general procedure C with potassium ((1R,2R,3R,5S)-2,6,6-trimethylbicyclo[3.1.1]heptan-3-yl)trifluoroborate (0.3 mmol, 74 mg) and triphenylcarbenium tetrafluoroborate (0.3 mmol, 99 mg) in diethyl ether. The crude product was purified by flash column chromatography (pentane) to afford **25** as a colorless oil (57 mg, 64%). The spectroscopic data are in agreement with those reported in the literature.¹⁵⁰

¹H NMR (400 MHz, CDCl₃): δ 4.21 (dt, *J* = 9.4, 4.5 Hz, 1H), 2.37 – 2.20 (m, 3H), 2.14 – 2.05 (m, 1H), 1.91 – 1.85 (m, 1H), 1.73 (td, *J* = 5.9, 2.4 Hz, 1H), 1.45 – 1.40 (m, 6H), 1.25 – 1.06 (m, 18H), 1.02 (d, *J* = 9.3 Hz, 1H), 0.88 (s, 6H). ¹³C NMR (100 MHz, CDCl₃): δ 82.4, 59.9 (2 C), 48.0, 44.5, 41.6, 40.8, 40.6, 38.5, 34.7 (3 C), 33.1, 27.6, 23.9, 22.0, 20.5 (2 C), 17.5.

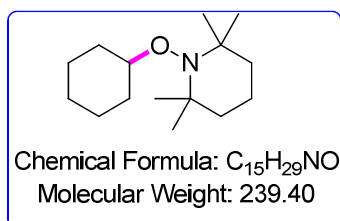
1-(Tert-butoxy)-2,2,6,6-tetramethylpiperidine (26)



Following general procedure C with potassium tert-butytrifluoroborate(0.3 mmol, 49 mg) and triphenylcarbenium tetrafluoroborate (0.3 mmol, 99 mg) in diethyl ether. The crude product was purified by flash column chromatography (pentane/diethyl ether, 99/1) to afford **26** as a colorless oil (16 mg, 25%). The spectroscopic data are in agreement with those reported in the literature.¹⁵⁰

¹H NMR (400 MHz, CDCl₃): δ 1.48– 1.44 (m, 6H), 1.18 (s, 9H), 1.12 (s, 6H), 1.07 (s, 6H). ¹³C NMR (100 MHz, CDCl₃): δ 77.3, 59.4 (2 C), 41.1 (2 C), 35.1 (2 C), 29.7 (3 C), 20.7 (2 C), 17.5.

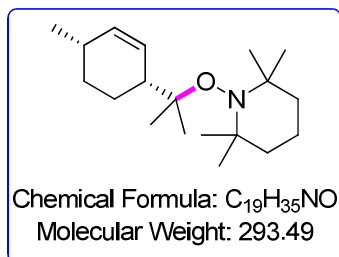
1-(Tert-butoxy)-2,2,6,6-tetramethylpiperidine (27)



Following general procedure C with cyclohexylsilicate **1**(0.3 mmol, 189 mg) and triphenylcarbenium tetrafluoroborate (0.3 mmol, 99 mg) in DMF. The crude product was purified by flash column chromatography (pentane/diethyl ether, 98/2) to afford **27** as a colorless oil (53%). The spectroscopic data are in agreement with those reported in the literature.⁶⁶

$^1\text{H NMR}$ (400 MHz, CDCl_3): δ 3.61– 3.55 (m, 1H), 2.07– 2.02 (m, 2H), 1.77– 1.75 (m, 2H), 1.70– 1.20 (m, 12H), 1.12 (s, 6H). $^{13}\text{C NMR}$ (100 MHz, CDCl_3): δ 81.5, 59.3, 40.1, 34.3, 32.6, 25.7, 24.8, 19.9, 17.1.

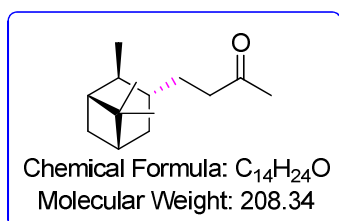
2,2,6,6-Tetramethyl-1-((2-((1R,4S)-4-methylcyclohex-2-en-1-yl)propan-2-yl)oxy)piperidine (28)



Following general procedure C with (1S,2R,3S,6R)-3,7,7-trimethylbicyclo[4.1.0]heptan-2-trifluoroborate(0.3 mmol, 65 mg) and triphenylcarbenium tetrafluoroborate (0.3 mmol, 99 mg) in DMF. The crude product was purified by flash column chromatography (pentane/diethyl ether, 99/1) to afford **28** as a colorless oil (48 mg, 67%). The spectroscopic data are in agreement with those reported in the literature.¹⁵⁰

$^1\text{H NMR}$ (400 MHz, CDCl_3): δ 5.76 (m, 1H), 5.67 (m, 1H), 2.53 (m, 1H), 2.18 (m, 1H), 1.74– 1.65 (m, 2H), 1.57– 1.40 (m, 6H), 1.30– 1.24 (m, 2H), 1.21 (s, 3H), 1.20 (s, 3H), 1.12 (s, 6H), 1.10 (s, 3H), 1.09 (s, 3H), 0.98 (d, $J = 7.2$ Hz, 3H). $^{13}\text{C NMR}$ (100 MHz, CDCl_3): δ 133.9, 128.8, 81.1, 59.5 (2 C), 47.2, 41.2 (2 C), 35.3, 35.1, 29.3, 29.0, 24.0, 23.8, 21.2, 21.0 (2 C), 20.7, 17.3.

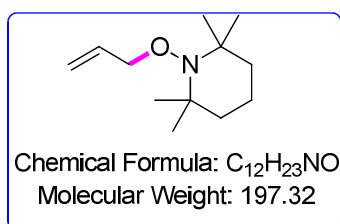
4-((1R,2S,3R,5R)-2,6,6-Trimethylbicyclo[3.1.1]heptan-3-yl)butan-2-one (29)



Following general procedure C with potassium potassium ((1R,2R,3R,5S)-2,6,6-trimethylbicyclo[3.1.1]heptan-3-yl)trifluoroborate(1 mmol, 244 mg), methyl vinyl ketone (5 mmol, 0.4 mL) and triphenylcarbenium tetrafluoroborate (1 mmol, 330mg). The crude product was purified by flash column chromatography (pentane) to afford **29** as a colorless oil (131 mg, 63%). The spectroscopic data are in agreement with those reported in the literature.¹⁵⁰

¹H NMR (400 MHz, CDCl₃): δ 2.46 (ddd, *J* = 16.5, 10.1, 5.9 Hz, 1H), 2.34 (ddd, *J* = 16.5, 10.4, 5.1 Hz, 1H), 2.30– 2.22 (m, 1H), 2.12 (s, 3H), 2.15– 2.06 (m, 1H), 1.91 – 1.85 (m, 1H), 1.85 – 1.70 (m, 2H), 1.68 – 1.50 (m, 2H), 1.45 – 1.34 (m, 2H), 1.16 (s, 6H), 0.99 (d, *J* = 7.0 Hz, 3H), 0.96 (s, 3H), 0.70 (d, *J* = 9.7 Hz, 1H). ¹³C NMR (100 MHz, CDCl₃): δ 209.5, 48.2, 43.7, 42.3, 42.0, 38.8, 36.1, 34.8, 34.5, 34.1, 30.0, 28.1, 23.0, 21.7.

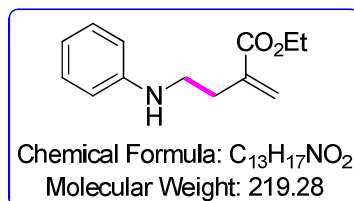
1-(Tert-butoxy)-2,2,6,6-tetramethylpiperidine (30)



The potassium allyl trifluoroborate (0.3 mmol, 44 mg) and 9-mesityl-10-methylacridinium perchlorate (0.03 mmol, 12.4 mg) and TEMPO (0.66 mmol, 103 mg) were added to a Schlenk flask. The Schlenk flask was evacuated / purged with vacuum / argon three times. Degassed DMF (3 mL) was introduced followed by two freeze-pump-thaw cycles and the reaction mixture was irradiated with blue LED (477 nm) at room temperature for 24h under an argon atmosphere. The reaction mixture was diluted with diethyl ether (50 mL), washed with saturated aqueous NaHCO₃ (2 times), brine (2 times), dried over MgSO₄ and evaporated under reduced pressure. The crude product was purified by flash column chromatography to afford **30** as a colorless oil (19 mg, 32%). The spectroscopic data are in agreement with those reported in the literature.⁶⁶

$^1\text{H NMR}$ (400 MHz, CDCl_3): δ 5.94– 5.84 (m, 1H), 5.26 (dq, $J = 17.3, 3.6$ Hz, 1H), 5.30 – 5.09 (m, 1H), 4.28 (dt, $J = 5.5, 1.5$ Hz, 2H), 1.58– 1.30 (m, 6H), 1.33 (s, 6H), 1.16 (s, 6H). $^{13}\text{C NMR}$ (100 MHz, CDCl_3): δ 134.2, 115.9, 78.3, 59.7 (2 C), 39.7 (2 C), 32.9 (2 C), 20.1 (2 C), 17.2.

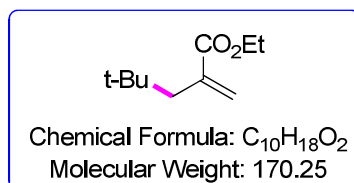
Ethyl 2-methylene-4-(phenylamino)butanoate (32)



Following general procedure D with **8** (0.3 mmol, 196.2 mg). The crude product was purified by flash column chromatography (pentane/ethyl acetate, 95/5) to afford **32** as a colorless oil (62 mg, 93%). The spectroscopic data are in agreement with those reported in the literature.^{116a}

$^1\text{H NMR}$ (300 MHz, CDCl_3): δ 7.22 – 7.16 (m, 2H), 7.74 – 7.69 (m, 2H), 6.65 – 6.62 (m, 2H), 6.27 (d, $J = 1.4$ Hz, 1H), 6.54 (d, $J = 1.3$ Hz, 1H), 4.25 (q, $J = 7.1$ Hz, 2H), 3.68 (bs, 1H), 3.31 (d, $J = 6.8$ Hz, 2H), 2.64 (td, $J = 6.8, 1.1$ Hz, 2H), 1.33 (t, $J = 7.1$ Hz, 3H). $^{13}\text{C NMR}$ (75 MHz, CDCl_3): δ 167.1, 148.0, 138.4, 129.3 (2 C), 126.7, 117.4, 112.9 (2 C), 61.0, 43.0, 32.1, 14.3.

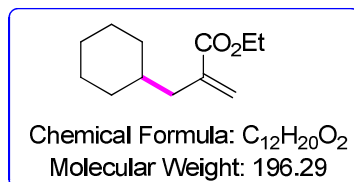
Ethyl 4,4-dimethyl-2-methylenepentanoate (**33**)



Following general procedure D with **21** (0.3 mmol, 129.5 mg). The crude product was purified by flash column chromatography (pentane/ethyl acetate, 95/5) to afford **33** as a colorless oil (48 mg, 94%). The spectroscopic data are in agreement with those reported in the literature.^{116a}

¹H NMR (400 MHz, CDCl₃): δ 6.17 (d, *J* = 1.4 Hz, 1H), 5.44 – 5.44 (m, 1H), 4.19 (q, *J* = 7.1 Hz, 2H), 2.28 (d, *J* = 0.8 Hz, 2H), 1.29 (t, *J* = 7.1 Hz, 3H), 0.88 (s, 9H). ¹³C NMR (100 MHz, CDCl₃): δ 168.2, 139.1, 126.8, 60.6, 53.4, 44.5, 31.5, 29.2 (3 C), 14.2.

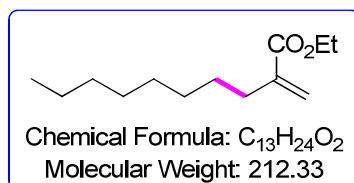
Ethyl 2-(cyclohexylmethyl)acrylate (**34**)



Following general procedure D with **1** (0.3 mmol, 189.3 mg). The crude product was purified by flash column chromatography (pentane/diethyl ether, 95/5) to afford **34** as a colorless oil (52 mg, 88%). The spectroscopic data are in agreement with those reported in the literature.^{116a}

¹H NMR (400 MHz, CDCl₃): δ 6.13 (d, *J* = 1.8 Hz, 1H), 5.45 (m, 1H), 4.19 (q, *J* = 7.1 Hz, 2H), 2.18 (dd, *J* = 7.1, 1.1 Hz, 2H), 1.72 – 1.61 (m, 5H), 1.46 – 1.41 (m, 1H), 1.29 (t, *J* = 7.1 Hz, 3H), 1.23 – 1.08 (m, 3H), 0.92 – 0.85 (m, 2H). ¹³C NMR (100 MHz, CDCl₃): δ 167.7, 139.8, 125.6, 125.5, 60.6, 40.1, 36.8, 33.4, 33.2, 26.7, 26.4, 14.3.

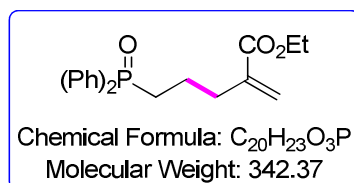
Ethyl 2-methylenenonanoate (35)



Following general procedure D with **2** (0.3 mmol, 184.7 mg). The crude product was purified by flash column chromatography (pentane/diethyl ether, 95/5) to afford **35** as a colorless oil (34 mg, 57%). The spectroscopic data are in agreement with those reported in the literature.^{116a}

¹H NMR (400 MHz, CDCl₃): δ 6.11 (d, *J* = 1.5 Hz, 1H), 5.50 (q, *J* = 1.5 Hz, 1H), 4.20 (q, *J* = 7.1 Hz, 2H), 2.31 – 2.27 (m, 2H), 1.47 – 1.42 (m, 2H), 1.32 – 1.25 (m, 12H), 0.87 (t, *J* = 7.1 Hz, 3H). **¹³C NMR** (100 MHz, CDCl₃): δ 167.7, 141.3, 124.2, 60.7, 32.0, 32.0, 29.3, 29.2, 28.6, 22.8, 14.4, 14.2.

Ethyl 5-(diphenylphosphoryl)-2-methylenepentanoate (36)

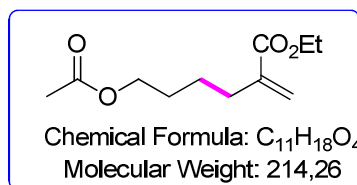


Following general procedure D with **16** (0.3 mmol, 233.1 mg). The crude product was purified by flash column chromatography (pentane/ethyl acetate, 80/20) to afford **36** as a colorless oil (48 mg, 46%).

¹H NMR (400 MHz, CDCl₃): δ 7.74 – 7.69 (m, 4H), 7.52 – 7.42 (m, 6H), 6.14 (d, *J* = 1.3 Hz, 1H), 5.49 (d, *J* = 1.3 Hz, 1H), 4.14 (q, *J* = 7.1 Hz, 2H), 2.42 – 2.38 (m, 2H), 2.29 – 2.22 (m, 2H), 1.84 – 1.80 (m, 2H), 1.22 (t, *J* = 7.1 Hz, 3H). **¹³C NMR** (100 MHz, CDCl₃): δ 167.0, 139.7, 133.1 (d, *J* = 98.2 Hz, 2 C), 131.8 (d, *J* = 2.7 Hz, 2 C), 130.9 (d, *J* = 9.2 Hz, 4 C), 128.7 (d, *J* = 11.6 Hz, 4 C), 125.6, 60.8, 32.9 (d, *J* = 15.3 Hz), 29.2 (d, *J* = 72.2 Hz), 20.5 (d, *J* = 3.4 Hz), 14.3. **³¹P NMR** (162 MHz, CDCl₃): δ 32.2. **IR** (neat): 3120, 2944, 1903, 1710, 1629,

1437, 1176, 1105, 717, 694 cm^{-1} . **HRMS** calc. for $[\text{C}_{20}\text{H}_{23}\text{NaO}_3\text{P}]^+$ 365.1277; found 365.1268, for $[(\text{C}_{20}\text{H}_{23}\text{O}_3\text{P})_2\text{Na}]^+$ 707.2662; found 707.2366 .

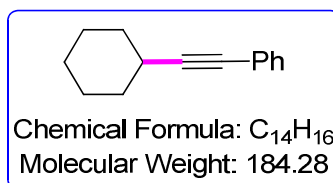
Ethyl 6-acetoxy-2-methylenehexanoate (**37**)



Following general procedure D with **17** (0.3 mmol, 194.6 mg). The crude product was purified by flash column chromatography (pentane/diethyl ether, 90/10) to afford **37** as a colorless oil (24 mg, 37%).

$^1\text{H NMR}$ (400 MHz, CDCl_3): δ 6.15 (d, $J = 1.5$ Hz, 1H), 5.52 (d, $J = 1.4$ Hz, 1H), 4.20 (q, $J = 7.1$ Hz, 2H), 4.07 (t, $J = 6.5$ Hz, 2H), 2.35 – 2.31 (m, 2H), 2.04 (s, 3H), 1.69 – 1.62 (m, 2H), 1.58 – 1.50 (m, 2H), 1.30 (t, $J = 7.1$ Hz, 3H). $^{13}\text{C NMR}$ (100 MHz, CDCl_3): δ 171.3, 167.3, 140.6, 124.8, 64.4, 60.8, 31.6, 28.3, 25.0, 21.1, 14.4. **IR** (neat): 2995, 2949, 1741, 1710, 1630, 1368, 1234, 1187, 1146, 1028, 944, 813cm^{-1} . **HRMS** calc. for $[\text{C}_{11}\text{H}_{18}\text{NaO}_4]^+$ 237.1097; found 237.1097.

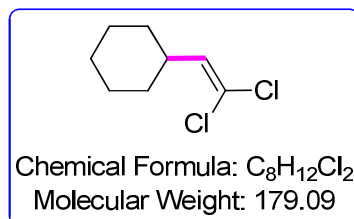
(Cyclohexylethynyl)benzene (**39**)



Following general procedure E with 1-phenyl-2-p-toluenesulfonylethyne (1.2 mmol, 307.6 mg). The crude product was purified by flash column chromatography (pentane) to afford **39** as a colorless oil (44 mg, 78%). The spectroscopic data are in agreement with those reported in the literature.^{116a}

¹H NMR (300 MHz, CDCl₃): δ 7.42 – 7.39 (m, 2H), 7.31 – 7.24 (m, 3H), 2.64 – 2.55 (m, 1H), 1.92 – 1.85 (m, 2H), 1.79 – 1.74 (m, 2H), 1.58 – 1.52 (m, 3H), 1.40 – 1.33 (m, 3H). **¹³C NMR** (75 MHz, CDCl₃): δ 131.7 (2 C), 128.3 (2 C), 127.5, 124.3, 94.6, 80.7, 32.9, 29.8, 26.1 (2 C), 25.1 (2 C).

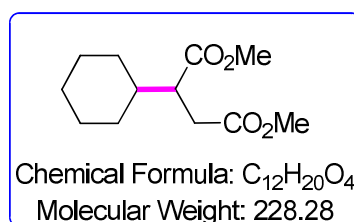
(2,2-Dichlorovinyl)cyclohexane (**41**)



Following general procedure E with trichloroethylene (1.2 mmol, 108 μL). The crude product was purified by flash column chromatography (pentane) to afford **41** as a colorless oil (39 mg, 70%). The spectroscopic data are in agreement with those reported in the literature.^{116a}

¹H NMR (300 MHz, CDCl₃): δ 5.70 (d, *J* = 9.2 Hz, 1H), 2.43 – 2.32 (m, 1H), 1.77 – 1.62 (m, 5H), 1.37 – 1.04 (m, 6H). **¹³C NMR** (75 MHz, CDCl₃): δ 135.2, 118.7, 39.3, 31.8 (2 C), 25.9, 25.7 (2 C).

Dimethyl 2-cyclohexylsuccinate (**43**)



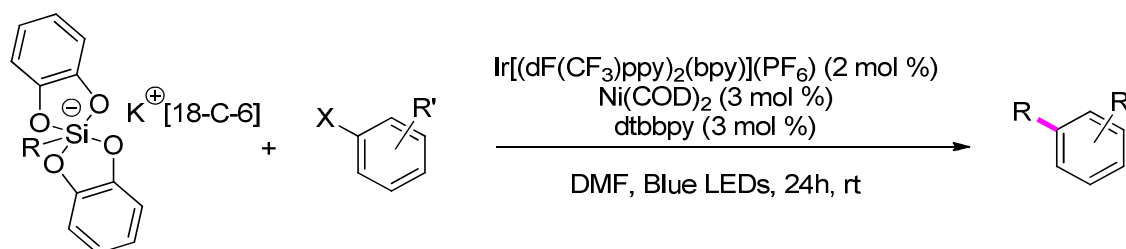
Following general procedure F with dimethyl maleate (1.2 mmol, 150 μL). The crude product was purified by flash column chromatography (pentane/ethyl acetate, 95/5) to afford **40** as a colorless oil (84 mg, 78%). The spectroscopic data are in agreement with those reported in the literature.^{116a}

¹H NMR (300 MHz, CDCl₃): δ 3.67 (s, 3 H), 3.64 (s, 3 H), 2.76 – 2.65 (m, 2 H), 2.48 – 2.38 (m, 1 H), 1.74 – 1.85 (m, 6 H), 1.29 – 0.97 (m, 5 H). **¹³C NMR** (100 MHz, CDCl₃): δ 175.0, 173.0, 51.80, 51.6, 47.1, 40.03, 33.3, 30.7, 30.2, 29.8, 26.4, 26.2.

5.6 Cross-coupling reactions: photoredox/nickel dual catalysis

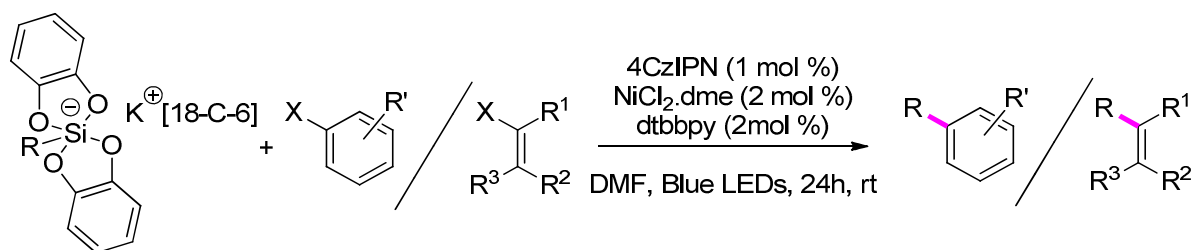
5.6.1 C(sp²)-C(sp³) bond formation

General procedure G for photoredox/nickel cross-coupling dual catalysis



To a Schlenk flask was added aryl or heteroaryl halide (1 eq., 0.3 mmol), silicate (1.5 eq., 0.45 mmol), Ir[(dF(CF₃)ppy)₂(bpy)](PF₆) (2 mol %, 6 μmol, 6 mg), and 4,4'-di-*tert*-butyl-2,2'-bipyridine (3 mol %, 9 μmol, 2.4 mg). The Schlenk flask was taken into a glovebox and Ni(COD)₂ (3 mol %, 9 μmol, 2.5 mg) was added. The Schlenk flask was sealed with a rubber septum, removed from the glovebox, and evacuated / purged with vacuum / argon three times. Degassed DMF (3 mL) was introduced (followed by the aryl or heteroaryl halide if liquid) and the reaction mixture was irradiated with blue LEDs (477 nm) for 24 hours. The reaction mixture was diluted with diethyl ether (50 mL), washed with saturated NaHCO₃ (2 times), brine (2 times), dried over MgSO₄ and evaporated under reduced pressure. The residue was purified by flash column chromatography on silica gel to afford the cross-coupling product.

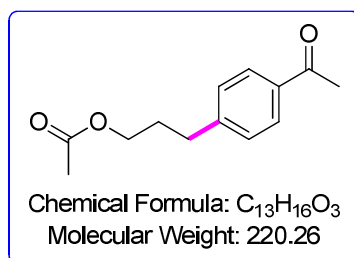
General procedure H for photoredox/nickel cross-coupling dual catalysis with aryl/heteroaryl halide or vinyl bromide



To a Schlenk flask was added aryl, heteroaryl halide or alkenyl halide (1 eq., 0.3 mmol), appropriate silicate (1.5 eq., 0.45 mmol), 4CzIPN (1 mol%, 3 μmol, 2.4 mg), and 4,4'-di-*tert*-

butyl-2,2'-bipyridine (2 mol %, 6 μ mol, 1.6 mg). The Schlenk flask was taken into a glovebox and NiCl₂.dme (2 mol %, 6 μ mol, 1.3 mg) was added. The Schlenk flask was sealed with a rubber septum, removed from the glovebox, and evacuated / purged with vacuum / argon three times. Degassed DMF (3 mL) was introduced (followed by the aryl or heteroaryl halide if liquid) and the reaction mixture was irradiated with blue LEDs (477 nm) for 24 hours. The reaction mixture was diluted with diethyl ether (50 mL), washed with saturated NaHCO₃ (2 times), brine (2 times), dried over MgSO₄ and evaporated under reduced pressure. The residue was purified by flash column chromatography on silica gel to afford the cross-coupling product.

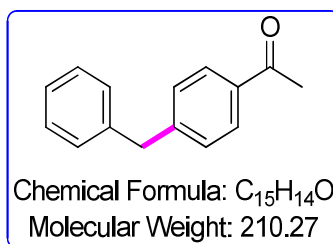
4'-(Acetoxypropyl)acetophenone (**45**)



Following general procedure G with acetoxypropylsilicate **17** (0.45 mmol, 292 mg) and 4'-bromoacetophenone **44** (0.3 mmol, 60 mg). The crude product was purified by flash column chromatography (pentane/diethyl ether, 99/1 then 95/5) to afford **45** as a colorless oil (56 mg, 85%).

¹H NMR (400 MHz, CDCl₃): δ 7.88 (d, J = 8.4 Hz, 2H), 7.27 (d, J = 8.4 Hz, 2H), 4.08 (t, J = 6.5 Hz, 2H), 2.76 – 2.72 (m, 2H), 2.57 (s, 3H), 2.04 (s, 3H), 2.01 – 1.94 (m, 2H). ¹³C NMR (100 MHz, CDCl₃): δ 197.7, 171.0, 147.0, 135.3, 128.6 (2 C), 128.6 (2 C), 63.5, 32.2, 29.8, 26.5, 20.9. IR (neat): 2900, 1735, 1679, 1606, 1233 cm⁻¹. HRMS calc for [C₁₃H₁₆NaO₃]⁺ 243.0992; found 243.0999.

4'-(Benzyl)acetophenone (**46**)

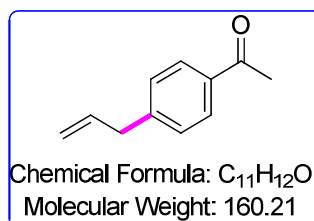


Following general procedure G with benzylsilicate **4** (0.45 mmol, 287 mg) and 4'-bromoacetophenone **44** (0.3 mmol, 60 mg). The crude product was purified by flash column chromatography (pentane/diethyl ether, 95/5) to afford **46** as a colorless oil (56 mg, 88%).

The spectroscopic data are in agreement with those reported in the literature.²¹⁰

¹H NMR (400 MHz, CDCl₃): δ 7.89 (d, *J* = 8.4 Hz, 2H), 7.32–7.17 (m, 7H), 4.04 (s, 2H), 2.58 (s, 3H). ¹³C NMR (100 MHz, CDCl₃): δ 197.8, 146.8, 140.1, 135.3, 129.1 (2 C), 129.0 (2 C), 128.7 (4 C), 126.40, 41.9, 26.6. IR (neat): 2937, 1678, 1602, 1265 cm⁻¹.

4'-(Allyl)acetophenone (**47**)



Following general procedure G with allylsilicate **10** (0.45 mmol, 265 mg) and 4'-bromoacetophenone **44** (0.3 mmol, 60 mg). The crude product was purified by flash column chromatography (pentane/diethyl ether, 98/2) to afford **47** as a colorless oil (41 mg, 86%).

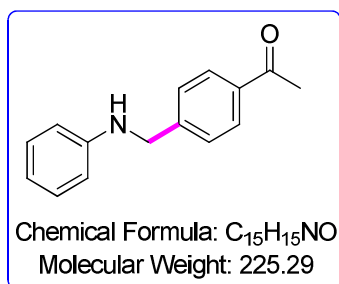
The spectroscopic data are in agreement with those reported in the literature.²¹¹

²¹⁰ M. Amatore and C. Gosmini, *Chem. Eur. J.*, 2010, 16, 5848–5852.

²¹¹ A. M. Echavarren and J. K. Stille, *J. Am. Chem. Soc.*, 1987, **109**, 5478–5486.

¹H NMR (400 MHz, CDCl₃): δ 7.90 (d, *J* = 8.4 Hz, 2H), 7.28 (d, *J* = 8.4 Hz, 2H), 5.95 (ddt, *J* = 17.1 Hz, 10.5 Hz, 6.7 Hz, 1H), 5.13–5.08 (m, 2H), 3.45 (d, *J* = 6.7 Hz, 2H), 2.59 (s, 3H). **¹³C NMR** (100 MHz, CDCl₃): δ 197.8, 145.8, 136.3, 135.3, 128.8 (2 C), 128.6 (2 C), 116.7, 40.1, 26.6. **IR** (neat): 3050, 1680, 1604, 1356, 1266 cm⁻¹.

4'-(Anilinomethyl)acetophenone (**48**)



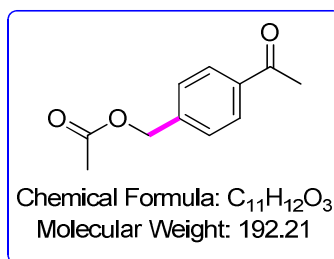
Following general procedure G with anilinomethylsilicate **8** (0.45 mmol, 294 mg) and 4'-bromoacetophenone **44** (0.3 mmol, 60 mg). The crude product was purified by flash column chromatography (pentane/diethyl ether, 80/20) to afford **48** as a colorless oil (62 mg, 91%).

The spectroscopic data are in agreement with those reported in the literature.²¹²

¹H NMR (400 MHz, CDCl₃): δ 7.93 (d, *J* = 8.4 Hz, 2H), 7.47 (d, *J* = 8.4 Hz, 2H), 7.17–7.15 (m, 2H), 6.75–6.71 (m, 1H), 6.66 – 6.60 (m, 2H), 4.42 (s, 2H), 4.16 (s, 1H), 2.59 (s, 3H). **¹³C NMR** (100 MHz, CDCl₃): δ 197.7, 147.7, 145.2, 136.2, 129.3 (2 C), 128.7 (2 C), 127.3 (2 C), 117.9, 112.9 (2 C), 47.9, 26.6. **IR** (neat): 3321, 1669, 1597, 1510 cm⁻¹.

²¹²G.-N. Wang, T.-H. Zhu, S.-Y. Wang, T.-Q. Wei and S.-J. Ji, *Tetrahedron* **2014**, 70, 8079–8083.

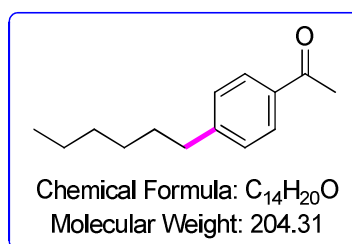
4'-(Acetoxymethyl)acetophenone (**49**)



Following general procedure G with acetoxymethylsilicate **18** (0.45 mmol, 279 mg) and 4'-bromoacetophenone **44** (0.3 mmol, 60 mg). The crude product was purified by flash column chromatography (pentane/diethyl ether, 99/1 then 95/5) to afford **49** as a colorless oil (38 mg, 66%).

¹H NMR (400 MHz, CDCl₃): δ 7.94 (d, *J* = 8.4 Hz, 2H), 7.43 (d, *J* = 8.4 Hz, 2H), 5.15 (s, 2H), 2.59 (s, 3H), 2.12 (s, 3H). ¹³C NMR (100 MHz, CDCl₃): δ 197.6, 170.6, 141.2, 136.8, 128.6 (2 C), 127.9 (2 C), 65.4, 26.6, 20.9. IR (neat): 2905, 2855, 1736, 1681, 1264, 1224 cm⁻¹. HRMS calc for [C₁₁H₁₂NaO₃]⁺ 215.0673; found 215.0679.

4'-(Hexyl)acetophenone (**50**)



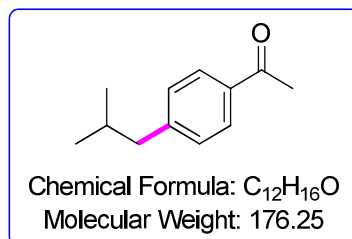
Following general procedure G with hexylsilicate **2** (0.45 mmol, 285 mg) and 4'-bromoacetophenone **44** (0.3 mmol, 60 mg). The crude product was purified by flash column chromatography (pentane/diethyl ether, 99/1) to afford **50** as a colorless oil (53 mg, 85%).

The spectroscopic data are in agreement with those reported in the literature.²¹³

²¹³A. Fernandes, C. Romão, C. Rosa, V. Vieira, A. Lopes, P. Silva and A. Maçanita, *Eur.J.Org. Chem.*, 2004, **23**, 4877–4883.

¹H NMR (400 MHz, CDCl₃): δ 7.87 (d, *J* = 8.2 Hz, 2H), 7.26 (d, *J* = 8.2 Hz, 2H), 2.68–2.64 (m, 2H), 2.58 (s, 3H), 1.67–1.58 (m, 2H), 1.38–1.26 (m, 6H), 0.88 (t, *J* = 6.8 Hz, 3H). **¹³C NMR** (100 MHz, CDCl₃): δ 198.0, 149.0, 135.1, 128.7 (2 C), 128.6 (2 C), 36.1, 31.8, 31.2, 29.0, 26.7, 22.7, 14.2. **IR** (neat): 2900, 1681, 1605, 1265 cm⁻¹.

4'-(Isobutyl)acetophenone (**51**)



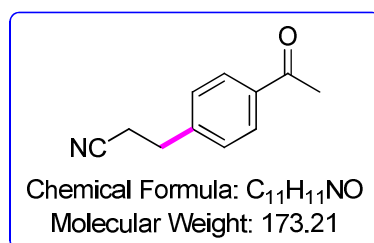
Following general procedure G with isopropylsilicate **5** (0.45 mmol, 272 mg) and 4'-bromoacetophenone **44** (0.3 mmol, 60 mg). The crude product was purified by flash column chromatography (pentane/diethyl ether, 98/2) to afford **51** as a colorless oil (39 mg, 75%).

The spectroscopic data are in agreement with those reported in the literature.²¹⁴

¹H NMR (400 MHz, CDCl₃): δ 7.87 (d, *J* = 8.3 Hz, 2H), 7.23 (d, *J* = 8.3 Hz, 2H), 2.58 (s, 3H), 2.53 (d, *J* = 7.2 Hz, 2H), 1.93 – 1.87 (m, 1H), 0.91 (d, *J* = 6.6 Hz, 6H). **¹³C NMR** (100 MHz, CDCl₃): δ 198.0, 147.7, 135.1, 129.4 (2 C), 128.4 (2 C), 45.5, 30.2, 29.7, 22.5 (2 C). **IR**(neat): 2909, 1680, 1605, 1265 cm⁻¹.

²¹⁴ E. V. Bellale, D. S. Bhalerao and K. G. Akamanchi, *J. Org. Chem.*, 2008, **73**, 9473–9475.

4'-(2-Cyanoethyl)acetophenone (**52**)

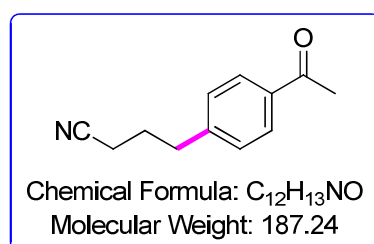


Following general procedure G with 2-cyanoethylsilicate **13** (0.45 mmol, 271 mg) and 4'-bromoacetophenone **44** (0.3 mmol, 60 mg). The crude product was purified by flash column chromatography (pentane/diethyl ether, 1/1) to afford **52** as a colorless oil (36 mg, 69%).

The spectroscopic data are in agreement with those reported in the literature.²¹⁵

¹H NMR (400 MHz, CDCl₃): δ 7.93 (d, *J* = 8.4 Hz, 2H), 7.33 (d, *J* = 8.4 Hz, 2H), 3.01 (t, *J* = 7.3 Hz, 2H), 2.65 (t, *J* = 7.3 Hz, 2H), 2.58 (s, 3H). ¹³C NMR (100 MHz, CDCl₃): δ 197.6, 143.3, 136.2, 129.0 (2 C), 128.6 (2 C), 118.7, 31.4, 26.6, 19.0. IR (neat): 2910, 2245, 1675, 1607, 1266 cm⁻¹.

4'-(3-Cyanopropyl)acetophenone (**53**)



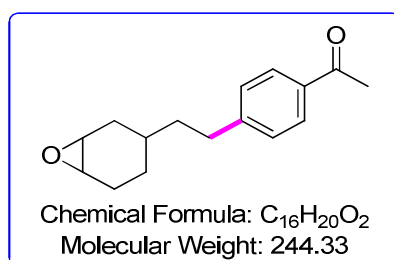
Following general procedure G with 2-cyanoethylsilicate **14** (0.45 mmol, 277 mg) and 4'-bromoacetophenone **44** (0.3 mmol, 60 mg). The crude product was purified by flash column chromatography (pentane/diethyl ether, 1/1) to afford **53** as a colorless oil (48 mg, 85%).

²¹⁵ M. Amatore, C. Gosmini and J. Périchon, *J. Org. Chem.*, 2006, **71**, 6130–6134.

The spectroscopic data are in agreement with those reported in the literature.²¹⁶

¹H NMR (400 MHz, CDCl₃): δ 7.90 (d, *J* = 8.4 Hz, 2H), 7.28 (d, *J* = 8.4 Hz, 2H), 2.86–2.82 (m, 2H), 2.58 (s, 3H), 2.33 (t, *J* = 7.0 Hz, 2H), 2.0 (dd, *J* = 7.5 Hz, 7.0 Hz, 2H). **¹³C NMR** (100 MHz, CDCl₃): δ 197.6, 145.3, 135.6, 128.8 (2 C), 128.6 (2 C), 119.1, 34.3, 26.5, 26.5, 16.4. **IR** (neat): 2905, 2258, 1675, 1605, 1266 cm⁻¹.

4'-(2-(7-Oxabicyclo-[4.1.0]hept-3-yl)ethyl)acetophenone (**54**)

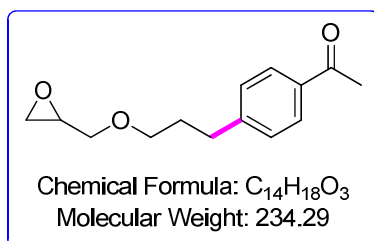


Following general procedure G with 2-(7-oxabicyclo-[4.1.0]hept-3-yl)ethylsilicate **11** (0.45 mmol, 303 mg) and 4'-bromoacetophenone **44** (0.3 mmol, 60 mg). The crude product was purified by flash column chromatography (pentane/diethyl ether, 80/20) to afford a 45/55 mixture of diastereoisomers of **54** as a colorless oil (48 mg, 65%).

¹H NMR (400 MHz, CDCl₃): δ 7.88–7.85 (m, 4H), 7.26–7.21 (m, 4H), 3.20–3.14 (m, 4H), 2.69–2.66 (m, 4H), 2.60 (s, 6H), 2.25–1.99 (m, 4H), 1.89–1.51 (m, 10H), 1.44–1.37 (m, 2H), 1.25–0.95 (m, 2H). **¹³C NMR** (100 MHz, CDCl₃): δ 197.8 (197.8), 148.4 (148.3), 135.0 (135.0), 128.5 (128.5), 128.5 (128.5), 53.0 (52.5), 51.8 (51.7), 38.1 (37.8), 33.3 (33.0), 32.1 (31.8), 30.6 (29.3), 27.0 (25.1), 26.5, 24.3 (23.5). **IR** (neat): 2935, 1671, 1604, 1568, 1298 cm⁻¹. **HRMS** calc for [C₁₆H₂₀NaO₂]⁺ 267.1365; found 267.1135.

²¹⁶ S. Sase, M. Jaric, A. Metzger, V. Malakhov and P. Knochel, *J. Org. Chem.*, 2008, **73**, 7380–7382.

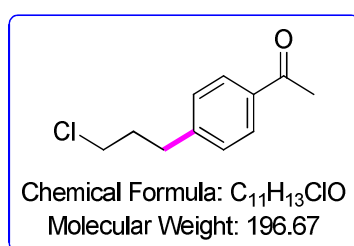
4'-(3-Glycidyoxypropyl)acetophenone (**55**)



Following general procedure G with 3-glycidyoxypropylsilicate **9** (0.45 mmol, 239 mg) and 4'-bromoacetophenone **44** (0.3 mmol, 60 mg). The crude product was purified by flash column chromatography (pentane/diethyl ether, 95/5) to afford **55** as a colorless oil (29 mg, 40%).

¹H NMR (400 MHz, CDCl₃): δ 7.88 (d, *J* = 8.4 Hz, 2H), 7.28 (d, *J* = 8.4 Hz, 2H), 3.73 (dd, *J* = 11.5 Hz, 2.9 Hz, 1H), 3.57–3.42 (m, 2H), 3.36 (dd, *J* = 11.5 Hz, 5.9 Hz, 1H), 3.21–3.07 (m, 1H), 2.85–2.64 (m, 3H), 3.60 (dd, *J* = 5.0 Hz, 2.7 Hz, 1H), 2.58 (s, 3H), 1.92 (ddt, *J* = 12.7 Hz, 7.6 Hz, 6.3 Hz, 2H). ¹³C NMR (100 MHz, CDCl₃): δ 197.8, 147.7, 135.1, 128.7 (2 C), 128.5 (2 C), 71.6, 70.3, 50.8, 44.2, 32.3, 30.9, 26.5. IR (neat): 2905, 1678, 1605, 1266, 1106 cm⁻¹. HRMS calc for [C₁₄H₁₈NaO₃]⁺ 257.1148; found 257.1155.

4'-(3-Chloropropyl)acetophenone (**56**)

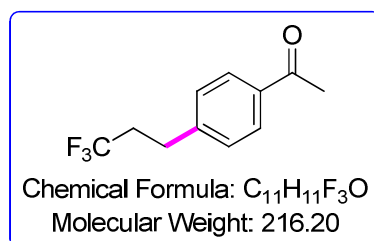


Following general procedure G with 3-chloropropylsilicate **12** (0.45 mmol, 282 mg) and 4'-bromoacetophenone **44** (0.3 mmol, 60 mg). The crude product was purified by flash column chromatography (pentane/diethyl ether, 80/20) to afford **56** as a colorless oil (42 mg, 71%).

The spectroscopic data are in agreement with those reported in the literature.²¹⁷

¹H NMR (400 MHz, CDCl₃): δ 7.89 (d, *J* = 8.4 Hz, 2H), 7.29 (d, *J* = 8.4 Hz, 2H), 3.52 (t, *J* = 6.4 Hz, 2H), 2.86– 2.82 (m, 2H), 2.58 (s, 3H), 2.13– 2.07 (m, 2H). **¹³C NMR** (100 MHz, CDCl₃): δ 197.8, 146.5, 135.5, 128.8 (2 C), 128.7 (2 C), 44.1, 33.6, 32.8, 26.6. **IR** (neat): 2935, 1678, 1605, 1358, 1265 cm⁻¹.

4'-(3,3,3-Trifluoropropyl)acetophenone(**57**)

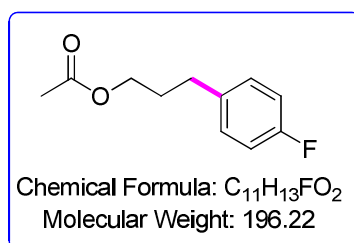


Following general procedure G with 3,3,3-trifluoropropylsilicate **13** (0.45 mmol, 290 mg) and 4'-bromoacetophenone **44** (0.3 mmol, 60 mg). The crude product was purified by flash column chromatography (pentane/diethyl ether, 99/1 then 95/5) to afford **57** as a colorless oil (52 mg, 80%).

¹H NMR (400 MHz, CDCl₃): δ 7.91 (d, *J* = 8.4 Hz, 2H), 7.30 (d, *J* = 8.4 Hz, 2H), 2.95 – 2.91 (m, 2H), 2.59 (s, 3H), 2.47 – 2.35 (m, 2H). **¹³C NMR** (100 MHz, CDCl₃): δ 197.6, 144.4, 135.8, 128.8 (2 C), 128.5 (2 C), 126.5 (q, *J* = 275 Hz), 35.1 (q, *J* = 28 Hz), 28.2 (q, *J* = 3 Hz), 26.5. **¹⁹F NMR** (376 MHz, CDCl₃): δ -66.57. **IR** (neat): 2871, 1677, 1607, 1266 cm⁻¹.

²¹⁷X.-Q. Li, W.-K. Wang, C. Zhang, *Adv. Synth. Catal.*, 2009, **351**, 2342–2350.

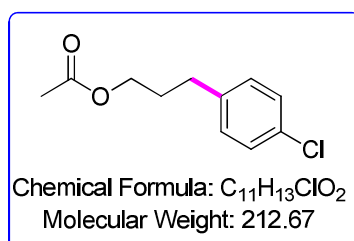
3-(4-Fluorophenyl)propylacetate (**58**)



Following general procedure G with acetoxypropylsilicate **17** (0.45 mmol, 292 mg) and 1-bromo-4-fluorobenzene (0.3 mmol, 33 μ l). The crude product was purified by flash column chromatography (pentane/diethyl ether, 80/20) to afford **58** as a colorless oil (45 mg, 75%).

¹H NMR (400 MHz, CDCl₃): δ 7.16–7.08 (m, 2H), 7.00–6.92 (m, 2H), 4.07 (t, J = 6.5 Hz, 2H), 2.68 – 2.64 (m, 2H), 2.05 (s, 3H), 1.95 – 1.89 (m, 2H). **¹³C NMR** (100 MHz, CDCl₃): δ 171.1, 161.3 (d, J = 243.7 Hz), 136.7 (d, J = 3.2 Hz), 129.7 (d, J = 7.8 Hz, 2 C), 115.1 (d, J = 21.1 Hz, 2 C), 63.6, 31.3, 30.3, 20.9. **¹⁹F NMR** (376 MHz, CDCl₃): δ -117.48. **IR** (neat): 2930, 1733, 1600, 1509, 1218, 1036 cm⁻¹. **HRMS** calc. for [C₁₁H₁₃FN₂O₂]⁺ 219.0797; found 219.0792

3-(4-Chlorophenyl)propyl acetate (**59**)



Following general procedure G with acetoxypropylsilicate **17** (0.45 mmol, 292 mg) and 1-bromo-4-chlorobenzene (0.3 mmol, 58 mg). The crude product was purified by flash column chromatography (pentane/diethyl ether, 90/10) to afford **59** as a colorless oil (51 mg, 80%).

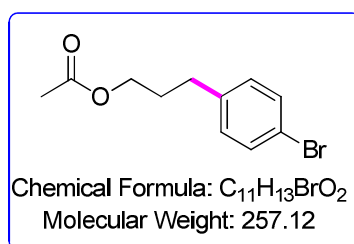
¹H NMR (400 MHz, CDCl₃): δ 7.25 (d, J = 8.6 Hz, 1H), 7.11 (d, J = 8.6 Hz, 1H), 4.07 (t, J = 6.5 Hz, 2H), 2.68 – 2.64 (m, 2H), 2.05 (s, 3H), 1.97 – 1.89 (m, 2H). **¹³C NMR** (100 MHz,

CDCl₃): δ 171.0, 139.6, 131.7, 129.7 (2 C), 128.5 (2 C), 63.6, 31.5, 30.1, 21.9. **IR** (neat): 2936, 1736, 1597, 1231, 836 cm⁻¹. **HRMS** calc. for [C₁₁H₁₃ClNaO₂]⁺235.0496; found 235.0505.

3-(4-Bromophenyl)propyl acetate (**60**) and 3-(4-iodophenyl)propyl acetate (**61**)

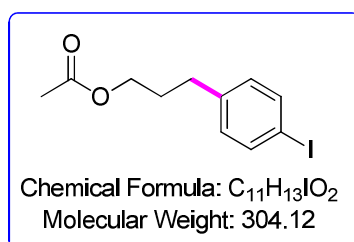
Following general procedure G with acetoxypropylsilicate **17** (0.45 mmol, 292 mg) and 1-bromo-4-iodobenzene (0.3 mmol, 85 mg). The crude product was purified by flash column chromatography (pentane/diethyl ether, 90/10) to afford a 10:1 mixture of **60** and **61** as a colorless oil (43 mg, 48%).

3-(4-Bromophenyl)propyl acetate (**60**)



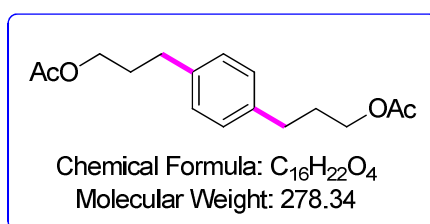
¹H NMR (400 MHz, CDCl₃): δ 7.40 (d, *J* = 8.4 Hz, 2H), 7.06 (d, *J* = 8.4 Hz, 2H), 4.07 (t, *J* = 6.6 Hz, 2H), 2.66 – 2.62 (m, 2H), 2.05 (s, 3H), 1.97 – 1.89 (m, 2H). **¹³C NMR** (100 MHz, CDCl₃): δ 171.1, 140.1, 131.5 (2 C), 130.1 (2 C), 119.8, 63.6, 31.6, 30.0, 20.9. **IR** (neat): 2940, 1735, 1591, 1299, 1231 cm⁻¹. **HRMS** calc. for [C₁₁H₁₃BrNaO₂]⁺ 278.9991; found 278.9991

3-(4-Iodophenyl)propyl acetate (**61**)



¹H NMR (400 MHz, CDCl₃): δ 7.60 (d, *J* = 8.4 Hz, 2H), 6.95 (d, *J* = 8.4 Hz, 2H), 4.07 (t, *J* = 6.6 Hz, 2H), 2.66 – 2.63 (m, 2H), 2.05 (s, 3H), 1.96 – 1.86 (m, 2H). **¹³C NMR** (100 MHz, CDCl₃): δ 171.1, 140.8, 137.5 (2 C), 130.5 (2 C), 119.8, 63.6, 31.7, 30.0, 20.9. **IR** (neat): 2940, 1735, 1591, 1299, 1231 cm⁻¹. **HRMS** calc. for [C₁₁H₁₃INaO₂]⁺ 326.9852; found 326.9847.

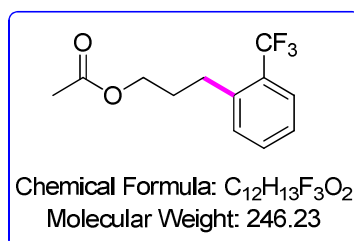
1,4-Phenylenebis(propane-3,1-diyl) diacetate (**62**)



Following general procedure G with acetoxypropylsilicate **17** (0.45 mmol, 292 mg) and 1,4-dibromobenzene (0.3 mmol, 71 mg). The crude product was purified by flash column chromatography (pentane/diethyl ether, 90/10 to 80/20) to afford **60** (51 mg, 66%) and **62** (14 mg, 16%).

¹H NMR (400 MHz, CDCl₃): δ 7.1 (s, 4H), 4.08 (t, *J* = 6.6 Hz, 4H), 2.67 – 2.64 (m, 4H), 2.05 (s, 6H), 1.98 – 1.90 (m, 4H). **¹³C NMR** (100 MHz, CDCl₃): δ 171.3, 139.0, 128.6, 64.0, 31.9, 30.4, 21.1. **HRMS** calc. for [C₁₆H₂₂INaO₄]⁺ 301.1410; found 301.1412.

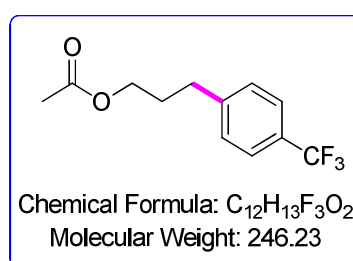
3-(2-(Trifluoromethyl)phenyl)propyl acetate (**63**)



Following general procedure G with acetoxypropylsilicate **17** (0.45 mmol, 292 mg) and 2-bromobenzotrifluoride (0.3 mmol, 42 μl). The crude product was purified by flash column chromatography (pentane/diethyl ether, 95/5) to afford **63** as a colorless oil (51 mg, 69%).

¹H NMR (400 MHz, Chloroform-*d*) δ 7.62 (dd, $J = 7.9, 1.3$ Hz, 1H), 7.47 (td, $J = 7.6, 1.3$ Hz, 1H), 7.36 – 7.27 (m, 2H), 4.13 (t, $J = 6.4$ Hz, 2H), 2.86 (ddd, $J = 9.7, 6.2, 1.3$ Hz, 2H), 2.06 (s, 3H), 2.01 – 1.91 (m, 2H). **¹³C NMR** (100 MHz, CDCl₃): δ 171.1, 140.1, 131.8 (d, $J = 0.8$ Hz), 131.0, 128.6 (q, $J = 29.8$ Hz), 126.2, 126.0 (q, $J = 5.8$ Hz), 124.6 (q, $J = 5.8$ Hz), 63.8, 30.4, 29.1 (d, $J = 1.7$ Hz), 20.9. **¹⁹F NMR** (376 MHz, CDCl₃): δ -59.7. **IR** (neat): 2940, 1737, 1608, 1311, 1111, 1030 cm⁻¹. **HRMS** calc. for [C₁₂H₁₃F₃LiO₂]⁺ 253.1022; found 253.1019.

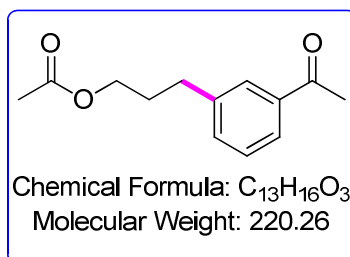
3-(4-(Trifluoromethyl)phenyl)propyl acetate (**64**)



Following general procedure G with acetoxypropylsilicate **17** (0.45 mmol, 292 mg) and 4-bromobenzotrifluoride (0.3 mmol, 41 μ l). The crude product was purified by flash column chromatography (pentane/diethyl ether, 90/10) to afford **64** as a colorless oil (70 mg, 94%).

¹H NMR (400 MHz, CDCl₃): δ 7.54 (d, $J = 8.0$ Hz, 2H), 7.29 (d, $J = 8.0$ Hz, 2H), 4.09 (t, $J = 6.5$ Hz, 2H), 2.77 – 2.73 (m, 2H), 2.05 (s, 3H), 1.99 – 1.94 (m, 2H). **¹³C NMR** (100 MHz, CDCl₃): δ 171.1, 145.3, 128.7, 128.5 (q, $J = 32.3$ Hz, 2 C), 125.4 (q, $J = 3.9$ Hz, 2 C), 124.3 (q, $J = 270$ Hz), 63.5, 32.1, 29.9, 21.9. **¹⁹F NMR** (376 MHz, CDCl₃): δ -62.4. **IR** (neat): 2922, 1737, 1584, 1232, 845 cm⁻¹. **HRMS** calc. for [C₁₂H₁₃F₃NaO₂]⁺ 269.0760; found 269.0752.

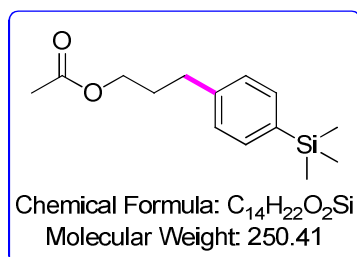
3-(3-Acetylphenyl)propyl acetate (**65**)



Following general procedure G with acetoxypropylsilicate **17** (0.45 mmol, 292 mg) and 3'-bromoacetophenone (0.3 mmol, 35 μ l). The crude product was purified by flash column chromatography (pentane/diethyl ether, 90/10) to afford **65** as a colorless oil (53 mg, 80%).

¹H NMR (400 MHz, CDCl₃): δ 7.80–7.71 (m, 2H), 7.40–7.34 (m, 2H), 4.08 (t, *J* = 6.5 Hz, 2H), 2.76 – 2.72 (m, 2H), 2.59 (s, 3H), 2.04 (s, 3H), 2.01 – 1.94 (m, 2H). ¹³C NMR (100 MHz, CDCl₃): δ 198.2, 171.1, 141.7, 137.3, 133.2, 128.6, 128.0, 126.3, 63.6, 32.0, 30.0, 26.6, 20.9. IR (neat): 2941, 1734, 1684, 1601, 1232, 839 cm⁻¹. HRMS calc. for [C₁₃H₁₆NaO₃]⁺ 243.0992; found 243.0992.

3-(4-(Trimethylsilyl)phenyl)propyl acetate (**66**)

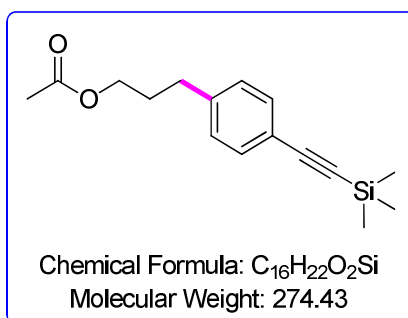


Following general procedure G with acetoxypropylsilicate **17** (0.45 mmol, 292 mg) and (4-bromophenyl)trimethylsilane (0.3 mmol, 59 μ l). The crude product was purified by flash column chromatography (pentane/diethyl ether, 90/10) to afford **66** as a colorless oil (54 mg, 72%).

¹H NMR (400 MHz, CDCl₃): δ 7.46 (d, *J* = 8.0 Hz, 2H), 7.19 (d, *J* = 8.0 Hz, 2H), 4.10 (t, *J* = 6.6 Hz, 2H), 2.71 – 2.67 (m, 2H), 2.06 (s, 3H), 1.99 – 1.91 (m, 2H), 0.27 (s, 9H). ¹³C

NMR(100 MHz, CDCl₃): δ 171.1, 141.8, 137.7, 133.5 (2 C), 127.9 (2 C), 63.6, 32.1, 30.0, 20.9, -1.1 (3 C). **IR** (neat): 2936, 1739, 1601, 1233 cm⁻¹. **HRMS** calc.for [C₁₄H₂₂NaO₂Si]⁺ 273.1281; found 273.1277.

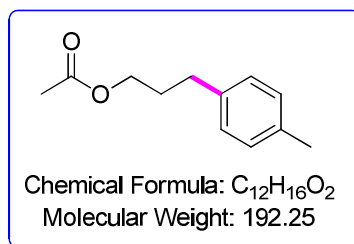
3-(4-((Trimethylsilyl)ethynyl)phenyl)propyl acetate (**67**)



Following general procedure G with acetoxypropylsilicate **17** (0.45 mmol, 292 mg) and ((4-bromophenyl)ethynyl)trimethylsilane (0.3 mmol, 76 mg). The crude product was purified by flash column chromatography (pentane/diethyl ether, 95/5) to afford **67** as a colorless oil (54 mg, 72%).

¹H NMR (400 MHz, CDCl₃): δ 7.38 (d, *J* = 8.3 Hz, 2H), 7.11 (d, *J* = 8.3 Hz, 2H), 4.06 (t, *J* = 6.5 Hz, 2H), 2.69 – 2.65 (m, 2H), 2.04 (s, 3H), 1.97 – 1.89 (m, 2H), 0.24 (s, 9H). **¹³C NMR** (100 MHz, CDCl₃): δ 171.0, 141.8, 132.0 (2 C), 128.3 (2 C), 120.8, 105.1, 93.6, 63.6, 32.21, 29.9, 20.9, 0.0 (3 C). **IR** (neat): 2944, 2156, 1738, 1608, 1233, 839 cm⁻¹. **HRMS** calc. for [C₁₆H₂₂NaO₂Si]⁺ 297.1281; found 297.1281.

3-(*p*-Tolyl)propyl acetate (**68**)

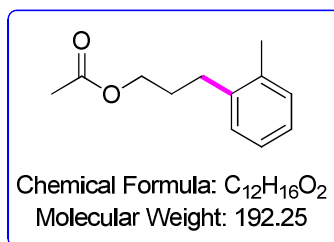


Following general procedure G with acetoxypropylsilicate **17** (0.45 mmol, 292 mg) and 4-bromotoluene (0.3 mmol, 51 mg). The crude product was purified by flash column chromatography (pentane/diethyl ether, 90/10) to afford **68** as a colorless oil (42 mg, 73%).

¹H NMR (400 MHz, CDCl₃): δ 7.12–7.07 (m, 4H), 4.09 (t, *J* = 6.6 Hz, 2H), 2.67 – 2.64 (m, 2H), 2.33 (s, 3H), 2.06 (s, 3H), 1.96 – 1.92 (m, 2H). ¹³C NMR (100 MHz, CDCl₃): δ 171.1, 138.1, 135.4, 129.1 (2 C), 128.2 (2 C), 63.8, 31.7, 30.3, 21.0 (2 C). * IR (neat): 2920, 1736, 1232, 1036 cm⁻¹. HRMS calc. for [C₁₂H₁₆NaO₂]⁺ 215.1043; found 215.1045.

*signal for both CH₃ (verified by HSQC)

3-(*o*-Tolyl)propyl acetate (**69**)

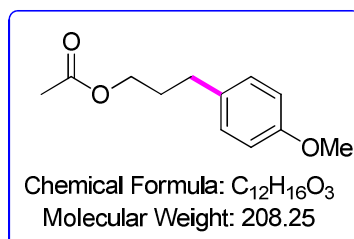


Following general procedure G with acetoxypropylsilicate **17** (0.45 mmol, 292 mg) and 2-bromotoluene (0.3 mmol, 36 μl). The crude product was purified by flash column chromatography (pentane/diethyl ether, 95/5) to afford **69** as a colorless oil (44 mg, 76%).

¹H NMR (400 MHz, CDCl₃): 7.17–7.11 (m, 4H), 4.13 (t, *J* = 6.5 Hz, 2H), 2.71 – 2.67 (m, 2H), 2.33 (s, 3H), 2.08 (s, 3H), 1.97 – 1.90 (m, 2H). ¹³C NMR (100 MHz, CDCl₃): δ 171.1,

139.4, 135.8, 130.2, 128.7, 126.1, 126.0, 64.0, 29.5, 29.0, 20.9, 19.2. **IR** (neat): 2942, 1736, 1601, 1231 cm^{-1} . **HRMS** calc. for $[\text{C}_{12}\text{H}_{16}\text{NaO}_2]^+$ 215.1043; found 215.1035.

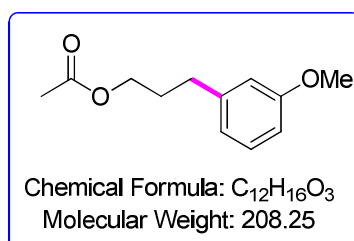
3-(4-Methoxyphenyl)propyl acetate (**70**)



Following general procedure G with acetoxypropylsilicate **17** (0.45 mmol, 292 mg) and 4-iodoanisole (0.3 mmol, 70 mg). The crude product was purified by flash column chromatography (pentane/diethyl ether, 90/10) to afford **70** as a colorless oil (29 mg, 46%).

^1H NMR (400 MHz, CDCl_3): δ 7.10 (d, $J = 8.7$ Hz, 2H), 6.83 (d, $J = 8.7$ Hz, 2H), 4.07 (t, $J = 6.6$ Hz, 2H), 3.79 (s, 3H), 2.65 – 2.61 (m, 2H), 2.05 (s, 3H), 1.96 – 1.89 (m, 2H). **^{13}C NMR** (100 MHz, CDCl_3): δ 171.2, 157.9, 133.2, 129.3 (2 C), 113.9 (2 C), 63.8, 55.3, 31.2, 30.4, 21.0. **IR** (neat): 2941, 1734, 1612, 1299, 1234 cm^{-1} . **HRMS** calc. for $[\text{C}_{12}\text{H}_{16}\text{NaO}_3]^+$ 231.0992; found 231.0989.

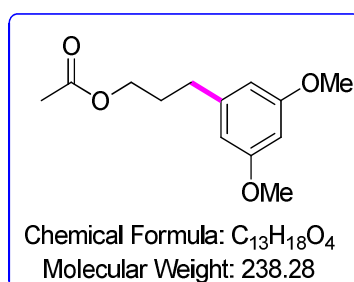
3-(3-Methoxyphenyl)propyl acetate (**71**)



Following general procedure G with acetoxypropylsilicate **17** (0.45 mmol, 292 mg) and 3-bromoanisole (0.3 mmol, 38 μl). The crude product was purified by flash column chromatography (pentane/diethyl ether, 90/10) to afford **71** as a colorless oil (34mg, 54%).

¹H NMR (400 MHz, CDCl₃): δ 7.22 – 7.18 (m, 1H), 6.79 – 6.74 (m, 3H), 4.09 (t, *J* = 6.6 Hz, 2H), 3.80 (s, 3H), 2.69 – 2.65 (m, 2H), 2.06 (s, 3H), 1.99 – 1.92 (m, 2H). **¹³C NMR** (100 MHz, CDCl₃): δ 171.1, 159.7, 142.8, 129.4, 120.8, 114.2, 111.2, 63.8, 55.1, 32.2, 30.1, 21.0. **IR** (neat): 2941, 1734, 1600, 1594, 1234, 1035 cm⁻¹. **HRMS** calc. for [C₁₂H₁₆NaO₃]⁺ 231.0992; found 231.0992.

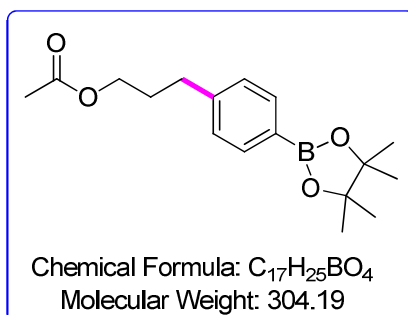
3-(3,5-Dimethoxyphenyl)propyl acetate (**72**)



Following general procedure G with acetoxypropylsilicate **17** (0.45 mmol, 292 mg) and 1-bromo-3,5-dimethoxybenzene (0.3 mmol, 65 mg). The crude product was purified by flash column chromatography (pentane/diethyl ether, 90/10) to afford **72** as a colorless oil (46 mg, 65%).

¹H NMR (400 MHz, CDCl₃): δ 6.37 – 6.29 (m, 3H), 4.09 (t, *J* = 6.6 Hz, 2H), 3.78 (s, 6H), 2.65 – 2.61 (m, 2H), 2.06 (s, 3H), 1.98 – 1.91 (m, 2H). **¹³C NMR** (100 MHz, CDCl₃): δ 171.3, 161.0, 143.7, 106.6 (2 C), 98.1 (2 C), 63.9, 55.4 (2 C), 32.6, 30.1, 21.1. **IR** (neat): 1734, 1594, 1236, 1204, 1147, 1036 cm⁻¹. **HRMS** calc. for [C₁₃H₁₈NaO₄]⁺ 261.1097; found 261.1087.

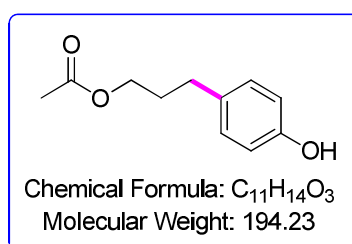
4-Acetoxypropylphenylboronic pinacol ester (**73**)



Following general procedure G with acetoxypropylsilicate **17** (0.45 mmol, 292 mg) and 4-bromophenylboronic acid pinacol ester (0.3 mmol, 85 mg). The crude product was purified by flash column chromatography (pentane/EtOAc, 90/10) to afford **73** as a brown oil (49 mg, 53%).

¹H NMR (400 MHz, CDCl₃): δ 7.74 (d, *J* = 8.0 Hz, 2H), 7.20 (d, *J* = 8.0 Hz, 2H), 4.08 (t, *J* = 6.6 Hz, 2H), 2.72 – 2.68 (m, 2H), 2.05 (s, 3H), 1.97 – 1.94 (m, 2H), 1.34 (s, 12H). ¹³C NMR (100 MHz, CDCl₃): δ 171.1, 144.6, 135.0 (2 C), 127.8 (2 C), 83.7 (2 C), 63.8, 32.4, 30.1, 24.9 (4 C), 21.0. ¹¹B NMR (128 MHz, CDCl₃): 30.6. IR (neat): 2960, 1737, 1611, 1357, 1235, 657 cm⁻¹. HRMS calc. for [C₁₇H₂₅BNaO₄]⁺ 327.1741; found 327.1754

3-(4-Hydroxyphenyl)propylacetate (**74**)



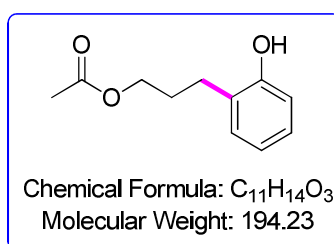
Following general procedure G with acetoxypropylsilicate **17** (0.45 mmol, 292 mg) and 4-bromophenylboronic acid pinacol ester (0.3 mmol, 85 mg). After 24h of reaction, the crude reaction mixture was filtered through a plug of celite, washing with THF (15 mL). The filtrate was concentrated by rotary evaporation. The resulting solution of DMF was diluted with THF (10 mL) and cooled to 0°C in an ice water bath. To the cold stirring solution was added 1M

NaOH (1.5 mL, 5 equiv.) and 30% aq. H₂O₂ (171 μL, 5 equiv.). After 30 min the mixture was diluted with water (10 mL) and diethyl ether (10 mL) and neutralized by addition of 1M HCl (2.5 mL). The organic layer was collected and washed with water (2 x 10mL), brine (2 x 10 mL), dried over MgSO₄ and evaporated under reduced pressure. The crude product was purified by flash column chromatography (pentane/EtOAc, 90/10) to afford **74** as a brown oil (41 mg, 69%).

The spectroscopic data are in agreement with those reported in the literature.²¹⁸

¹H NMR (400 MHz, CDCl₃): δ 7.04 (d, *J* = 8.5 Hz, 2H), 6.76 (d, *J* = 8.5 Hz, 2H), 5.19 (s, 1H) 4.08 (t, *J* = 6.6 Hz, 2H), 2.63 – 2.59 (m, 2H), 2.06 (s, 3H), 1.95 – 1.89 (m, 2H). ¹³C NMR (100 MHz, CDCl₃): δ 171.5, 153.9, 133.2, 129.4 (2 C), 115.3 (2 C), 63.9, 31.2, 30.4, 21.0. IR (neat): 3356, 2978, 1707, 1595, 1514, 1227, 1035 cm⁻¹.

3-(2-Hydroxyphenyl)propylacetate (**75**)



Following general procedure G with acetoxypropylsilicate **17** (0.45 mmol, 292 mg) and 2-bromophenylboronic acid pinacol ester (0.3 mmol, 67 μL). After 24h of reaction, the crude reaction mixture was filtered through a plug of celite, washing with THF (15 mL). The filtrate was concentrated by rotary evaporation. The resulting solution of DMF was diluted with THF (10 mL) and cooled to 0°C in an ice water bath. To the cold stirring solution was added 1M NaOH (1.5 mL, 5 equiv.) and 30% aq. H₂O₂ (171 μL, 5 equiv.). After 30 min the mixture was diluted with water (10 mL) and diethyl ether (10 mL) and neutralized by addition of 1M HCl (2.5 mL). The organic layer was collected and washed with water (2 x 10mL), brine (2 x 10 mL), dried over MgSO₄ and evaporated under reduced pressure. The crude product was

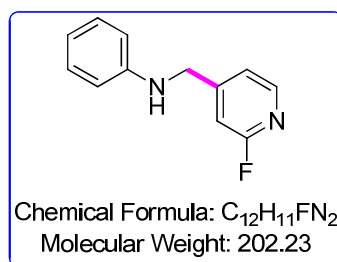
²¹⁸ Y. M. Chiang, H. K. Liu, J. M. Lo, S. C. Chien, Y. F. Chan, T. H. Lee, J. K. Su, Y. H. Kuo, *J. Chin. Chem. Soc.*, 2003, **50**, 161-166.

purified by flash column chromatography (pentane/EtOAc, 90/10) to afford **75** as a colorless oil (34 mg, 58%).

The spectroscopic data are in agreement with those reported in the literature.²¹⁹

¹H NMR (400 MHz, CDCl₃): δ 7.12 – 7.06 (m, 2H), 6.88 – 6.84 (m, 1H), 6.77 – 6.75 (m, 1H), 5.43 (s, 1H), 4.12 (t, *J* = 6.5 Hz, 2H), 2.72 – 2.68 (m, 2H), 2.07 (s, 3H), 1.99 – 1.94 (m, 2H), **¹³C NMR** (100 MHz, CDCl₃): δ 171.6, 153.7, 130.3, 127.4, 127.3, 120.7, 115.4, 64.2, 28.6, 26.3, 21.0. **IR** (neat): 3355, 2999, 1707, 1491, 1236, 1032 cm⁻¹.

4-Anilinomethyl-2-fluoropyridine (**77**)

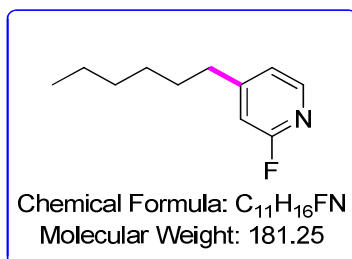


Following general procedure G with anilinomethylsilicate **8** (0.45 mmol, 294 mg) and 4-bromo-2-fluoropyridine **76** (0.3 mmol, 31 μl). The crude product was purified by flash column chromatography (pentane/EtOAc, 80/20) to afford **77** as a colorless oil (53 mg, 86%).

¹H NMR (400 MHz, CDCl₃): δ 8.15 (d, *J* = 5.2 Hz, 1H), 7.20 – 7.16 (m, 3H), 6.94 (s, 1H), 6.78 – 6.74 (m, 1H), 6.58 – 6.56 (m, 2H), 4.41 (s, 2H), 4.41 (s, 1H (N-H)). **¹³C NMR** (100 MHz, CDCl₃): δ 164.3 (d, *J* = 238.8 Hz), 155.5 (d, *J* = 7.5 Hz), 147.7 (d, *J* = 15.1 Hz), 147.1, 129.34, 119.7 (d, *J* = 3.9 Hz), 118.3, 112.8, 107.7 (d, *J* = 37.8 Hz), 46.8 (d, *J* = 3.2 Hz). **¹⁹F NMR** (376 MHz, CDCl₃): δ -68.12. **IR** (neat): 3345, 3060, 1602, 1264, 732 cm⁻¹. **HRMS** calc. for [C₁₂H₁₂FN₂]⁺ 203.0979; found 203.0977.

²¹⁹ P. Allevi, P. Ciuffreda, A. Longo, M. Anastasia, *Tetrahedron: Asymmetry*, **1998**, 9, 2915-2924.

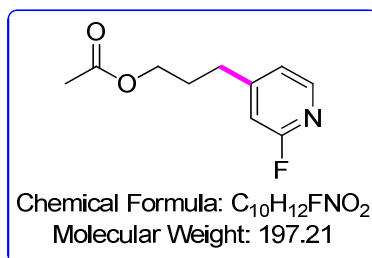
2-Fluoro-4-hexylpyridine (78)



Following general procedure G with hexylsilicate **2** (0.45 mmol, 285 mg) and 4-bromo-2-fluoropyridine **76** (0.3 mmol, 31 μ L). The crude product was purified by flash column chromatography (pentane/diethyl ether, 99/1 then 95/5) to afford **78** as a colorless oil (47 mg, 87%).

¹H NMR (400 MHz, CDCl₃): δ 8.07 (d, J = 5.1 Hz, 1H), 6.98 (dt, J = 5.1, 1.7 Hz, 1H), 6.72 (t, J = 1.8 Hz, 1H), 2.68 – 2.56 (m, 2H), 1.68 – 1.56 (m, 2H), 1.30 - 1.28 (m, 6H), 0.87 (t, J = 6.8 Hz, 3H). ¹³C NMR (100 MHz, CDCl₃): δ 164.2 (d, J = 237.9 Hz), 158.0 (d, J = 7.8 Hz), 147.3 (d, J = 15.5 Hz), 121.7 (d, J = 4.2 Hz), 109.1 (d, J = 36.3 Hz), 35.2 (d, J = 2.7 Hz), 31.6, 30.1, 28.9, 22.6, 14.1. ¹⁹F NMR (376 MHz, CDCl₃): δ -69.4. IR (neat): 2955, 2925, 2857, 1612, 1567, 1481, 1465, 1410, 1276, 1146, 1096, 1072 cm⁻¹. HRMS calc. for [C₁₁H₁₆FNNa]⁺ 204.1159; found 204.1166.

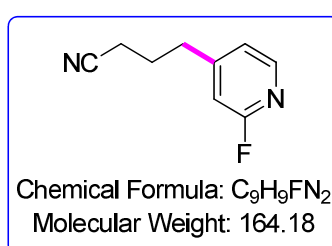
3-(2-Fluoropyridin-4-yl)propyl acetate (79)



Following general procedure G with acetoxypropylsilicate **17** (0.45 mmol, 292 mg) and 4-bromo-2-fluoropyridine **76** (0.3 mmol, 31 μ L). The crude product was purified by flash column chromatography (pentane/EtOAc, 80/20) to afford **79** as a colorless oil (48 mg, 81%).

¹H NMR (400 MHz, CDCl₃): δ8.09 (d, *J* = 5.2 Hz, 1H), 7.02 – 6.98 (m, 1H), 6.74 (s, 1H), 4.08 (t, *J* = 6.4 Hz, 2H), 2.74 – 2.71 (m, 2H), 2.03 (s, 3H), 2.02 – 1.95 (m, 2H). **¹³C NMR** (100 MHz, CDCl₃): δ170.9, 164.1 (d, *J* = 238.5 Hz), 156.2 (d, *J* = 7.7 Hz), 147.5 (d, *J* = 15.4 Hz), 121.5 (d, *J* = 3.9 Hz), 109.1 (d, *J* = 36.9 Hz), 63.2, 31.5 (d, *J* = 3.0 Hz), 28.9, 20.8. **¹⁹F NMR** (376 MHz, CDCl₃): δ -68.84. **IR** (neat): 2935, 1733, 1612, 1411, 1233 cm⁻¹. **HRMS** calc. for [C₁₀H₁₂FLiNO₂]⁺ 204.1007; found 204.1015.

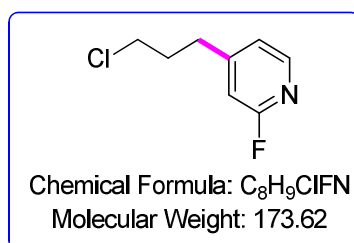
4-(2-Fluoropyridin-4-yl)butanenitrile (**80**)



Following general procedure G with cyanopropylsilicate **14** (0.45 mmol, 277 mg) and 4-4-bromo-2-fluoropyridine **76** (0.3 mmol, 31 μl). The crude product was purified by flash column chromatography (pentane/EtOAc, 80/20) to afford **80** as a colorless oil (29 mg, 59%).

¹H NMR (400 MHz, CDCl₃): δ8.15 (d, *J* = 5.1 Hz, 1H), 7.04 – 7.01 (m, 1H), 6.78 – 6.74 (m, 1H), 2.85 – 2.81 (m, 2H), 2.39 – 2.36 (m, 2H), 2.05 – 1.98 (m, 2H). **¹³C NMR** (100 MHz, CDCl₃): δ164.2 (d, *J* = 239.0 Hz), 154.6 (d, *J* = 7.7 Hz), 147.9 (d, *J* = 15.3 Hz), 121.5 (d, *J* = 4.0 Hz), 118.7, 107.7 (d, *J* = 37.0 Hz), 33.5 (d, *J* = 3.0 Hz), 25.6, 16.5. **¹⁹F NMR** (376 MHz, CDCl₃): δ -68.10. **IR** (neat): 3060, 1672, 1613, 1412, 1265, 731 cm⁻¹. **HRMS** calc. for [C₉H₁₀FN₂]⁺ 165.0823; found 165.0822

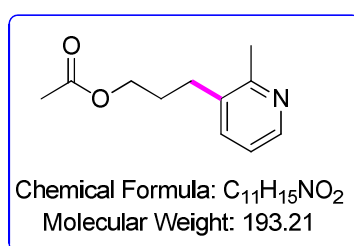
4-(3-Chloropropyl)-2-fluoropyridine (**81**)



Following general procedure G with 3-chloropropylsilicate **12** (0.45 mmol, 281 mg) and 4-bromo-2-fluoropyridine **76** (0.3 mmol, 31 μ L). The crude product was purified by flash column chromatography (pentane/diethyl ether, 99/1 then 95/5) to afford **81** as a colorless oil (42 mg, 81%).

¹H NMR (400 MHz, CDCl₃): δ 8.12 (d, *J* = 5.1 Hz, 1H), 7.02 (dt, *J* = 5.0, 1.6 Hz, 1H), 6.85 – 6.68 (m, 1H), 3.53 (t, *J* = 6.3 Hz, 2H), 2.83 (dd, *J* = 8.4, 6.8 Hz, 2H), 2.19 – 2.02 (m, 2H). ¹³C NMR (100 MHz, CDCl₃): δ 164.1 (d, *J* = 239.5 Hz), 155.7 (d, *J* = 7.7 Hz), 147.6, 121.7, 109.3 (d, *J* = 38.0 Hz), 43.6, 32.5, 31.9 (d, *J* = 2.8 Hz). ¹⁹F NMR (376 MHz, CDCl₃): δ -68.6. IR (neat): 2926, 1613, 1558, 1411, 1275, 1148, 908, 728 cm⁻¹. HRMS calc. for [C₈H₉ClFNNa]⁺ 196.0300; found 196.0306.

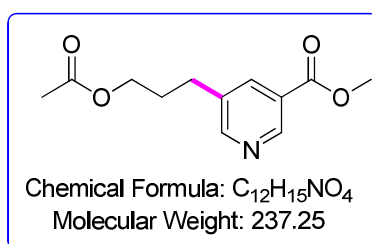
3-(2-methylpyridin-3-yl)propylacetate (**82**)



Following general procedure G with acetoxypropylsilicate **17** (0.45 mmol, 292 mg) and 3-bromo-2-methylpyridine (0.3 mmol, 35 μ L). The crude product was purified by flash column chromatography (pentane/diethyl ether, 50/50) to afford **82** as a colorless oil (39 mg, 67%).

¹H NMR (300 MHz, CDCl₃): δ8.34 (d, *J* = 3.5 Hz, 1H), 7.40 (d, *J* = 7.5, 1H), 7.06 (dd, *J* = 7.6 Hz, *J* = 3.5 Hz, 1H), 4.10 (t, *J* = 6.4 Hz, 2H), 2.70 – 2.65 (m, 2H), 2.53 (s, 3H), 2.05 (s, 3H) 1.96 – 1.87 (m, 2H). **¹³C NMR** (75 MHz, CDCl₃): δ171.0, 156.5, 147.7, 136.3, 134.4, 121.3, 63.6, 29.0, 28.5, 22.0, 20.9. **IR** (neat): 2942, 1736, 1574, 1441, 1232, 1035, 729 cm⁻¹. **HRMS** calc. for [C₁₁H₁₅NNaO₂]⁺ 216.0995; found 216.1003.

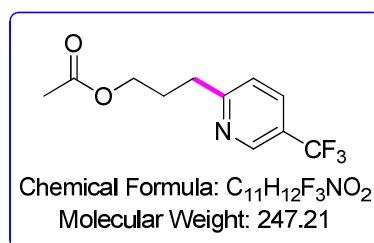
Methyl 5-(3-acetoxypropyl)nicotinate (**83**)



Following general procedure G with acetoxypropylsilicate **17** (0.45 mmol, 292 mg) and methyl 5-bromopyridine-3-carboxylate (0.3 mmol, 65 mg). The crude product was purified by flash column chromatography (pentane/ethyl acetate, 60/40) to afford **83** as a colorless oil (47 mg, 75%).

¹H NMR (400 MHz, CDCl₃): δ9.05 (d, *J* = 1.7 Hz, 1H), 8.61 (d, *J* = 1.9, 1H), 8.12 (dd, *J* = 1.9 Hz, *J* = 1.7 Hz, 1H), 4.09 (t, *J* = 6.4 Hz, 2H), 3.94 (s, 3H), 2.78 – 2.74 (m, 2H), 2.04 (s, 3H) 2.02 – 1.95 (m, 2H). **¹³C NMR** (100 MHz, CDCl₃): δ 171.0, 165.8, 153.4, 148.6, 136.8, 136.5, 125.8, 63.3, 52.4, 29.7, 29.2, 20.9. **IR** (neat): 2942, 1722, 1426, 1231, 1027, 765 cm⁻¹. **HRMS** calc. for [C₁₂H₁₅NNaO₄]⁺ 260.0893; found 260.0897.

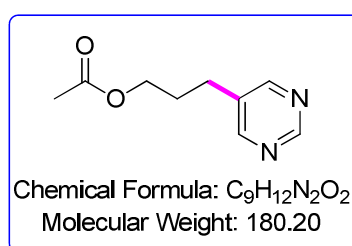
3-(5-(trifluoromethyl)pyridin-2-yl)propyl acetate (**84**)



Following general procedure G with acetoxypropylsilicate **17** (0.45 mmol, 292 mg) and 2-bromo-5-(trifluoromethyl)pyridine (0.3 mmol, 67 mg). The crude product was purified by flash column chromatography (pentane/diethyl ether, 80/20) to afford **84** as a colorless oil (30 mg, 40%).

¹H NMR (400 MHz, CDCl₃): δ 8.80 (d, *J* = 0.8 Hz, 1H), 7.84 (dd, *J* = 8.1 Hz, *J* = 1.9 Hz, 1H), 7.30 (d, *J* = 8.1 Hz, 1H), 4.10 (t, *J* = 6.4 Hz, 2H), 2.97 – 2.94 (m, 2H), 2.16 – 2.09 (m, 2H), 2.04 (s, 3H). ¹³C NMR (75 MHz, CDCl₃): δ 171.1, 165.0(d, *J* = 1.3 Hz), 146.3 (q, *J* = 4.1 Hz), 133.5(q, *J* = 3.5 Hz), 124.4 (q, *J* = 30 Hz), 123.7 (q, *J* = 270 Hz), 122.6, 63.6, 34.6, 28.2, 20.9. ¹⁹F NMR (376 MHz, CDCl₃): δ -62.3. IR (neat): 2940, 1737, 1608, 1326, 1232, 1125, 732 cm⁻¹. HRMS calc. for [C₁₁H₁₂F₃NNaO₂]⁺ 270.0712; found 270.0707.

3-(Pyrimidin-5-yl)propyl acetate (**85**)

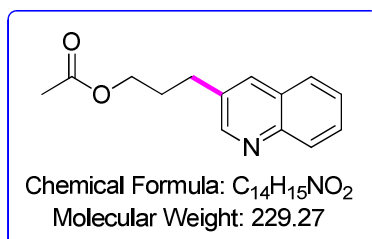


Following general procedure G with acetoxypropylsilicate **17** (0.45 mmol, 292 mg) and 5-bromopyrimidine (0.3 mmol, 48 mg). The crude product was purified by flash column chromatography (pentane/ethylacetate, 50/50) to afford **85** as a colorless oil (18 mg, 33%).

¹H NMR (300 MHz, CDCl₃): δ 9.09 (s, 1H), 8.60 (s, 2H), 4.12 (t, *J* = 6.3 Hz, 2H), 2.73 – 2.68 (m, 2H), 2.05 (s, 3H), 2.03 – 1.94 (m, 2H). ¹³C NMR (75 MHz, CDCl₃): δ 170.9, 156.9 (2 C),

156.7, 134.2, 63.1, 29.4, 27.0, 20.9. **IR** (neat): 2942, 1734, 1232, 1040, 697 cm^{-1} . **HRMS** calc. for $[\text{C}_9\text{H}_{12}\text{N}_2\text{NaO}_2]^+$ 203.0791; found 203.0797.

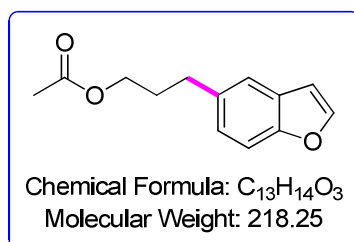
3-(Quinolin-3-yl)propylacetate (**86**)



Following general procedure G with acetoxypropylsilicate **17** (0.45 mmol, 292 mg) and 4-bromoquinoline (0.3 mmol, 41 μl). The crude product was purified by flash column chromatography (pentane/diethyl ether, 90/10) to afford **86** as a colorless oil (45 mg, 65%).

^1H NMR (400 MHz, CDCl_3): δ 8.78 (d, $J = 2.2$ Hz, 1H), 8.07 (d, $J = 8.5$ Hz, 1H), 7.92 (d, $J = 2.2$ Hz, 1H), 7.76 (d, $J = 8.2$ Hz, 1H), 7.68 – 7.62 (m, 1H), 7.58 – 7.50 (m, 1H), 4.14 (t, $J = 6.6$ Hz, 2H), 2.90 – 2.85 (m, 2H), 2.10 – 2.06 (m, 2H), 2.05 (s, 3H). **^{13}C NMR** (100 MHz, CDCl_3): δ 171.0, 151.9, 146.9, 134.2, 133.8, 129.2, 128.8, 128.0, 127.3, 126.7, 63.5, 29.8, 29.6, 20.9. **IR** (neat): 2938, 1732, 1605, 1494, 1365, 1232 cm^{-1} . **HRMS** calc. for $[\text{C}_{14}\text{H}_{16}\text{NO}_2]^+$ 230.1176; found 230.1183.

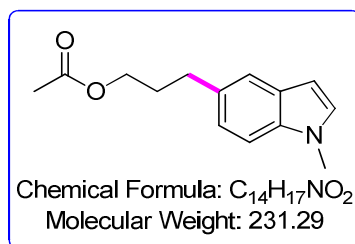
3-(benzofuran-5-yl)propylacetate (**87**)



Following general procedure G with acetoxypropylsilicate **17** (0.45 mmol, 292 mg) and 5-bromobenzofuran (0.3 mmol, 38 μl). The crude product was purified by flash column chromatography (pentane/diethyl ether, 95/5) to afford **87** as a colorless oil (48mg, 73%).

¹H NMR (400 MHz, CDCl₃): δ 7.60 (d, *J* = 2.2 Hz, 1H), 7.41 (m, 2H), 7.12 (dd, *J* = 8.4 Hz, *J* = 1.7 Hz, 1H), 6.71 (dd, *J* = 2.2 Hz, *J* = 0.9 Hz, 1H), 4.10 (t, *J* = 6.6 Hz, 2H), 2.80 – 2.77 (m, 2H), 2.06 (s, 3H) 2.03 – 1.96 (m, 2H). **¹³C NMR** (100 MHz, CDCl₃): δ 171.1, 153.6, 145.2, 135.6, 127.6, 124.8, 120.5, 111.1, 106.3, 63.8, 32.0, 30.8, 21.0. **IR** (neat): 2948, 1733, 1467, 1234, 1030, 734 cm⁻¹. **HRMS** calc. for [C₁₃H₁₄NaO₃]⁺ 241.0835; found 241.0841.

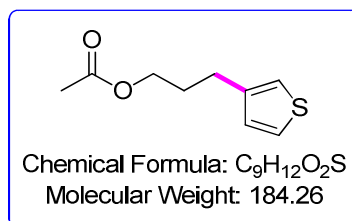
3-(1-Methyl-1H-indol-5-yl)propyl acetate (**88**)



Following general procedure G with acetoxypropylsilicate **17** (0.45 mmol, 292 mg) and 5-bromo-1-methyl-1H-indole (0.3 mmol, 63 mg). The crude product was purified by flash column chromatography (pentane/diethyl ether, 90/10) to afford **88** as a colorless oil (12 mg, 17%).

¹H NMR (400 MHz, CDCl₃): δ 7.47 – 7.42 (m, 1H), 7.28 (s, 1H), 7.09 – 7.04 (m, 2H), 6.44 (d, *J* = 3.1 Hz, *J* = 1.8 Hz, 1H), 4.13 (t, *J* = 6.6 Hz, 2H), 3.80 (s, 3H), 2.84 – 2.79 (m, 2H), 2.10 – 2.05 (m, 3H), 2.04 – 2.00 (m, 2H). **¹³C NMR** (100 MHz, CDCl₃): δ 171.2, 135.5, 132.0, 129.0, 128.7, 122.4, 120.1, 109.1, 100.5, 64.0, 32.8, 32.2, 31.0, 21.0. **IR** (neat): 2912, 1732, 1615, 1239, 1101, 1036, 718 cm⁻¹. **HRMS** calc. for [C₁₄H₁₇NNaO₂]⁺ 254.11151; found 254.1153.

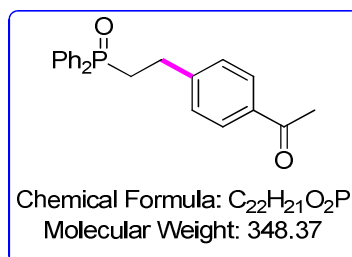
3-(Thiophen-3-yl)propyl acetate (**89**)



Following general procedure G with acetoxypropylsilicate **17** (0.45 mmol, 292 mg) and 3-bromothiophene (0.3 mmol, 29 μ l). The crude product was purified by flash column chromatography (pentane/diethyl ether, 90/10) to afford **89** as a colorless oil (28 mg, 50%).

¹H NMR (400 MHz, CDCl₃): δ 7.13 (dd, $J = 5.2$ Hz, $J = 1.2$ Hz, 1H), 6.92 (dd, $J = 5.1$ Hz, $J = 3.4$ Hz, 1H), 6.80 (s, 1H), 4.12 (t, $J = 6.4$ Hz, 2H), 2.95 – 2.90 (m, 2H), 2.06 (s, 3H), 2.04 – 1.99 (m, 2H). ¹³C NMR (100 MHz, CDCl₃): δ 171.1, 143.9, 126.8, 124.5, 123.2, 63.5, 30.5, 26.3, 20.9. IR (neat): 2942, 1734, 1232, 1040, 697 cm⁻¹. HRMS calc. for [C₉H₁₂SLiO₂]⁺ 191.0713; found 191.0710.

1-(3-(2-(Diphenylphosphoryl)ethyl)phenyl)ethan-1-one (**90**)

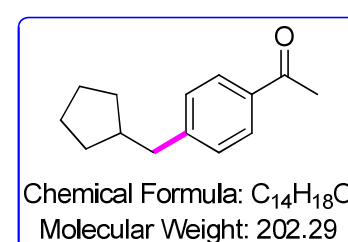
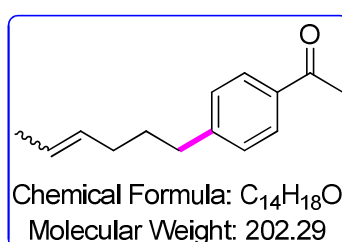
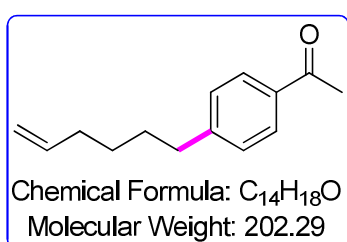


Following general procedure F with 2-(diphenylphosphine oxide)ethylsilicate **16** (0.45 mmol, 350 mg) and 4'-bromoacetophenone **44** (0.3 mmol, 60 mg). The crude product was purified by flash column chromatography (dichloromethane/ethyl acetate, 60/40 to 40/60) to afford **90** contaminated with 15% of ethyldiphenylphosphine oxide as a white solid (79 mg, 68%).

¹H NMR (400 MHz, CDCl₃): δ 7.82 (d, $J = 8.3$ Hz, 2H), 7.77 – 7.72 (m, 4H), 7.53 – 7.43 (m, 6H), 7.23 (d, $J = 8.3$ Hz, 2H), 3.06 – 2.87 (m, 2H), 2.60 – 2.54 (m, 2H), 2.53 (s, 3H).

^{13}C NMR (100 MHz, CDCl_3): δ 197.7, 146.8 (d, $J = 14.6$ Hz), 135.5, 132.6 (d, $J = 98.8$ Hz, 2 C), 132.0 (d, $J = 2.7$ Hz, 2 C), 130.8 (d, $J = 9.2$ Hz, 4 C), 128.8 (d, $J = 11.2$ Hz, 4 C), 128.8 (2 C), 128.4 (2 C), 31.5 (d, $J = 69.8$ Hz), 27.7 (d, $J = 3.0$ Hz), 26.6. ^{31}P NMR (162 MHz, CDCl_3): 31.11. IR (neat): 3015, 2895, 2257, 1904, 1674, 1601, 1437, 1264, 1174, 1111, 747, 725 cm^{-1} . HRMS calc. for $[\text{C}_{22}\text{H}_{21}\text{NaO}_2\text{P}]^+$ 371.1171; found 371.1159.

4'-(Acetoxymethyl)acetophenone (91), 1-(4-(hex-4-en-1-yl)phenyl)ethan-1-one (91') and 1-(4-(cyclopentylmethyl)phenyl)ethan-1-one (91'')



Following general procedure H with hex-5-enylsilicate **3** (0.45 mmol, 279 mg) and 4'-bromoacetophenone **44** (0.3 mmol, 60 mg). The crude product was purified by flash column chromatography (pentane/diethyl ether, 90/10) to afford a mixture of **91**, **91'** and **91''** in a ratio of 10:13:77 as a colorless oil (51 mg, 88%).

The spectroscopic data are in agreement with those reported in the literature.

Compound 91 (characteristic signals)

^1H NMR (400 MHz, C_6D_6): δ 7.80 (d, $J = 8.3$ Hz, 2H), 6.97 (d, $J = 8.4$ Hz, 2H), 5.72 (ddt, $J = 16.9, 10.2, 6.7$ Hz, 1H), 5.03 – 4.96 (m, 2H), 2.15 (s, 3H), 1.98 – 1.83 (m, 2H). ^{13}C NMR (100 MHz, CDCl_3): δ 196.2, 138.8, 114.8.

Compound 91' (characteristic signals)

$^1\text{H NMR}$ (400 MHz, C_6D_6): δ 5.54 – 5.35 (m, 2H), 1.97 – 1.85 (m, 2H), 1.45 – 1.39 (m, 3H).

$^{13}\text{C NMR}$ (100 MHz, CDCl_3): δ 196.2, 130.3, 124.6, 12.9.

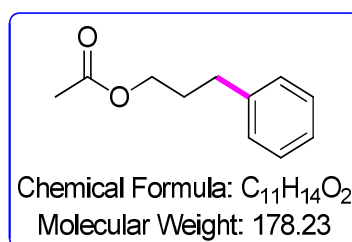
Compound 91'',²²⁰

$^1\text{H NMR}$ (400 MHz, C_6D_6): δ 7.80 (d, $J = 8.3$ Hz, 2H), 6.97 (d, $J = 8.4$ Hz, 2H), 2.40 (d, $J =$

7.5 Hz, 2H), 2.16 (s, 3H), 1.94 – 1.83 (m, 1H), 1.61 – 1.38 (m, 5H), 1.08 – 0.99 (m, 1H). $^{13}\text{C NMR}$ (100 MHz, CDCl_3): δ 196.2, 147.7, 135.7, 129.1, 128.7, 42.2, 42.0, 32.7, 26.2, 25.2.

HRMS calc. for $[\text{C}_{14}\text{H}_{18}\text{NaO}_2]^+$ 225.1250; found 225.1247.

3-Phenylpropyl acetate (92)



Following general procedure H with acetoxypropylsilicate **17** (0.45 mmol, 292 mg) and bromobenzene (0.3 mmol, 32 μl). The crude product was purified by flash column chromatography (pentane/diethyl ether, 95/5) to afford **92** as a colorless oil (41 mg, 76%).

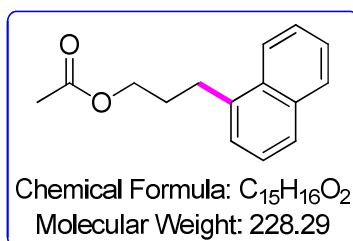
The spectroscopic data are in agreement with those reported in the literature.²²¹

$^1\text{H NMR}$ (400 MHz, CDCl_3): δ 7.30 – 7.23 (m, 2H), 7.20 – 7.15 (m, 2H), 4.07 (t, $J = 6.5$ Hz, 2H), 2.70 – 2.65 (m, 2H), 2.04 (s, 3H), 2.03 – 1.90 (m, 2H). $^{13}\text{C NMR}$ (100 MHz, CDCl_3): δ 171.2, 141.3, 128.5 (2C), 128.5 (2C), 126.1, 63.9, 32.3, 30.3, 21.1.

²²⁰ R. Ortiz and M. Yus, *Tetrahedron*, 2005, **61**, 1699–1707.

²²¹ B. Karimi, H. M. Mirzaei, A. Mobaraki and H. Vali, *Catal. Sci. Technol.*, **2015**, *5*, 3624–3631.

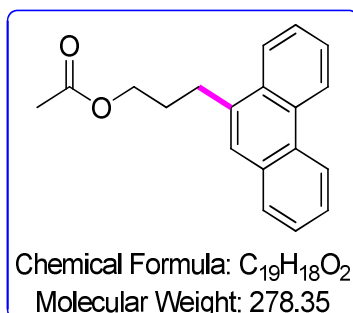
3-(Naphthalen-1-yl)propylacetate (**93**)



Following general procedure H with acetoxypropylsilicate **17** (0.45 mmol, 292 mg) and 1-bromonaphthalene (0.3 mmol, 42 μ l). The crude product was purified by flash column chromatography (pentane/diethyl ether, 95/5) to afford **93** as a colorless oil (43 mg, 63%).

¹H NMR (400 MHz, CDCl₃): δ 8.03 (dt, J = 7.8, 0.9 Hz, 1H), 7.87 (dd, J = 8.2, 1.3 Hz, 1H), 7.74 – 7.72 (m, 1H), 7.55 – 7.46 (m, 2H), 7.42 – 7.39 (m, 1H), 7.34 – 7.32 (m, 1H), 4.17 (t, J = 6.5 Hz, 2H), 3.18 – 3.15 (m, 2H), 2.14 – 2.07 (m, 2H), 2.09 (s, 3H). **¹³C NMR** (100 MHz, CDCl₃): δ 171.2, 137.2, 133.9, 131.8, 128.8, 126.9, 126.1, 125.9, 125.5, 125.5, 123.6, 64.1, 29.5, 29.3, 21.0. **IR** (neat): 2052, 2953, 1930, 1733, 1592, 1360, 1234, 1040, 738 cm⁻¹. **HRMS** calc. for [C₁₅H₁₆NaO₂]⁺ 251.1043; found 251.1041.

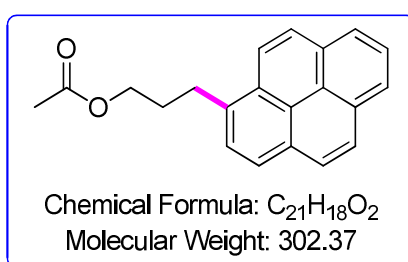
3-(Phenanthren-9-yl)propylacetate (**94**)



Following general procedure H with acetoxypropylsilicate **17** (0.45 mmol, 292 mg) and 9-bromophenanthrene (0.3 mmol, 77 mg). The crude product was purified by flash column chromatography (pentane/diethyl ether, 95/5) to afford **94** as a colorless oil (38 mg, 45%).

¹H NMR (400 MHz, CDCl₃): δ 8.76– 8.74 (m, 1H), 8.68 – 8.65 (m, 1H), 8.11– 8.07 (m, 1H), 7.85 – 7.82 (m, 1H), 7.70 – 7.56 (m, 5H), 4.23 (t, *J* = 6.5 Hz, 2H), 3.23 – 3.19 (m, 2H), 2.20 – 2.14 (m, 2H), 2.10 (s, 3H). **¹³C NMR** (100 MHz, CDCl₃): δ 171.3, 135.5, 131.9, 131.28, 130.9, 129.9, 128.2, 126.8, 126.8, 126.4, 126.4, 126.3, 124.3, 123.5, 122.6, 64.3, 29.9, 29.1, 21.2. **IR** (neat): 2917, 1957, 1929, 1722, 1245, 1067, 1031, 755, 736 cm⁻¹. **HRMS** calc. for [C₁₉H₁₈NaO₂]⁺ 301.1199; found 301.1195.

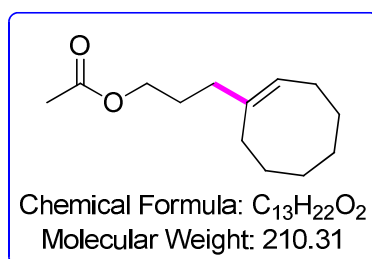
3-(Pyren-1-yl)propyl acetate (**95**)



Following general procedure H with acetoxypropylsilicate **17** (0.45 mmol, 292 mg) and 9-bromophenanthrene (0.3 mmol, 84.3 mg). The crude product was purified by flash column chromatography (pentane/diethyl ether, 95/5) to afford **95** as a colorless oil (58 mg, 64%).

¹H NMR (600 MHz, CDCl₃): δ 8.26 (d, *J* = 9.2 Hz, 1H), 8.18 – 8.16 (m, 2H), 8.12 (d, *J* = 9.2 Hz, 2H), 8.05 – 8.02 (m, 2H), 8.00 (t, *J* = 7.6 Hz, 1H), 7.87 (d, *J* = 7.7 Hz, 1H), 4.21 (t, *J* = 6.4 Hz, 2H), 3.45 – 3.42 (m, 2H), 2.23– 2.19(m, 2H), 2.11 (s, 3H). **¹³C NMR** (150 MHz, CDCl₃) δ 171.3, 135.5, 131.6, 131.0, 130.1, 128.8, 127.6, 127.6, 127.3, 126.9, 126.0, 125.3, 125.1, 125.1, 125.0, 124.9, 123.2, 64.1, 30.6, 29.9, 21.2. **IR** (neat): 3140, 2953, 2895, 1728, 1361, 1238, 1036, 836, 769, 708 cm⁻¹. **HRMS** calc. for [C₂₁H₁₈NaO₂]⁺ 325.1199; found 325.1209.

(E)-3-(Cyclooct-1-en-1-yl)propyl acetate (**96**)

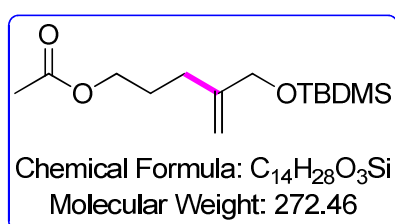


Following general procedure H with acetoxypropylsilicate **17** (0.45 mmol, 292 mg) and (E)-1-bromocyclooct-1-ene (0.3 mmol, 44 μ l). The crude product was purified by flash column chromatography (pentane/diethyl ether, 95/5) to afford **96** as a colorless oil (29 mg, 46%).

The spectroscopic data are in agreement with those reported in the literature.¹⁸⁸

¹H NMR (400 MHz, CDCl₃): δ 5.34 (t, J = 8.1 Hz, 1H), 4.05 (t, J = 6.7 Hz, 2H), 2.15 – 2.12 (m, 2H), 2.09 – 2.01 (m, 4H), 2.04 (s, 3H), 1.78 – 1.70 (m, 2H), 1.53 – 1.43 (m, 8H). ¹³C NMR (100 MHz, CDCl₃): δ 171.3, 139.6, 124.5, 64.6, 33.7, 30.1, 29.0, 28.9, 27.1, 26.7, 26.4, 26.4, 21.2.

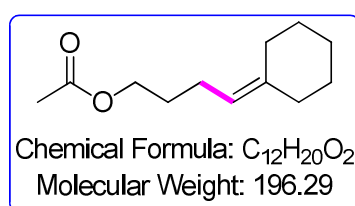
4-(((*tert*-Butyldimethylsilyl)oxy)methyl)pent-4-en-1-yl acetate(**97**)



Following general procedure H with acetoxypropylsilicate **17** (0.45 mmol, 292 mg) and ((2-bromoallyl)oxy)(*tert*-butyl)dimethylsilane (0.3 mmol, 68 μ l). The crude product was purified by flash column chromatography (pentane/diethyl ether, 95/5) to afford **97** as a colorless oil (46 mg, 56%).

¹H NMR (300 MHz, CDCl₃): δ 5.05 (dt, *J* = 1.6, 0.8 Hz, 1H), 4.83 (t, *J* = 1.5 Hz, 1H), 4.10 – 4.05 (m, 4H), 2.11 – 2.06 (m, 2H), 2.04 (s, 3H), 1.84 – 1.74 (m, 2H), 0.91 (s, 9H), 0.07 (s, 6H). **¹³C NMR** (75 MHz, CDCl₃): δ 171.3, 147.6, 109.3, 66.0, 64.3, 29.1, 26.9, 26.1 (3 C), 21.1, 18.5, -5.2 (2 C). **IR** (neat): 2972, 2945, 2885, 2852, 1740, 1653, 1465, 1361, 1237, 1116, 1078, 1039, 839, 773 cm⁻¹. **HRMS** calc. for [C₁₄H₂₈NaSiO₃]⁺ 295.1700; found 295.1710.

Cyclohexylidenebutyl acetate (**98**)

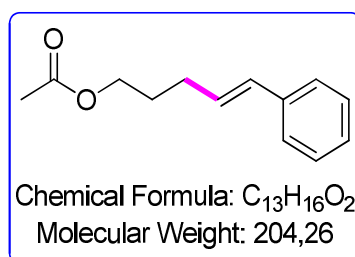


Following general procedure H with acetoxypropylsilicate **17** (0.45 mmol, 292 mg) and bromomethylenecyclohexane (0.3 mmol, 40 μl). The crude product was purified by flash column chromatography (pentane/diethyl ether, 95/5) to afford **98** as a colorless oil (32 mg, 55%).

The spectroscopic data are in agreement with those reported in the literature.¹⁸⁸

¹H NMR (400 MHz, CDCl₃): δ 5.09 – 4.93 (m, 1H), 4.04 (t, *J* = 6.8 Hz, 2H), 2.12 – 2.03 (m, 6H), 2.04 (s, 3H), 1.65 (p, *J* = 6.8 Hz, 2H), 1.56 – 1.45 (m, 6H). **¹³C NMR** (100 MHz, CDCl₃): δ 171.2, 140.8, 119.7, 64.0, 37.2, 28.9, 28.7, 28.6, 27.8, 26.90, 23.3, 21.

(E)-5-Phenylpent-4-en-1-yl acetate (**99**)

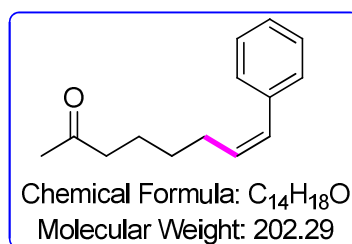


Following general procedure H with acetoxypropylsilicate **17** (0.45 mmol, 292 mg) and (E)-(2-bromovinyl)benzene (0.3 mmol, 39 μ l). The crude product was purified by flash column chromatography (pentane/diethyl ether, 90/10) to afford **99** as a colorless oil (46 mg, 75%).

The spectroscopic data are in agreement with those reported in the literature.¹⁸⁸

¹H NMR (400 MHz, CDCl₃): δ 7.41 – 7.31(m, 4H), 7.28 – 7.23(m, 1H), 6.50 – 6.44(m, 1H), 6.25 (dt, J = 15.8, 6.8 Hz, 1H), 4.18 (t, J = 6.6 Hz, 2H), 2.39 – 2.31 (m, 2H), 2.11 (s, 3H), 1.92 – 1.83 (m, 2H). **¹³C NMR** (100 MHz, CDCl₃): δ 171.2, 137.7, 130.8, 129.5, 128.6 (2C), 127.2, 126.1 (2C), 64.1, 29.5, 28.5, 21.1.

(Z)-5-Phenylpent-4-en-1-yl acetate (**100**)

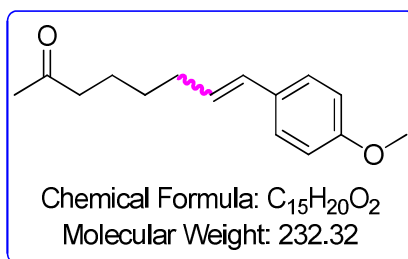


Following general procedure H with acetoxypropylsilicate **17** (0.45 mmol, 292 mg) and (Z)-(2-bromovinyl)benzene (0.3 mmol, 39 μ l). The crude product was purified by flash column chromatography (pentane/diethyl ether, 90/10) to afford **100** as a colorless oil (39 mg, 65%).

The spectroscopic data are in agreement with those reported in the literature.¹⁸⁸

¹H NMR (400 MHz, CDCl₃): δ 7.41 – 7.36 (m, 2H), 7.34 – 7.26 (m, 3H), 6.53 – 6.51 (m, 1H), 5.70 (dt, J = 11.5, 7.3 Hz, 1H), 4.13 (t, J = 6.6 Hz, 2H), 2.46 (qd, J = 7.4, 1.8 Hz, 2H), 2.05 (s, 3H), 1.87 – 1.80 (m, 2H). **¹³C NMR** (100 MHz, CDCl₃): δ 171.2, 137.5, 131.4, 130.0, 128.8 (2 C), 128.3 (2 C), 126.8, 64.0, 28.9, 25.1, 21.0.

5-Phenylpent-4-en-1-yl acetate (**101**)



Following general procedure H with acetoxypropylsilicate **17** (0.45 mmol, 292 mg) and (E)-1-(2-chlorovinyl)-4-methoxybenzene (0.3 mmol, 50.6 mg). The crude product was purified by flash column chromatography (pentane/diethyl ether, 90/10) to afford **101** as a colorless oil (46 mg, 65%, Z/E:8/92). The spectroscopic data are in agreement with those reported in the literature.¹⁸⁸

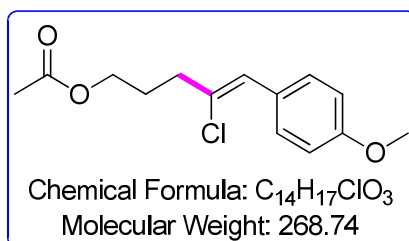
(E) isomer:

¹H NMR (600 MHz, CDCl₃): δ 7.27 (d, *J* = 8.8 Hz, 2H), 6.84 (d, *J* = 8.7 Hz, 2H), 6.35 (d, *J* = 15.8 Hz, 1H), 6.05 (dt, *J* = 15.8, 7.1 Hz, 1H), 4.12 (t, *J* = 6.6 Hz, 2H), 3.80 (s, 3H), 2.26 (qd, *J* = 7.1, 1.5 Hz, 1H), 2.05 (s, 3H), 1.82 – 1.78 (m, 2H). ¹³C NMR (150 MHz, CDCl₃) δ 171.3, 158.9, 130.5, 130.2, 127.2, 127.2 (2 C), 114.0 (2 C), 64.1, 55.4, 29.5, 28.6, 21.1.

(Z) isomer:

¹H NMR (600 MHz, CDCl₃): δ 7.21 (d, *J* = 8.7 Hz, 2H), 6.87 (d, *J* = 8.7 Hz, 2H), 6.39 (d, *J* = 11.7 Hz, 1H), 5.54 (dt, *J* = 11.6, 7.3 Hz, 1H), 4.08 (t, *J* = 6.6 Hz, 2H), 3.81 (s, 3H), 2.40 (qd, *J* = 7.3, 1.9 Hz, 2H), 2.01 (s, 3H), 1.80 – 1.76 (m, 2H). ¹³C NMR (150 MHz, CDCl₃) δ 171.2, 158.4, 130.1, 130.0, 129.8, 129.4 (2 C), 113.7 (2 C), 64.0, 55.4, 29.0, 25.1, 21.0.

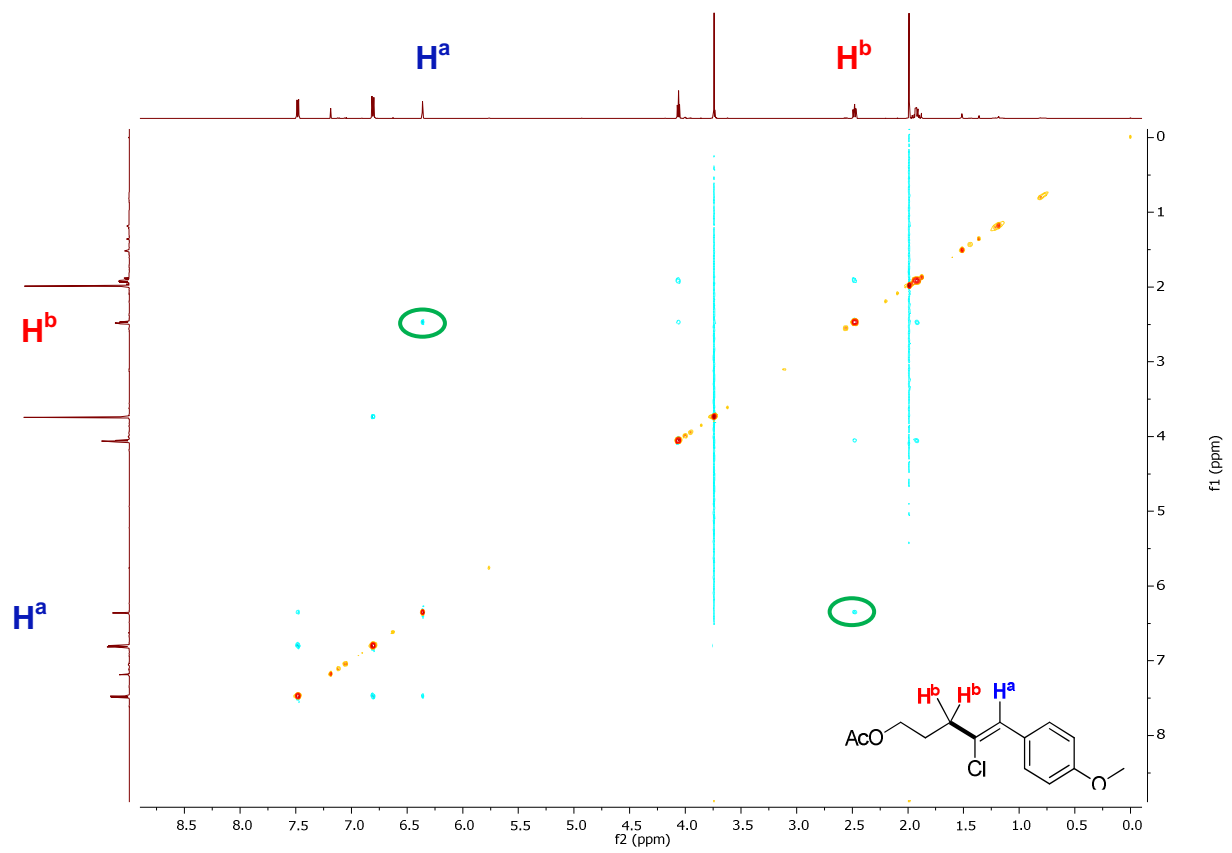
(Z)-4-Chloro-5-(4-methoxyphenyl)pent-1-en-1-yl acetate (102)



Following general procedure H with acetoxypropylsilicate **17** (0.45 mmol, 292 mg) and 1-(2,2-dichlorovinyl)-4-methoxybenzene (0.3 mmol, 61 mg). The crude product was purified by flash column chromatography (pentane/diethyl ether, 90/10) to afford **102** as a colorless oil (44 mg, 54%). Geometry of the double bond determined by NOESY experiment (see below).

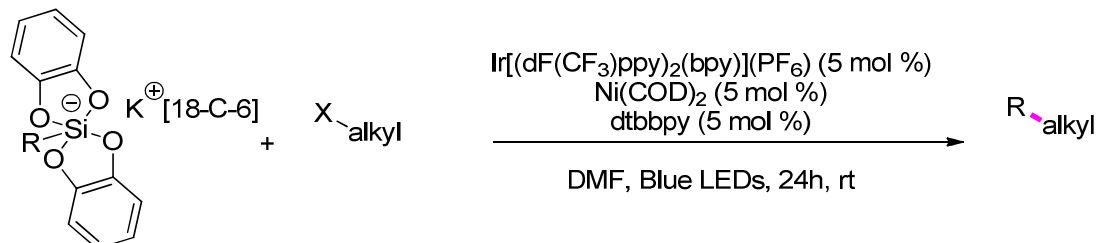
¹H NMR (400 MHz, CDCl₃): δ 7.55 (d, *J* = 8.7 Hz, 2H), 6.88 (d, *J* = 8.7 Hz, 2H), 6.43 (s, 1H), 4.14 (t, *J* = 6.4 Hz, 2H), 3.82 (s, 3H), 2.55 (td, *J* = 7.3, 0.9 Hz, 2H), 2.06 (s, 3H), 2.04 – 1.98 (m, 2H). **¹³C NMR** (100 MHz, CDCl₃) δ 171.2, 159.1, 131.6, 130.4 (2 C), 127.6, 124.7, 113.7 (2 C), 63.4, 55.4, 37.8, 26.9, 21.1. **IR** (neat): 2948, 2846, 1734, 1605, 1508, 1361, 1240, 1175, 1032, 819, 609 cm⁻¹. **HRMS** calc. for [C₁₄H₁₇ClNaO₃]⁺ 291.0758; found 291.0763.

NOESY of 102



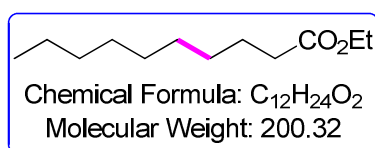
5.6.2 C(sp³)-C(sp³) bond formation

General procedure I for photoredox/nickel cross-coupling dual catalysis



To a Schlenk flask was added alkyl halide (1 eq., 0.3 mmol), silicate (1.5 eq., 0.45 mmol), Ir[(dF(CF₃)ppy)₂(bpy)](PF₆) (5 mol %, 15 μmol, 15 mg), and 2,2'-bipyridine (3 mol %, 9 μmol, 2.4 mg). The Schlenk flask was taken into a glovebox and Ni(COD)₂ (3 mol %, 9 μmol, 2.5 mg) was added. The Schlenk flask was sealed with a rubber septum, removed from the glovebox, and evacuated / purged with vacuum / argon three times. Degassed DMF (3 mL) was introduced (followed by the aryl or heteroaryl halide if liquid) and the reaction mixture was irradiated with blue LEDs (477 nm) for 24 hours. The reaction mixture was diluted with diethyl ether (50 mL), washed with saturated NaHCO₃ (2 times), brine (2 times), dried over MgSO₄ and evaporated under reduced pressure. The residue was purified by flash column chromatography on silica gel to afford the cross-coupling product.

Ethyl decanoate (104)



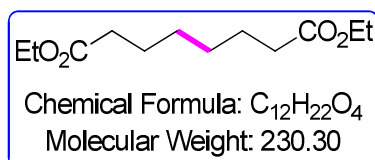
Following general procedure I with ethyl 4-bromobutyrate **103** (0.3 mmol, 43 μl) and hexylsilicate **2** (0.45 mmol, 284 mg). The crude product was purified by flash column chromatography (pentane/diethyl ether, 98/2) to afford **104** as a colorless oil (26 mg, 43%).

The spectroscopic data are in agreement with those reported in the literature.²²²

²²²M. Blümel, J.-M. Noy, D. Enders, M. H. Stenzel, T. V. Nguyen, *Org. Lett.*, 2016, **18**, 2208–2211.

¹H NMR (400 MHz, CDCl₃): δ 4.12 (q, *J* = 7.1 Hz, 2H), 2.30– 2.26 (m, 2H), 1.65 – 1.58 (m, 2H), 1.35 – 1.25 (m, 12H), 1.25 (t, *J* = 7.1 Hz, 3H), 0.88 (t, *J* = 6.8 Hz, 3H). **¹³C NMR** (100 MHz, CDCl₃): δ 174.1, 60.3, 34.6, 32.0, 29.6, 29.4, 29.4, 29.3, 25.2, 22.8, 14.4, 14.2.

Diethyl octanedioate (**105**)

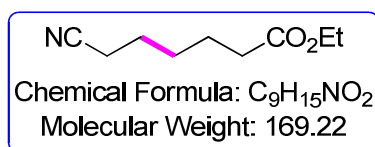


Following general procedure I with ethyl 4-bromobutyrate **103** (0.3 mmol, 43 μl) and hexylsilicate **2** (0.45 mmol, 284 mg). The crude product was purified by flash column chromatography (pentane/diethyl ether, 90/10) to afford **105** as a colorless oil (26 mg, 38%).

The spectroscopic data are in agreement with those reported in the literature.²²³

¹H NMR (400 MHz, CDCl₃): δ 4.12 (q, *J* = 7.1 Hz, 4H), 2.28 (t, *J* = 7.5 Hz, 4H), 1.66– 1.58 (m, 4H), 1.35 – 1.31 (m, 4H), 1.25 (t, *J* = 7.1 Hz, 6H). **¹³C NMR** (100 MHz, CDCl₃): δ 173.9 (2 C), 60.3 (2 C), 34.4 (2 C), 28.9 (2 C), 24.9 (2 C), 14.4 (2 C).

Ethyl 6-cyanoheptanoate (**106**)



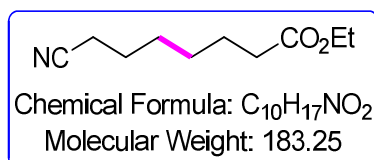
Following general procedure I with ethyl 4-bromobutyrate **103** (0.3 mmol, 43 μl) and cyanoethylsilicate **13** (0.45 mmol, 271 mg). The crude product was purified by flash column chromatography (pentane/diethyl ether, 80/20) to afford **106** as a colorless oil (10 mg, 20%).

The spectroscopic data are in agreement with those reported in the literature.²²⁴

²²³Y. Cai, X. Qian, C. Gosmini, *Adv.Synth. Catal.*, 2016, **358**, 2427–2430

¹H NMR (400 MHz, CDCl₃): δ 4.13 (q, *J* = 7.1 Hz, 2H), 2.35 (t, *J* = 7.1 Hz, 2H), 2.32 (t, *J* = 7.3 Hz, 2H), 1.72– 1.63 (m, 4H), 1.53– 1.45 (m, 2H), 1.26 (t, *J* = 7.1 Hz, 3H). **¹³C NMR** (100 MHz, CDCl₃): δ 173.4, 119.7, 60.5, 34.0, 28.3, 25.3, 24.2, 17.2, 14.4.

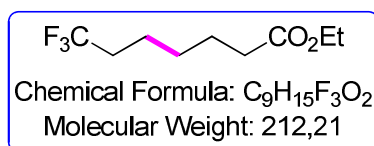
Ethyl 7-cyanoheptanoate (**107**)



Following general procedure I with ethyl 4-bromobutyrate **103** (0.3 mmol, 43 μl) and cyanopropylsilicate **14** (0.45 mmol, 277 mg). The crude product was purified by flash column chromatography (pentane/diethyl ether, 80/20) to afford **107** as a colorless oil (15 mg, 27%).

¹H NMR (400 MHz, CDCl₃): δ 4.12 (q, *J* = 7.1 Hz, 2H), 2.35 – 2.28 (m, 4H), 1.70– 1.60 (m, 4H), 1.51– 1.42 (m, 2H), 1.40– 1.32 (m, 2H), 1.25 (t, *J* = 7.1 Hz, 3H). **¹³C NMR** (100 MHz, CDCl₃): δ 173.5, 119.7, 60.3, 34.1, 28.3, 28.2, 25.2, 24.6, 17.1, 14.2. **HRMS** calc. for [C₁₀H₁₇NNaO₂]⁺ 206.1151; found 206.1153. **IR** (neat): 3058, 2988, 2939, 2863, 2365, 2328, 1728, 1264, 1188, 734 cm⁻¹.

Ethyl 7,7,7-trifluoroheptanoate (**108**)



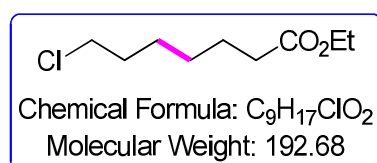
Following general procedure I with ethyl 4-bromobutyrate **103** (0.3 mmol, 43 μl) and 3,3',3''-trifluoropropylsilicate **6** (0.45 mmol, 290 mg). The crude product was purified by flash column chromatography (pentane/diethyl ether, 95/5) to afford **108** in a mixture with the starting material **103** in a (1/0.9) ratio as a colorless oil (30 mg, 25%).

²²⁴ M. Tokuda, Y. Watanabe, M. Itoh, *Bulletin of the Chemical Society of Japan*, 1978, **51**, 905 – 908.

The spectroscopic data are in agreement with those reported in the literature.²²⁵

¹H NMR (400 MHz, CDCl₃): δ 4.14 (d, *J* = 7.1 Hz, 2H), 2.31 (t, *J* = 7.4 Hz, 2H), 2.13– 2.01 (m, 2H), 1.69– 1.62 (m, 2H), 1.60– 1.54 (m, 2H), 1.44– 1.36 (m, 2H), 1.26 (t, *J* = 7.1 Hz, 3H). **¹³C NMR** (100 MHz, CDCl₃): δ 173.6, 127.3 (d, *J* = 276.3 Hz), 60.5, 34.1, 33.7 (q, *J* = 28.4 Hz), 28.3, 24.6, 21.8 (q, *J* = 2.9 Hz), 14.4. **¹⁹F NMR** (376 MHz, CDCl₃): -66.44.

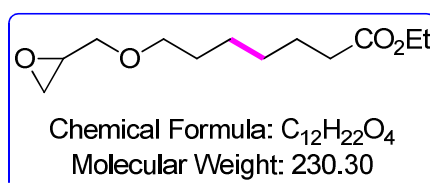
Ethyl 7-chloroheptanoate (**109**)



Following general procedure I with ethyl 4-bromobutyrate **103** (0.3 mmol, 43 μl) and chloropropylsilicate **12** (0.45 mmol, 281 mg). The crude product was purified by flash column chromatography (pentane/diethyl ether, 95/5) to afford **109** as a colorless oil (19 mg, 33%).

¹H NMR (400 MHz, CDCl₃): δ 4.12 (q, *J* = 7.1 Hz, 2H), 3.52 (t, *J* = 6.7 Hz, 2H), 2.29 (t, *J* = 7.5 Hz, 2H), 1.81 – 1.74 (m, 2H), 1.67 – 1.60 (m, 2H), 1.49 – 1.42 (m, 2H), 1.39 – 1.31 (m, 2H), 1.25 (t, *J* = 7.1 Hz, 2H). **¹³C NMR** (100 MHz, CDCl₃): δ 173.8, 60.4, 45.1, 34.3, 32.5, 28.5, 26.7, 24.9, 14.4. **HRMS** calc. for [C₉H₁₇ClNaO₂]⁺ 215.0809; found 215.0806. **IR** (neat): 2961, 2922, 2854, 2364, 2329, 1739, 1459, 1374 cm⁻¹.

Ethyl 7-(oxiran-2-ylmethoxy)heptanoate (**110**)



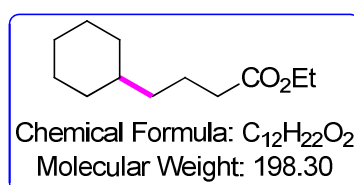
Following general procedure I with ethyl 4-bromobutyrate **103** (0.3 mmol, 43 μl) and 3-glycidyloxypropylsilicate **9** (0.45 mmol, 298 mg). The crude product was purified by flash

²²⁵ Y. Imagawa, S. Yoshikawa, T. Fukuhara and S. Hara, *Chem. Commun.*, 2011, **47**, 9191–9193.

column chromatography (pentane/diethyl ether, 80/20) to afford **110** as a colorless oil (19mg, 27%).

¹H NMR (400 MHz, CDCl₃): δ 4.12 (q, *J* = 7.1 Hz, 2H), 3.70 (dd, *J* = 11.5, 3.1 Hz, 1H), 3.48 (qt, *J* = 9.3, 6.6 Hz, 2H), 3.37 (dd, *J* = 11.5, 5.7 Hz, 1H), 3.14 (ddt, *J* = 5.8, 4.1, 2.9 Hz, 1H), 2.79 (dd, *J* = 5.1, 4.1 Hz, 1H), 2.60 (dd, *J* = 5.1, 2.7 Hz, 1H), 2.29 (t, *J* = 7.5 Hz, 2H), 1.66 – 1.55 (m, 4H), 1.41 – 1.29 (m, 4H), 1.25 (t, *J* = 7.1 Hz, 3H). **¹³C NMR** (100 MHz, CDCl₃): δ 173.9, 71.7, 71.6, 60.3, 51.0, 44.5, 34.4, 29.7, 29.1, 25.9, 25.1, 14.4. **HRMS** calc. for [C₁₂H₂₂NaO₄]⁺ 253.1410; found 253.1420. **IR** (neat): 2994, 2935, 2862, 2365, 2329, 1728, 1463, 1104, 1030 cm⁻¹.

Ethyl 4-cyclohexylbutanoate (**111**)



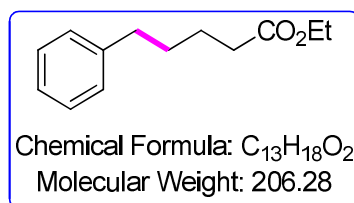
Following general procedure I with ethyl 4-bromobutyrate **103** (0.3 mmol, 43 μl) and cyclohexylsilicate **1** (0.45 mmol, 282 mg). The crude product was purified by flash column chromatography (pentane/diethyl ether, 98/2) to afford **111** as a colorless oil (19 mg, 31%).

The spectroscopic data are in agreement with those reported in the literature.²²⁶

¹H NMR (400 MHz, CDCl₃): δ 4.11 (q, *J* = 7.2 Hz, 2H), 2.26 (t, *J* = 7.6 Hz, 2H), 1.70– 1.58 (m, 7H), 1.25 (t, *J* = 7.2 Hz, 3H), 1.27– 1.11 (m, 6H), 0.90 – 0.81 (m, 2H). **¹³C NMR** (100 MHz, CDCl₃): δ 174.0, 60.3, 37.5, 37.1, 34.8, 33.4 (2 C), 26.8, 26.5 (2 C), 22.5, 14.4.

²²⁶ A. E. Jensen and P. Knochel, *J. Org. Chem.*, 2002, **67**, 79–85.

Ethyl 5-phenylpentanoate (**112**)

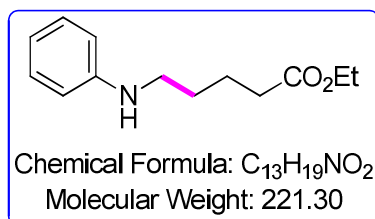


Following general procedure I with ethyl 4-bromobutyrate **103** (0.3 mmol, 43 μ l) and benzylsilicate **4** (0.45 mmol, 287 mg). The crude product was purified by flash column chromatography (pentane/diethyl ether, 95/5) to afford **112** in a mixture with the starting material in a (1/0.3) ratio as a colorless oil (18 mg, 18%).

The spectroscopic data are in agreement with those reported in the literature.²²⁷

¹H NMR (400 MHz, CDCl₃): δ 7.30– 7.25 (m, 2H), 7.20– 7.16 (m, 3H), 4.12 (q, J = 7.1 Hz, 2H), 2.65– 2.61 (m, 2H), 2.34– 2.30 (m, 2H), 1.69– 1.66 (m, 4H), 1.25 (t, J = 7.1 Hz, 3H). ¹³C NMR (100 MHz, CDCl₃): δ 173.8, 142.3, 128.5 (2 C), 128.4 (2 C), 125.9, 60.4, 35.7, 34.4, 31.1, 24.8, 14.4.

Ethyl 5-(phenylamino)pentanoate (**113**)



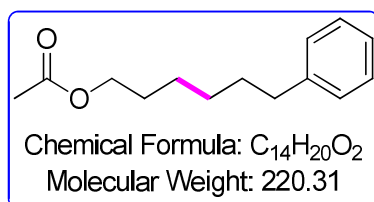
Following general procedure I with ethyl 4-bromobutyrate **103** (0.3 mmol, 43 μ l) and anilinomethylsilicate **8** (0.45 mmol, 294 mg). The crude product was purified by flash column chromatography (pentane/diethyl ether, 80/20) to afford **113** as a white solid (26 mg, 38%).

¹H NMR (400 MHz, CDCl₃): δ 7.19– 7.15 (m, 2H), 6.71– 6.67 (m, 1H), 6.62– 6.59 (m, 2H), 4.14 (q, J = 7.1 Hz, 2H), 3.66 (bs, 1H), 3.14 (t, J = 6.8 Hz, 2H), 2.36 (t, J = 7.2 Hz, 2H), 1.79–

²²⁷ M. Yoshida, H. Otaka and T. Doi, *Eur. J. Org. Chem.*, 2014, 27, 6010–6016.

1.72 (m, 2H), 1.70– 1.62 (m, 2H), 1.26 (t, $J = 7.1$ Hz, 3H). ^{13}C NMR (100 MHz, CDCl_3): δ 173.6, 148.4, 129.4 (2 C), 117.4, 112.8 (2 C), 60.5, 43.7, 34.2, 29.1, 22.7, 14.4. HRMS calc. for $[\text{C}_{13}\text{H}_{19}\text{NNaO}_2]^+$ 244.1308; found 244.1301. IR (neat): 3052, 2986, 2932, 2861, 1722, 1601, 1551, 1323, 1266, 1171 cm^{-1} .

6-Phenylhexyl acetate (**117**)

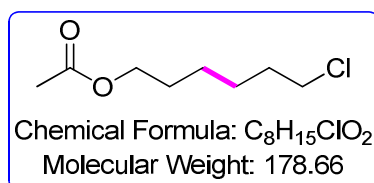


Following general procedure I with 1-bromo-3-phenylpropane (0.3 mmol, 46 μl) and acetoxypropylsilicate **17** (0.45 mmol, 292 mg). The crude product was purified by flash column chromatography (pentane/diethyl ether, 95/5) to afford **117** as a colorless oil (26 mg, 37%).

The spectroscopic data are in agreement with those reported in the literature.²²⁸

^1H NMR (400 MHz, CDCl_3): δ 7.26– 7.22 (m, 2H), 7.16– 7.13 (m, 3H), 4.02 (t, $J = 6.7$ Hz, 2H), 2.59 – 2.56 (m, 2H), 2.01 (s, 3H), 1.62 – 1.55 (m, 4H), 1.38 – 1.30 (m, 4H). ^{13}C NMR (100 MHz, CDCl_3): δ 171.3, 142.8, 128.5 (2 C), 128.4 (2 C), 125.8, 64.7, 36.0, 31.5, 29.0, 28.7, 26.0, 21.1.

6-Chlorohexyl acetate (**118**)



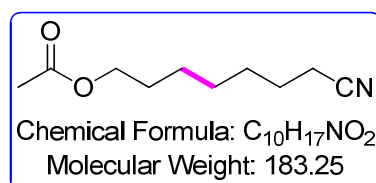
²²⁸ A. Fürstner, R. Martin, H. Krause, G. Seidel, R. Goddard and C.W. Lehmann, *J. Am. Chem. Soc.*, 2008, **130**, 8773–8787.

Following general procedure I with 1-bromo-3-chloropropane (0.3 mmol, 30 μ l) and acetoxypropylsilicate **17** (0.45 mmol, 292 mg). The crude product was purified by flash column chromatography (pentane/diethyl ether, 95/5) to afford **118** as a colorless oil (16 mg, 28%).

The spectroscopic data are in agreement with those reported in the literature.²²⁹

¹H NMR (400MHz, CDCl₃): δ 4.06 (t, J = 6.7 Hz, 2H), 3.53 (t, J = 6.7 Hz, 1H), 2.04 (s, 3H), 1.82 – 1.75 (m, 2H), 1.68 – 1.61 (m, 2H), 1.51 – 1.34 (m, 4H). **¹³C NMR** (100 MHz, CDCl₃): δ 171.3, 64.5, 45.1, 32.6, 28.6, 26.7, 25.4, 21.1.

7-Cyanoheptyl acetate (**119**)

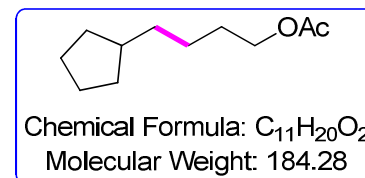
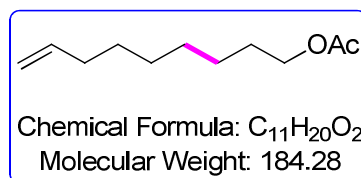
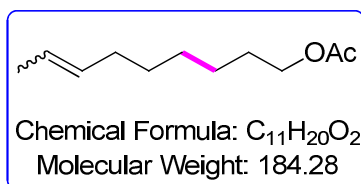


Following general procedure I with 5-bromopentanenitrile (0.3 mmol, 37 μ l) and acetoxypropylsilicate **17**(0.45 mmol, 292 mg). The crude product was purified by flash column chromatography (pentane/diethyl ether, 70/30) to afford **119** as a colorless oil (15 mg, 27%).

¹H NMR (400 MHz, CDCl₃): δ 4.06 (t, J = 6.7 Hz, 2H), 2.34 (t, J = 7.1 Hz, 2H), 2.05 (s, 3H), 1.70 – 1.60 (m, 4H), 1.49 – 1.41 (m, 2H), 1.39 – 1.33 (m, 4H). **¹³C NMR** (100 MHz, CDCl₃): δ 171.7, 120.2, 64.8, 29.0, 28.9, 28.9, 26.1, 25.7, 21.5, 17.6. **HRMS** calc.for [C₁₇H₂₀NNaO₂]⁺ 206.1151; found 206.1149. **IR** (neat): 2930, 2858, 2356, 2329, 2246, 1734, 1463, 1429, 1365, 1237, 1034, 733 cm⁻¹.

²²⁹ P.Doláková, M. Dracínský, J. Fanfrlík and Antonín Holý, *Eur. J. Org. Chem.*, 2009, 1082–1092.

Non-8-en-1-yl acetate (120), non-7-en-1-yl acetate (120'), 4-cyclopentylbutyl acetate (120'')



Following general procedure I with 6-bromo-1-hexene (0.3 mmol, 33 μ l) and acetoxypopylsilicate **17** (0.45 mmol, 292 mg). The crude product was purified by flash column chromatography (pentane/diethyl ether, 95/5) to afford a (3/2/5) mixture of **118**, **118'** and **118''** as a colorless oil (18 mg, 32%).

The spectroscopic data are in agreement with those reported in the literature.²²⁷

Compound 120 (characteristic signals)

¹H NMR (400 MHz, CDCl₃): δ 5.94 – 5.77 (m, 1H), 5.10 – 4.80 (m, 2H). ¹³C NMR (100 MHz, CDCl₃): δ 139.1, 114.2, 64.6, 25.1.

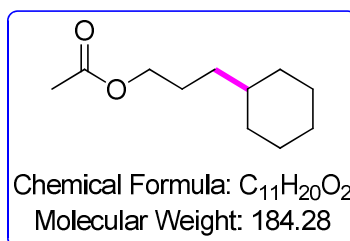
Compound 120' (characteristic signals)

¹H NMR (400 MHz, CDCl₃): δ 5.69 – 5.58 (m, 1H), 5.51 – 5.38 (m, 2H). ¹³C NMR (100 MHz, CDCl₃): δ 131.4, 1303.3, 124.8.

Compound 120''

¹H NMR (400 MHz, CDCl₃): δ 4.05 (t, *J* = 6.8 Hz, 2H), 2.04 (s, 3H), 1.83 – 1.70 (m, 1H), 1.68 – 1.58 (m, 3H), 1.54 – 1.47 (m, 1H), 1.47 – 1.20 (m, 8H), 1.16 – 1.01 (m, 1H), 0.98 – 0.83 (m, 1H). ¹³C NMR (100 MHz, CDCl₃): δ 171.2, 64.7, 40.0, 35.8, 33.7, 32.7, 28.9, 28.6, 25.9, 25.2, 21.0.

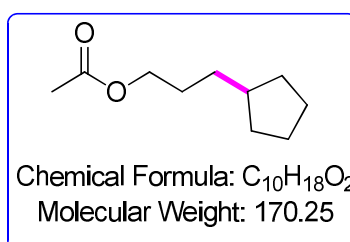
3-Cyclohexylpropyl acetate (**121**)



Following general procedure I with bromocyclohexane (0.3 mmol, 37 μ l) and acetoxypropylsilicate **17** (0.45 mmol, 292 mg). The crude product was purified by flash column chromatography (pentane/diethyl ether, 95/5) to afford **121** as a colorless oil (9 mg, 16%).

¹H NMR (400 MHz, CDCl₃): δ 4.03 (t, J = 6.8 Hz, 2H), 2.04 (s, 3H), 1.71 – 1.59 (m, 6H), 1.28 – 1.11 (m, 7H), 0.92 – 0.86 (m, 2H). **¹³C NMR** (100 MHz, CDCl₃): δ 171.4, 65.1, 37.5, 33.7, 33.4, 26.8, 26.5, 26.1, 21.2. **HRMS** calc. for [C₁₁H₂₀NaO₂]⁺ 207.1356; found 217.1352. **IR** (neat): 2925, 2852, 2386, 2289, 1731, 1455, 1365, 1285, 1243, 1038 cm⁻¹.

3-Cyclohexylpropyl acetate (**122**)

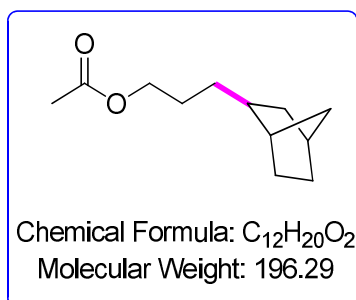


Following general procedure I with bromocyclopropane (0.3 mmol, 32 μ l) and acetoxypropylsilicate **17** (0.45 mmol, 292 mg). The crude product was purified by flash column chromatography (pentane/diethyl ether, 95/5) to afford **122** as a colorless oil (10 mg, 19%).

¹H NMR (400 MHz, CDCl₃): δ 3.98 (t, J = 6.8 Hz, 2H), 1.97 (s, 3H), 1.75 – 1.64 (m, 2H), 1.64 – 1.38 (m, 6H), 1.34 – 1.22 (m, 2H), 1.10 – 0.95 (m, 2H), 0.83 – 0.74 (m, 1H). **¹³C NMR** (100 MHz, CDCl₃): δ 171.2, 64.9, 39.8, 32.7, 32.3, 29.7, 27.9, 25.2 (2 C), 21.0. **HRMS** calc.

for $[\text{C}_{10}\text{H}_{18}\text{NaO}_2]^+$ 193.1199; found 193.1194. Ir (neat): 2954, 2922, 2856, 2364, 2329, 1741, 1459, 1366, 1239, 1037 cm^{-1} .

3-((1R,2R,4S)-bicyclo[2.2.1]heptan-2-yl)propyl acetate (123)

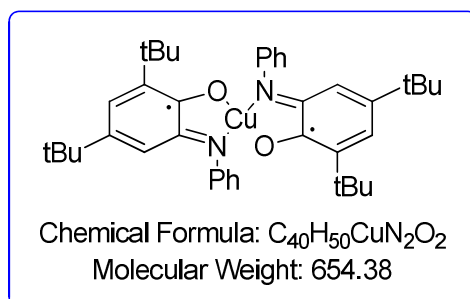


Following general procedure I with *exo*-2-bromonorbornane (0.3 mmol, 39 μl) and acetoxypropylsilicate **17** (0.45 mmol, 292 mg). The crude product was purified by flash column chromatography (pentane/diethyl ether, 95/5) to afford **123** as a colorless oil (21 mg, 35%).

$^1\text{H NMR}$ (400 MHz, CDCl_3): δ 4.05 (t, $J = 6.8$ Hz, 2H), 2.28 – 2.15 (m, 1H), 2.06 (s, 3H), 2.00 – 1.89 (m, 1H), 1.70 – 1.53 (m, 2H), 1.53 – 1.24 (m, 6H), 1.23 – 1.06 (m, 4H), 1.06 – 0.95 (m, 1H). $^{13}\text{C NMR}$ (100 MHz, CDCl_3): δ 171.3, 64.0, 42.1, 41.2, 38.3, 36.7, 35.4, 33.1, 30.3, 28.9, 27.2, 21.2. **HRMS** calc. for $[\text{C}_{12}\text{H}_{20}\text{NaO}_2]^+$ 219.1356; found 219.1350. Ir (neat): 2948, 2863, 2364, 2329, 1739, 1456, 1363, 1237, 1042 cm^{-1} .

5.7 Synthesis of non-innocent ligand complexes

Synthesis of complex $\text{Cu}(\text{L}_{\text{SQ}})_2$ (**125**)

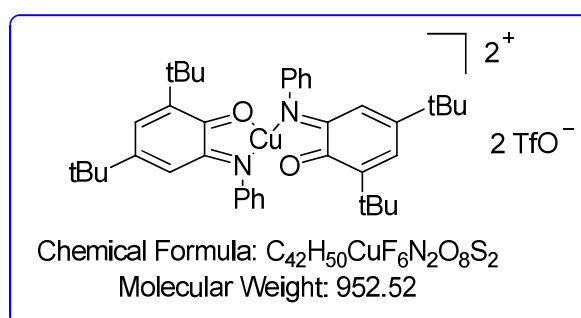


To a colorless solution of 2-(3,5-dimethoxyanilino)-4,6-di-*tert*-butylphenol, prepared following a previously reported procedure,¹⁰⁶ (3.56 mmol, 2 equiv.) in acetonitrile (40 mL), were added at 40°C, CuCl (176 mg, 1.78 mmol, 1 equiv.) and triethylamine (992 μL , 7.12 mmol, 4 equiv.). The resulting dark green mixture was refluxed for 2 h under air. After cooling down to room temperature, the dark green complex formed was filtered and washed with cold acetonitrile.

The UV-vis data were consistent with those reported in the literature.¹⁰⁶

UV-vis [CH_2Cl_2 ; λ nm (ϵ , $\text{M}^{-1}\cdot\text{cm}^{-1}$): 307 (21000), 460 (4610), 795 (7270).

Synthesis of complex $\text{Cu}(\text{L}_{\text{BQ}})_2(\text{OTf})_2$ (**127**)



To a flame-dried Schlenk flask was introduced complex **125** (200 mg, 0.31 mmol, 1 equiv.). The flask was back-filled three times with argon and degassed DCM (9 mL) was added. A 2.8M solution of bromine in DCM (111 μL , 0.31 mmol, 1 equiv.) was added and the

resulting dark-red solution was stirred for 1 h at room temperature. After evaporation of the solvent, the residue was triturated in hexane and filtered to afford a red-brown solid (quantitative). This Cu(L_{BQ})₂Br₂ complex (249 mg, 0.31 mmol, 1 equiv.) and silver triflate (157 mg, 0.62 mmol, 2 equiv.) were introduced into a Schlenk flask under an argon atmosphere. Degassed acetonitrile (5 mL) was added and the resulting mixture stirred for 2 h at room temperature. The suspension was filtered, and the filtrate was evaporated. The residue was dissolved in DCM and filtered. The filtrate was concentrated to give complex **127** (245 mg, 83%).

The UV-vis data were consistent with those reported in the literature.¹⁰⁶

UV-vis [CH₂Cl₂; λ nm (ε, M⁻¹.cm⁻¹): 290 (14100), 434 (6970), 504 (7370)

General Conclusion

The visible-light photoredox catalysis has proved to be an efficient alternative to toxic tin-mediated radical transformations and redox processes involving a stoichiometric amount of organometallic complexes, for the generation of radical species. This catalytic approach and the use of visible-light offers several advantages in terms of mild, selective and more eco-compatible process.

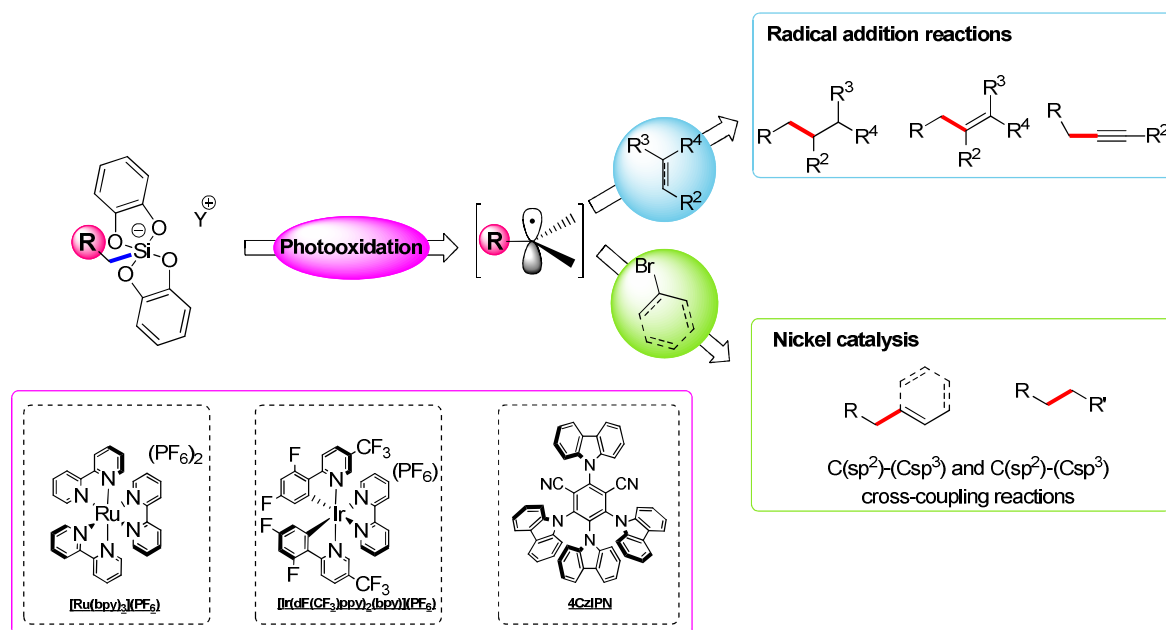
In this manuscript, we first reported the formation of non-stabilized alkyl radicals under photooxidative conditions. Photooxidation of alkyl bis-catecholato silicates, simply obtained from organosilanes, which are substrates of sol-gel processes, by a photoactive iridium complex under visible-light irradiation can provide alkyl radicals. Electrochemical studies of bis-catecholato silicates showed lower oxidation potentials than alkyl trifluoroborates or carboxylates. Spin-trapping experiments revealed that the silicates are good radical precursors. Further experiments demonstrated the ability of the generated radicals to be engaged in radical addition reactions such as allylation, vinylation or Giese-type reaction. In addition, the organic dye 4CzIPN (1,2,3,5-tetrakis-(carbazol-yl)-4,6-dicyanobenzene), proved to be an efficient photocatalyst as well.

The second part of this Ph. D. thesis focuses especially on a promising and growing application of photoredox catalysis: the merge of photoredox and organometallic catalysis. In conjunction with photooxidative processes, nickel catalysis showed to be a suitable candidate to perform cross-coupling reactions. With an iridium based photocatalyst and a nickel complex, alkyl bis-catecholato silicates were coupled to (hetero)aryl bromides *via* the formation of alkyl radicals. A “greener” version was further developed with 4CzIPN without loss of performance. The conditions for C(sp³)-C(sp²) cross-coupling reactions were compatible to aryl and alkenyl halides. Subsequently, the C(sp³)-C(sp³) bond formation in photoredox/nickel dual catalysis was studied. However, the methodology developed suffers of a side reaction of homocoupling which affects the yield of the reactions.

Finally, the ability of alkyl bis-catecholato silicates to be easily oxidized provides an opportunity to engage these precursors in others redox catalytic systems. Organometallic complexes with non-innocent ligands can participate to the generation of radicals by a single electron transfer through oxidation or reduction. Preliminary results concerning the oxidation

of silicates by a bis-iminobenzoquinone copper(II) complex are promising but still require more investigations.

The alkyl bis-catecholato silicates previously used as Lewis-acid proved to be excellent radical precursors upon photooxidation and thus versatile substrates for synthetic applications.



Photooxydation de silicates hypervalents pour la génération de radicaux carbonés: processus radicalaires et catalyse duale

La catalyse photoredox en lumière visible a réussi à s'imposer comme une méthode douce et éco-compatible de formation d'espèces radicalaires, et plus particulièrement de radicaux carbonés. Bien que cette catalyse ait su prouver son efficacité pour la formation de liaisons carbone-carbone/hétéroatome, les radicaux carbonés formés sont très souvent stabilisés. A l'inverse, les alkyles bis-catécholato silicates ont montré leur capacité à engendrer des radicaux alkyles non stabilisés par photooxydation à l'aide de complexes polypyridine de métaux de transition (Ru, Ir) photoactifs en lumière visible mais aussi de photocatalyseurs organiques. Les radicaux formés peuvent ainsi être piégés par différents accepteurs radicalaires. En outre, les alkyles bis-catécholato silicates sont engagés en présence d'électrophiles comme des halogénures éthyléniques ou (hétéro)aromatiques dans des conditions de catalyse duale photoredox/nickel afin de former des liaisons $C(sp^2) - C(sp^3)$. La méthodologie a été étendue au couplage $C(sp^3) - C(sp^3)$ avec toutefois quelques limitations. D'autre part, une étude comparant les silicates et les « ate-complexes » de bore pour la formation de radicaux par processus d'oxydation est présentée. Enfin, des travaux prometteurs sur l'oxydation des silicates par des complexes de cuivre portant des ligands non-innocents ont été amorcés.

Mots clés: Catalyse photoredox, photooxydation, photocatalyseur, silicate, radical, couplage croisé, catalyse duale, catalyse au nickel

Photooxidation of hypervalent silicon species for the formation of carbon centered radicals: radical processes and dual catalysis

Photoredox catalysis in visible light has succeeded in establishing itself as a gentle and eco-compatible method of formation of radical species, and more particularly of carbon radicals. Although this catalysis has proved to be efficient for the formation of carbon-carbon/heteroatom bonds, the generated carbon centered radicals are often very stabilized. Conversely, bis-catecholato silicates have shown to be capable of generating alkyl radicals that are not stabilized by photooxidation using polypyridine complexes of transition metals (Ru, Ir) that are photoactive in visible light but also organic photocatalysts. The radicals formed can thus be trapped by various radical acceptors. In addition, the bis-catecholato silicates can be employed in cross-coupling reactions with alkene halides and (hetero)aromatic halides under photoredox/nickel dual catalysis conditions for the formation of $C(sp^2) - C(sp^3)$ bonds. The methodology can also be extended to $C(sp^3) - C(sp^3)$ with some limitations. On the other hand, a study comparing the silicates and the "ate-complex" of boron for the formation of radicals by oxidation process is presented. Finally, promising works on the oxidation of silicates by copper complexes bearing non-innocent ligands have been initiated.

Key words: Photoredox catalysis, Dual catalysis, photooxidation, photocatalyst, silicate, radical, cross-coupling